

The role of soil in the transmission of chronic wasting disease and the inactivation of prions by peroxymonosulfate

By
Alexandra Rae Chesney

A dissertation submitted in partial fulfillment of
the requirements for the degree of

Doctor of Philosophy
(Molecular and Environmental Toxicology)

at the

UNIVERSITY OF WISCONSIN-MADISON
2016

Date of final oral examination: February 17th, 2016

The dissertation is approved by the following members of the final oral committee:

Joel A. Pedersen, Professor, Soil Science

Warren Porter, Professor, Zoology

Christopher Bradfield, Professor, Oncology

Corinna Burger, Associate Professor, Neurology

Christopher Johnson, Research Biologist, National Wildlife Health Center, USGS

ACKNOWLEDGEMENTS

I would like to acknowledge and thank the many people who were involved in the research described here. First and foremost, I would like to thank my advisors and committee, Drs. Chris Bradfield, Chris Johnson, Corinna Burger, and Warren Porter. I have been fortunate throughout my tertiary-education in that my advisors have always been excellent scientists who were kind but firm in their guidance.

In particular I would like to thank my major advisor, Dr. Joel Pedersen. I consider myself extremely lucky to have found an advisor so detail oriented and critical, yet willing to allow me to explore my professional independence, both in and out of the lab. I am sincerely thankful for the opportunities Joel has provided, and the professional respect developed in the last four years.

I would also like to give special thanks to Dr. Chad Johnson, a fantastic molecular biologist whom I have worked with throughout my PhD work. Chad was an amazing and involved mentor during his tenure in the Pedersen lab. After moving to a new field, he was willing to continue to coach me in my growth as a PhD scientist. I am thankful for his long-time support, his aspirations for me, and his mentorship in all things prion and PMCA.

Thank you also to Drs. Jeff and Delinda Johnson, who brought *in vivo* disease investigation into focus during this project and challenged me in developing a variety of new laboratory skills. I am immensely grateful for the wonderful laboratory colleagues in the Pedersen lab, the J. Johnson Lab at the School of Pharmacy, the C. Johnson lab at the National Wildlife Health Center at the United States Geological Survey, and the University of Wisconsin, Madison as a whole. In particular my lab-mates, Dr. Clarissa Shaffer, Prof. Christen Bell Smith, Dr. Kurt Jacobson, Dr. Thomas Keuch, Dr. Mercedes Ruiz, Kartik Kumar, Eric Melby, Debra Garvey, Emily Caudill and other past lab mates who not only helped me with experiments and critical thinking but who also became good friends.

I am deeply grateful for the social camaraderie and intellectual challenges from members of the NWHC lab of Chris Johnson: Dr. Christina Carlson, Dr. Jeanette Ducett, and Matt Keating; and members past and present of the Jeff Johnson group: Dr. Hannah Brautigam, Dr. Kahlilia Blanco, Dr. Kelley Salem, Dr. Jason Fuchs, Dr. Tim Rhoads, Rasa Valiauga, Calvin Harberg, and Trish Hoang. Your help troubleshooting Western blots, sharing resources, and cursing failed experiments, as well as all of your crazy, wonderfully high spirits and positive attitudes were instrumental in getting through the last half of this process. I cannot begin to thank you all enough.

I would like to thank other members of the UW science community for their friendship and support. I was lucky to be peripherally related to the Center for Sustainable Nanotechnology and I am grateful for the commitment and help I received from multiple members of this great group of scientists, in particular Dr. Lee Bishop, Arielle Mensch, and Mimi Hang of the research group of Robert Hamers.

I would like to thank the following individuals for their assistance as co-authors or other research support; Dr. Lingjun Li, Dr. Christopher Leitz, Dr. Tracey Nichols, as well as Guilherme Ludwig

for his patience and guidance in statistical analysis, Daniel Barr and Delwyn Keane at the Wisconsin Veterinary Diagnostic Laboratory for their excellent histological preparation and staining.

My graduate program, the Molecular and Environmental Toxicology Center, has been instrumental in my success as a graduate student. I would like to especially thank my cohort: Justin Clements, Jake Olson, Mike Shea, Carlos Ivan Rodriguez, Emmanuel Vazquez-Rivera, Morten Seirup, and Cherry Tsai Brown. From day one in fall 2011 I felt welcomed and accepted. Throughout the last five years we've been a team, both figuratively and literally (softball, flag football, volleyball, etc.). I'm honored to have been accepted into the METC program with such a talented, intelligent, creative, and sociable group of scientist. In addition, I would like to thank the administrative trio for METC, Barb Lewis, Eileen Stevens, and Mark Marohl for their support and help navigating academic deadlines and policies. I would like to especially thank Christopher Bradfield, the chair of METC for his unwavering support and dedication to the success of the METC program and all METC students.

Much of the work here was done with the help of a number of fantastic undergraduate assistants. In particular I would like to thank Hannah Kornely who was enthusiastic about nearly everything I threw at her. Her assistance and positive attitude were indispensable. I would also like to thank Dania Shoukfeh, who took a leap of faith and dove headfirst into the world of tissue processing. I would also like to thank Gabe Epstein and Rose Millevolte, who stepped in to help me in the last year of my projects.

Thank you to the mentors throughout my life who have inspired and pushed me to always strive for more. I cannot underscore the importance of a few powerful mentors: my rowing coaches, Becky Robinson and Julie Domina, for their endless encouragement and mentorship; Wisconsin's women's rowing coach Bebe Bryans, for getting me back on the water in graduate school; Professor Bethia King at Northern Illinois University, for taking a chance on me; and Victor Nguyen for his understanding, wisdom, patience, and many long chats in the pharmacy. Thank you to you all for pushing me further than I ever thought I could go.

My deepest thanks go to my friends and family. I particularly have to thank my road trip buddy, Chicago pizza pal, and advocate of all things adventure, Marisa Houlton. I look forward to many more spontaneous trips with you and reunions with everyone in Chicago at Lou's. I wouldn't be here if it weren't for the high expectations and support from my family. Thank you to my mother, Vicki Chesney, who kept me grounded throughout this journey. Your care packages were very much appreciated. Thank you to my father, Dr. David Chesney, for first nurturing my enthusiasm for science by coaching my Science Olympiad team in high school. Thank you also for all the chemistry guidance throughout all these years. You were a resource the typical student would never have had and I'm truly appreciative I had a tutor just a phone call away.

Finally, thank you to my Joe. Thank you for being with me through this long, arduous, stressful journey. Thank you for making me take breaks when I needed them, and pushing me when I needed to get the ball rolling. Thank you for providing me with a home, a sanctuary, and a safe haven. Thank you for not giving up on me, and believing me when I said that this graduate school thing wouldn't last forever.

DEDICATION

I would like to dedicate this work to:

- My grandmother, Loretta Theisen; the rock of our family, and the enduring legacy of kindness and love. I think of you every day.
- Nyx, the most patient pit bull puppy.
- My family and friends, who believed in me; thank you, it has meant the world.

TABLE OF CONTENTS

Acknowledgements	i
Dedication	iii
Table of Contents	iv
List of Tables	v
List of Figures	vi
Chapter 1: Introduction	1
Chapter 2: Peroxymonosulfate Rapidly Inactivates the Disease-associated Prion Protein	32
Chapter 2 Appendix	65
Chapter 3: Degradation of pathogenic prion protein from soil microparticles by peroxymonosulfate	74
Chapter 3 Appendix	104
Chapter 4: Extraction, detection, and decontamination of chronic wasting disease agent from soil	115
Chapter 4 Appendix	149
Chapter 5: Microparticles Alter Early Disease Tissue Tropism and Accumulation of Chronic Wasting Disease Prions in White-Tailed Deer.	156
Chapter 5 Appendix	186
Chapter 6: Overall conclusions and future research needs	192

LIST OF TABLES

Table 2.1 Inactivation of prions by chemical oxidants	60
Table 3.S1 Chemical composition of microparticles	105
Table 3.S2 Characterizations of prepared smectites	106
Table 4.1 Extraction buffers.	140
Table 5.S1 Tissues analyzed by mbPMCA for the presence of PrP ^{TSE}	187

LIST OF FIGURES

Figure 1.1	Structural regions of the prion protein.	28
Figure 1.2	Representation of PrP ^{TSE} transmission in the environment.	29
Figure 1.3	Two potential models of PrP conversion	30
Figure 1.4	Protein Misfolding Cyclic Amplification.	31
Figure 2.1	Peroxymonosulfate degrades pathogenic prion protein in the absence of transition metal cations	61
Figure 2.2	Activation of HSO ₅ ⁻ by CoCl ₂ enhances degradation of PrP ^{TSE}	62
Figure 2.3	Treatment with HSO ₅ ⁻ ± CoCl ₂ reduces the <i>in vitro</i> PrP ^C -to-PrP ^{TSE} converting ability of CWD agent by a factor of at least 10 ^{5.9}	63
Figure 2.4	Exposure of pathogenic prion protein to HSO ₅ ⁻ results in oxidative modification to tryptophan and methionine residues	64
Figure 2.S1	Sodium thiosulfate does not inhibit detection of PrP by immunoblotting	70
Figure 2.S2	Antibody epitopes and residues determined to be oxidized by peroxymonosulfate	71
Figure 2.S3	Antibody epitopes and residues easily oxidized and determined to be oxidized by peroxymonosulfate	72
Figure 2.S4	Transmission electron micrographs of purified prion protein exposed to 50 mM peroxymonosulfate for the indicated time period	73
Figure 2.S5	Peroxymonosulfate degrades recombinant mouse PrP in the α-helix-rich conformation (α-mo-recPrP) without activation to the sulfate radical	74
Figure 2.S6	Ethanol and <i>tert</i> -butyl alcohol do not quench inactivation of CWD prions by peroxymonosulfate (± CoCl ₂)	75

Figure 3.1	Concentration of HSO_5^- over time is dependent on the presence of certain microparticles and pH	100
Figure 3.2	Clay microparticles do not inhibit inactivation of CWD prion protein by HSO_5^-	101
Figure 3.3	Inactivation of prions bound to SWy-2 microparticles by HSO_5^- is not dependent on temperature or pH	102
Figure 3.4	Iron (oxy)hydroxide presence in HSO_5^- does not impact PrP^{TSE} inactivation	103
Figure 3.S1	X-ray diffraction data of prepared smectites	107
Figure 3.S2	SDS extraction recovered PrP^{TSE} from soil microparticles	108
Figure 3.S3	The presence of iron oxides do not inhibit detection of PrP^{TSE} by Western blot	109
Figure 3.S4	HSO_5^- previously exposed to microparticles still degrade prions	110
Figure 3.S5	Concentration decline of pH-buffered HSO_5^- -microparticle solutions	111
Figure 3.S6	Concentration of peroxymonosulfate over time in the presence of iron oxides	112
Figure 3.S7	Clay microparticles do not inhibit inactivation of CWD prion protein by HSO_5^-	113
Figure 3.S8	Densitometry of PrP^{TSE} exposed to 25 mM or 125 mM HSO_5^- for 30 or 60 minutes.	114
Figure 4.1	Degradation of CWD prions by peroxymonosulfate is not inhibited by sorption to soils	141
Figure 4.2	In vitro converting ability of CWD PrP^{TSE} is reduced after 1 h exposure to 125 mM peroxymonosulfate	142
Figure 4.3	Colony forming units from soil after saturation in peroxymonosulfate	144

Figure 4.4	Soil saturated with peroxymonosulfate was able to produce grass	146
Figure 4.5	Sod Toxicity (buffered and unbuffered)	147
Figure 4.S1	Extracts from Elliot and Defore soils reduce PMCAb amplification of PrP ^{TSE}	150
Figure 4.S2	Effect of extraction buffer on recovery of PrP ^{TSE} from soil and its detection by (A) immunoblotting or (B) protein misfolding cyclic amplification	152
Figure 4.S3	Effect of humic acid (HA) or fulvic acid (FA) on PMCAb	153
Figure 4.S4	PTA precipitation coupled with PMCAb reduce the inhibitory effect of soil extracts on PMCA	155
Figure 5.1	Accumulation of disease-associated prion protein (PrP ^{TSE}) is higher in white-tailed deer orally exposed to chronic wasting disease (CWD) prions + montmorillonite (Mte) relative to those inoculated with prions alone	183
Figure 5.2	The amount of prions was higher in animals inoculated with chronic wasting disease (CWD) prions associated with montmorillonite (Mte) microparticles than in those dosed with CWD prions alone	185
Figure 5.S1	Immunohistochemical analysis fails to detect CWD PrP in white-tailed deer tissues harvested at 3 and 42 dpi that test CWD-positive by mbPMCA	188
Figure 5.S2	Dilution series of PrP ^{TSE} in CWD-infected brain tissue analyzed by mbPMCA	189
Figure 5.S3	Detection of PrP ^{TSE} by mbPMCA in tissues of white-tailed deer at 42 days post oral challenge with CWD in the presence and absence of montmorillonite.	190
Figure 5.S4	Variation of semi-quantitative content due to treatment type, rather than tissue type	191

Chapter 1

Introduction: Current State of Knowledge

1.1 Prion Diseases

Transmissible spongiform encephalopathies (TSEs) are a class of progressive neurodegenerative diseases caused by prions.^{1,2} Prions are a unique infectious agent that catalytically converts a normal, biologically functional protein, PrP^C, to the misfolded and disease-associated conformation.³⁻⁶ Although the nomenclature for the disease-associated protein is varied depending on certain properties, including the size of the protein or the associated disease or strain, we will refer to the abnormally folded prion protein as PrP^{TSE}, unless otherwise indicated. Available evidence suggests that, unlike other pathogens, prions proliferate by a nucleic acid-independent method.^{1,7} Prion diseases affect a variety of mammalian species including humans (Creutzfeldt-Jakob disease, kuru, fatal familial insomnia, and Gerstmann–Sträussler–Scheinker syndrome), cattle (bovine spongiform encephalopathy or “mad cow” disease),^{8,9} sheep and goats (scrapie), and North American cervids (chronic wasting disease).^{4,8,10-13} Scrapie has been a documented sheep disease since 1732 in England and in Germany and France in the late 1760s.¹⁴ William Hadlow made the connection between scrapie and kuru, a disease afflicting the indigenous people of Papua New Guinea in the 1950s and noted the similarities of the diseases in a 1959 letter to *The Lancet*.¹⁵ These similarities included the prolonged incubation time, clinical symptoms, inevitable death and the neurohistological hallmark of prion diseases: the degeneration of the cerebellar cortex.¹⁶

1.2 Structure of normal and disease-associated PrP conformers

The cellular prion protein, PrP^C, is a 33-35 kDa sialoglycoprotein encoded by a single copy gene, *Prnp*.¹⁷ The gene is highly conserved among mammalian species and is expressed in neural and non-neural tissues, the highest expression being seen at the synapse of neurons.¹⁸⁻²⁰

The N-terminus of the protein contains a signal peptide, which is cleaved in a post-translational modification, followed by a series of octapeptide repeats containing primarily proline and glycine residues (Figure 1). The C-terminus contains a signal that controls the attachment of a glycosyl-phosphatidylinositol (GPI) anchor. Additionally, the protein contains two consensus sites for N-linked glycosylation as well as two cysteine residues that participate in a disulfide bond linkage. Secondary structure analysis by solution state NMR spectroscopy, X-ray crystallography, Fourier transform infrared spectroscopy and circular dichroism indicate that PrP^C has a high α -helical content.²¹⁻²⁴ This folding primarily occurs within the C-terminal domain (aa 121-231) and the N-terminus (aa 23-121) has no influence in its folding as the folding of the C-terminal domain is preserved in N-terminally truncated PrP forms.²² Although the differences in protein tertiary structure between PrP^C and the disease-associated PrP^{TSE} is not completely known, all structural models suggest that the infectious conformation of the prion protein contains a rich β -sheet structure.^{24,25} The change in structure also confers a resistance to typical sterilization and degradation methods such as proteinase digestion, most chemical treatments, and most typical heat-based sterilization measures.^{26,27} The disease agent is also resistant to irradiation, as it lacks nucleic acid. Resistance to proteinase K degradation is useful to distinguish between the host-expressed PrP^C and the pathogenic PrP^{TSE}; where PrP^C would be completely hydrolyzed, all but approximately 86-88 residues at the N-terminus of PrP^{TSE} resists Proteinase K digestion and the remaining protein maintains infectivity.²²

The infectious conformation is able to leave the cell surface by disassociating from the GPI anchor²⁸ and can aggregate into oligomers, protofibrils and amyloid plaques.^{2,25} Aggregates of PrP^{TSE} accumulate during disease progression and coincide with clinical symptoms such as ataxia, neuropathological lesions, spongiform vacuolations, and neuron depletion.²⁹ All TSEs are

invariably fatal and are distinguishable from other dementia diseases by their rapid progression of clinical symptoms after an extended asymptomatic period.^{10,12,30,31} The key event in all prion diseases is the conformational conversion of host-expressed PrP^{C} to PrP^{TSE} . Although the exact mechanism is unknown, available evidence suggests that polymeric PrP^{TSE} acts as a seed and becomes a template for the refolding of PrP^{C} into the growing polymer, and conversion may occur with polyanions acting as catalysts.^{21,32-34} This model is called the seeding-nucleation model.³⁵⁻³⁷ The spontaneous post-translational misfolding of PrP^{C} is thermodynamically unfavorable without the infectious seed, therefore the sporadic initiation of disease is rare.³⁸ In an alternative model, template directed misfolding, PrP^{TSE} induces the conformational transition of PrP^{C} through a cycle of unfolding and refolding reactions. During the reaction, the two conformations form a heterodimer at an intermediate stage and the resulting two PrP^{TSE} molecules dissociate and restart the reaction.² Prion disease progression relies on the expression of PrP^{C} on the cell membrane of infected tissues; previous studies have shown that PrP^{C} knockout mice ($\text{PrP}^{0/0}$) resist TSE infection.³⁹⁻⁴¹

1.3 Prion Disease Pathogenesis

Previous immunohistochemical studies suggest that following oral inoculation or ingestion, PrP^{TSE} enter the mucosal wall probably via transcytoplasmic tunneling of the M-cells and contact the mucosa-associated lymphoid system, including Peyer's patches.^{42,43} An alternative route may be through large lysosomal-associated membrane protein 1 (LAMP1)-positive endosomes of enterocytes.⁴⁴ LAMP1 is a type of glycoprotein that is involved with cell adhesion and endocytosis and is co-expressed with areas of PrP^{TSE} recruitment into the enterocyte cell body.⁴⁴ These enterocytes may capture and transport PrP^{TSE} from the gut lumen to

the Peyer's patches. Here, it is proposed, within the sub-epithelial dome, macrophages take up PrP^{TSE} by endocytosis for cellular degradation and follicular dendritic cells in the germinal centers accumulate PrP^{TSE} on their surfaces where replication is thought to begin.⁴⁴⁻⁴⁷

Mechanisms of further prion transport to other compartments of the lympho-reticular system (LRS) are still unclear. Following oral infection, fluorescently tagged PrP^{TSE} trafficked to axillary lymph nodes within two hours and were present in Peyer's patches, axillary and mesenteric lymph nodes up to 8 hours post infection, and PrP^{TSE} accumulates in other dendritic cells and probably sympathetic nerve endings in the LRS.³⁹ After infectivity has reached a certain plateau in the LRS, PrP^{TSE} likely gains contact with the CNS via splanchnic nerves at the level of the thoracic spinal cord. Accumulation of PrP^{TSE} in the central and peripheral nervous system of naturally infected deer provides evidence that disease spreads to the brain via the enteric nervous system. In clinically infected mule deer, high levels of PrP^{TSE} were detected in peripheral nervous system tissues associated with the digestive tract, including dorsal motor nucleus of the vagus nerve and the myenteric plexus.⁴⁸ This same tissue tropism of PrP^{TSE} accumulation was seen in hunter-harvested deer positive for CWD by immunohistochemistry (IHC) where the earliest tropism of PrP^{TSE} in the brain was the motor nucleus of the vagus nerve.⁴⁹ The exact role of the individual cells and the exact timing in PrP^{TSE} replication and transmission in each tissue is currently unknown. Differences in replication rates and locations of accumulation may differ between PrP^{TSE} alone and PrP^{TSE} bound to microparticles. Distinct differences in disease routes may exist between different sizes of PrP^{TSE} particles and the conditions of interactions between PrP^{TSE} and microparticles.

Terminal stages of TSEs are usually histologically characterized by large amyloid deposits of misfolded proteins. Studies using flow field-flow fractionation⁵⁰ and sedimentation

velocity show that non-fibrillar oligomers of around 300-600 kDa (equivalent to approximately 14-28 PrP^{res} molecules) are the most efficient initiators of TSE disease.^{50,51} It is generally agreed that oligomers and protofibrils (4-11 nm in diameter and less than 200 nm in length)^{50,52} are more toxic and more efficient at disease initiation than larger amyloid fibrils (approximately 10-14 nm in diameter and several μ m in length).⁵⁰⁻⁵⁴ Smaller molecules are more unstable compared to fibrils of 14-28 monomers, and are more likely to be captured and degraded by macrophages before replication can accumulate enough PrP^{TSE} to the point of exponential replication seen in disease progression.⁵² Isolated sizes of fractionated PrP^{TSE} adsorbed to Mte may also illustrate a difference in disease transmission based on a certain size of fibril associated with Mte that is unclear in heterogeneous inoculum.

Progressive neurodegeneration is the inevitable outcome of prion disease, however the mechanism of neurotoxicity remains unknown. Several groups have hypothesized that the neurodegeneration is a result of loss of PrP^C function, however this hypothesis has been tested by the development of PrP knockout mice where it was confirmed that PrP is not required for growth and development in mice; PrP knockout mice develop normally to adulthood, indicating PrP has a non-essential role.⁵⁵ Other groups have claimed that PrP^{TSE} or an intermediate has neurotoxic properties. Several factors likely play a role in prion-disease associated cell death, and cell toxicity may come from both hypothesized causes. A strong argument for loss of PrP^C function coupled with increased stress resulting in neuronal toxicity comes from an experiment where *Prnp* transgenic mice expressing hamster PrP only in the astrocytes were challenged and became infected with hamster-adapted scrapie agent.⁵⁶ This indicates that PrP^{TSE} in the astrocytes results in neurotoxic signaling that PrP knockout mice are not susceptible to.

1.4 Evidence for oral environmental transmission of prion disease

Most natural TSE transmission occurs via the oral route.^{44,57,58} The occurrence of bovine spongiform encephalopathy in the 1980s and 90s was due to infectious material being included in meat and bone meal fed to cattle, and the subsequent transmission to humans (variant Creutzfeldt-Jakob disease) was strongly implicated to be due to consumption of infected beef products.^{8,9,59} Kuru was spread by ritualistic cannibalism of deceased relatives.^{10,12,16,60} Some TSEs do, however, result from genetic mutations, such as fatal familial insomnia and familial Creutzfeldt-Jakob disease (CJD),¹⁰ both in humans, and CJD has been shown to spread iatrogenically.¹⁰ Scrapie and chronic wasting disease (CWD) are unique among other TSEs in that indirect horizontal transmission occurs from infected to naïve animals via an environmental reservoir of infectivity.^{61,62} Evidence suggests that prions enter the environment through urine, saliva, blood, placenta, or feces from infected animals or decomposed diseased carcasses (Figure 2).^{61,63-68} The quantity of prion shedding changes throughout the course of the disease depending on the tissue or excretion, mule deer are capable of producing titers of approximately 100 infectious units per mL of saliva ($\text{IU}_{50} \text{ mL}^{-1}$; an IU_{50} is the median infectious dose, the amount of infectious agent needed to infect half the test animal population),⁶⁹ and infectivity in feces is estimated at titers of $10^{2.5} \text{ IU}_{50} \text{ g}^{-1}$ wet feces cumulative over the course of a 10 month window where deer shed prions but do not yet show clinical symptoms of disease.^{67,70} Infectivity from decomposing carcasses depend on the state of disease progression. Improper disposal of infectious material may be an additional route of PrP^{TSE} entry into the environment, such as buried infected carcasses,^{72,73} and deposition of waste products (e.g., from slaughterhouses) into the environment.⁷⁴⁻⁷⁶ Pathogenesis of prion diseases differ among species, and prion shedding in the cases of scrapie and CWD may implicate increased peripheral tissue accumulation as a factor

in natural disease transmission.⁷⁷

The transmission of scrapie from diseased to naïve animals via an environmental reservoir has been long supported by anecdotal evidence, including up to 16 years between diseased animal presence and naïve animal exposure.⁷⁸ An experiment by Greig (1940) investigated this transmission by housing naïve sheep in enclosed fields previously housing scrapie-infected sheep.⁷⁹ The sheep contracted the disease despite having no direct contact with diseased animals. More recently, contaminated environments were shown to harbor levels of prions sufficient for disease transmission for up to 36 days,⁸⁰ and several fomites (i.e., materials or objects harboring infectivity) such as metal fencing, plastic scratching posts and wooden fence posts were implicated in the transmission of scrapie at a sheep farm.⁸¹

Extensive evidence has shown CWD infectivity persists in the environment. An unsuccessful attempt to decontaminate animal facilities previously housing diseased mule deer (*Odocoileus hemionus*) was an early demonstration of the environmental transmissibility of CWD.⁸² This same group later investigated the transmission of CWD in the environment and determined that in paddocks where diseased animals had been previously housed, naïve animals contracted the disease after 2.2 years, and that in paddocks where CWD-infected carcasses had been allowed to decompose in situ, naïve animals contracted the disease after introduction 1.8 years later.⁶¹ Fomites including feed buckets, water and bedding from pens housing experimentally challenged white-tailed deer (*Odocoileus virginianus*) in the preclinical stage of infection were sufficient to transmit the disease to naïve animals.⁸¹

1.5 Effect of soil microparticles on disease transmission

The amount of PrP^{TSE} shed from diseased animals is low (between -1.1 and $0.4 \log \text{ID}_{50}$ units/mL)⁸³ and oral transmission is less efficient than inoculation directly into the cerebrum by a factor of $\sim 10^5$ for mice.⁶⁷ Given that the amount of infectious material released into the environment is so low, successful environmental transmission is not widely expected, however it appears to be one of the primary routes of transmission of CWD and scrapie.^{61,62} Factors that are expected to influence the susceptibility of animals to the infectious agent include species of the host, and route of infection (e.g., inhalation, ingestion, scarification). The behavior of the animal (e.g., grazing in areas of animal congregation, rubbing on fence posts) is also a contributing factor as their physical exposure to infected environments or fomites likely adds to the likelihood of transmission.

Oral transmission of both scrapie and CWD is likely to occur through exposure to contaminated soils; ungulates ingest large quantities of soil and previous work from our group has shown that PrP^{TSE} strongly binds to specific soil constituents,^{73,84,85} and remarkably, this adsorption maintains prion infectivity and enhances oral transmissibility.^{85,86} Cervids and ruminants ingest large amounts of soils both to supplement nutrients and inadvertently while grazing (e.g., 8-30 g/day in the case of mule deer).⁸⁷ Analysis of CWD incidence and soil property data revealed that for every 1% increase of clay particle content in soil, the deer in that habitat have an 8.9% increase in their odds of being infected with CWD,⁸⁸ therefore prion infectivity in the soil is of particular concern due to this observed correlative enhancement in disease transmission. Almberg et al. (2011) examined CWD epizootic dynamics using a discrete, aspatial, susceptible-exposed-infectious-clinical model to examine the effect of infectious prion

persistence in soil. They found the duration of TSE agent persistence would drive CWD prevalence and the severity of cervid population decline.⁸⁹

The properties of soil plays a role in disease transmission,⁸⁵ a positive correlation was found between clay content of soils (i.e., soil particles $\leq 2 \mu\text{m}$) and CWD infection in northern Colorado's free-ranging mule deer population.⁸⁸ Transmission is also likely affected by the location of prion deposition in the soil (surface deposition from pre-clinical and clinical stage shedding vs. diseased carcass burial below soil surface), interaction strength between prions and soil constituents, environmental conditions (e.g., temperature, soil pH, water content and flux), and the presence of microorganisms, environmental enzymes,^{90,91} and/or minerals⁹² capable of degrading the infectious agent.⁹³

1.6 Prion and PrP^{TSE} detection methods

Detection methods for prions and PrP^{TSE} are differentiated into those that detect infectivity and those that measure PrP, or, when PK treated, PrP^{TSE}. Animal infectivity bioassays measure prion infectivity directly and are performed in whole animals via oral, intracranial ("IC"), intraperitoneal ("IP") or other routes of infection depending on the investigation question (e.g., inhalation, sublingual, environmental exposure such as the paddock experiments previously described, etc.). Long considered the "gold standard" for detection of prion infectivity, bioassays have a limit of detection of approximately 5.3 fg.⁹⁴ Animal bioassays have been used as an end-point measurement to determine the dilution at which a set proportion of the population of infected animals acquire disease.⁹⁵ Alternatively, bioassays have been used as way to measure incubation time, where animals are inoculated and the time until disease onset is measured.⁹⁶ Practical limitations of bioassays include the length of time until disease onset, cost to purchase

and maintain large quantities of animals, and considerations for genotype and background variety of certain animal strains.

1.6.1 In vitro methods of prion detection

In vitro methods to detect and diagnose prion diseases include immune-detection assays such as western blots, enzyme linked immunosorbant assays (ELISA) and immunohistochemistry, which typically provide direct detection of the prion protein in both the normal and misfolded form, although some only detect PrP^{TSE}.^{94,97,98} IHC is currently considered the diagnostic gold standard and provides direct visualization of the prion amyloid deposits present in tissues. IHC is instrumental in mapping prion distribution throughout tissues, as well as differentiating between prion phenotypes such as punctate verse diffuse amyloid staining. Western blots and ELISAs also use antibodies to directly detect the presence of prions in a liquid sample and are commonly used for disease diagnostics.

1.6.2 Protein Misfolding Cyclic Amplification

Protein misfolding cyclic amplification (PMCA) is a PrP^{TSE} detection method that exploits the ability of PrP^{TSE} to convert the cellular prion protein to the disease-associated conformer. Amplification is achieved through repeated cycles of sonication and incubation (Figure 4).^{94,99,100} Cellular prion protein from uninfected brain homogenate is used as a substrate, and a small amount of starting material containing PrP^{TSE} seeds the conversion. Samples are sonicated with one (microplate-based PMCA, mbPMCA) or two Teflon beads (bead assisted PMCA, PMCAb) to disrupt PrP^{TSE} aggregates and incubated to allow PrP^C-to-PrP^{TSE} conversion before repeating the cycle. One “round” of PMCA consists of multiple cycles (96-144). During serial PMCA, the substrate is replenished between rounds. The level of amplification can be determined by immunoblotting after proteinase K digestion, and samples can be used to estimate

the quantity of PrP^{TSE} present in each sample using semi-quantitative methods. The newly converted PrP^{TSE} has physiochemical properties identical to the seed and remains infectious in bioassay.¹⁰⁰ The inclusion of polymeric beads is a recent advancement that has improved the robustness and repeatability of the technique.^{99,100} We have shown that PMCAb increased the detection sensitivity of CWD agent by a factor of 10^5 .¹⁰⁰ Our group has shown previously that the sensitivity of PMCAb is such that CWD-positive brain homogenate can be detected in dilutions up to 6.7×10^{-13} after three 96-cycle rounds with no additional detection after a fourth round.¹⁰⁰ This sensitivity exceeds by $\sim 10^5$ that of detection by bioassay when conducted in transgenic mice (cervid prion protein expressed) where clinical disease symptoms were observed in half the mice at 10^{-7} dilution.¹⁰⁰

Recently, Moudjou et al. (2014) adapted PMCA/PMCAb to a 96 well microplate format (mbPMCA) where the amount of substrate and seed is reduced 60% and only one Teflon bead is used. In addition to reducing materials, the 96-well plate format allows higher throughput of samples. We have seen a noticeable improvement in PMCA reproducibility using mbPMCA, with the limit of detection reaching a $10^{-13.6}$ dilution from CWD brain. We found that mbPMCA is more sensitive than immunohistochemistry by a factor exceeding $\geq 10^{6.3}$.

1.7 Resistance of prions to physical, chemical, and enzymatic inactivation

Prions are resistant to conventional sterilization methods that inactivate conventional pathogens (e.g., viruses, bacteria, protozoans), such as ionizing, microwave, and ultraviolet radiation,¹⁰¹⁻¹⁰³ dry heat, boiling,¹⁰¹ standard autoclaving,¹⁰⁴ or exposure to formalin,¹⁰⁵ or 1-8 M urea.¹⁰⁶ Effective treatments include autoclaving at 132 °C for 4.5 hours or at 121 °C for 90 minutes in the presence of 1 M NaOH, exposure to the denaturing chaotropic salt guanidinium

thiocyanate (>6M),¹⁰⁶ incineration (15 min at 1000 °C),¹⁰⁷ and exposure to the phenolic disinfectant Environ LpH (1% for 30 min),¹⁰⁸ exposure to 2% sodium hypochlorite for 1 h,¹⁰⁹ exposure to acidic 1% SDS (pH ≤ 4.5) at 65 °C for 2 h following exposure to 4% SDS (neutral pH) at 65 °C for 30 min.¹¹⁰ Additional oxidation techniques that have been attempted for prion inactivation are reviewed in Table 1 in Chapter 2.

Prions generally resist degradation by microorganisms and isolated proteases.^{90,111} Several examples of proteolytic degradation of prions have been reported, such as via composting,¹¹²⁻¹¹⁴ via microbial communities on the surface of ripened cheeses,¹¹⁵ and via lichen proteases.¹¹⁶ Some isolated enzymes, primarily serine proteases, have shown the ability to degrade prions, however, challenges associated with proteolytic degradation of prions include requirements of harsh conditions for prion degradation (extensive exposure times, elevated temperature, alkaline pH, presence of a detergent).⁹⁰ Prionzyme (Genecor), a proprietary serine protease derived from *Bacillus subtilis*, was able to reduce prion detection to less than threshold for Western blot, but required up to 7 d for this depletion to occur at mild conditions (pH 7.4 and 22 °C) and, significantly, infectivity was not reduced.¹¹⁷

In some studies, protease-induced reduction in the detected amount of pathogenic prion protein does not correlate with declines in prion infectivity,^{25,90,118} indicating that after exposure to potentially proteolytic enzymes in which immunoblot detection of the protein decreased, the prions remained infectious. These results suggest that not only the type of enzyme used, but also the conditions of prion incubation with enzymes can have a significant effect in reducing prion infectivity.

1.9 Summary and concluding remarks

Despite the many advances in prion research, many questions remain, specifically regarding the role of soil in both disease transmission dynamics and the role of PrP^{TSE} associated with soil particles in efforts to inactivate the disease agent, especially in the environment. Chronic wasting disease continues to spread throughout the United States; since the work described here began in 2011, seven states reported new incidents of CWD in captive or wild cervids. Now, more than ever, it is imperative that inactivation techniques be developed and translated to environmental applications and that wildlife management strategies consider the role of environmental factors in prion disease transmission.

1.10 Introduction to the research in this dissertation

The main goal of the current research is to gain a greater understanding of CWD prion inactivation and CWD transmission dynamics with respect to prion association with soil particles. **The overall hypothesis for this thesis is that CWD prions associated with soil components play a role in inactivation as well as disease progression once orally ingested.** Utilizing diagnostic methods and subclinical disease tissue assays, we addressed the following research questions:

Question 1: Are prions susceptible to inactivation by oxidation with peroxymonosulfate?

Currently, efficient prion degradation techniques are not realistic for environmental applications, yet the spread of CWD continues with extensive evidence implicating horizontal transmission through an environmental reservoir. Here, we

investigate the ability of peroxymonosulfate to inactivate two strains of prions: CWD, an environmentally relevant prion strain; and the HY strain of hamster-adapted transmissible mink encephalopathy. Peroxymonosulfate rapidly inactivates both strains, with enhanced degradation seen when peroxymonosulfate is activated to sulfate radical by addition of the transition metal cobalt. We showed, using liquid chromatography-tandem mass spectrometry, that four residues are consistently oxidized by peroxymonosulfate, and by using transmission electron microscopy, we see the entire protein fibril structure is affected. By using protein misfolding cyclic amplification, we show that peroxymonosulfate reduces PrP^C to PrP^{TSE} in vitro conversion by a factor greater than $10^{5.9}$. Because of these results, we considered further studies essential, especially studies to investigate the ability of peroxymonosulfate to inactivate prions associated with soil components.

Question 2: Can oxidation by peroxymonosulfate inactivate CWD prions associated with isolated clay and iron oxide soil particles?

Here, we extended the investigation with prion inactivation by peroxymonosulfate by examining the extent of degradation when CWD prions are associated with soil particles. In addition to association with soil components and environmental factors such as pH, and temperature were examined for their effect on oxidation efficiency. We show that despite binding to clay microparticles, peroxymonosulfate is able to inactivate the associated CWD prions. Furthermore, relevant environmental temperatures (4-50 °C) and pH (3-9) do not significantly affect prion inactivation. Our results suggest that peroxymonosulfate may be an option for future CWD prion remediation efforts.

Question 3: Is peroxymonosulfate able to degrade CWD prions associated with whole soils at concentrations not toxic to environmental flora?

In addition to clay and iron oxide microparticles, whole soils are complex and include a combination of minerals, mineral and organic matter. The assessment of the ability of peroxymonosulfate to inactivate prions associated with soil is a key step towards environmental application. In addition to assessing degradation, it is essential that the toxicity of peroxymonosulfate is well understood before its environmental application. We showed that peroxymonosulfate is able to inactivate prions associated with six different whole soils, and, using protein misfolding cyclic amplification, we showed in vitro conversion is significantly reduced. Furthermore, we show that although the concentration used to inactivate PrP^{TSE} is lethal to soil microflora and turfgrass, grass seeded on soil exposed to high concentrations of peroxymonosulfate is able to grow, and bacterial and fungal colonies are likely able to recover. These results indicate that peroxymonosulfate may be a viable option for remediation of prion infected soil in the environment and may contribute to limiting the horizontal spread of CWD.

Question 4: Do CWD prions associated with soil microparticles affect prion accumulation and prion tissue tropism in vivo?

The transmission of prion disease is enhanced when prions are associated with microparticles. This effect has already been shown in hamster models, however we cannot assume this enhancement holds true in cervids due to inherent differences in rodent vs. cervid intestinal anatomy and potential prion strain differences. In addition to investigating an increased disease penetrance in cervids, other questions remain from the earlier studies.

Here, we examined the accumulation of PrP^{TSE} in tissues from white-tailed deer orally inoculated with CWD brain homogenate with or without clay microparticles. We used protein misfolding cyclic amplification to detect prions in the palatine tonsil, submandibular lymph node, retropharyngeal lymph node, and ileum. Importantly, our results showed that animals given inoculum containing clay microparticles had larger amounts of accumulated PrP^{TSE} and PrP^{TSE} was detected in a larger number of tissues compared to animals given inoculum without particles. Although the mechanism of enhanced disease transmission is not yet established, our results indicate that tissue tropism is altered and accumulation is increased when the disease agent is associated with microparticles.

1.12 References

1. Prusiner, S. B., Prions. *Proc. Natl. Acad. Sci. U S A*. **1998**, *95*, (23), 13363-13383.
2. Prusiner, S. B., Molecular biology of prion diseases. *Science*. **1991**, *252*, (5012), 1515-1522.
3. Bolton, D. C.; Bendheim, P. E.; Marmorstein, A. D.; Potempska, A., Isolation and structural studies of the intact scrapie agent protein. *Arch. Biochem. Biophys.* **1987**, *258*, (2), 579-590.
4. McKinley, M. P.; Bolton, D. C.; Prusiner, S. B., A protease-resistant protein is a structural component of the scrapie prion. *Cell*. **1983**, *35*, 57-62.
5. Prusiner, S. B., Novel proteinaceous infectious particles cause Scrapie. *Science*. **2011**, *216*, (4542), 136-144.
6. Prusiner, S. B.; Groth, D. F.; Cochran, S. P.; Masiarz, F. R.; McKinley, M. P.; Martinez, H. M., Molecular properties, partial purification, and assay by incubation period measurements of the hamster scrapie agent. *Biochemistry*. **1980**, *19*, 4883-4891.
7. Barria, M. A.; Mukherjee, A.; Gonzalez-Romero, D.; Morales, R.; Soto, C., De novo generation of infectious prions in vitro produces a new disease phenotype. *PLoS Pathog.* **2009**, *5*, (5), e1000421.
8. Anderson, R. M.; Donnelly, C. A.; Ferguson, N. M.; Woolhouse, M. E.; Watt, C. J.; Udy, H. J.; MaWhinney, S.; Dunstan, S. P.; Southwood, T. R.; Wilesmith, J. W.; Ryan, J. B.; Hoinville, L. J.; Hillerton, J. E.; Austin, A. R.; Wells, G. A., Transmission dynamics and epidemiology of BSE in British cattle. *Nature*. **1996**, *382*, (6594), 779-788.
9. Hope, J., Bovine spongiform encephalopathy: a tipping point in One Health and Food Safety. *Curr. Top. Microbiol. Immunol.* **2013**, *366*, 37-47.
10. Sikorska, B.; Liberski, P. P., Human prion diseases: from Kuru to variant Creutzfeldt-Jakob disease. *Subcell. Biochem.* **2012**, *65*, 457-496.
11. Bolton, D. C.; McKinley, M. P.; Prusiner, S. B., Identification of a protein that purifies with the scrapie prion. *Science*. **1982**, *218*, (4579), 1309-1311.
12. Liberski, P. P., Historical overview of prion diseases: a view from afar. *Folia. Neuropathol.* **2012**, *50*, (1), 1-12.
13. Williams, E. S.; Miller, M. W.; Kreeger, T. J.; Kahn, R. H.; Thorne, E. T., Chronic wasting disease of deer and elk: A review with recommendations for management. *J. Wildl. Manage.* **2002**, *66*, 551-563.

14. Plummer, P. J., Scrapie - a disease of sheep. *Can. J. Comp. Med. Vet. Sci.* **1946**, *10*, (2), 49-54.
15. Hadlow, W. J., Scrapie and kuru. *Lancet.* **1959**, *2*, (7097), 289-290.
16. Hadlow, W. J., Neuropathology and the scrapie-kuru connection. *Brain. Pathol.* **1995**, *5*, 27-31.
17. Oesch, B.; Westaway, D.; Walchli, M.; McKinley, M. P.; Kent, S. B. H.; Aebersold, R.; Barry, R. A.; Tempst, P.; Teplow, D. B.; Hood, L. E.; Prusiner, S. B.; Weissmann, C., A cellular gene encodes scrapie PrP 27-30 protein. *Cell.* **1985**, *40*, 735-746.
18. Kretzschmar, H. A.; Prusiner, S. B.; Stowring, L. E.; Dearmond, S. J., Scrapie prion proteins are synthesized in neurons. *Am. J. Pathol.* **1986**, *122*, 1-5.
19. Sales, N.; Rodolfo, K.; Hassig, R.; Faucheux, B.; Di Giamberardino, L.; Moya, K. L., Cellular prion protein localization in rodent and primate brain. *Eur. J. Neurosci.* **1998**, *10*, 2464-2471.
20. Herms, J.; Tings, T.; Gail, S.; Madlung, A.; Giese, A.; Siebert, H.; Schurmann, P.; Windl, O.; Brose, N.; Kretzschmar, H. A., Evidence of presynaptic location and function of the prion protein. *Neuroscience.* **1999**, *19*, (20), 8866-8875.
21. Govaerts, C.; Wille, H.; Prusiner, S. B.; Cohen, F. E., Evidence for assembly of prions with left-handed beta-helices into trimers. *Proc. Natl. Acad. Sci. U S A.* **2004**, *101*, (22), 8342-8347.
22. Sajnani, G.; Requena, J. R., Prions, proteinase K and infectivity. *Prion.* **2012**, *6*, (5), 430-2.
23. Silva, C. J.; Vazquez-Fernandez, E.; Onisko, B.; Requena, J. R., Proteinase K and the structure of PrP^{Sc}: The good, the bad and the ugly. *Virus. Res.* **2015**, *207*, 120-126.
24. Pan, K. M.; Baldwin, M.; Nguyen, J.; Gasset, M.; Serban, A.; Groth, D.; Mehlhorn, I.; Huang, Z.; Fletterick, R. J.; Cohen, F. E.; Prusiner, S. B., Conversion of α -helices into β -sheet features in the formation of the scrapie prion proteins. *Proc. Natl. Acad. Sci. U S A.* **1993**, *90*, 10962-10966.
25. Aguzzi, A.; Sigurdson, C.; Heikenwaelder, M., Molecular mechanisms of prion pathogenesis. *Annu. Rev. Pathol.* **2008**, *3*, 11-40.
26. Taylor, D. M., Inactivation of prions by physical and chemical means. *J. Hosp. Infect.* **1999**, *43 Suppl*, S69-76.
27. Rutala, W. A.; Weber, D. J.; Society for Healthcare Epidemiology of, A., Guideline for disinfection and sterilization of prion-contaminated medical instruments. *Infect. Control. Hosp. Epidemiol.* **2010**, *31*, (2), 107-117.

28. Harris, D. A., Cellular biology of prion diseases. *Clin. Microbiol. Rev.* **1999**, *12*, (3), 429-444.
29. Davies, G. A.; Bryant, A. R.; Reynolds, J. D.; Jirik, F. R.; Sharkey, K. A., Prion diseases and the gastrointestinal tract. *Can. J. Gastroenterol.* **2006**, *20*, (1), 18-24.
30. Colby, D. W.; Prusiner, S. B., Prions. *Cold. Spring. Harb. Perspect. Biol.* **2011**, *3*, (1), a006833.
31. Aguzzi, A.; Nuvolone, M.; Zhu, C., The immunobiology of prion diseases. *Nat. Rev. Immunol.* **2013**, *13*, (12), 888-902.
32. Apostol, M. I.; Perry, K.; Surewicz, W. K., Crystal structure of a human prion protein fragment reveals a motif for oligomer formation. *J. Am. Chem. Soc.* **2013**, *135*, (28), 10202-10205.
33. Soto, C., Prion hypothesis: the end of the controversy? *Trends. Biochem. Sci.* **2011**, *36*, (3), 151-158.
34. Fernandez-Borges, N.; Erana, H.; Elezgarai, S. R.; Harrathi, C.; Gayosso, M.; Castilla, J., Infectivity versus Seeding in Neurodegenerative Diseases Sharing a Prion-Like Mechanism. *Int. J. Cell. Biol.* **2013**, *2013*, 583498.
35. Come, J. H.; Fraser, P. E.; Lansbury, P. T., Jr., A kinetic model for amyloid formation in the prion diseases: Importance of seeding. *Proc. Natl. Acad. Sci. U S A.* **1993**, *90*, 5959-5963.
36. Aguzzi, A.; Calella, A. M., Prions: protein aggregation and infectious diseases. *Physiol. Rev.* **2009**, *89*, (4), 1105-1152.
37. Jarrett, J. T.; Lansbury, P. T., Seeding one-dimensional crystallization of amyloid - a pathogenic mechanism in Alzheimer's disease and scrapie. *Cell.* **1993**, *73*, (6), 1055-1058.
38. Kupfer, L.; Hinrichs, W.; Groschup, M. H., Prion protein misfolding. *Curr. Mol. Med.* **2009**, *9*, 826-835.
39. Takakura, I.; Miyazawa, K.; Kanaya, T.; Itani, W.; Watanabe, K.; Ohwada, S.; Watanabe, H.; Hondo, T.; Rose, M. T.; Mori, T.; Sakaguchi, S.; Nishida, N.; Katamine, S.; Yamaguchi, T.; Aso, H., Orally administered prion protein is incorporated by m cells and spreads into lymphoid tissues with macrophages in prion protein knockout mice. *Am. J. Pathol.* **2011**, *179*, (3), 1301-1309.
40. Mallucci, G. R.; Ratte, S.; Asante, E. A.; Linehan, J.; Gowland, I.; Jeffreys, J. G. R.; Collinge, J., Post-natal knockout of prion protein alters hippocampal CA1 properties, but does not result in neurodegeneration. *EMBO J.* **2002**, *21*, (3), 202-210.
41. Blattler, T., Transmission of prion disease. *APMIS.* **2002**, *110*, 71-78.

42. Press, C. M.; Heggebo, R.; Espenes, A., Involvement of gut-associated lymphoid tissue of ruminants in the spread of transmissible spongiform encephalopathies. *Adv. Drug. Deliv. Rev.* **2004**, *56*, (6), 885-899.
43. Jeffrey, M.; Gonzalez, L.; Espenes, A.; Press, C. M.; Martin, S.; Chaplin, M.; Davis, L.; Landsverk, T.; MacAldowie, C.; Eaton, S.; McGovern, G., Transportation of prion protein across the intestinal mucosa of scrapie-susceptible and scrapie-resistant sheep. *J. Pathol.* **2006**, *209*, (1), 4-14.
44. Kujala, P.; Raymond, C. R.; Romeijn, M.; Godsave, S. F.; van Kasteren, S. I.; Wille, H.; Prusiner, S. B.; Mabbott, N. A.; Peters, P. J., Prion uptake in the gut: identification of the first uptake and replication sites. *PLoS Pathog.* **2011**, *7*, (12), e1002449.
45. McCulloch, L.; Brown, K. L.; Bradford, B. M.; Hopkins, J.; Bailey, M.; Rajewsky, K.; Manson, J. C.; Mabbott, N. A., Follicular dendritic cell-specific prion protein (PrP) expression alone is sufficient to sustain prion infection in the spleen. *PLoS Pathog.* **2011**, *7*, (12), e1002402.
46. Michel, B.; Meyerett-Reid, C.; Johnson, T.; Ferguson, A.; Wyckoff, C.; Pulford, B.; Bender, H.; Avery, A.; Telling, G.; Dow, S.; Zabel, M. D., Incunabular immunological events in prion trafficking. *Sci. Rep.* **2012**, *2*, 1-12.
47. Krejciova, Z.; De Sousa, P.; Manson, J.; Ironside, J. W.; Head, M. W., Human tonsil-derived follicular dendritic-like cells are refractory to human prion infection in vitro and traffic disease-associated prion protein to lysosomes. *Am. J. Pathol.* **2014**, *184*, (1), 64-70.
48. Sigurdson, C.; Spraker, T. R.; Miller, M. W.; Oesch, B.; Hoover, E. A., PrPCWD in the myenteric plexus, vagosympathetic trunk and endocrine glands of deer with chronic wasting disease. *J. Gen. Virol.* **2001**, *82*, 2327-2334.
49. Spraker, T. R.; Zink, R. R.; Cummins, B. A.; Sigurdson, C.; Miller, M. W.; O'Rourke, K. I., Distribution of protease-resistant prion protein and spongiform encephalopathy in free-ranging mule deer (*Odocoileus hemionus*) with chronic wasting disease. *Vet. Pathol.* **2002**, *39*, 546-556.
50. Silveira, J. R.; Raymond, G. J.; Hughson, A. G.; Race, R. E.; Sim, V. L.; Hayes, S. F.; Caughey, B., The most infectious prion protein particles. *Nature.* **2005**, *437*, (7056), 257-261.
51. Caughey, B.; Baron, G. S.; Chesebro, B.; Jeffrey, M., Getting a grip on prions: oligomers, amyloids, and pathological membrane interactions. *Annu. Rev. Biochem.* **2009**, *78*, 177-204.
52. Moreno-Gonzalez, I.; Soto, C., Misfolded protein aggregates: mechanisms, structures and potential for disease transmission. *Semin. Cell. Dev. Biol.* **2011**, *22*, (5), 482-487.

53. Diaz-Espinoza, R.; Soto, C., High-resolution structure of infectious prion protein: the final frontier. *Nat. Struct. Mol. Biol.* **2012**, *19*, (4), 370-377.
54. Nelson, R.; Sawaya, M. R.; Balbirnie, M.; Madsen, A. O.; Riek, C.; Grothe, R.; Eisenberg, D., Structure of the cross- β spine of amyloid-like fibrils. *Nature*. **2005**, *435*, (7043), 773-778.
55. Büeller, H.; Fischer, M.; Lang, Y.; Bluethmann, H.; Lipp, H.; DeArmond, S. J.; Prusiner, S. B.; Aguet, M.; Weissmann, C., Normal development and behaviour of mice lacking the neuronal cell-surface PrP protein. *Nature*. **1992**, *356*, 577-582.
56. Raeber, A. J.; Race, R. E.; Brandner, S.; Priola, S. A.; Sailer, A.; Bessen, R. A.; Mucke, L.; Manson, J.; Aguzzi, A.; Oldstone, M. B. A.; Weissmann, C.; Chesebro, B., Astrocyte-specific expression of hamster prion protein (PrP) renders PrP knockout mice susceptible to hamster scrapie. *EMBO J.* **1997**, *16*, (20), 6057-6065.
57. Da Costa Dias, B.; Jovanovic, K.; Weiss, S. F. T., Alimentary prion infections. *Prion*. **2014**, *5*, (1), 6-9.
58. Beekes, M.; McBride, P. A., The spread of prions through the body in naturally acquired transmissible spongiform encephalopathies. *FEBS J.* **2007**, *274*, (3), 588-605.
59. Imran, M.; Mahmood, S., An overview of human prion diseases. *Virology*. **2011**, *8*, (559), 1-9.
60. Rhodes, R., *Deadly feasts: the "prion" controversy and the public's health*. Simon and Schuster: 1998.
61. Miller, M. W.; Williams, E. S.; Hobbs, N. T.; Wolfe, L. L., Environmental sources of prion transmission in mule deer. *Emerg. Infect. Dis.* **2004**, *10*, (6), 1003-1006.
62. Seidel, B.; Thomzig, A.; Buschmann, A.; Groschup, M. H.; Peters, R.; Beekes, M.; Tertytze, K., Scrapie agent (strain 263K) can transmit disease via the oral route after persistence in soil over years. *PLoS One*. **2007**, *2*, (5), e435.
63. Haley, N. J.; Seelig, D. M.; Zabel, M. D.; Telling, G. C.; Hoover, E. A., Detection of CWD prions in urine and saliva of deer by transgenic mouse bioassay. *PLoS One*. **2009**, *4*, (3), e4848.
64. Henderson, D. M.; Manca, M.; Haley, N. J.; Denkers, N. D.; Nalls, A. V.; Mathiason, C. K.; Caughey, B.; Hoover, E. A., Rapid antemortem detection of CWD prions in deer saliva. *PLoS One*. **2013**, *8*, (9), e74377.
65. Mathiason, C. K.; Powers, J. G.; Dahmes, S. J.; Osborn, D. A.; Miller, K. V.; Warren, R. J.; Mason, G. L.; Hays, S. A.; Hayes-Klug, J.; Seelig, D. M.; Wild, M. A.; Wolfe, L. L.; Spraker, T. R.; Miller, M. W.; Sigurdson, C. J.; Telling, G. C.; Hoover, E. A., Infectious

- prions in the saliva and blood of deer with chronic wasting disease. *Science*. **2006**, *314*, (5796), 133-136.
66. Safar, J. G.; Lessard, P.; Tamguney, G.; Freyman, Y.; Deering, C.; Letessier, F.; Dearmond, S. J.; Prusiner, S. B., Transmission and detection of prions in feces. *J. Infect. Dis.* **2008**, *198*, (1), 81-89.
 67. Tamgüney, G.; Miller, M. W.; Wolfe, L. L.; Sirochman, T. M.; Glidden, D. V.; Palmer, C.; Lemus, A.; DeArmond, S. J.; Prusiner, S. B., Asymptomatic deer excrete infectious prions in faeces. *Nature* **2009**, *461*, (7263), 529-532.
 68. Gough, K. C.; Maddison, B. C., Prion transmission: prion excretion and occurrence in the environment. *Prion*. **2010**, *4*, (4), 275-282.
 69. Lax, A. J.; Millson, G. C.; Manning, E. J., Involvement of protein in scrapie agent infectivity. *Res. Vet. Sci.* **1983**, *34*, (2), 155-158.
 70. Tamgüney, G.; Miller, M. W.; Wolfe, L. L.; Sirochman, T. M.; Glidden, D. V.; Palmer, C.; Lemus, A.; DeArmond, S. J.; Prusiner, S. B., Asymptomatic deer excrete infectious prions in faeces. *Nature*. **2010**, *466*, (7306), 652-652.
 71. Race, R.; Jenny, A.; Sutton, D., Scrapie infectivity and proteinase K-resistant prion protein in sheep placenta, brain, spleen, and lymph node: implications for transmission and antemortem diagnosis. *J. Infect. Dis.* **1998**, *178*, 949-953.
 72. Jacobson, K. H.; Lee, S.; McKenzie, D.; Benson, C. H.; Pedersen, J. A., Transport of the pathogenic prion protein through landfill materials. *Environ. Sci. Technol.* **2009**, *43*, (6), 2022-2028.
 73. Jacobson, K. H.; Lee, S.; Somerville, R. A.; McKenzie, D.; Benson, C. H.; Pedersen, J. A., Transport of the pathogenic prion protein through soils. *J. Environ. Qual.* **2010**, *39*, (4), 1145-1152.
 74. Hinckley, G. T.; Johnson, C. J.; Jacobson, K. H.; Bartholomay, C.; McMahon, K. D.; McKenzie, D.; Aiken, J. M.; Pedersen, J. A., Persistence of pathogenic prion protein during simulated wastewater treatment processes. *Environ. Sci. Technol.* **2008**, *42*, 5254-5259.
 75. Gale, P.; Standfield, G., Towards a quantitative risk assessment for BSE in sewage sludge. *J. Appl. Microbiol.* **2001**, *91*, 563-569.
 76. Pedersen, J. A.; McMahon, K. D.; Benson, C. H., Prions: novel pathogens of environmental concern? *J. Environ. Eng.* **2006**, *132*, (9), 967-969.
 77. Fox, K. A.; Jewell, J. E.; Williams, E. S.; Miller, M. W., Patterns of PrPCWD accumulation during the course of chronic wasting disease infection in orally inoculated mule deer (*Odocoileus hemionus*). *J. Gen. Virol.* **2006**, *87*, (Pt 11), 3451-3461.

78. Georgsson, G.; Sigurdarson, S.; Brown, P., Infectious agent of sheep scrapie may persist in the environment for at least 16 years. *J. Gen. Virol.* **2006**, *87*, (Pt 12), 3737-3740.
79. Greig, J. R., Scrapie: Observations on the transmission of the disease by mediate contact. *Vet. J.* **1940**, *96*, 203-206.
80. Dexter, G.; Tongue, S. C.; Heasman, L.; Bellworthy, S. J.; Davis, A.; Moore, S. J.; Simmons, M. M.; Sayers, A. R.; Simmons, H. A.; Matthews, D., The evaluation of exposure risks for natural transmission of scrapie within an infected flock. *BMC Vet. Res.* **2009**, *5*, 38.
81. Mathiason, C. K.; Hays, S. A.; Powers, J.; Hayes-Klug, J.; Langenberg, J.; Dahmes, S. J.; Osborn, D. A.; Miller, K. V.; Warren, R. J.; Mason, G. L.; Hoover, E. A., Infectious prions in pre-clinical deer and transmission of chronic wasting disease solely by environmental exposure. *PLoS One.* **2009**, *4*, (6), e5916.
82. Miller, M. W.; Williams, E. S., Horizontal prion transmission in mule deer. *Nature.* **2003**, *425*, 35-36.
83. Tamguney, G.; Richt, J. A.; Hamir, A. N.; Greenlee, J. J.; Miller, M. W.; Wolfe, L. L.; Sirochman, T. M.; Young, A. J.; Glidden, D. V.; Johnson, N. L.; Giles, K.; DeArmond, S. J.; Prusiner, S. B., Salivary prions in sheep and deer. *Prion.* **2012**, *6*, (1), 52-61.
84. Schramm, P. T.; Johnson, C. J.; Mathews, N. E.; McKenzie, D.; Aiken, J. M., Potential role of soil in the transmission of prion disease. *Rev. Mineral. Geochem.* **2006**, *64*, 135-152.
85. Johnson, C. J.; Pedersen, J. A.; Chappell, R. J.; McKenzie, D.; Aiken, J. M., Oral transmissibility of prion disease is enhanced by binding to soil particles. *PLoS Pathog.* **2007**, *3*, (7), e93.
86. Johnson, C. J.; Phillips, K. E.; Schramm, P. T.; McKenzie, D.; Aiken, J. M.; Pedersen, J. A., Prions adhere to soil minerals and remain infectious. *PLoS Pathog.* **2006**, *2*, (4), e32.
87. Alldredge, A. W.; Arthur, W. J., Soil ingestion by mule deer in northcentral Colorado. *J. Range. Manage.* **1979**, *32*, 67-71.
88. Walter, D. W.; Walsh, D. P.; Farnsworth, M. L.; Winkelman, D. L.; Miller, M. W., Soil clay content underlies prion infection odds. *Nat. Commun.* **2011**, *2*, 200.
89. Almberg, E. S.; Cross, P. C.; Johnson, C. J.; Heisey, D. M.; Richards, B. J., Modeling routes of chronic wasting disease transmission: environmental prion persistence promotes deer population decline and extinction. *PLoS One.* **2011**, *6*, (5), e19896.
90. Booth, C. J.; Johnson, C. J.; Pedersen, J. A., Microbial and enzymatic inactivation of prions in soil environments. *Soil. Biol. Biochem.* **2013**, *59*, 1-15.

91. Booth, C. J., Novel chemical and biological routes of prion degradation in soil. *PhD Thesis, University of Wisconsin-Madison* **2014**.
92. Russo, F.; Johnson, C. J.; Johnson, C. J.; McKenzie, D.; Aiken, J. M.; Pedersen, J. A., Pathogenic prion protein is degraded by a manganese oxide mineral found in soils. *J. Gen. Virol.* **2009**, *90*, (Pt 1), 275-280.
93. Smith, C. B.; Booth, C. J.; Wadzinski, T. J.; Legname, G.; Chappell, R.; Johnson, C. J.; Pedersen, J. A., Humic substances interfere with detection of pathogenic prion protein. *Soil. Biol. Biochem.* **2014**, *68*, 309-316.
94. Saa, P.; Castilla, J.; Soto, C., Ultra-efficient replication of infectious prions by automated protein misfolding cyclic amplification. *J. Biol. Chem.* **2006**, *281*, (46), 35245-25252.
95. Reed, L. J.; Muench, H., A simple method of estimating fifty per cent endpoints. *Am. J. Epidemiol.* **1938**, *27*, (3), 493-497.
96. Prusiner, S. B.; Cochran, S. P.; Groth, D. F.; Downey, D. E.; Bowman, K. A.; Martinez, H. M., Measurement of the Scrapie agent using an incubation time interval assay. *Ann. Neurology.* **1982**, *11*, 353-358.
97. Hibler, C. P.; Wilson, K. L.; Spraker, T. R.; Miller, M. W.; Zink, R. R.; DeBuse, L. L.; Andersen, E.; Schweitzer, D.; Kennedy, J. A.; Baeten, L. A.; Smeltzer, J. F.; Salman, M. D.; Powers, B. E., Field validation and assessment of an enzyme-linked immunosorbent assay for detecting chronic wasting disease in mule deer (*Odocoileus hemionus*), white-tailed deer (*Odocoileus virginianus*), and Rocky Mountain elk (*Cervus elaphus nelsoni*). *J. Vet. Diagn. Invest.* **2003**, *15*, 311-319.
98. Spraker, T. R.; O'Rourke, K. I.; Balachandran, A.; Zink, R. R.; Cummins, B. A.; Miller, M. W.; Powers, B. E., Validation of monoclonal antibody F99/97.6.1 for immunohistochemical staining of brain and tonsil in mule deer (*Odocoileus hemionus*) with chronic wasting disease. *J. Vet. Diagn. Invest.* **2002**, *14*, 3-7.
99. Gonzalez-Montalban, N.; Makarava, N.; Ostapchenko, V. G.; Savtchenk, R.; Alexeeva, I.; Rohwer, R. G.; Baskakov, I. V., Highly efficient protein misfolding cyclic amplification. *PLoS Pathog.* **2011**, *7*, (2), e1001277.
100. Johnson, C. J.; Aiken, J. M.; McKenzie, D.; Samuel, M. D.; Pedersen, J. A., Highly efficient amplification of chronic wasting disease agent by protein misfolding cyclic amplification with beads (PMCAb). *PLoS One.* **2012**, *7*, (4), e35383.
101. Taylor, D. M.; Diprose, M. F., The response of the 22A strain of scrapie agent to microwave irradiation compared with boiling. *Neuropathol. Appl. Neurobiol.* **1996**, *22*, (3), 256-258.

102. Gibbs Jr, C. J.; Gajdusek, C. D.; Latarjet, R., Unusual resistance to ionizing radiation of the viruses of kuru, Creutzfeldt-Jakob disease, and scrapie. *Proc. Natl. Acad. Sci. U S A.* **1978**, *75*, (12), 6268-6270.
103. Bellinger-Kawahara, C.; Cleaver, J. E.; Diener, T. O.; Prusiner, S. B., Purified scrapie prions resist inactivation by UV irradiation. *J. Virol.* **1987**, *61*, (1), 159-166.
104. Brown, P.; Liberski, P. P.; Wolff, A.; Gadjusek, D. C., Resistance of scrapie infectivity to steam autoclaving after formaldehyde fixation and limited survival after ashing at 360°C: practical and theoretical implications. *J. Infect. Dis.* **1990**, *161*, (3), 467-472.
105. Brown, P.; Rohwer, R. G.; Green, E. M.; Gadjusek, D. C., Effect of chemicals, heat, and histopathologic processing on high-infectivity hamster-adapted scrapie virus. *J. Infect. Dis.* **1982**, *145*, (5), 683-687.
106. Prusiner, S. B.; Groth, D.; Serban, A.; Stahl, N.; Gabizon, R., Attempts to restore scrapie prion infectivity after exposure to protein denaturants. *Proc. Natl. Acad. Sci. U S A.* **1993**, *90*, 2793-2797.
107. Brown, P.; Rau, E. H.; Lemieux, P.; Johnson, B. K.; Bacote, A. E.; Gajdusek, D. C., Infectivity studies of both ash and air emissions from simulated incineration of scrapie-contaminated tissues. *Environ Sci Technol* **2004**, *38*, (22), 6155-6160.
108. Race, R. E.; Raymond, G. J., Inactivation of Transmissible Spongiform Encephalopathy (Prion) Agents by Environ LpH. *J. Virol.* **2004**, *78*, (4), 2164-2165.
109. Kimberlin, R. H.; Walker, C. A.; Millson, G. C.; Taylor, D. M.; Robertson, P. A.; Tomlinson, A. H.; Dickinson, A. G., Disinfection studies with two strains of mouse-passaged scrapie agent. Guidelines for Creutzfeldt-Jakob and related agents. *J. Neurol. Sci.* **1983**, *59*, (3), 355-369.
110. Peretz, D.; Supattapone, S.; Giles, K.; Vergara, J.; Freyman, Y.; Lessard, P.; Safar, J. G.; Glidden, D. V.; McCulloch, C.; Nguyen, H. O.; Scott, M.; Dearmond, S. J.; Prusiner, S. B., Inactivation of prions by acidic sodium dodecyl sulfate. *J. Virol.* **2006**, *80*, (1), 322-331.
111. Fraise, A. P.; Maillard, J.-Y.; Sattar, S., *Russell, Hugo and Ayliffe's principles and practice of disinfection, preservation and sterilization*. 5th ed.; Wiley-Blackwell: Oxford, 2012.
112. Huang, H.; Spencer, J. L.; Soutyrine, A.; Guan, J.; Rendulich, J.; Balachandran, A., Evidence for degradation of abnormal prion protein in tissues from sheep with scrapie during composting. *Can. J. Vet. Res.* **2007**, *71*, 34-40.
113. Huang, H.; Spencer, J. L.; Guan, J., In Vitro Microbial Degradation of Abnormal Prions in Central Nervous System from Scrapie Affected Sheep. *Open Vet. J.* **2010**, *4*, (1), 20-26.
114. Xu, S.; Reuter, T.; Gilroyed, B. H.; Mitchell, G. B.; Price, L. M.; Dudas, S.; Braithwaite, S. L.; Graham, C.; Czub, S.; Leonard, J. J.; Balachandran, A.; Neumann, N. F.; Belosevic, M.;

- McAllister, T. A., Biodegradation of prions in compost. *Environ. Sci. Technol.* **2014**, *48*, (12), 6909-6918.
115. Muller-Hellwig, S.; Groschup, M. H.; Pichner, R.; Gareis, M.; Martlbauer, E.; Scherer, S.; Loessner, M. J., Biochemical evidence for the proteolytic degradation of infectious prion protein PrP^{Sc} in hamster brain homogenates by foodborne bacteria. *Syst. Appl. Microbiol.* **2006**, *29*, (2), 165-171.
116. Johnson, C. J.; Bennett, J. P.; Biro, S. M.; Duque-Velasquez, J. C.; Rodriguez, C. M.; Bessen, R. A.; Rocke, T. E., Degradation of the disease-associated prion protein by a serine protease from lichens. *PLoS One*. **2011**, *6*, (5), e19836.
117. Saunders, S. E.; Bartz, J. C.; Vercauteren, K. C.; Bartelt-Hunt, S. L., Enzymatic digestion of chronic wasting disease prions bound to soil. *Environ. Sci. Technol.* **2009**, *44*, 4129-4135.
118. Miyazawa, K.; Emmerling, K.; Manuelidis, L., High CJD infectivity remains after prion protein is destroyed. *J. Cell. Biochem.* **2011**, *112*, (12), 3630-3637.

1.12 Figures

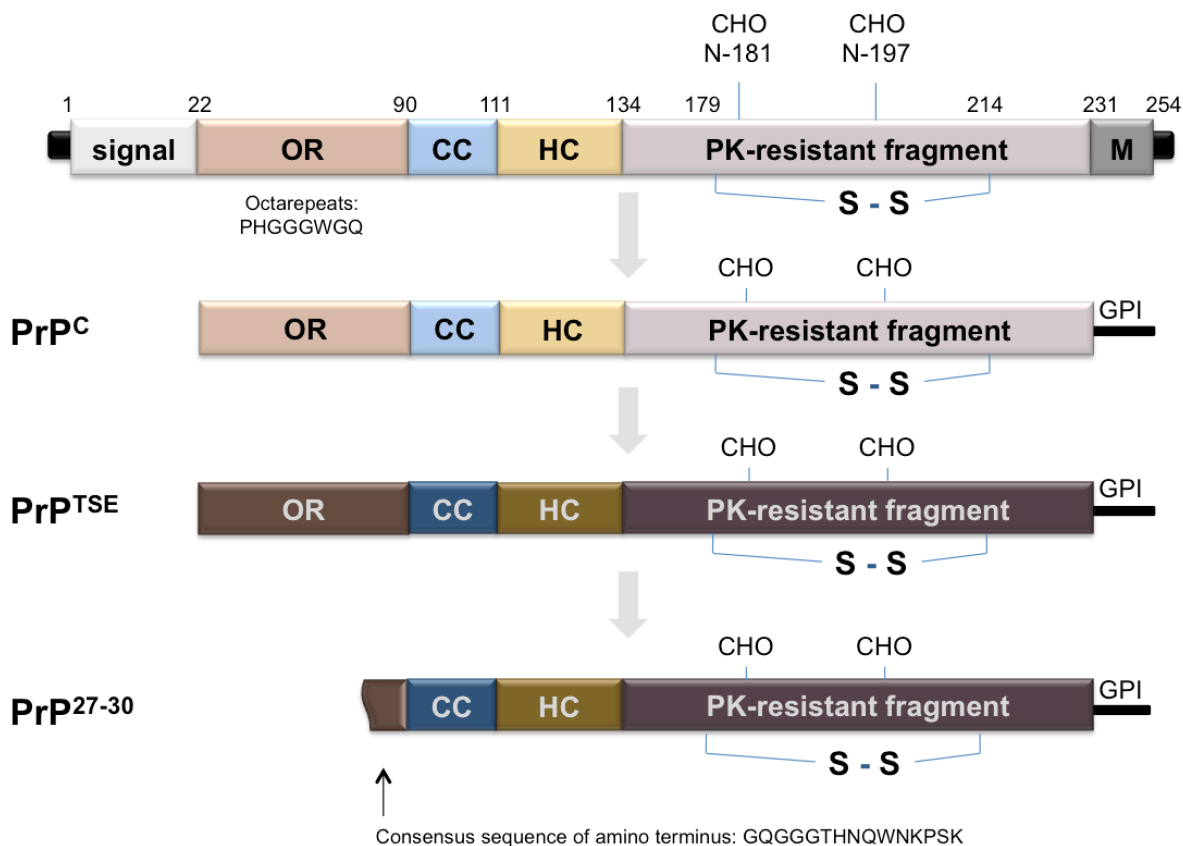


Figure 1. Structural regions of the prion protein. Compiled functional regions from studies of mouse, human, hamster, and sheep prions. Abbreviations: OR, octapeptide repeats; CC, conserved core; HC, conserved hydrophobic core; PK, proteinase K; GPI, glycosylphosphatidylinositol; S, serine.

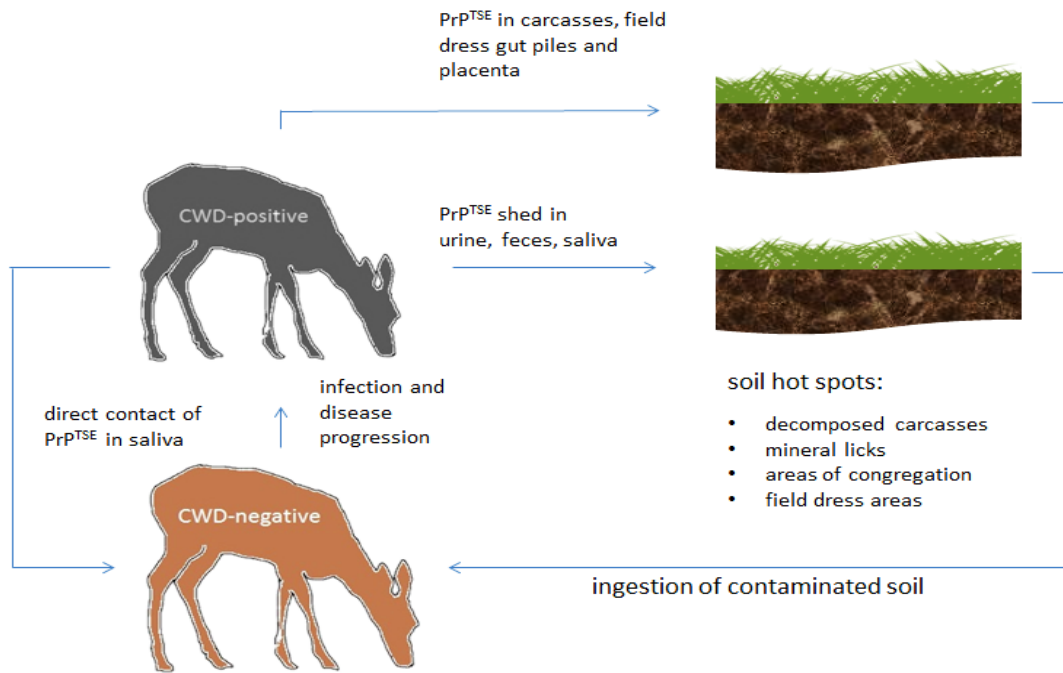
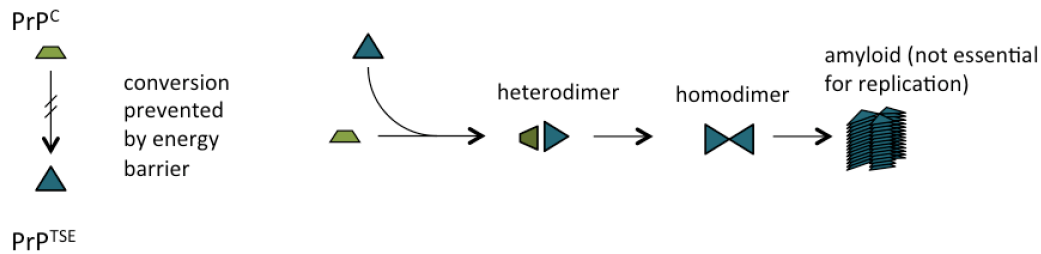


Figure 2. Representation of PrP^{TSE} transmission in the environment.

template directed refolding



seeded nucleation

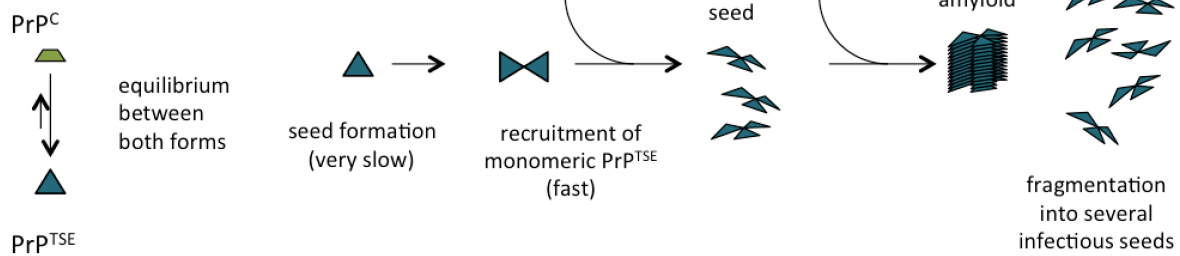


Figure 3. Two potential models of PrP conversion. In template directed misfolding, PrP^{TSE} induces the conformational transition of PrP^{C} through a cycle of unfolding and refolding reactions. During the reaction, the two conformations form a heterodimer at an intermediate stage and the resulting two PrP^{TSE} molecules dissociate and restart the reaction. In the seeded nucleation model of PrP^{C} to PrP^{TSE} conversion, PrP^{TSE} acts as a seed and becomes a template for the refolding of PrP^{C} into the growing polymer, and conversion may occur with polyanions acting as catalysts.

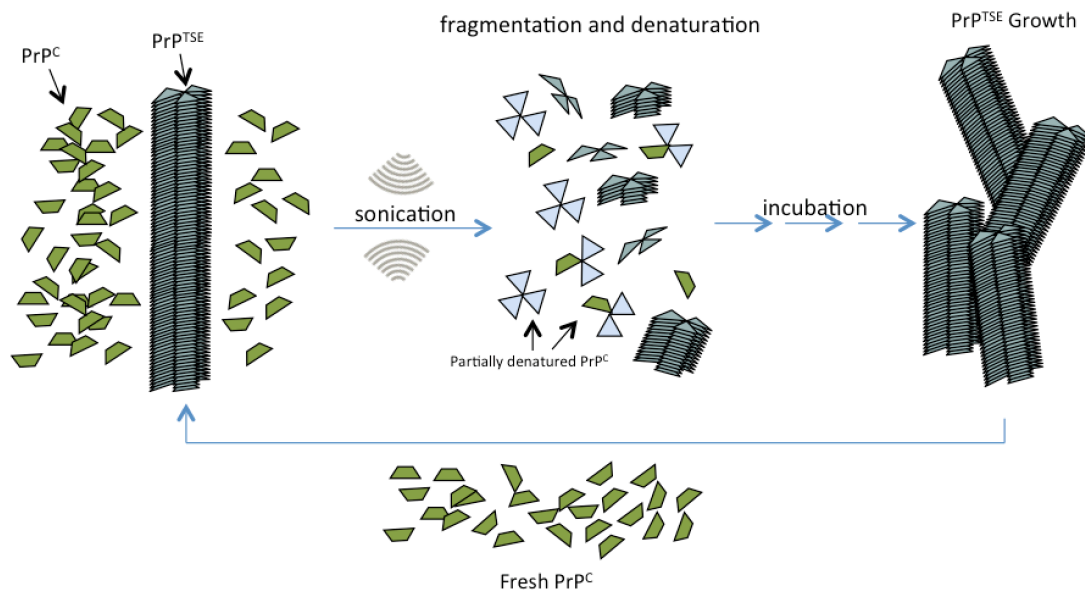


Figure 4. Protein Misfolding Cyclic Amplification. A sample containing pathogenic prions (PrP^{TSE}) is placed in an excess of normal prion protein (PrP^{C}) and subjected to successive rounds of incubation of sonication until sufficient pathogenic prion protein has been formed to allow detection by immunoblotting.

Chapter 2

Peroxymonosulfate Rapidly Inactivates the Disease-associated Prion Protein*

*A version of this chapter will be submitted to *Environmental Science & Technology* with Booth, C.J., Lietz, C.B., Li, L., and Pedersen, J.A. as co-authors.

*Chris Lietz conducted the LC MS/MS analysis

2.1 ABSTRACT.

Prions, the etiological agents in transmissible spongiform encephalopathies, exhibit remarkable resistance to most methods of inactivation that are effective against conventional pathogens. Prions are composed of pathogenic conformers of the prion protein (PrP^{TSE}). Some prion diseases are transmitted, in part, through environmental routes. The recalcitrance of prions to inactivation may lead to a persistent reservoir of infectivity that contributes to the environmental maintenance of epizootics. At present, few methods exist to remediate prion-contaminated lands. Here we examined the ability of peroxymonosulfate to degrade PrP^{TSE} as an initial step toward developing an *in situ* chemical oxidation process to inactivate prions. We find that peroxymonosulfate rapidly degrades PrP^{TSE} from two species. Transition metal-catalyzed decomposition of peroxymonosulfate to produce sulfate radicals appears to enhance degradation. We further demonstrate that exposure to peroxymonosulfate significantly reduced PrP^{C} -to- PrP^{TSE} converting ability as measured by protein misfolding cyclic amplification, used as a proxy for infectivity. Liquid chromatography-tandem mass spectrometry revealed that exposure to peroxymonosulfate results in oxidative modifications to methionine and tryptophan residues. This study indicates that peroxymonosulfate may hold promise for *in situ* remediation of prion-contaminated surfaces.

2.2 INTRODUCTION

Prions are the etiological agents of transmissible spongiform encephalopathies (TSEs) or prion diseases.^{1,2} Prion diseases are a group of fatal, neurodegenerative disorders affecting a number of mammalian species including humans (kuru, Creutzfeldt-Jakob disease), sheep and goats (scrapie), cattle (bovine spongiform encephalopathy; “mad cow” disease), and North American members of the deer family (chronic wasting disease; CWD). Prions appear to be composed primarily, if not solely of misfolded conformers (PrP^{TSE}) of the host-encoded cellular prion protein (PrP^{C}).^{1,2} The central molecular event in prion diseases is the conformational conversion of PrP^{C} into PrP^{TSE} ,^{1,3} which induces profound changes in the biophysical properties of the protein. Whereas PrP^{C} is primarily α -helical, detergent soluble and labile with respect to proteolysis, PrP^{TSE} exhibits high β -sheet content, is largely insoluble in water and most detergents, and displays remarkable resistance to a variety of chemical and physical inactivation methods.⁴⁻⁷ Treatments that are effective for inactivating conventional microbial pathogens (e.g., boiling, ultraviolet irradiation, ethanol, formalin, conventional autoclaving) do not eliminate prion infectivity.⁸ Sterilization procedures recommended by the World Health Organization include > 1 h exposure to 1 N sodium hydroxide or 2% sodium hypochlorite, or autoclaving in 1 N sodium hydroxide at 121 °C for 30 min.⁸

Chronic wasting disease of North American members of the deer family (cervids) and scrapie in sheep and goats are spread in part via environmental reservoirs of prion infectivity.⁹ Past studies indicate that indirect transmission via environmental routes may play an important role in the long-term dynamics of CWD in North America.¹⁰ Infected animals shed prions in feces, urine, and saliva.¹¹⁻¹⁵ Prion infectivity can persist in the environment for years.^{13,16-18} The persistence of prions in the environment is attributed to the intrinsic stability of PrP^{TSE} fibrils and

may be enhanced by association with soil constituents,¹⁹⁻²¹ one explanation invoked for the preservation of intrinsically labile organic matter.^{22,23}

Remediation of prion-contaminated lands poses a challenge; decontamination methods that have been demonstrated to be effective in inactivating prions are difficult to apply in the environment.²⁴ Several oxidants used for *in situ* chemical oxidation of recalcitrant organic contaminants²⁵⁻²⁹ have been investigated for their ability to degrade PrP^{TSE} including hydrogen peroxide,³⁰ ozone,³¹⁻³³ permanganate,³⁴⁻³⁶ and the Fenton reagent.³⁷⁻³⁹ Table 1 provides a summary of selected studies that have demonstrated the ability of oxidants to inactivate prions. Most oxidants investigated to date are either insufficiently effective against prions (e.g., H₂O₂, permanganate) or possess features that may limit their utility for application to soils (e.g., the gaseous nature of O₃, low pH needed for optimal application of Fenton reagent). Peroxymonosulfate (HSO₅⁻) has been investigated for *in situ* chemical oxidation,⁴⁰⁻⁴³ but has not previously been investigated for its ability to inactivate prions. Peroxymonosulfate is a monosubstituted derivative of H₂O₂ that is less prone to spontaneous decomposition in water than hydrogen peroxide and is frequently more reactive than H₂O₂ kinetically despite having only a slightly higher standard reduction potential (E_H^0 (HSO₅⁻/HSO₄⁻) = +1.82 V vs. E_H^0 (H₂O₂/H₂O) = +1.776 V).⁴⁴⁻⁴⁶ Peroxymonosulfate is reactive over a broad pH range, but its stability declines as pK_{a,2} is approached (9.9 at 20 °C).^{47,48} Peroxymonosulfate can oxidize organic moieties including acetals to alcohols,⁴⁹ alkenes to ketones,⁵⁰ sulfides to sulfones,⁵¹ and phosphines to phosphine oxides.⁵²

Peroxymonosulfate can be activated thermally,⁴⁵ radiolytically,⁵³ photolytically ($\lambda < 419$ nm),⁵⁴ and in the presence of transition metals to produce sulfate radical (SO₄^{•-}).^{41,55-57} Much previous work with peroxymonosulfate used Co(II) to catalytically decompose

peroxymonosulfate to $\text{SO}_4^{\cdot-}$.^{40-43,54,57,58} The estimated standard reduction potential of $\text{SO}_4^{\cdot-}$, $E_H^0(\text{SO}_4^{\cdot-}/\text{SO}_4^{2-})$, is 2.5 to 3.1 V,⁵⁹ similar to or higher than that for hydroxyl radical ($\cdot\text{OH}$; $E_H^0(\cdot\text{OH}/\text{H}_2\text{O}) = 2.59$ or 2.7 V).⁶⁰ The reduction potential for sulfate radical does not vary with pH for proton activities typical of the environment while that for hydroxyl radical does, making the formal potential of $\text{SO}_4^{\cdot-}$ larger than that of $\cdot\text{OH}$ at $\text{pH} > 3.4$ (assuming $E_H^0(\text{SO}_4^{\cdot-}/\text{SO}_4^{2-})$ and $E_H^0(\cdot\text{OH}/\text{H}_2\text{O})$ are 2.5 V and 2.7 V, respectively; all activities unity other than that for protons). Cobalt-activated peroxymonosulfate has been employed to treat diesel-contaminated soil,⁴⁰ polychlorinated biphenyls,⁶¹ atrazine,⁵⁴ and landfill leachates.⁶² Activated peroxymonosulfate can degrade peptidic cyanobacterial toxins⁶³ and some amino acids.⁶⁴ The ability of (activated) peroxymonosulfate to inactivate prions has not been previously reported.

The objectives of this study were to determine the extent to which peroxymonosulfate degrades and inactivates pathogenic prion protein unaided, and when activated by cobalt. To achieve these objectives we used immunoblotting to investigate degradation of PrP^{TSE} from white-tailed deer (*Odocoileus virginianus*; CWD agent) and golden hamsters (*Mesocricetus auratus*; HY agent) by (Co(II)-activated) peroxymonosulfate as a function of time and peroxymonosulfate concentration. We used protein misfolding cyclic amplification (PMCA) to examine (activated) peroxymonosulfate-induced reductions in the PrP^{C} -to- PrP^{TSE} converting ability of prions as a proxy for infectivity. We investigated modifications to the primary structure of PrP^{TSE} due to exposure to (activated) peroxymonosulfate by liquid chromatography-tandem mass spectrometry (LC-MS/MS).

2.3 EXPERIMENTAL

2.3.1 Prion protein sources. Hamster-adapted transmissible mink encephalopathy agent (HY strain) and cervid (CWD) agent were obtained from brain tissue of experimentally inoculated Syrian golden hamsters and an experimentally inoculated white-tailed deer,⁶⁵ respectively. Animals were cared for in accordance with protocols approved by the Institutional Animal Care and Use Committee of the University of Wisconsin – Madison (Assurance Number 3464-01). Brain tissue was homogenized in 1× Dulbecco’s phosphate buffered saline (DPBS; 137 mM NaCl, 8.1 mM NaHPO₄²⁻, 1.47 mM H₂PO₄; pH 7), and the resultant 10% (w/v) brain homogenate (BH) was stored at –80 °C until use. When elimination of PrP^C was needed, BH was treated with 50 µg·mL⁻¹ PK (final concentration) for 1 h at 37 °C. Proteinase K activity was halted by addition of PMSF to a final concentration of 4 mM. Some experiments were conducted with purified HY PrP^{TSE}, wherein the P4 pellet was isolated from eight hamster brains following the procedure of Bolton et al.³ as modified by McKenzie et al.⁶⁶ The P4 pellet was resuspended in 1× DPBS, pH 7.4. Total protein concentration in the purified preparation was measured using a BCA protein assay (Pierce), and PrP^{TSE} concentrations were estimated to be > 90% of total protein.²⁰ Purified, full-length (23-230) recombinant murine PrP (residues 23-231, lacking a His-tag) in the α-helix-rich conformation (α-mo-recPrP) was acquired from Prionatis AG (RPA0101, Alpnach Dorf, Switzerland).

2.3.2 Reaction of peroxymonosulfate with prions. Pathogenic prion protein, either in the form of purified preparation (HY strain) or 10% BH (HY or CWD strains) was mixed with solutions of peroxymonosulfate and/or CoCl₂ under the conditions indicated in the Results and Discussion. All concentrations presented for peroxymonosulfate, CoCl₂, and

quenching agents reflect final concentrations. The molar ratio of peroxymonosulfate to CoCl_2 was 125:3 unless otherwise specified. All experiments were conducted at room temperature ($\sim 25^\circ\text{C}$) in polypropylene microcentrifuge tubes in the dark. Some experiments employed α -mo-recPrP. Reactions with peroxymonosulfate and/or CoCl_2 were halted by addition of an equal volume of 0.5 M sodium thiosulfate (unless otherwise specified). In some cases, samples were pre-treated with sodium thiosulfate to prevent oxidation by peroxymonosulfate and radical species. All experiments were conducted in triplicate unless otherwise specified. Final solution pH of peroxymonosulfate was stable at approximately 1.5. For experiments with α -mo-recPrP pH was controlled by preparing peroxymonosulfate solutions in 100 mM phosphate and brought to the desired pH with 0.1 M NaOH or 0.1 M H_2SO_4 .

2.3.3 Immunoblot detection of PrP^{TSE}. Following treatment, PrP^{TSE} samples were prepared for SDS-PAGE as previously described.⁶⁷ Briefly, a 20 μL aliquot was removed from the reaction vessel and mixed with 10 μL of 10 \times SDS sample buffer (100 mM Tris; pH 8, 10% SDS, 7.5 mM EDTA, 100 mM dithiothreitol, 30% glycerol). Samples were then heated at 100°C for 10 min and fractionated on 12% bis-tris polyacrylamide gels (Invitrogen). Proteins were electrotransferred from the gel to a 0.45 μm polyvinyl difluoride membrane (Millipore). Membranes were blocked with 5% nonfat dry milk (prepared in 1 \times Tris-buffered saline containing 0.1% Tween 20) overnight at 4°C . Membrane-bound hamster PrP was probed with monoclonal antibody 3F4 (Covance, 1:40,000 dilution; epitope: 109-112) or SAF83 (Cayman Chemical, 1:200, epitope: 126-164). Cervid PrP and murine recPrP were probed with monoclonal antibodies 8G8 (Cayman Chemical, 1:1000, epitope: 97-102) and Bar224 (Cayman Chemical, 1:10000, epitope: 141-151). Primary antibodies were detected with horseradish peroxidase-conjugated goat-anti-mouse immunoglobulin G (BioRad, 1:10,000 dilution) and

Super Signal West Pico chemiluminescent substrate (Pierce Biotechnology). Densitometric analysis of immunoblot bands was conducted using Image J Software.

2.3.4 Protein misfolding cyclic amplification. Bead-assisted protein misfolding cyclic amplification (PMCA) was conducted following the methods of Johnson et al.,⁶⁸ adapted to a microplate format⁶⁹ and designated mbPMCA. Detection of CWD prions was achieved using PrP^C in normal brain homogenate from uninfected transgenic mice hemizygous for the cervid prion gene (Tg(CerPrP)1535[±] mice)⁷⁰ as substrate for the PMCA reaction. Mice were euthanized by CO₂ asphyxiation and immediately perfused with 1× modified DPBS without Ca²⁺ or Mg²⁺ (Thermo Scientific, amended with 5 mM EDTA). Brains were rapidly removed, flash frozen in liquid nitrogen, and stored at −80 °C until use. Brain tissue was homogenized on ice to 10% (w/v) in PMCA conversion buffer (Ca²⁺- and Mg²⁺-free DPBS supplemented with 150 mM NaCl, 1% Triton X-100, 0.05% saponin (Mallinckrodt), 5 mM EDTA, and 1 tablet Roche Complete EDTA-free protease inhibitors cocktail (Fisher) per 50 mL conversion buffer). Brain homogenates were clarified by centrifugation (2 min, 2,000g). Supernatant was transferred to pre-chilled microcentrifuge tubes, flash frozen in liquid nitrogen, and stored at −80 °C until use.

Seeds for mbPMCA were prepared from CWD-positive white-tailed deer brain tissue by serially diluting 10% BH (made up in DPBS) five-fold in normal brain homogenate (NBH) to generate a dilution series. Sample dilutions were used to seed 36 µL NBH (4 µL seed) in 96-well PCR microplate (Axygen, Union City, CA, USA) with one 2.38 mm Teflon[®] bead (McMaster-Carr, #9660K12). Experimental plates were placed in a rack in a Misonix S-4000 microplate horn, and the reservoir was filled with ultrapure water. Each round of mbPMCA consisted of 96 cycles (30 s sonication at 40-60% of maximum power, 1770 s incubation at 37 °C). At the completion of 96 cycles, new NBH was reseeded with 4 µL of the reaction product for serial

mbPMCA. After completing the last round of mbPMCA, 20 μL of each sample was PK digested (50 $\mu\text{g}\cdot\text{mL}^{-1}$, 1 h, 37 $^{\circ}\text{C}$) and analyzed by SDS-PAGE with immunoblot detection (*vide supra*).

2.3.5 Liquid chromatography-tandem mass spectrometry. To prepare samples for LC-MS/MS analysis, we exposed ~ 2.4 μg of HY PrP^{TSE} (PK-treated purified preparation) with 9.6 mM peroxymonosulfate in the absence or presence of 230 μM CoCl_2 for 15 or 60 min. At the end of the exposure, samples were quenched with an equal volume of 0.5 M sodium thiosulfate, and the total sample volume (~ 26 μL) was dried down using a SpeedVacTM (Thermo Scientific). To achieve high sequence coverage in LC-MS/MS analysis, samples were digested with multiple proteases: samples were digested by a combination of endoprotease Lys-C and trypsin (which cleaves C-terminal to lysine and arginine), or by chymotrypsin (which cleaves C-terminal to tryptophan, tyrosine, phenylalanine, and leucine) as detailed in the SI. Dry pellets were resuspended in 20 μL of 8 M urea (in 50 mM Tris-HCl, pH 8) and sonicated for 30 s. Cysteine residues were reduced and alkylated as outlined in the SI.

Peptides were extracted and desalted using 100 μL reversed-phase C18 Omix SPE pipette tips (Agilent Technologies) following manufacturer recommendations and dried down using a SpeedVac (Thermo Scientific). The sample was then resuspended in 0.1% formic acid (prepared in LCMS grade water). The peptide fragments were analyzed on a nanoAcquity UPLC (Waters Corp.) with an integrated nano-electrospray ionization (nESI) emitter. Upon elution from the column, sample was electrosprayed into the nESI source of an Orbitrap Elite mass spectrometer (Thermo Fisher). The selected ions were isolated and fragmented individually, and each fragmentation spectrum was recorded. Samples were prepared in two technical replicates and analyzed in duplicate by LC-MS/MS. Details on the method and subsequent data analysis are described in the SI.

2.4 RESULTS AND DISCUSSION

2.4.1 Peroxymonosulfate rapidly degrades pathogenic prion protein. Prion strains exhibit different susceptibilities to inactivation methods.^{71,72} We therefore examined the ability of peroxymonosulfate to degrade PrP^{TSE} from two prion strains: laboratory model strain HY and an environmentally relevant CWD strain. We exposed 10% HY brain homogenate, purified HY preparation or 10% CWD brain homogenate to 125 mM peroxymonosulfate for 60 min. Peroxymonosulfate reactions were quenched with up to 1 M Na₂S₂O₃. (This concentration of Na₂S₂O₃ did not affect detection of PrP^{TSE} by immunoblotting; Figure S1.) Densitometry values from the resulting immunoblots are presented in Figure 1A (inset) relative to the control (PrP^{TSE} in ultrapure water). Following a 1-h treatment with peroxymonosulfate, immunoreactivity of all forms of PrP^{TSE} was reduced to $\leq 13\%$ of control (i.e., $13 \pm 1\%$, $8 \pm 3\%$, and $8 \pm 2\%$ of control immunoblot intensity for HY BH, HY prep, and CWD BH, respectively). The reproducibility of PrP^{TSE} immunoblots was consistent with that of general protein immunoblotting, in which errors associated with quantitative comparisons are often $\geq 10\%$.⁷³ The results described here for HY were obtained using monoclonal antibodies (mAbs) 3F4 and SAF83 (SI), which bind to non-overlapping residues 109-112 and 126-164 respectively in hamster PrP; immunoblots for CWD were probed with mAbs 8G8 and Bar224, which are directed against residues 97-102 and 141-151, respectively, of deer PrP (epitopes are mapped onto a molecular model for PrP^{TSE} in Figure S2).⁷⁴ The results in Figure 1A (inset) indicate that HSO₅⁻ either induced alteration of at least two separate antibody epitopes in PrP (fragments) from each species or fragmented the protein so extensively that the fragments were not retained on the gel (i.e., fragment molecular mass $\lesssim 10$ kDa) or both. All epitopes probed contain easily oxidizable amino acid residues (i.e., histidine (H), tryptophan (W), and tyrosine (Y), and

methionine (M).⁷⁵ The cervid and hamster prion proteins both contain 42 easily oxidizable residues spaced approximately evenly throughout the protein (Figure S3), leading to the expectation of oxidation of residues throughout the protein. These results demonstrate that peroxymonosulfate is able to degrade pathogenic prion protein from two different prion strains (HY and CWD) and furthermore, that this degradation can occur even in the presence of a large excess of other biomolecules (e.g., other proteins, nucleic acids, lipids, glycans in brain homogenate).⁷⁶⁻⁷⁸

We investigated the concentration-dependence of PrP^{TSE} degradation by peroxymonosulfate by incubating PrP^{TSE} (10% CWD brain homogenate) with a range of peroxymonosulfate concentrations for 30 min at a constant ratio of 125:3. Immunoblot band intensity for CWD PrP^{TSE} was significantly reduced at peroxymonosulfate concentrations ≥ 25 mM ($p < 0.0001$) (Figure 1A). These data suggest that substantial PrP^{TSE} degradation ($\geq 75\%$) is achieved within 30 min at 25 mM peroxymonosulfate.

We then examined the kinetics of PrP^{TSE} degradation by peroxymonosulfate at two concentrations. We added 15 μ L 10% BH (CWD) to ultrapure water, or 25 or 125 mM peroxymonosulfate for 1 to 60 min (Figure 1B). Immunoreactivity of CWD PrP^{TSE} was diminished after 5 min incubation ($p < 0.01$) with 125 mM peroxymonosulfate, and after 15 min incubation, CWD PrP^{TSE} was substantially reduced, and in some replicates, no longer detectable. Contact with 125 mM peroxymonosulfate for durations exceeding 1 min significantly reduced immunoreactivity compared to controls ($p < 0.01$). In contrast, contact with 25 mM peroxymonosulfate did not result in significantly reduced band intensity until 15 min exposure ($p < 0.01$). At both peroxymonosulfate concentrations, CWD PrP^{TSE} immunoreactivity was undetectable after 60 min exposure (Figure 1B, $p < 0.01$).

To gain further insight into the degradation of PrP^{TSE} achieved by exposure to HSO₅⁻ we imaged protein aggregates from purified prion preparations⁷⁹ by TEM (Methods in SI) after 10, 30, and 60 min and 24 h exposure to 50 mM peroxymonosulfate (Figure S4). The control (unexposed) and samples exposed for 10 min exhibited definitive rod-like structures characteristic of pathogenic prion protein fibrils. Samples exposed to HSO₅⁻ for longer time periods had fewer fibril-like structures; the 24 h exposure showed no discernable structures. These data indicate that peroxymonosulfate extensively altered prion protein aggregates.

2.4.2 Peroxymonosulfate degrades recombinant prion protein in the absence of transition metal catalysts. Peroxymonosulfate is a strong oxidant capable of direct oxidation of primary amines, alkenes, azides, and sulfides in aqueous solution without activation to form radical species.^{80,81} The results presented above indicate that peroxymonosulfate can degrade PrP^{TSE} in brain homogenate and in purified preparations without addition by an exogenous transition metal (i.e., cobalt) to activate HSO₅⁻. Brain homogenate and purified PrP^{TSE} preparations contain transition metals (e.g., iron, copper)^{82,83} that can activate HSO₅⁻.^{56,84-86} For example, ~2.4 µg Cu²⁺ per mg PrP^{TSE} has been estimated to be present in brain tissue of sporadic Creutzfeldt-Jakob disease patients.⁸³ The benign, normal form of the prion protein, PrP^C, associates with copper with a binding stoichiometry of approximately two copper atoms per PrP molecule under physiologically relevant conditions;⁸² the binding stoichiometry of PrP^{TSE} has not been worked out, however some replacement of copper by manganese and zinc has been reported.^{83,87}

We sought to establish whether HSO₅⁻ could transform prion protein in the absence of transition metals that might activate peroxymonosulfate to produce radical species. To do this we used α -mo-recPrP because available sources of PrP^{TSE} were expected to include transition

metals. We incubated ~15 ng of α -mo-recPrP with 12.5 mM peroxymonosulfate in the absence and presence of 300 μ M cupric chloride (CuCl_2) for 1 h, and quenched the reaction at the end of the incubation period or pre-treated samples with 50 mM $\text{Na}_2\text{S}_2\text{O}_3$. Recombinant prion proteins are typically purified using immobilized metal affinity chromatography, and His-tagged proteins purified in this manner may contain transition metal contaminants.⁸⁸ To exclude this possibility, we used α -mo-recPrP not bearing a His-tag. Under the experimental conditions employed, exposure to HSO_5^- completely eliminated α -mo-recPrP immunoreactivity (Figure S5) indicating that activation of peroxymonosulfate to form radical species was not prerequisite to degrade prion protein. Exposure to peroxymonosulfate + CuCl_2 also eliminated α -mo-recPrP immunoreactivity. Pre-treatment of samples with sodium thiosulfate prevented loss of α -mo-recPrP immunoreactivity in treatments of peroxymonosulfate with and without CuCl_2 (S5). These results indicate that peroxymonosulfate can directly oxidize prion protein without metal activation.

2.4.3 Cobalt accelerates degradation of pathogenic prion protein exposed to peroxymonosulfate. We next assessed whether activation of peroxymonosulfate by Co(II) accelerates degradation of PrP^{TSE} . We incubated 10% HY brain homogenate, purified HY preparation or 10% CWD brain homogenate with 125 mM peroxymonosulfate and 3 mM CoCl_2 for 60 min and found immunoreactivity to be diminished to $5 \pm 0.3\%$, $3 \pm 1\%$, and $2 \pm 1\%$ of control (identical to treatments except that HSO_5^- was excluded), respectively (Figure 2A, inset). Examination of the concentration-dependence of Co(II)-activated peroxymonosulfate transformation of PrP^{TSE} (10% CWD brain homogenate) revealed substantial decrease immunoreactivity at 25 mM HSO_5^- by 30 min exposure (Figure 2A); in contrast, substantial degradation by peroxymonosulfate without added CoCl_2 was not observed at concentrations

below 50 mM HSO_5^- for this exposure period (Figure 1A). Exposure of PrP^{TSE} to 125 mM HSO_5^- in the absence or presence of CoCl_2 resulted in elimination of immunoreactivity by 15 min (Figure 1B and 2B). When PrP^{TSE} was exposed to 25 mM HSO_5^- in the presence of 600 μM CoCl_2 , immunoblot band intensity was substantially reduced after 15 min ($p = 0.0013$) and completely eliminated at longer exposure times (Figure 2B). In the absence of cobalt, equivalent PrP^{TSE} degradation required longer exposure (1 h, Figure 1B). These data demonstrate that addition of cobalt enhances the effectiveness of PrP^{TSE} degradation by peroxymonosulfate.

The experiments described above used a 125:3 molar ratio of HSO_5^- to Co^{2+} . This ratio is within ranges reported for optimal degradation of diesel-contaminated soil and 2,4-dichlorophenol.^{57,40} We investigated the effect of the HSO_5^- -to- CoCl_2 ratio on degradation at constant HSO_5^- concentrations of 25 and 125 mM and found no difference ($p > 0.05$) in the extent of degradation after 20 min for HSO_5^- -to- CoCl_2 ratios between 10:1 and 100:1; after 1 h, immunoreactivity was no longer detectable for these treatments (data not shown).

2.4.4 Formation of sulfate and hydroxyl radicals is not necessary for rapid degradation of PrP^{TSE} . Activation of peroxymonosulfate by transition metals produces sulfate and hydroxyl radicals. To assess whether the formation of either of these radical species was required for the rapid transformation of PrP^{TSE} , we employed ethanol and *tert*-butyl alcohol as radical quenchers in exposures of PrP^{TSE} to peroxymonosulfate with or without added CoCl_2 . Ethanol reacts rapidly with hydroxyl and sulfate radicals ($\cdot\text{OH}$: $k' = 1.2$ to $2.8 \times 10^9 \text{ M}^{-1}\text{s}^{-1}$; $\text{SO}_4\cdot^-$: $k' = 1.6$ to $7.7 \times 10^7 \text{ M}^{-1}\text{s}^{-1}$),^{41,56,60,89,90} quenching reactions with these radicals. (We note that ethanol also quenches chloride radical ($\text{Cl}\cdot$), $k' = 1 \times 10^9 \text{ M}^{-1}\text{s}^{-1}$).⁹¹ In contrast, the second-order rate constant for *tert*-butyl alcohol reaction with $\cdot\text{OH}$ ($k' = 3.8$ to $7.6 \times 10^8 \text{ M}^{-1}\text{s}^{-1}$) is three

orders of magnitude larger than that for $\text{SO}_4^{\cdot-}$ ($k' = 4.0$ to $9.1 \times 10^5 \text{ M}^{-1}\text{s}^{-1}$),^{60,90} allowing it to be used to discriminate between the two radical species.^{43,56}

We exposed PrP^{TSE} (10% CWD brain homogenate) to 25 mM PMS \pm 600 μM CoCl_2 for 5 min, and either quenched at the end of the incubation period with $\text{Na}_2\text{S}_2\text{O}_3$ or pre-treated samples with 17.1 M ethanol or 10.4 M *tert*-butyl alcohol (molar ratios of 684:1 and 416:1 for ethanol- and *tert*-butyl alcohol-to- HSO_5^- , respectively). Degradation of PrP^{TSE} proceeded with sufficient rapidity to abolish detectable immunoreactivity within 5 min in the presence of the alcohol quenchers (Figure S6). This result indicates that the formation of hydroxyl or sulfate (or chloride) radicals is not requisite for rapid transformation of PrP^{TSE} . The species responsible for transformation of PrP^{TSE} may be HSO_5^- itself. Peroxymonosulfate is not quenched by ethanol and has been shown to transform all common proteinogenic amino acids investigated (cysteine not tested) with the largest pseudo-first-order rate constants for methionine, tryptophan, tyrosine and histidine.⁹² A second possibility is peroxymonosulfate radical ($\text{SO}_5^{\cdot-}$), a species formed from the oxidation of peroxymonosulfate by either sulfate radical or hydroxyl radical.⁹² The second-order rate constant for $\text{SO}_5^{\cdot-}$ reaction with ethanol ($k'_{\text{EtOH},\text{SO}_5^{\cdot-}} < 10^3 \text{ M}^{-1}\text{s}^{-1}$) is small compared to that of sulfate radical or hydroxyl radical ($k'_{\text{EtOH},i} > 10^7 \text{ M}^{-1}\text{s}^{-1}$, $i = \text{SO}_4^{\cdot-}$ or $\cdot\text{OH}$),^{59,60,89} making ethanol an inefficient quencher of reactions with this radical.

Interestingly, for samples exposed to peroxymonosulfate alone, pre-exposure of PrP^{TSE} to ethanol or *tert*-butyl alcohol appeared to enhance degradation (compare lanes 9 and 12 with lane 3 in Figure S6). This result may be attributable to partial denaturation of the protein by the alcohol, allowing HSO_5^- access to more of the structure. Ethanol can induce (partial) unfolding of proteins in a concentration-dependent manner.⁹³ Increased branching of the hydrocarbon

portion of alcohols generally reduces their effectiveness in denaturing proteins making *tert*-butyl alcohol a less effective denaturant than ethanol.⁹³

2.4.5 Effect of peroxymonosulfate on the *in vitro* converting ability of PrP^{TSE}.

The biochemical data presented thus far demonstrate that exposure to peroxymonosulfate in the absence or presence of Co²⁺ effects substantial degradation of PrP^{TSE}. The detection method employed (immunoblotting) has two limitations that are important for assessing the effectiveness of HSO₅⁻ for inactivating prions: (1) immunoblotting has detection limit (~4 ng PrP) that is orders of magnitude higher than the amount of PrP^{TSE} required to initiate disease (for mice, 725,000 times less sensitive than intracerebral inoculation);⁹⁴ and (2) declines in immunoreactivity do not always parallel reductions in prion infectivity.^{69,95-97} Protein misfolding cyclic amplification exploits the ability of PrP^{TSE} to induce conformational conversion of PrP^C to misfolded, protease K-resistant forms of the protein and has emerged as a sensitive technique for detecting low levels of pathogenic prion protein (detection limit of 1×10^{-12} dilution of 10% BH from hamsters infected with the 263K strain of hamster-adapted scrapie; estimated to be equivalent of 1.3 ag PrP^{TSE}, or approximately 26 molecules).^{94,98} Here we use a form of PMCA adapted to a microplate format and including Teflon beads (mbPMCA) to measure the *in vitro* converting ability of prions as a proxy for infectivity and to sensitively detect PrP^{TSE}.

We exposed PrP^{TSE} (15 μ L PK-treated 10% CWD BH) to 125 mM HSO₅⁻ with and without 3 mM CoCl₂ for 1 h. Samples were either quenched at the end of the exposure or pre-treated with 0.5 M Na₂S₂O₃. A 4 μ L aliquot of the reaction mixture was then added to 36 μ L NBH and subjected to two rounds of 96 cycles of mbPMCA. Immunoreactivity was not detected at any dilution examined in samples that had been exposed to HSO₅⁻ regardless of whether Co²⁺ had been added to the sample (Figure 3). Pre-treatment with thiosulfate allowed detection of

PrP^{TSE} immunoreactivity for dilutions of CWD-positive deer BH to the 10^{-7.6} dilution. These results indicate that 1-h treatment with 125 mM peroxymonosulfate + 3 mM CoCl₂ decreased the PrP^C-to-PrP^{TSE} converting ability of PrP^{TSE} by a factor of at least 10^{5.9}. This factor was arrived at by considering that the lowest (10⁻²) and highest dilutions (10^{-7.9}) at which untreated controls could be amplified and treated samples could not.

2.4.6 Modifications to PrP^{TSE} induced by exposure to peroxymonosulfate.

The immunoblotting results presented above demonstrate that peroxymonosulfate in the absence or presence of added CoCl₂ is capable of degrading pathogenic prion protein. To gain insight into modifications to pathogenic prion protein induced by exposure to peroxymonosulfate ± CoCl₂, we analyzed PrP^{TSE} following such treatment by LC-MS/MS. We incubated PrP^{TSE} (PK-treated purified HY preparation) with 9.6 mM HSO₅⁻ in the absence and presence of 230 μM CoCl₂ for 15 or 60 min. Samples were either quenched at the end of each time point or pre-treated with 0.5 M sodium thiosulfate.

Exposure to peroxymonosulfate in the absence and presence of CoCl₂ resulted in oxidative modifications to tryptophan and methionine residues. Reproducible tryptophan hydroxylation was observed on chymotryptic peptide fragments containing W⁵⁶ (GNDW(o)EDRY) and W¹⁰ (GQGGGTHNQW(o)), where (o) indicates oxidative modification. In Figure 4, we show the intensity ratios of these peptide fragments with and without modified tryptophan residues for samples exposed to HSO₅⁻ for 15 min. Substantially higher levels of oxidized tryptophan residues were present at both locations in samples containing unquenched peroxymonosulfate, consistent with a previous report of oxidative modification of free tryptophan.⁹² The location of these residues are displayed on the molecular model of PrP^{TSE} (Figure S2).

Reproducible methionine modifications were detected near the C-terminus of the protein on tryptic (+ endoprotease Lys-C) peptides containing M¹¹⁷ (GENFTETDIKIM(sulfone)ER) and M¹²⁴ (VVEQM(sulfone)CTTQYQK) (Figure 4C, and D; mapped onto the molecular model of PrP^{TSE}, Figure S2). The modified methionine residues were absent in samples not exposed to peroxymonosulfate or pre-treated with sodium thiosulfate. Following incubation with peroxymonosulfate in the absence of cobalt, the methionine sulfone-containing peptides were detected at similar intensities after both 15- and 60-min exposures. The same modification, but at substantially lower intensities was observed in 15- and 60-min reactions with peroxymonosulfate + CoCl₂ (data not shown). This result may reflect a true reduction in intensity of the sulfone modification, or enhanced protein degradation by peroxymonosulfate + CoCl₂ leading to reduced production of these particular peptide fragments, consistent with individual methionine amino acid modifications seen previously.⁹² Similar results were seen by Requena et al.³⁰ wherein hydrogen peroxide exposure led to the oxidation of methionine residues 109, 112, 129, and 134 in recombinant PrP (SHa, 29-231).

2.4.7 Environmental Implications. Prions are remarkably resistant to inactivation,⁸ and their persistence in the environment creates a need to develop effective *in situ* remediation methods for prion-contaminated lands. We have demonstrated that peroxymonosulfate can rapidly degrade and inactivate pathogenic prion protein. We further showed that Co(II)-catalyzed decomposition of HSO₅⁻ to SO₄⁻ accelerated prion degradation. The extent of prion inactivation suggested by the reduction of template-directed misfolding ability as measured by mbPMCA ($\geq 5.9 \log_{10}$ reduction for 1-h exposure to 125 mM HSO₅⁻ \pm 3 mM CoCl₂) compares favorably with that for other oxidants that have been tested for their ability to inactivate prions (Table 1). Peroxymonosulfate possesses advantages over some of the other oxidants listed in Table 1 for *in*

situ chemical oxidation. Peroxymonosulfate does not require low pH as does Fenton's reagent for optimal hydroxyl radical production⁹⁹ or the addition of toxic metals as does Cu²⁺-catalyzed decomposition of H₂O₂ to produce ·OH.¹⁰⁰ Reductions of infectivity of >6 log have been achieved via exposure to the Fenton reagent, but at elevated temperature (50 °C for 22 h).³⁹ Heterogeneous photocatalytically produced ·OH have been shown to reduce prion infectivity,¹⁰¹ but the utility of such methods for *in situ* chemical oxidation is limited because the photic zone in soils is on the order of 0.5 mm.^{102,103} While ozone has been demonstrated to inactivate prions,³¹⁻³³ its use to inactivate prions in soil is complicated by the gaseous nature of the oxidant. In some soil environments, the deposition of SO₄²⁻ may represent a concern for the application of peroxymonosulfate for *in situ* chemical oxidation.

Oxidative modifications to proteins can make them more susceptible to proteolytic degradation.¹⁰⁴ This suggests that if peroxymonosulfate effected only partial PrP^{TSE} degradation in the environment, the resulting oxidative modifications may render it susceptible to *in situ* degradation by native or added proteases. Our results strongly suggest that peroxymonosulfate, even without activation to radical species via transition metal activation, high temperatures or UV exposure, holds promise for *in situ* remediation of prion-contaminated land surfaces. Future research directed at the efficacy of peroxymonosulfate in degrading pathogenic prion protein and inactivating prions associated with soil constituents is warranted. We also note that peroxymonosulfate may prove useful in decontaminating medical instruments.

2.5 ACKNOWLEDGMENTS

This research was funded by NIH grant R01 NS060034. ARC was supported by NIEHS predoctoral training grant number T32ES007015. CBL acknowledges an NIH-supported Chemistry Biology Interface Training Program Predoctoral Fellowship (grant number T32-GM008505) and an NSF Graduate Research Fellowship (DGE-1256259). We thank Glenn Telling for the Tg(CerPrP) mice and Cédric Govaerts and Holge Wille for the PrP^{TSE} trimer protein database file. The Orbitrap Elite MS instrument was purchased through funding from NIH S10 RR029531. Article contents are solely the responsibility of the authors and do not represent official views of the sponsors.

2.6 REFERENCES

1. Prusiner, S. B. Prions. *Proc. Natl. Acad. Sci. USA* **1998**, *95*, 13363-13383.
2. Prusiner, S. B. Molecular biology of prion diseases. *Science*. **1991**, *252*, 1515-1522.
3. Bolton, D. C.; Bendheim, P. E.; Marmorstein, A. D.; Potempska, A. Isolation and structural studies of the intact scrapie agent protein. *Arch. Biochem. Biophys.* **1987**, *258*, 579-590.
4. Caughey, B.; Raymond, G. J.; Kocisko, D. A.; Lansbury, P. T., Jr. Scrapie infectivity correlates with converting activity, protease resistance, and aggregation of scrapie-associated prion protein in guanidine denaturation studies. *J. Virol.* **1997**, *71*, 4107-4110.
5. McKinley, M. P.; Bolton, D. C.; Prusiner, S. B. A protease-resistant protein is a structural component of the scrapie prion. *Cell* **1983**, *35*, 57-62.
6. Prusiner, S. B.; Cochran, S. P.; Groth, D. F.; Downey, D. E.; Bowman, K. A.; Martinez, H. M. Measurement of the scrapie agent using an incubation time interval assay. *Ann. Neurol.* **1982**, *11*, 353-358.
7. Prusiner, S. B.; Groth, D. F.; Cochran, S. P.; Masiarz, F. R.; McKinley, M. P.; Martinez, H. M. Molecular properties, partial purification, and assay by incubation period measurements of the hamster scrapie agent. *Biochem.* **1980**, *19*, 4883-4891.
8. Taylor, D. M. Inactivation of prions by physical and chemical means. *J. Hosp. Infect.* **1999**, *43 Suppl*, S69-76.
9. Pedersen, J. A.; Somerville, R. A. Why and how are CWD and Scrapie sometimes spread via environmental routes? In *Decontamination of Prions*, Reisner, D.; Deslys, J.-P., Eds. Dusseldorf University Press: Dusseldorf Germany, 2012; pp. 19-37.
10. Almberg, E. S.; Cross, P. C.; Johnson, C. J.; Heisey, D. M.; Richards, B. J. Modeling routes of chronic wasting disease transmission: Environmental prion persistence promotes deer population decline and extinction. *PLoS ONE* **2011**, *6*, e19896.
11. Haley, N. J.; Seelig, D. M.; Zabel, M. D.; Telling, G. C.; Hoover, E. A., Detection of CWD prions in urine and saliva of deer by transgenic mouse bioassay. *PLoS ONE* **2009**, *4*, e4848.
12. Mathiason, C. K.; Powers, J. G.; Dahmes, S. J.; Osborn, D. A.; Miller, K. V.; Warren, R. J.; Mason, G. L.; Hays, S. A.; Hayes-Klug, J.; Seelig, D. M.; Wild, M. A.; Wolfe, L. L.; Spraker, T. R.; Miller, M. W.; Sigurdson, C. J.; Telling, G. C.; Hoover, E. A. Infectious prions in the saliva and blood of deer with chronic wasting disease. *Science*. **2006**, *314*, 133-136.
13. Miller, M. W.; Williams, E. S.; Hobbs, N. T.; Wolfe, L. L. Environmental sources of prion transmission in mule deer. *Emerg. Infect. Dis.* **2004**, *10*, 1003-1006.

14. Race, R.; Jenny, A.; Sutton, D. Scrapie infectivity and proteinase K-resistant prion protein in sheep placenta, brain, spleen, and lymph node: Implications for transmission and antemortem diagnosis. *J. Infect. Dis.* **1998**, *178*, 949-953.
15. Tamguney, G.; Miller, M. W.; Wolfe, L. L.; Sirochman, T. M.; Glidden, D. V.; Palmer, C.; Lemus, A.; DeArmond, S. J.; Prusiner, S. B. Asymptomatic deer excrete infectious prions in faeces. *Nature* **2009**, *461*, 529-532.
16. Brown, P.; Gajdusek, D. C. Survival of scrapie virus after 3 years' interment. *Lancet* **1991**, *337*, 269-770.
17. Georgsson, G.; Sigurdarson, S.; Brown, P. Infectious agent of sheep scrapie may persist in the environment for at least 16 years. *J. Gen. Virol.* **2006**, *87*, 3737- 3740.
18. Seidel, B.; Thomzig, A.; Buschmann, A.; Groschup, M. H.; Peters, R.; Beekes, M.; Terytze, K. Scrapie agent (strain 263K) can transmit disease via the oral route after persistence in soil over years. *PLoS ONE* **2007**, *2*, e435.
19. Cooke, C. M.; Rodger, J.; Smith, A.; Fernie, K.; Shaw, G.; Somerville, R. A. Fate of prions in soil: Detergent extraction of PrP from soils. *Environ. Sci. Technol.* **2007**, *41*, 811-817.
20. Johnson, C. J.; Phillips, K. E.; Schramm, P. T.; McKenzie, D.; Aiken, J. M.; Pedersen, J. A. Prions adhere to soil minerals and remain infectious. *PLoS Pathog.* **2006**, *2*, e32.
21. Ma, X.; Benson, C. H.; McKenzie, D.; Aiken, J. M.; Pedersen, J. A. Adsorption of pathogenic prion protein to quartz sand. *Environ. Sci. Technol.* **2007**, *41*, 2324-2330.
22. Boyd, S. A.; Mortland, M. M. Enzyme interactions with clays and clay-organic matter complexes. In *Soil Biochemistry*, Stotzky, G.; Bollag, J.-M. Eds. Marcel Dekker: New York, 1990; Vol. 6, pp. 1-28.
23. Nielsen, K. M.; Calamai, L.; Pietramellara, G. Stabilization of extracellular DNA and proteins by transient binding to various soil components. In *Nucleic Acids and Proteins in Soil*, Nannipieri, P.; Smalla, K. Eds. Springer: Germany, 2006; Vol. 8, pp. 142-157.
24. Williams, E. S.; Miller, M. W.; Kreeger, T. J.; Kahn, R. H.; Thorne, E. T. Chronic wasting disease of deer and elk: A review with recommendations for management. *J. Wildl. Manag.* **2002**, *66*, 551-563.
25. Chamarro, E.; Marco, A.; Esplugas, S. Use of Fenton reagent to improve organic chemical biodegradability. *Wat. Res.* **2001**, *35*, 1047-1051.
26. Liang, C.; Huang, C. F.; Chen, Y. J. Potential for activated persulfate degradation of BTEX contamination. *Wat. Res.* **2008**, *42*, 4091-4100.
27. Tsitonaki, A.; Petri, B.; Crimi, M.; Mosbæk, H.; Siegrist, R. L.; Bjerg, P. L. In situ chemical oxidation of contaminated soil and groundwater using persulfate: A review. *Crit. Rev. Environ. Sci. Technol.* **2010**, *40*, 55-91.

28. Matta, R.; Hanna, K.; Chiron, S. Fenton-like oxidation of 2,4,6-trinitrotoluene using different iron minerals. *Sci. Total Environ.* **2007**, *385*, 242-251.
29. Furman, O.; Laine, D. F.; Blumenfeld, A.; Teel, A. L.; Shimizu, K.; Cheng, I. F.; Watts, R. J. Enhanced reactivity of superoxide in water-soild matrices. *Environ. Sci. Technol.* **2009**, *43*, 1528-1533.
30. Requena, J. R.; Dimitrova, M. N.; Legname, G.; Teijeira, S.; Prusiner, S. B.; Levine, R. L. Oxidation of methionine residues in the prion protein by hydrogen peroxide. *Arch. Biochem. Biophys.* **2004**, *432*, 188-195.
31. Ding, N.; Neumann, N. F.; Price, L. M.; Braithwaite, S. L.; Balachandran, A.; Belosevic, M.; El-Din, M. G. Inactivation of template-directed misfolding of infectious prion protein by ozone. *Appl. Environ. Microbiol.* **2012**, *78*, 613-620.
32. Ding, N.; Neumann, N. F.; Price, L. M.; Braithwaite, S. L.; Balachandran, A.; Belosevic, M.; Gamal El-Din, M. Ozone inactivation of infectious prions in rendering plant and municipal wastewaters. *Sci. Total Environ.* **2014**, *470-471*, 717-725.
33. Ding, N.; Neumann, N. F.; Price, L. M.; Braithwaite, S. L.; Balachandran, A.; Mitchell, G.; Belosevic, M.; Gamal El-Din, M. Kinetics of ozone inactivation of infectious prion protein. *Appl. Environ. Microbiol.* **2013**, *79*, 2721-30.
34. Rutala, W. A.; Weber, D. J.; Society for Healthcare Epidemiology of, A. Guideline for disinfection and sterilization of prion-contaminated medical instruments. *Infect. Control. Hosp. Epidemiol.* **2010**, *31*, 107-117.
35. Brown, P.; Rohwer, R. G.; Gajdusek, C. D. Newer data on the inactivation of scrapie virus or Creutzfeldt Jakob Disease virus in brain tissue. *J. Infect. Dis.* **1986**, *153*, 1145-1148.
36. Brown, P.; Rohwer, R. G.; Green, E. M.; Gadjusek, D. C. Effect of chemicals, heat, and histopathologic processing on high-infectivity hamster-adapted scrapie virus. *J. Infect. Dis.* **1982**, *145*, 683-687.
37. Park, S. J.; Kim, N. H.; Jeong, B. H.; Jin, J. K.; Choi, J. K.; Park, Y. J.; Kim, J. I.; Carp, R. I.; Kim, Y. S. The effect of Fenton reaction on protease-resistant prion protein (PrP^{Sc}) degradation and scrapie infectivity. *Brain Res.* **2008**, *1238*, 172-180.
38. Paspaltsis, I.; Berberidou, C.; Poulis, I.; Sklaviadis, T. Photocatalytic degradation of prions using the photo-Fenton reagent. *J. Hosp. Infect.* **2009**, *71*, 149-156.
39. Suyama, K.; Yoshioka, M.; Akagawa, M.; Murayama, Y.; Horii, H.; Takata, M.; Yokoyama, T.; Mohri, S. Assessment of prion inactivation by Fenton reaction using protein misfolding cyclic amplification and bioassay. *Biosci. Biotechnol. Biochem.* **2007**, *71*, 2069-2071.

40. Do, S. H.; Jo, J. H.; Jo, Y. H.; Lee, H. K.; Kong, S. H. Application of a peroxymonosulfate/cobalt (PMS/Co(II)) system to treat diesel-contaminated soil. *Chemosphere* **2009**, *77*, 1127-1131.
41. Anipsitakis, G. P.; Dionysiou, D. D. Degradation of organic contaminants in water with sulfate radicals generated by the conjugation of peroxymonosulfate with cobalt. *Environ. Sci. Technol.* **2003**, *37*, 4790-4797.
42. Anipsitakis, G. P.; Tufano, T. P.; Dionysiou, D. D. Chemical and microbial decontamination of pool water using activated potassium peroxymonosulfate. *Wat. Res.* **2008**, *42*, 2899-2910.
43. Anipsitakis, G. P. Cobalt/peroxymonosulfate and related oxidizing reagents for water treatment. *Thesis*. University of Cincinnati, Cincinnati, OH, 2005.
44. Lou, X.; Wu, L.; Guo, Y.; Chen, C.; Wang, Z.; Xiao, D.; Fang, C.; Liu, J.; Zhao, J.; Lu, S. Peroxymonosulfate activation by phosphate anion for organics degradation in water. *Chemosphere* **2014**, *117*, 582-585.
45. Yang, S.; Wang, P.; Yang, X.; Shan, L.; Zhang, W.; Shao, X.; Niu, R. Degradation efficiencies of azo dye Acid Orange 7 by the interaction of heat, UV and anions with common oxidants: Persulfate, peroxymonosulfate and hydrogen peroxide. *J. Hazard. Mater.* **2010**, *179*, 552-558.
46. Steele, W. J.; Appelman, E. H. The standard enthalpy of formation of peroxymonosulfate (HSO_5^-) and the standard electrode potential of the peroxymonosulfate-bisulfate couple. *J. Chem. Thermodynamics*, **1982**, *14*, 337-344.
47. Ball, D. L.; Edwards, J. O. The kinetics and mechanism of the decomposition of Caro's acid. *J. Am. Chem. Soc.* **1956**, *78*, 1125-1129.
48. DuPont. DuPont oxone technical attributes. In DuPont, Ed. 2008.
49. Curini, M.; Epifano, F.; Marcotullio, M. C.; Rosati, O. Oxone®: A convenient reagent for the oxidation of acetals. *Synlett*. **1999**, *6*, 777-779.
50. Denmark, S. E.; Forbes, D. C.; Hays, D. S.; DePue, J. S.; Wilde, R. G. Catalytic epoxidation of alkenes with oxone. *J. Org. Chem.* **1995**, *60*, 1391-1407.
51. Trost, B. M.; Curran, D. P. Chemoselective oxidation of sulfides to sulfones with potassium hydrogen persulfate. *Tetrahedron Lett.* **1981**, *22*, 1287-1290.
52. Wozniak, L. A.; Stec, W. J. Oxidation in organophosphorus chemistry: Potassium peroxymonosulphate. *Tetrahedron Lett.* **1999**, *40*, 2637-2640.
53. Liu, H.; Bruton, T. A.; Doyle, F. M.; Sedlak, D. L. In situ chemical oxidation of contaminated groundwater by persulfate: Decomposition by Fe(III)- and Mn(IV)-containing oxides and aquifer materials. *Environ. Sci. Technol.* **2014**, *48*, 10330-10336.

54. Chan, K. H.; Chu, W. Degradation of atrazine by cobalt-mediated activation of peroxymonosulfate: Different cobalt counteranions in homogenous process and cobalt oxide catalysts in photolytic heterogeneous process. *Wat. Res.* **2009**, *43*, 2513-2521.
55. Anipsitakis, G. P.; Dionysiou, D. D. Transition metal/UV-based advanced oxidation technologies for water decontamination. *Appl. Catal. B* **2004**, *54*, 155-163.
56. Anipsitakis, G. P.; Dionysiou, D. D. Radical generation by the interaction of transition metals with common oxidants. *Environ. Sci. Technol.* **2004**, *38*, 3705-3712.
57. Anipsitakis, G. P.; Dionysiou, D. D.; Gonzalez, M. A. Cobalt-mediated activation of peroxymonosulfate and sulfate radical attack on phenolic compounds. Implications of chloride ions. *Environ. Sci. Technol.* **2006**, *40*, 1000-1007.
58. Ji, Y.; Dong, C.; Kong, D.; Lu, J. New insights into atrazine degradation by cobalt catalyzed peroxymonosulfate oxidation: Kinetics, reaction products and transformation mechanisms. *J. Hazard. Mater.* **2015**, *285*, 491-500.
59. Neta, P.; Hule, R. E.; Ross, A. B. Rate constants for reactions of inorganic radicals in aqueous solution. *J. Phys. Chem. Ref. Data* **1988**, *17*, 1027-1284.
60. Buxton, G. V.; Greenstock, C. L.; Helman, P. W.; Ross, A. B. Critical review of rate constants for reactions of hydrated electrons, hydrogen atoms and hydroxyl radicals. *J. Phys. Chem. Ref. Data* **1988**, *17*, 513-886.
61. Rastogi, A.; Al-Abed, S. R.; Dionysiou, D. D. Sulfate radical-based ferrous–peroxymonosulfate oxidative system for PCBs degradation in aqueous and sediment systems. *Appl. Catal. B* **2009**, *85*, 171-179.
62. Rivas, F. J.; Beltran, F. J.; Carvalho, F.; Alvarez, P. M. Oxone-promoted wet air oxidation of landfill leachates. *Ind. Eng. Chem. Res.* **2005**, *44*, 749-758.
63. He, X.; de la Cruz, A. A.; Dionysiou, D. D. Destruction of cyanobacterial toxin cylindrospermopsin by hydroxyl radicals and sulfate radicals using UV-254nm activation of hydrogen peroxide, persulfate and peroxymonosulfate. *J. Photochem. Photobiol. A* **2013**, *251*, 160-166.
64. Paradkar, V. M.; Latham, T. B.; Demko, D. M. Oxidative decarboxylation of alpha-amino acids with insitu generated dimethyl dioxirane. *Synlett.* **1995**, 1059-1060.
65. Johnson, C. J.; Herbst, A.; Duque-Velasquez, C.; Vanderloo, J. P.; Bochsler, P.; Chappell, R.; McKenzie, D. Prion protein polymorphisms affect chronic wasting disease progression. *PLoS ONE* **2011**, *6*, e17450.
66. McKenzie, D.; Bartz, J.; Mirwald, J.; Olander, D.; Marsh, R.; Aiken, J. M. Reversibility of scrapie inactivation is enhanced by copper. *J. Biol. Chem.* **1998**, *273*, 25545-25547.

67. Smith, C. B.; Booth, C. J.; Wadzinski, T. J.; Legname, G.; Chappell, R.; Johnson, C. J.; Pedersen, J. A. Humic substances interfere with detection of pathogenic prion protein. *Soil Biol. Biochem.* **2014**, *68*, 309-316.
68. Johnson, C. J.; Aiken, J. M.; McKenzie, D.; Samuel, M. D.; Pedersen, J. A. Highly efficient amplification of chronic wasting disease agent by protein misfolding cyclic amplification with beads (PMCAb). *PLoS ONE* **2012**, *7*, e35383.
69. Moudjou, M.; Sibille, P.; Fichet, G.; Reine, F.; Chapuis, J.; Herzog, L.; Jaumain, E.; Laferriere, F.; Richard, C. A.; Laude, H.; Andreoletti, O.; Rezaei, H.; Beringue, V. Highly infectious prions generated by a single round of microplate-based protein misfolding cyclic amplification. *MBio.* **2014**, *5*, e00829-13.
70. Browning, S. R.; Mason, G. L.; Seward, T.; Green, M.; Eliason, G. A.; Mathiason, C.; Miller, M. W.; Williams, E. S.; Hoover, E.; Telling, G. C. Transmission of prions from mule deer and elk with chronic wasting disease to transgenic mice expressing cervid PrP. *J. Virol.* **2004**, *78*, 13345-13350.
71. Peretz, D.; Supattapone, S.; Giles, K.; Vergara, J.; Freyman, Y.; Lessard, P.; Safar, J. G.; Glidden, D. V.; McCulloch, C.; Nguyen, H. O.; Scott, M.; Dearmond, S. J.; Prusiner, S. B. Inactivation of prions by acidic sodium dodecyl sulfate. *J. Virol.* **2006**, *80*, 322-331.
72. Somerville, R. A.; Gentles, N. Characterization of the effect of heat on agent strains of the transmissible spongiform encephalopathies. *J. Gen. Virol.* **2011**, *92*, 1738-1748.
73. Pitre, A.; Pan, Y.; Pruett, S.; Skalli, O. On the use of ratio standard curves to accurately quantitate relative changes in protein levels by Western blot. *Anal. Biochem.* **2007**, *361*, 305-307.
74. Govaerts, C.; Wille, H.; Prusiner, S. B.; Cohen, F. E. Evidence for assembly of prions with left-handed β -helices into trimers. *Proc. Natl. Acad. Sci. USA* **2004**, *101*, 8342-8347.
75. Davies, K. J. A. Protein damage and degradation by oxygen radicals. *J. Biol. Chem.* **1987**, *262*, 9895-9901.
76. Aiken, J. M.; Williamson, J. L.; Borchardt, L. M.; Marsh, R. F. Presence of mitochondrial D-loop DNA in scrapie-infected brain preparations enriched for the prion protein. *J. Virol.* **1990**, *64*, 3265-3268.
77. Kellings, K.; Meyer, N.; Mirenda, C.; Prusiner, S. B.; Riesner, D. Analysis of nucleic acids in purified scrapie prion preparations. *Arch. Virol. Suppl.* **1993**, *7*, 215-225.
78. Moore, R. A.; Timmes, A.; Wilmarth, P. A.; Priola, S. A. Comparative profiling of highly enriched 22L and C handler mouse scrapie prion protein preparations. *Proteomics* **2010**, *10*, 2858-2869.
79. Raymond, G. J.; Chabry, J. Purification of the pathological isoform of prion protein (PrP^{Sc} or PrP^{res}) from transmissible spongiform encephalopathy-affected brain tissue. In

- Techniques in Prion Research*, Lehmann, S.; Grassi, J. Eds. Birkhäuser Verlag: Basel, 2004; pp. 16-26.
80. Zhu, W.; Ford, W. T. Oxidation of alkenes with aqueous potassium peroxymonosulfate and no organic solvent. *J. Org. Chem.* **1991**, *56*, 7022-7026.
 81. Betterton, E. A.; Hoffmann, M. R. Oxidation of aqueous SO₂ by peroxymonosulfate. *Environ. Sci. Technol.* **1988**, *92*, 5962-5965.
 82. Stockel, J.; Safar, J. G.; Wallace, A. C.; Cohen, F. E.; Prusiner, S. B. Prion protein selectively binds copper(II) ions. *Biochem.* **1998**, *37*, 7185-7193.
 83. Wong, B.-S.; Chen, S. G.; Colucci, M.; Xie, Z.; Pan, T.; Liu, T.; Li, R.; Gambetti, P.; Sy, M.-S.; Brown, D. R. Aberrant metal binding by prion protein in human prion disease. *J. Neurochem.* **2001**, *78*, 1400-8.
 84. Ren, Y.; Lin, L.; Ma, J.; Yang, J.; Feng, J.; Fan, Z. Sulfate radicals induced from peroxymonosulfate by magnetic ferrosin MF₂O₄ (M = Co, Cu, Mn, and Zn) as heterogeneous catalysts in the water. *Appl. Catal. B* **2015**, *165*, 572-578.
 85. Kim, J.; Edwards, J. O. A study of cobalt catalysis and copper modification in the coupled decompositions of hydrogen peroxide and peroxomonosulfate ion. *Inorg. Chim. Acta* **1995**, *235*, 9-13.
 86. Gilbert, B. C.; Stell, J. K. Mechanisms of peroxide decomposition: An electron paramagnetic resonance study of the reaction of the peroxymonosulfate anion (HOOSO₃⁻) with Cu. *J. Chem. Soc. Faraday. Trans.* **1990**, *86*, 3261-3266.
 87. Brown, D. R. Metal toxicity and therapeutic intervention: Copper and prion disease. *Biochem. Soc. Trans.* **2002**, *30*, 742-745.
 88. Nilsson, J.; Stahl, S.; Lundberg, J.; Uhlen, M.; Nygren, P.A. Affinity fusion strategies for detection, purification, and immobilization of recombinant proteins. *Protein Express. Purif.* **1997**, *11*, 1-16.
 89. Hayon, E.; Treinin, A.; Wilf, J. Electronic spectra, photochemistry, and autoxidation mechanism of the sulfite-bisulfite-pyrosulfite systems. The SO₂⁻, SO₃⁻, SO₄⁻, and SO₅⁻ radicals. *J. Am. Chem. Soc.* **1971**, *94*, 47-57.
 90. Neta, P.; Madhavan, V.; Zemel, H.; Fessenden, R. W. Rate constants and mechanism of reaction of SO₄⁻ with aromatic compounds. *J. Am. Chem. Soc.* **1976**, *99*, 163-164.
 91. Khmenlinskii, I. V.; Plyusnin, V. F.; Grivin, V. P. Mechanism of the formation of the Cl₂⁻ ion radical in the photolysis of the FeCl₄⁻ complex in ethanol saturated with HCl. *Russ. J. Phys. Chem.* **1989**, *63*, 1494-1497.

92. Ruiz Vélez, M. Oxidation of amino acids by peroxymonosulfate and sorption of antibiotics to natural organic matter. Ph.D. Dissertation. University of Wisconsin – Madison, Madison, WI, 2015.
93. Herskovits, T. T.; Gadegbeku, B.; Jaillet, H. On the structural stability and solvent denaturation of proteins. *J. Biol. Chem.* **1970**, *245*, 2588-2598.
94. Saá, P.; Castilla, J.; Soto, C. Ultra-efficient replication of infectious prions by automated protein misfolding cyclic amplification. *J. Biol. Chem.* **2006**, *281*, 35245-35452.
95. Klingeborn, M.; Race, B.; Meade-White, K. D.; Chesebro, B. Lower specific infectivity of protease-resistant prion protein generated in cell-free reactions. *Proc. Natl. Acad. Sci. USA* **2011**, *108*, E1244-53.
96. Shikiya, R. A.; Bartz, J. C. In vitro generation of high-titer prions. *J. Virol.* **2011**, *85*, 13439-13442.
97. Weber, P.; Giese, A.; Piening, N.; Mitteregger, G.; Thomzig, A.; Beekes, M.; Kretzschmar, H. A. Cell-free formation of misfolded prion protein with authentic prion infectivity. *Proc. Natl. Acad. Sci. USA* **2006**, *103*, 15818-15823.
98. Silveira, J. R.; Raymond, G. J.; Hughson, A. G.; Race, R. E.; Sim, V. L.; Hayes, S. F.; Caughey, B. The most infectious prion protein particles. *Nature* **2005**, *437*, 257-261.
99. Gogate, P. R.; Pandit, A. B. A review of imperative technologies for wastewater treatment I: Oxidation technologies at ambient conditions. *Adv. Environ. Res.* **2004**, *8*, 501-551.
100. Solassol, J.; Pastore, M.; Crozet, C.; Perrier, V.; Lehmann, S. A novel copper-hydrogen peroxide formulation for prion decontamination. *J. Infect. Dis.* **2006**, *194*, 865-869.
101. Paspaltsis, I.; Kotta, K.; Lagoudaki, R.; Grigoriadis, N.; Poullos, I.; Sklaviadis, T. Titanium dioxide photocatalytic inactivation of prions. *J. Gen. Virol.* **2006**, *87*, 3125-3130.
102. Hebert, V. R.; Miller, G. C. Depth dependence of direct and indirect photolysis on soil surfaces. *J. Agric. Food Chem.* **1990**, *38*, 913-918.
103. Geddes, J.; Miller, G. C. Photolysis of organics in the environment. In *Perspectives in Environmental Chemistry*, Macalady, D. L., Ed. Oxford University Press: New York, NY, 1998; pp. 195-209.
104. Climent, I.; Tsai, L.; Levine, R. L. Derivatization of γ -glutamyl semialdehyde residues in oxidized proteins by fluoresceinamine. *Anal. Biochem.* **1989**, *182*, 226-32.
105. Russo, F.; Johnson, C. J.; Johnson, C. J.; McKenzie, D.; Aiken, J. M.; Pedersen, J. A. Pathogenic prion protein is degraded by a manganese oxide mineral found in soils. *J. Gen. Virol.* **2009**, *90*, 275-280.

2.7 TABLES

Table 1. Inactivation of prions by chemical oxidants

Oxidant	Concentration (mM)	Contact Time (min)	Reduction in Infectivity \log_{10}	Ref.
HOCl	19 ^b	30	4.4	36
O ₃	0.3 (pH 4.4, 4 °C)	5	>4.1	33
Fenton(-like) reagent (·OH)	[H ₂ O ₂] = 100, [Cu ²⁺] = 0.5	30	>5.2	100
	[H ₂ O ₂] = 2131, [Fe ²⁺] = 15.8 (50 °C)	1320	>6	39
Heterogeneous photocatalysis (·OH)	[H ₂ O ₂] = 118, [TiO ₂] _s = 50	720	ND	101
HSO ₅ ⁻	125	60	≥5.9 ^c	this study
H ₂ O ₂	1279	1, 24	0.84	36
permanganate	253-506	15, 60	1, 2-2.3	35
	6.3	15, 60, 1440	0.51, 1.17, 0.84	36
δ-MnO ₂ (s)	102 (pH 4)	960	>4 ^c	35, 105

^a ND, not determined. ^b Attributing all free residual chlorine to HOCl. ^c Based on reduction of template-directed conversion ability as measured by PMCA.

2.8 Figures

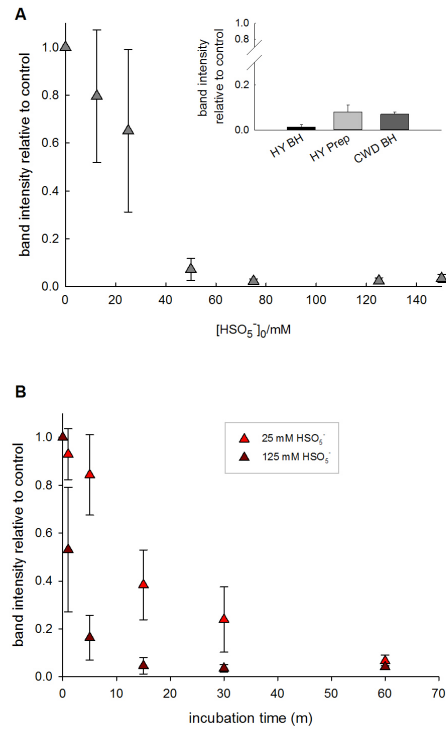


Figure 1. Peroxymonosulfate degrades pathogenic prion protein in the absence of transition metal cations. (A) CWD BH (10% wt/vol) was incubated with between 0 and 150 mM peroxymonosulfate for 30 min. Substantial degradation of PrP^{TSE} was seen at 50 mM. (Inset) Peroxymonosulfate substantially degrades CWD and HY prions (PrP^{TSE} (10% HY BH (15 μ L), purified HY preparation (0.5 μ g) or 10% CWD BH (15 μ L) was incubated with 125 mM peroxymonosulfate for 1 h. (B) Immunoblot detection of PrP^{TSE} was substantially reduced after 5 min when exposed to 125 mM peroxymonosulfate, and after 15-30 min when exposed to 25 mM peroxymonosulfate. All immunoblot detection was eliminated when PrP^{TSE} was exposed to both concentrations after 1-h incubation. PrP^{TSE} (15 μ L 10% CWD BH) was incubated with between 0 and up to 150 mM for 30 min. Immunoblot densitometry values normalized to PrP^{TSE} in ultrapure water ($n = 4$). Error bars represent standard deviations of experimental triplicates. Immunoblots were probed with mAb 3F4 (HY) or mAb 8G8/Bar224 (CWD). Error bars represent one standard deviation.

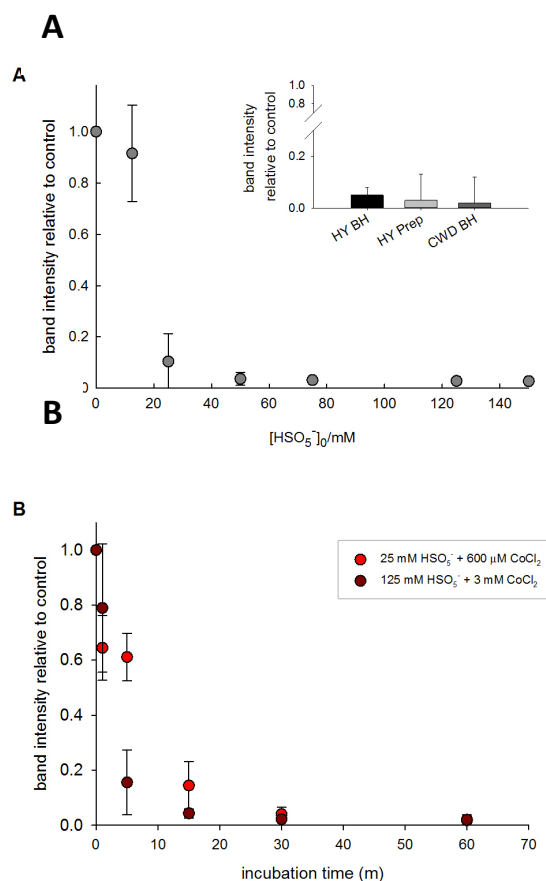


Figure 2. Activation of HSO_5^- by CoCl_2 enhances degradation of PrP^{TSE} . (A) CWD BH (10% wt/vol) was incubated with between 0 and 150 mM peroxymonosulfate in the presence of CoCl_2 (125:3 molar ratio) for 30 min. Substantial degradation of PrP^{TSE} was seen at 25 mM. (Inset) Peroxymonosulfate activated by CoCl_2 substantially degrades CWD and HY prions. PrP^{TSE} (10% HY BH (15 μL), purified HY preparation (0.5 μg) or 10% CWD BH (15 μL) was incubated with 125 mM peroxymonosulfate for 1 h. (B) Immunoblot detection of PrP^{TSE} was substantially reduced after 5 min when exposed to 125 mM peroxymonosulfate with 3 mM CoCl_2 , and after 15 min when exposed to 25 mM peroxymonosulfate with 600 mM CoCl_2 . All immunoblot detection was eliminated when PrP^{TSE} was exposed to both concentrations after 30 min incubation. Error bars represent standard deviations of experimental triplicates. Immunoblots were probed with mAb 3F4 (HY) or mAb 8G8/Bar224 (CWD). Immunoblot densitometry values normalized to PrP^{TSE} in ultrapure water ($n = 4$). Error bars represent one standard deviation.

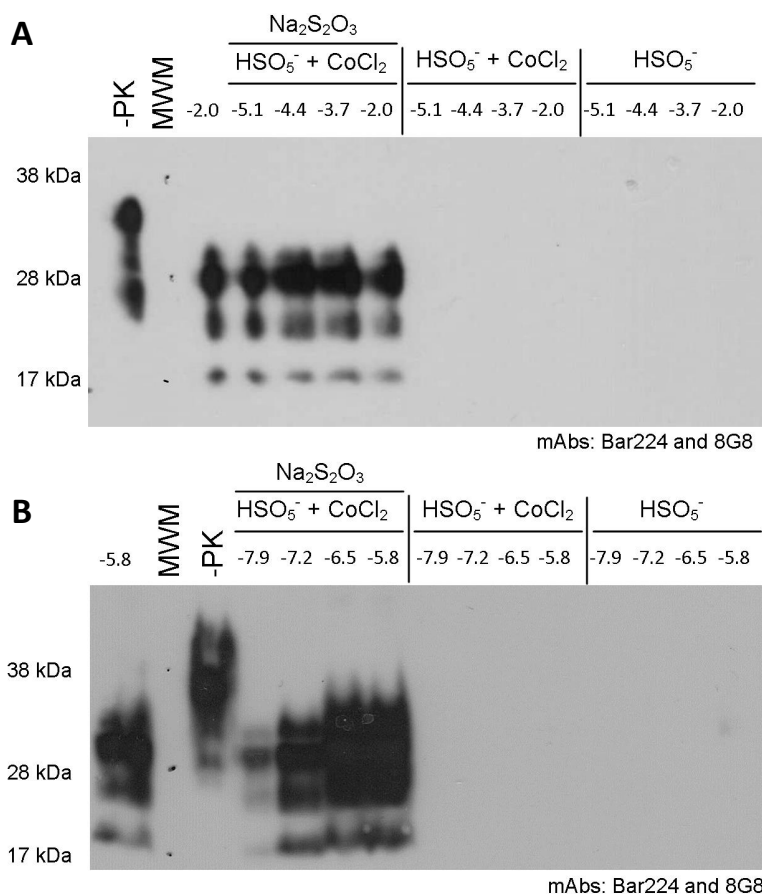


Figure 3. Treatment with peroxymonosulfate \pm CoCl₂ reduces the *in vitro* PrP^C-to-PrP^{TSE} converting ability of CWD agent by a factor of at least 10^{5.9}. PrP^{TSE} (15 μ L PK-treated 10% CWD BH) was incubated with 125 mM peroxymonosulfate with or without 3 mM CoCl₂ for 1 h. Samples were either quenched at the end of the experimental time point or pre-treated with 0.3 M Na₂S₂O₃. A 4 μ L aliquot of resulting sample was added to 36 μ L NBH and subjected to two rounds of 96 cycles of PMCAb. (A) PrP^{TSE} immunoreactivity is present in a 10^{-7.9} dilution from 10% brain homogenate from a white-tailed deer clinically affected by chronic wasting disease when peroxymonosulfate and CoCl₂ is pre-treated with thiosulfate, but not detected at any dilution (up to 10^{-2.0}, B) examined when exposed to peroxymonosulfate + CoCl₂ or peroxymonosulfate alone. Values above lanes indicate dilution from CWD brain homogenate. Immunoblots were probed with mAbs 8G8 and Bar224. Blot is representative of three replicates.

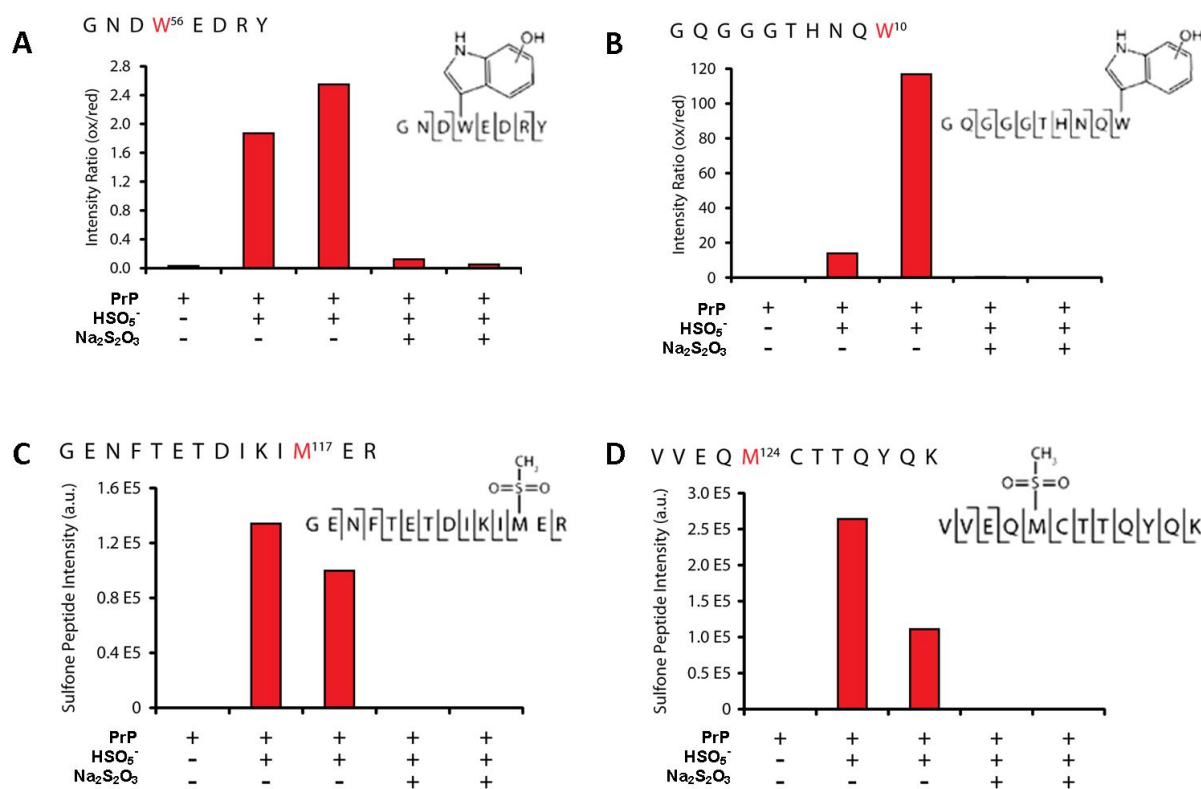


Figure 4. Exposure of pathogenic prion protein to peroxymonosulfate results in oxidative modification to tryptophan and methionine residues. PrP^{TSE} (proteinase K-treated purified HY preparation) was incubated with ultrapure water or 9.6 mM peroxymonosulfate for 15 min. After quenching with 0.5 M Na₂S₂O₃, samples were digested with chymotrypsin (panels a and b) or trypsin + endoprotease Lys-C (panels c and d) and analyzed by LC-MS/MS. Hydroxytryptophan (W⁵⁶, a; W¹⁰, b) and methionine sulfone (M¹¹⁷, c; M¹²⁴, d) were detected in samples treated with peroxymonosulfate that were not pre-quenched with 0.5 M Na₂S₂O₃. Bars indicate replicates of precursor ions.

2.9 APPENDIX

Supporting Information for Chapter 2

Peroxymonosulfate Rapidly Inactivates the Disease-associated Prion Protein*

*A version of this chapter will be submitted to *Environmental Science & Technology* with Booth, C.J., Lietz, C.B., Li, L., and Pedersen, J.A. as co-authors.

Table of Contents

	Page
2.9.1 Materials	66
2.9.2 Methods for Transmission Electron Microscopy	66
2.9.3 Methods for LC-MS/MS	67
2.9.4 Figures	70
S1. Sodium thiosulfate does not inhibit detection of PrP by immunoblotting.	70
S2. Antibody epitopes and residues determined to be oxidized by peroxymonosulfate.	71
S3. Antibody epitopes and residues easily oxidized and determined to be oxidized by peroxymonosulfate.	72
S4. Transmission electron micrographs of purified prion protein exposed to 50 mM peroxymonosulfate for the indicated time period.	73
S5. Peroxymonosulfate degrades recombinant mouse PrP in the α -helix-rich conformation (α -mo-recPrP) without activation to the sulfate radical.	74
S6. Ethanol and <i>tert</i> -butyl alcohol do not quench inactivation of CWD prions by peroxymonosulfate (\pm CoCl ₂).	75
2.9.5 References	76

2.9.1. Materials

We purchased proteinase K (PK) (from *Tritirachium album*, 30 units·mg_{protein}⁻¹) and phenylmethanesulfonyl fluoride (PMSF) (>98.5%) from Sigma-Aldrich. We obtained peroxymonosulfate as a potassium triple salt (2KHSO₅·KHSO₄·K₂SO₄, Oxone[®], 95%) and potassium dihydrogen phosphate (≥98%) from Alfa Aesar. Cobalt(II) chloride hexahydrate (>98%) was procured from MP Biomedicals. Cobalt(II) nitrate hexahydrate (99+%) and cobalt(II) sulfate heptahydrate (99+%) were from Acrōs Organics. Copper(II) chloride dihydrate, sodium thiosulfate pentahydrate (99%), methanol (>99.9%), sodium hydroxide (>97%), sulfuric acid (95-98%), sodium chloride (>99.9%), sodium phosphate dibasic anhydrous (>99%), and Tris base (>99.9%) were acquired from Fisher. Ethyl alcohol (99.9%) was from Decon Laboratories, Inc., and *tert*-butyl alcohol (99%) was purchased from TCI. These chemicals were used without further purification. All solutions were prepared in ultrapure water (18.2 MΩ·cm resistivity, Barnstead GenPure Pro) unless otherwise specified.

2.9.2 Methods for Transmission Electron Microscopy (TEM)

Purified HY PrP^{TSE} preparations were suspended to a concentration of 400 (± 27) µg·mL⁻¹ in ultrapure water, as measured by BCA assay. Prions were exposed to 50 mM peroxymonosulfate for 10, 30, 60 min or 24 h, quenched with 1 M Na₂S₂O₃, coated on to carbon grids, negatively stained with methylamine tungstate, and dried. Representative transmission electron micrographs of purified HY prion protein with the *N*-terminal truncated by treatment with PK were collected using a Philips CM120 (Amsterdam, Netherlands) operating at 80 keV.

2.9.3 Methods for LC-MS/MS

Preparation of proteolytic peptides for LC-MS/MS analysis. To prepare samples for LC-MS/MS analysis, we exposed $\sim 2.4 \mu\text{g}$ of HY PrP^{TSE} (PK-treated purified preparation) with 9.6 mM peroxymonosulfate in the absence or presence of 230 μM CoCl₂ for 15 or 60 min. At the end of the exposure, samples were quenched with an equal volume of 0.5 M sodium thiosulfate, and the total sample volume ($\sim 26 \mu\text{L}$) was dried down using a SpeedVacTM (Thermo Scientific). To achieve high sequence coverage in LC-MS/MS analysis, samples were digested with multiple proteases: samples were digested by a combination of endoprotease Lys-C and trypsin (which cleaves C-terminal to lysine and arginine), or by chymotrypsin (which cleaves C-terminal to tryptophan, tyrosine, phenylalanine, and leucine). Dry pellets were resuspended in 20 μL of 8 M urea (in 50 mM Tris-HCl, pH 8) and sonicated for 30 s. To reduce cysteine residues, dithiothreitol (DTT) (Promega) (prepared in 50 mM Tris-HCl, pH 8) was added to samples to a final concentration of 5 mM and incubated (room temperature, 1 h). To alkylate cysteine residues, iodoacetamide (Fisher) prepared in 50 mM Tris-HCl, pH 8 was then added to a final concentration of 15 mM and incubated (room temperature, 30 min) in the dark. A volume of DTT solution equal to the initial DTT aliquot was then added to quench alkylation. Samples were diluted with 50 mM Tris-HCl until the urea concentration was $< 6 \text{ M}$ or $< 1 \text{ M}$ for Lys-C/trypsin digestions or chymotryptic digestions, respectively. For Lys-C/trypsin, the pre-mixed enzymes (sequencing grade, Promega) were added at an enzyme:protein ratio of 1:25 (w/w), and the sample was incubated (room temperature, 3 h). Samples were diluted again with 50 mM Tris-HCl until the urea concentration $< 1 \text{ M}$ and incubated (30 °C, 17 h). For chymotryptic digestions, chymotrypsin (sequencing grade, Promega) was added at an enzyme:protein ratio of 1:50 (w/w).

and incubated (room temperature, 17 h). Digestions were halted with trifluoroacetic acid (Fisher), and samples were stored at -80°C until further use.

Liquid chromatography-tandem mass spectrometry. The nanoAcquity UPLC (Waters Corp.) liquid-chromatography column was self-packed with an integrated nano-electrospray ionization (nESI) emitter. Fused silica (360 μm OD, 75 μm ID) was pulled with a laser puller, and the emitter was etched with hydrofluoric acid. The packing material was reversed-phased bridged ethylene hybrid C18 beads (diameter: 1.7 μm , pore size: 130 Å; Waters Corp.) packed to ~ 15 cm in length. After sample loading (~ 3.0 to 3.5 μL), reversed phase solvents (A: 5% DMSO, 0.1% formic acid in LCMS-grade water; B: 5% DMSO, 0.1% formic acid in LCMS-grade acetonitrile) were ramped according to the following gradient: 0.0 min, 100% A; 0.1 min, 95% A; 80.0 min, 70% A; 80.5 min, 25% A; 90.0 min, 25% A; 90.5 min, 5% A; 100.0 min, 5% A; 100.5 min, 100% A; 115.0 min, 100% A. The flow rate was ~ 0.325 $\mu\text{L}\cdot\text{min}^{-1}$. Upon elution from the column, sample was electrosprayed into the nESI source of an Orbitrap Elite mass spectrometer (Thermo Fisher). Mass resolution was run at 30,000 (at a mass-to-charge ratio (m/z) 400), and mass accuracies were typically 2-5 ppm. MS/MS fragmentation was performed by higher energy collisional dissociation (HCD), and the resulting fragments were analyzed at high resolution (30,000). Experiments were performed with a semi-targeted, data-dependent method. A list of theoretical m/z charge ratios for doubly, triply, and quadruply protonated tryptic or chymotryptic PrP fragments (allowing up to two miscleavages) was constructed. The instrument searched for match between the m/z of eluted peptide ions and known PrP fragments from the list, and the ten most abundant multiply charged ions were chosen for fragmentation. If ten from the list could not be found, the most abundant multiply charged ions present filled the void. The selected ions were isolated and fragmented individually, and each fragmentation spectrum was

recorded. Samples were prepared in two technical replicates and analyzed in duplicate by LC-MS/MS.

Data analysis. Resulting peptide fragment spectra were searched against a target-decoy database using the open mass spectrometry search algorithm (OMSSA) on the COMPASS v1.4 software suite.¹ The database was constructed from the UniProt genome-predicted protein database for *Mescocricetus auratus* and digested by trypsin or chymotrypsin *in silico*. Database search criteria included the following: 20 ppm precursor mass tolerance, 0.01 Th fragment mass tolerance, trypsin or chymotrypsin enzyme, two missed cleavage maximum, and carbamidomethyl cysteine static modifications. Methionine sulfoxide, methionine sulfone, and tryptophan oxidations were included as variable modifications. Fragmentation spectra matching PrP peptides were validated by manual *de novo* sequencing. Relative quantitation was performed using the height of the extracted ion chromatogram (XIC) peaks. The XIC was constructed by plotting the intensity of experimental PrP peptide m/z (± 2.5 ppm) against retention time.

2.9.4 Figures

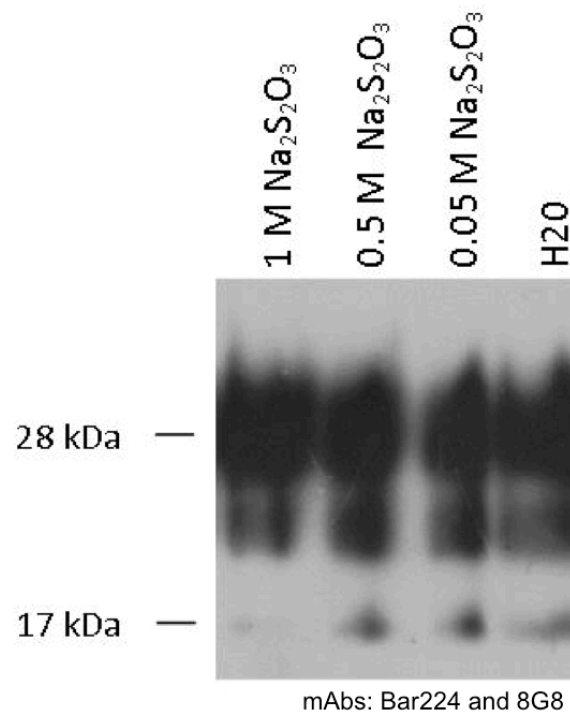


Figure S1. Sodium thiosulfate does not inhibit detection of PrP by immunoblotting. PrP^{TSE} (15 μL proteinase K-treated 10% brain homogenate from a white-tailed deer clinically positive for chronic wasting disease) was incubated with water or 0.05–1 M of $\text{Na}_2\text{S}_2\text{O}_3$ for 1 h. Detection of immunoreactivity by immunoblotting was not inhibited by $\text{Na}_2\text{S}_2\text{O}_3$ at any tested concentration. Immunoblot is representative of three replicates and was probed with Bar224 and 8G8.

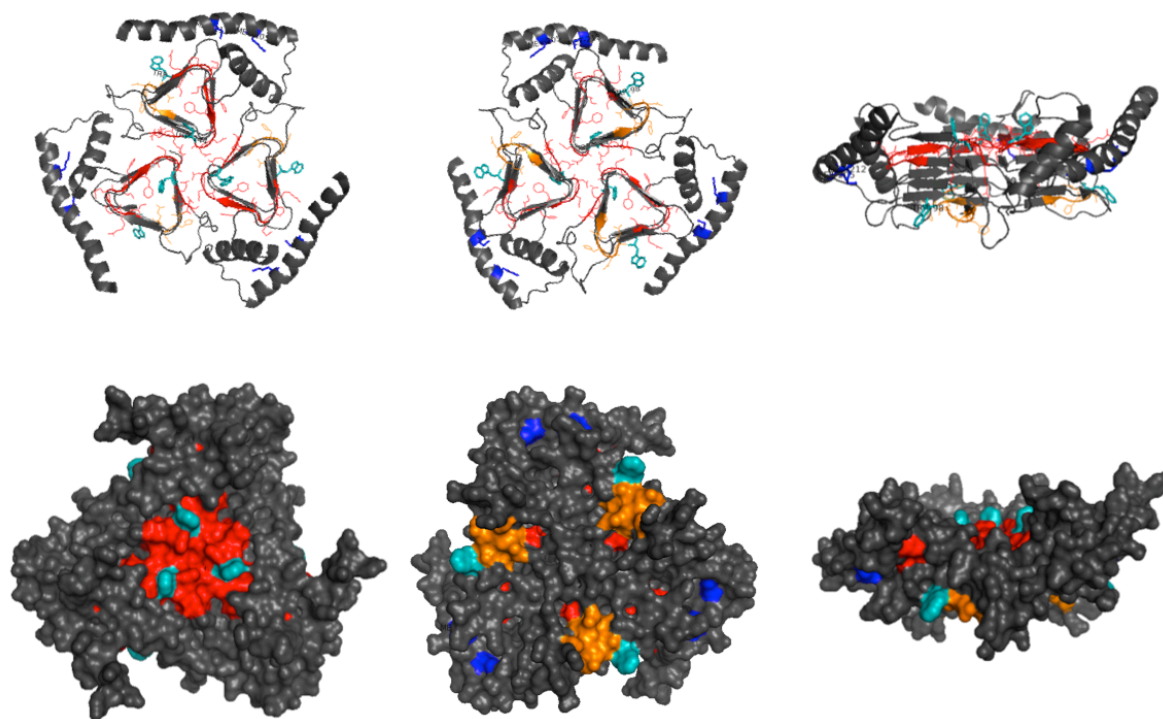


Figure S2. Antibody epitopes and residues determined to be oxidized by peroxymonosulfate. The proposed 3D structure of the mouse PrP^{TSE} with colors indicating the Bar224 (red) and 8G8 (orange) antibody epitopes (white-tailed deer PrP) and the oxidized residues (teal: tryptophan residues; blue: methionine residues) identified by LC-MS/MS.² PDB file kindly provided by Holger Wille.



Figure S3. Antibody epitopes and residues easily oxidized and determined to be oxidized by peroxymonosulfate. (A) The amino acid sequence for white-tailed deer (*Odocoileus hemionus*; residues 1-254) where one underline designates the epitope region for mAb 8G8 and double underline designates the epitope region for mAb Bar224. (B) The amino acid sequence for golden hamster (*Mesocricetus auratus*; residues 1-254) where one underline designates the epitope region for mAb 3F4 and double underline designates the epitope region for mAb SAF83. (A and B) Red letters represent easily oxidizable residues (methionine (M), tyrosine (Y), tryptophan (W), and histidine(H)). Sequences courtesy of NCBI, accession number AF009181.2 and B34759.

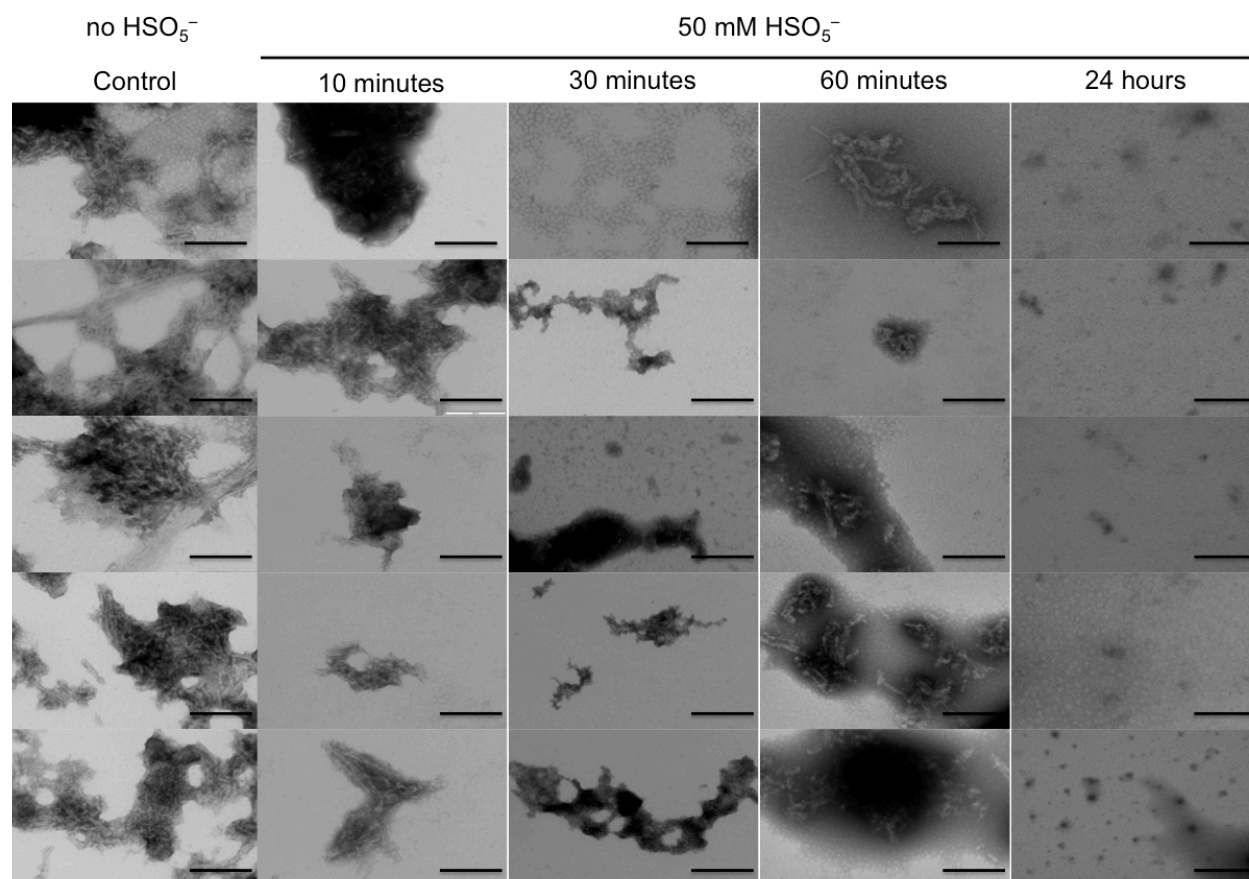


Figure S4. Transmission electron micrographs of purified prion protein exposed to 50 mM peroxymonosulfate for the indicated time period. Representative transmission electron micrographs of PrP²⁷⁻³⁰. Black bars are 200 nm. Purified preparations were suspended to a concentration of $400 \mu\text{g}\cdot\text{mL}^{-1} \pm 27 \mu\text{g}\cdot\text{mL}^{-1}$ in ultrapure water, exposed to 50 mM peroxymonosulfate for 10, 30, 60 min or 24 h, quenched with 1 M $\text{Na}_2\text{S}_2\text{O}_3$, coated onto carbon grids, negatively stained with methylamine tungstate, and dried. Images were collected using a Philips CM120 (Amsterdam, The Netherlands) operating at 80 keV.

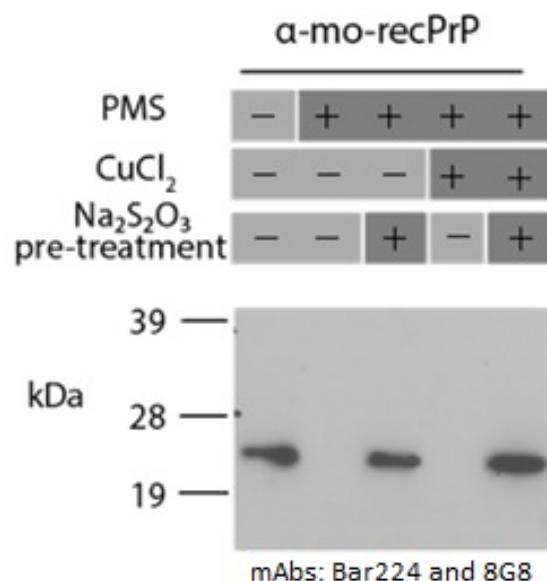


Figure S5. Peroxymonosulfate degrades recombinant mouse PrP in the α -helix-rich conformation (α -mo-recPrP) without activation to the sulfate radical. Murine recombinant PrP (15 ng, no His-tag) in the α -helix-rich conformation was incubated with 25 mM HSO₅[−] in the absence and presence of 375 μ M CuCl₂. Peroxymonosulfate solution was buffered to pH 7 with 100 mM sodium phosphate. Lanes 3 and 5 represent samples that were pre-treated with 50 mM Na₂S₂O₃. Immunoblot was probed with mAbs 8G8 and Bar224.

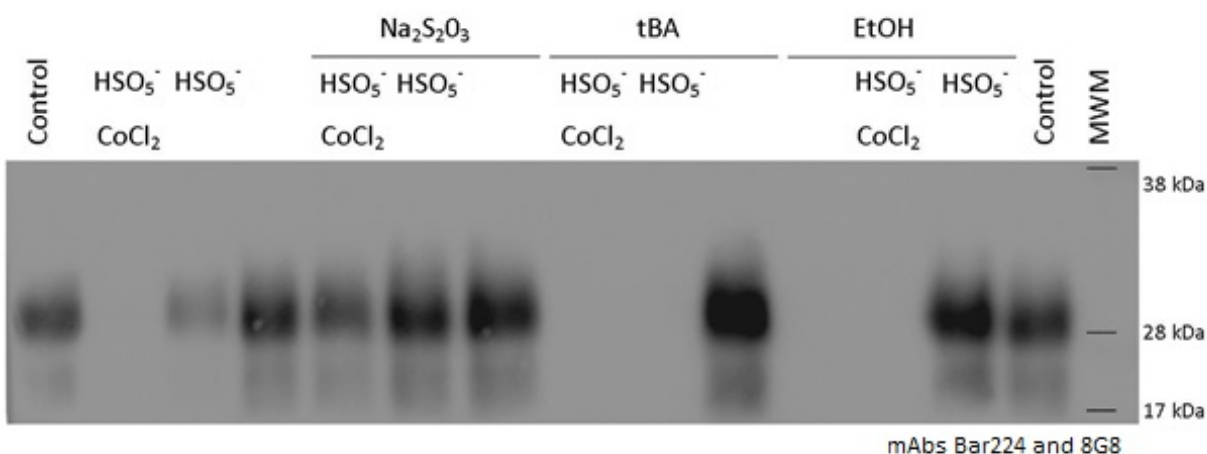


Figure S6 Ethanol and *tert*-butyl alcohol do not quench inactivation of CWD prions by peroxymonosulfate (\pm CoCl₂). Peroxymonosulfate (25 mM) was pre-treated with ultrapure water, sodium thiosulfate (1 M), pure ethanol (EtOH; 17.1 M), or pure *tert*-butyl alcohol (tBA; 10.4 M) for 1 h prior to exposing 10% CWD brain homogenate (20 μ L) for 5 min. Reactions were halted with addition of 1 M sodium thiosulfate. Immunoblot is representative of three replicates. Immunoblots probed with mAbs Bar224 and 8G8.

2.9.5 REFERENCES

1. Wenger, C. D.; Phanstiel, D. H.; Lee, M. V.; Bailey, D. J.; Coon, J. J. COMPASS: A suite of pre- and post-search proteomics software tools for OMSSA. *Proteomics*. **2011**, *11*, 1064-1074.
2. Govaerts, C.; Wille, H.; Prusiner, S. B.; Cohen, F. E. Evidence for assembly of prions with left-handed β -helices into trimers. *Proc. Natl. Acad. Sci. USA*. **2004**, *101*, 8342-8347.

Chapter 3

Degradation of pathogenic prion protein from soil microparticles by peroxymonosulfate*

*A version of this chapter will be submitted to *Environmental Science & Technology* with Epstein, G, Millevolte, R, and Pedersen, J.A. as co-authors.

3.1 ABSTRACT.

Environmental routes of transmission are implicated in epizootics of prion diseases of sheep (scrapie) and deer, elk, and moose (chronic wasting disease). Strong evidence suggests that soil may serve as an environmental reservoir for prions, the etiological agent of scrapie and chronic wasting disease. Prions can persist in soil for years, as they are remarkably resistant to inactivation, which is particularly relevant in environmental settings. We previously showed that exposure to peroxymonosulfate (HSO_5^-), alone and in the presence of cobalt, degrades pathogenic prions and substantially diminishes in vitro converting ability, as measured by protein misfolding cyclic amplification. Due to the high affinity of prions for many soil particle surfaces and the presence of iron (oxy)hydroxides and other compounds in soils that could potentially activate HSO_5^- to radical species, the ability of HSO_5^- to inactivate prions in a soil environment needs to be considered. Here, we investigate the ability of HSO_5^- to degrade the disease-associated, misfolded form of the prion protein, PrP^{TSE} , adsorbed to soil mineral particles (phyllosilicate clays, silica, and iron (oxy)hydroxides) as a function of HSO_5^- concentration, solution pH, and temperature. We also investigated the potential for the iron (oxy)hydroxides goethite and ferrihydrite to activate HSO_5^- to form radical species. Recovery of pathogenic prion protein from microparticles declined following 30- and 60-min exposure to HSO_5^- , indicating degradation of prions occurs regardless of interaction with clay or iron (oxy)hydroxides microparticles. Our results suggest that despite PrP^{TSE} adsorption to purified soil particles, exposure to HSO_5^- degrades PrP^{TSE} at environmentally relevant pH and temperatures. Furthermore, we anticipate HSO_5^- to be a useful tool in the environmental remediation of chronic wasting disease prions, and by extension, potentially other prion diseases.

3.2 INTRODUCTION

Transmissible spongiform encephalopathies (TSEs, prion diseases) are a class of fatal neurodegenerative diseases that include bovine spongiform encephalopathy, scrapie of sheep and goats, chronic wasting disease (CWD) of deer, elk and moose, transmissible mink encephalopathy (TME) of farmed mink, and Creutzfeldt-Jakob disease in humans.^{1,2} The central molecular event in TSE pathogenesis is the conversion of the normal, benign cellular prion protein, PrP^C, into an abnormally folded conformation associated with disease, designated PrP^{TSE}.^{1,3} Available evidence indicates that prions, the etiological agents of TSEs, are composed mostly, if not solely, of PrP^{TSE}.^{1,4}

Scrapie and CWD are unique among TSEs in that environmental routes of transmission appear to sustain TSE epizootics.⁵ Evidence for environmental transmission of scrapie and CWD includes observations that healthy animals contract TSEs following habitation in areas once holding infected animals or carcasses of diseased animals.⁶⁻⁹ Soil has been widely proposed as a potential reservoir of TSE infectivity in the environment.^{5, 7, 9-11} Prions enter the environment and, consequently, the soil when shed or excreted from infected animals in feces, urine, and saliva.^{6, 12-15} The mobility of prions in soils is limited^{7, 9, 16} and the bulk of infectivity is expected to be maintained near soil surfaces, suggesting the presence of soil “hot spots” of prion infectivity. Multiple studies have assessed the persistence of prion infectivity in soil for several years,^{7,9} and prion infectivity can persist in some environments for at least 16 years.⁸

Proteins in soil bind to charged surfaces of clay constituents,¹⁷ and the affinity of prions to attach to soil microparticles, especially aluminosilicate clay microparticles is well established.¹⁸⁻²² Attachment of prions to microparticles of montmorillonite, an aluminosilicate clay, enhances oral transmission by a factor of ~680 relative to free prions in Syrian hamsters.²³

We have previously shown that binding to montmorillonite particles alters in vivo tissue tropism of CWD agent and enhances PrP^{TSE} accumulation in orally inoculated white-tailed deer compared with animals given unbound PrP^{TSE} (Chesney et al. *PLoS Pathog.*, in review).

There is profound change in stability associated with the biophysical structure of the disease-associated PrP^{TSE} conformation compared to PrP^C, making prions remarkably resistant to sterilization methods used to inactivate conventional pathogens (e.g., viruses, bacteria, protozoans) including exposure to UV and ionizing radiation, or chemical disinfectants, and heat treatments.²⁴ Effective prion infectivity inactivation methods include autoclaving in 1 N NaOH at 121 °C, >1 h exposure to 1 N NaOH or 2% sodium hypochlorite, or incineration.²⁵ The resistance of prions to inactivation methods is consistent with its stability in the environment and the maintenance of infectivity. These inactivation methods are impractical for application in prion-contaminated environments.

Investigations of prion degradation using chemical oxidation has involved the use of in situ chemical oxidation techniques such as ozone,^{27, 28} hydroxyl radicals produced by the Fenton reagent,²⁹⁻³² and hydroxyl radicals formed via supra-bandgap irradiation of TiO₂.³³ However, most of the oxidants that have previously been investigated are either insufficiently effective against prions (e.g., H₂O₂) or have requirements that may limit their utility for application to soils (e.g., the gaseous nature of O₃, low pH needed for optimal application of Fenton reagent). We have previously shown that HSO₅⁻ (both alone and activated to a radical species by a transition metal) can inactivate PrP^{TSE} from two species (CWD and HY, a hamster-adapted form of TME). Prions adsorbed to metal surfaces have been shown to be significantly more resistant to inactivation compared to prions in brain homogenate (BH),³⁴ and an enhancement in transmission occurs when PrP^{TSE} is bound to certain soil and dietary mineral microparticles.^{23, 35}

Thus, to investigate the ability of HSO_5^- to inactivate PrP^{TSE} adsorbed to soil mineral microparticles, purified clay, silicon dioxide, and iron (oxy)hydroxide particles were used as a first step to assess the potential for its environmental application. The use of oxidation methods for prion decontamination in environmentally relevant conditions, including circumneutral pH, ambient temperature, and when the PrP^{TSE} is bound to soil constituents has not previously been examined. We previously showed that cobalt, a transition metal that activates HSO_5^- to radical species,^{36, 37} enhances degradation of PrP^{TSE} . (article in review) However, transition metal activation is not required for PrP^{TSE} inactivation and, due to introduction of a potentially toxic metal (e.g. cobalt) in the environment, is not desirable and therefore not used in this work.

The objective of this study was to ascertain the ability of HSO_5^- to degrade CWD PrP^{TSE} attached to mineral microparticles. The inactivation of PrP^{TSE} attached to soil microparticles by HSO_5^- was assessed by exposing phyllosilicate clay minerals, SiO_2 , iron (oxy)hydroxides microparticle-bound CWD prions to HSO_5^- , quenching the oxidation reaction with up to 1 M sodium thiosulfate, and extracting the prions to determine the extent of degradation. The ability of proteins to bind to soil constituents is influenced by pH, cation exchange capacity of minerals, and temperature.³⁸⁻⁴⁰ We investigated the reduction in immunoblot signal of prions as a function of microparticle mineralogy, HSO_5^- concentration, solution pH, and temperature.

3.3 EXPERIMENTAL

3.3.1 Materials. Proteinase K (PK) from *Tritirachium album*, 30 units·mg_{protein}⁻¹) and phenylmethanesulfonyl fluoride (PMSF) (>98.5%) was purchased from Sigma-Aldrich. Peroxyonosulfate was obtained as a triple salt ($2\text{KHSO}_5 \cdot \text{KHSO}_4 \cdot \text{K}_2\text{SO}_4$, Oxone[®], 95%, manufactured by DuPont). Potassium dihydrogen phosphate ($\geq 98\%$) was obtained from Alfa

Aesar. Sodium hydroxide (>97%), sulfuric acid (95-98%), sodium chloride (>99.9%), sodium phosphate dibasic anhydrous (>99%), and Tris base (>99.9%) were acquired from Fisher. These chemicals were used without further purification. All solutions were prepared in ultrapure water (18.2 MΩ·cm resistivity, Barnstead GenPure Pro) unless otherwise specified.

3.3.2 Prion protein sources. The CWD agent was obtained from brain tissue of an experimentally inoculated white-tailed deer.⁴¹ Brain homogenate (BH) was prepared by adding brain tissue to a final concentration of 10% (w/v) in 1× Dulbecco's phosphate buffered saline (DPBS) without Ca^{2+} or Mg^{2+} (137 mM NaCl, 8.1 mM HPO_4^{2-} , 1.47 mM H_2PO_4^- ; pH 7), homogenized in a Dounce homogenizer and stored at -80°C until use. Brain homogenates were treated with proteinase-K (PK), a serine protease that digests PrP^{C} and cleaves the N-terminus of PrP^{TSE} . The PK-treated PrP^{TSE} contains PrP antibody-specific epitopes and maintains infectivity equivalent to untreated PrP^{TSE} .⁴² In addition to removing PrP^{C} , PK treatment reduces the complexity of the BH matrix, towards what we would expect in decomposed tissues. Proteinase K-treated brain homogenates were prepared by incubating homogenized tissue with $50\ \mu\text{g}\cdot\text{mL}^{-1}$ PK for 1 h at 37°C . Proteinase K activity was inhibited by adding PefaBloc SC (Roche Applied Science, Germany) to a final concentration of 1 mM, and complete protease inhibitor EDTA-free (Roche Applied Science, Germany) was added to the PK-treated brain homogenates (BH) at 5× the manufacturer's recommended concentration.

3.3.3 Preparation of mineral particles. The montmorillonite (SWy-2) and kaolinite (KGa-1) particles were chosen due to previous demonstration that prion disease transmission in Syrian hamsters was enhanced when the disease agent was adsorbed to these particles. We chose additional smectite clay minerals to represent a wide range of cation exchange capacities (CEC) and surface area, provided in Table S2. Two kaolinites were chosen as KGa-1 is low-defect and

well crystalized, whereas KGa-2 is high defect and less crystallized. Both kaolinities have similar CEC (KGa-1 has a CEC of 20 $\mu\text{mol}_\text{c}/\text{g}$ and KGa-2 has a CEC of 33 $\mu\text{mol}_\text{c}/\text{g}$), however the surface area of KGa-2 is more than double KGa-1.

Montmorillonite (SWy-2, Crook County, Wyoming, USA; SAz-1, Apache County, Arizona, USA), kaolinite (KGa-1, Washington County, Georgia, USA; KGa-2, Warren County, Georgia, USA), hectorite (SHCa-1, San Bernardino County, California, USA) were purchased from the Clay Minerals Society Source Clays Repository (West Lafayette, Indiana, United States), and were size-fractionated by wet sedimentation (hydrodynamic diameter, $d_h = 0.5\text{--}2\ \mu\text{m}$) and saturated with sodium as previously described,⁴³ freeze-dried, ground and stored at room temperature until use. Properties and x-ray diffraction analysis of the microparticles are provided in Table S2. Quartz sand (Iota-6, Unimin Corporation, New Canaan, CT) was size fractionated by wet sedimentation/flotation to obtain the 0.18-0.25 mm particle size fraction, soaked in 12 N HCl for 24 h to remove impurities, rinsed with distilled deionized water, freeze dried, and stored at room temperature until use.²⁰

Ferrihydrite and goethite were prepared by the lab of Matt Ginder Vogel at the University of Wisconsin – Madison. Goethite was synthesized by adding 110 mL of 1 M NaHCO_3 to an anoxic 1 L solution of 0.036 M ferrous sulfate. The mixture was purged with air at a flow rate of 30-40 $\text{mL}\cdot\text{min}^{-1}$ for 48 h. Two-line ferrihydrite was synthesized by rapid titration of a 0.29 M ferric chloride solution with NaOH to pH 7.0. The Fe (hydr)oxides were washed three times with ultrapure water by centrifugation and freeze dried. Quartz sand, montmorillonite, kaolinite, hectorite, ferrihydrite, and goethite were sterilized by autoclaving at 121 °C for 30 min.

The phyllosilicate clay minerals used have been extensively characterized previously.⁴⁴⁻⁴⁶ The chemical composition of the microparticles are shown in Table S1. A clay slurry for X-ray

diffraction was prepared by making a 0.01 % w/ v suspension of the prepared microparticles of each smectite (SWy-2, SAz-1, and SHCa-1) in 10 mM NaCl. Samples were vortexed and centrifuged (10 min, 16,000g). The bulk of the supernatant was removed and the layer just above the pellet was layered on silica wafers and allowed to dry overnight (12-18 h). The basal d_{001} spacings of the near homoionic smectites (Na^+ -SWy-2, Na^+ -SAz-1, and Na^+ -SHCa-1) were determined by X-ray diffraction on a Scintag PAD V diffractometer (Cupertino, California, US) using $\text{CuK}\alpha$ with a step size of 0.02° and a dwell time of 2s (Table S2 and Figure S1).

3.3.4 Recovery of attached PrP^{TSE} from mineral particles. Larger prion aggregates were removed from suspension by one 5 min centrifugation at 800g. The supernatant (clarified BH) was collected, diluted 1:10 in 10 mM NaCl and added (100 μL) to 400 μg of microparticles in 400 μL 10 mM NaCl, or in the case of quartz, 20 mg in 400 μL 10 mM NaCl, and vortexed (10 min, 1200 rpm). Samples were incubated in sealed microcentrifuge tubes and rocked gently for 2 h at ambient temperature (clay and quartz particles, 1 hour in the case of the iron (oxy)hydroxide particles). Prions were extracted from the samples with 1 mL 1% SDS (smectites; SWy-2, SAz-1, and SHCa-1, and iron (oxy)hydroxides; ferrihydrite and goethite) or 1 mL of 1% SDS in 100 mM sodium phosphate, pH 7 (KGa-1 and KGa-2), vortexed, shaken at 37°C for 1 h, then heated to 100°C in $5\times$ SDS-PAGE sample buffer (100 mM Tris, 7.5 mM EDTA, 100 mM dithiothreitol (DTT), 350 mM SDS pH 8.0) for 10 min. After extraction, samples were prepared for analysis by SDS polyacrylamide gel electrophoresis (SDS-PAGE) with immunoblot detection.

3.3.5 Reaction of HSO_5^- with prions. Pathogenic prion protein adsorbed to microparticles were mixed with HSO_5^- under the conditions indicated in the Results and Discussion. Concentrations presented for HSO_5^- and sodium thiosulfate reflect final

concentrations. All experiments were conducted at room temperature ($\sim 25\text{ }^{\circ}\text{C}$) unless otherwise indicated, and in polypropylene microcentrifuge tubes in the dark. Reactions with HSO_5^- were halted by addition of an equal volume of 0.5 M sodium thiosulfate (unless otherwise specified). In some cases, samples were pre-treated with sodium thiosulfate to prevent oxidation by HSO_5^- and radical species. Final solution pH of HSO_5^- was stable at approximately 1.5, unless buffered with phosphate as indicated in Results and Discussion.

The iron (oxy)hydroxides goethite ($\text{Fe}^{\text{III}}\text{O}(\text{OH})$) and ferrihydrite ($(\text{Fe}^{\text{III}})_2\text{O}_3 \cdot 0.5\text{H}_2\text{O}$) were added to 50 mM HSO_5^- in concentrations ranging from 0.02-20% w/v final concentrations and incubated for 1 h at room temperature. The suspension was then added to CWD brain homogenate for final (oxy)hydroxide concentrations of 0.01-10% w/v. After 1 h the reaction was quenched with 0.5 M $\text{Na}_2\text{S}_2\text{O}_3$ and the PrP^{TSE} extracted using 1% SDS and prepared for immunoblot detection. Where indicated, HSO_5^- -iron (oxy)hydroxide samples were pre-quenched with 0.5 M $\text{Na}_2\text{S}_2\text{O}_3$ prior to addition of PrP^{TSE} .

3.3.6 Immunoblot detection of PrP^{TSE} . All protein samples were prepared for NuPAGE by adding LDS sample buffer (7 μL) and NuPAGE sample reducing agent (3 μL) containing 500 mM DTT (Invitrogen), and heating (10 min, $90\text{ }^{\circ}\text{C}$). Protein samples (16 μL) were fractionated on 12% bis-tris polyacrylamide gels (Invitrogen) and electrotransferred to polyvinyl difluoride membranes. Membranes were blocked in 5% non-fat dry milk in Tris-buffered saline containing 0.1% Tween 20 overnight at $4\text{ }^{\circ}\text{C}$. PrP was probed with mAb 8G8 and Bar224 (1:5000 and 1:10,000 dilution, respectively, Cayman Chemical). Detection was achieved with HRP-conjugated goat anti-mouse immunoglobulin G (1:10,000; BioRad) and Super Signal West Pico chemiluminescent substrate (Pierce Biotechnology, Rockford, IL). The intensity of immunoreactivity in blots was measured using density histograms of the protein bands and

converted to intensity relative to the corresponding no-soil control (Image J). We present the error associated with this method as the standard deviation of relative intensity measurements of triplicate immunoblots.

3.3.8 Iodometric titrations of HSO_5^- during exposures of microparticles and iron (oxy)hydroxides. Prepared clay or iron (oxy)hydroxide microparticles were added to 25 mM HSO_5^- to a final concentration of 1% w/v and vortexed. Iodometric titrations were used to determine changes in concentration following the manufacturer's protocol.⁴⁷ Briefly, a 10 mL aliquot of 25 mM HSO_5^- was added to 30 mL 1% w/v potassium iodide with 1 M sulfuric acid and immediately titrated with 25 mM thiosulfate solution until the solution turned pale yellow. After adding 1 mL starch indicator solution, titrant was added until the reaction was colorless. Between time points, sample tubes were covered with foil and rocked in the dark for up to two weeks. The pH was recorded at each time point indicated.

3.4 RESULTS AND DISCUSSION

3.4.1 PrP^{TSE} sorption to and extraction from soil microparticles. Washing PrP^{TSE} bound to microparticles with background buffer, centrifuging and analyzing the supernatant for protein by immunoblotting did not show detachment of PrP^{TSE} except from the pure quartz particles (data not shown). These results are consistent with previous reports. Johnson et al. showed PrP^{TSE} in the pellet from clay particles but not quartz, and this was attributable to the smaller specific surface area of quartz microparticles compared to kaolinite and montmorillonite surfaces.¹⁸ Compared to unbound controls, PrP^{TSE} was fully extractable from montmorillonite and hectorite samples (SWy-2, SAz-1, and SHCa-1; Figure S2) with 1% SDS extraction buffer. Strong interactions between PrP^{TSE} and montmorillonite have been shown

previously by a relatively large sorption capacity ($87\text{--}174 \mu\text{g}_{\text{protein}} \cdot \text{mg}_{\text{sorbent}}^{-1}$) and resistance to extraction.¹⁸ Extraction of PrP^{TSE} from iron (oxy)hydroxides by 1% SDS was conducted after 1 h incubation. At all concentrations of iron (oxy)hydroxides for both ferrihydrite and goethite (0.01-10% w/v), PrP^{TSE} was extracted comparable to controls containing equivalent BH concentrations (Figure S3).

Prions adsorbed to kaolinite (KGa-1 and KGa-2), a nonexpandable phyllosilicate clay, required the SDS to be buffered to pH 7 with phosphate to recover amounts comparable to unbound controls (Figure S2). The aluminum oxide/hydroxide gibbsite layer of kaolinite likely increased protein binding affinity at the clay edges, as aluminum oxide/hydroxyl moieties added to the montmorillonite tetrahedral plane increased the binding affinity of DNA molecules compared to montmorillonite alone.⁴⁸ In 1:1 clays, such as kaolinite, hydroxyl groups from the octahedral sheet form hydrogen bonds with the oxygens of the tetrahedral sheet, preventing protein binding of internal surface area and restricting adsorption to the external crystal structure and the edges of the clay; unlike montmorillonite, for each tactoid of kaolinite, one gibbsite plane is exposed.⁴⁹

3.4.2 Effect of microparticle presence on HSO_5^- .

Iodometric titration of 25 mM HSO_5^- from immediately following addition of microparticles to 168 h (1 week) after exposure resulted in substantial decline in HSO_5^- concentration only for samples containing hectorite (SHCa-1; Figure 1A). Hectorite also buffered the solution pH to a larger degree than did the other microparticles investigated (Figure 1B). Hectorite was the only microparticle examined that contained a large proportion of calcium and magnesium oxides (Table S1). The higher pH in the hectorite- HSO_5^- solution is consistent with the alkalinity from the alkali earth oxides present, calcium and magnesium oxide ($\text{p}K_{\text{a}} =$

12.8⁵⁰ and 13.09,⁵¹ respectively), which likely neutralizes a substantial amount of the acid to form a conjugate weak base that results in a pH 6 solution. This suggests the reduction in concentration of HSO_5^- in hectorite may be attributable to its ability to buffer the pH of the solution (Figure 1B). HSO_5^- in the presence of hectorite declined in concentration over time consistent with that seen in the sample when the solution pH was adjusted to pH 3-4 with phosphate buffer (Figure S5). In the iodometric titrations of phosphate-buffered HSO_5^- in the presence of microparticles, the final concentrations of microparticle-exposed HSO_5^- were not significantly different from each other or HSO_5^- alone, however the HSO_5^- concentration between start and 48 h incubation was statistically different for HSO_5^- ($p = 0.0270$), kaolinite ($p = 0.0183$), and hectorite ($p = 0.0037$). This is different from the unbuffered HSO_5^- concentrations where only the HSO_5^- exposed to hectorite was significantly different from the starting concentration at 48 h (Figure 1A).

Ferrihydrite and goethite were exposed to HSO_5^- to determine change in HSO_5^- concentration over time in the presence of iron (oxy)hydroxide particles (Figure S6). The pH of each iron (oxy)hydroxides - HSO_5^- solution was stable at approximately 2-3 throughout 72 h. After 48 h incubation, the concentration of HSO_5^- in the goethite- HSO_5^- solution was significantly decreased from the starting concentration ($p = 0.0414$), and this significance increased for the next 24 hours as the concentration continued to drop. The ferrihydrite- HSO_5^- solution was significantly decreased from the starting concentration ($p = 0.0408$) at 72 h incubation time. Because the pH of the iron (oxy)hydroxides did not change substantially over this time period, it is likely that the iron acts as an activator of HSO_5^- to sulfate radical. To test this hypothesis, iodometric titrations should be repeated in the presence of alcohols that quench radical species.

To test whether the presence of microparticles has an effect on the ability of HSO_5^- to inactivate PrP^{TSE} , we incubated 250 mM HSO_5^- with the kaolinites, montmorillonites, hectorite and quartz for 24 h, centrifuged the samples to remove the microparticles in the pellet, and exposed prions to the supernatant with a final concentration of 125 mM HSO_5^- for 1 h. After quenching the reaction with 1 M sodium thiosulfate and detecting via immunoblot, no PrP^{TSE} was detected in any of the HSO_5^- -exposed samples (Figure S4).

3.4.3 Recovery of PrP^{TSE} from soil minerals after exposure to HSO_5^- . As an initial step toward understanding PrP^{TSE} inactivation when the protein is associated with microparticles, we examined the effect of exposure to HSO_5^- on PrP^{TSE} adsorbed to montmorillonite (SWy-2 and SAz-1) or kaolinite (KGa-1 and KGa-2) (Figure 2). We note that we have previously investigated the ability of HSO_5^- to degrade PrP^{TSE} after being quenched by sodium thiosulfate and showed that inactivation of PrP^{TSE} does not occur,(article in review) and all reactions with HSO_5^- were quenched with sodium thiosulfate prior to protein extraction. Following 30 or 60-min incubation in 125 mM HSO_5^- , the relative intensity of PrP^{TSE} signal decreased to background levels (<10% of control band by densitometry) for all microparticles, except hectorite (SHCa-1) where the band intensity decreased to $11.0 \pm 0.01\%$ after 30 min but was below background after 60 min (Figure 2). A similar trend was seen for exposure to 25 mM HSO_5^- (Figure S7).

We note that after 60 min exposure to 125 mM HSO_5^- , some immunoreactivity below the threshold for densitometry background (<10% of control band) is observable, along with higher-than-expected molecular mass bands in the immunoblot for both kaolinites. This immunoreactivity was consistently seen in both kaolinites, but no other particle. The mechanism for the immunoreactivity is unknown. We suspect that PrP^{TSE} oxidation by HSO_5^- results in

partial protein aggregation that may be supported by unknown properties of kaolinite. Previous research supports this; exposure of bovine serum albumin (BSA) to hydroxyl radical led to the formation of higher molecular weight products (dimers, trimers, and higher) indicating protein aggregation or coupling.⁵² Additionally, the remaining protein may be attributed to greater aggregation of PrP^{TSE} when associated with kaolinite. It is possible that the HSO₅⁻ adsorbed to the positively charged gibbsite surface of the kaolinite, or that the kaolinite activated HSO₅⁻ to sulfate radical species, however no decrease in HSO₅⁻ concentration or change in pH was observed after exposure to kaolinite.

3.4.4 Effect of temperature. Degradation of PrP^{TSE} bound to SWy-2 was examined as a function of temperatures (4 °C, 10 °C, 20 °C, 30 °C, 40 °C, 50 °C). The investigation was not extended to higher temperatures because HSO₅⁻ can be activated to radical species at temperatures >70 °C^{47, 53, 54} and temperatures above 50 °C are unlikely during environmental decontamination attempts. Peroxymonosulfate is stable, and has a half-life of 600 days at 25 °C (unbuffered, pH stable at approximately 1.5),⁵⁵ although a similar compound, persulfate, was shown to have a half-life of ~200 days in the presence of SWy-2 montmorillonite, compared to a half life of >400 days in the presence of silica at the same temperature (solids mass loading 50 g/L, pH 8.0).⁵⁵ Peroxymonosulfate decreased immunoblot detection of PrP^{TSE} bound to SWy-2 montmorillonite at all temperatures tested (Figure 3A). The reaction rate of sodium thiosulfate decreases with temperature, and the rate difference between 4 °C and 10 °C may be large enough for the small variance in observed prion detection, although this same observable decrease in detection at 4 and 10 °C was still seen when the sample temperatures were adjusted to 20 °C for five min prior to addition of sodium thiosulfate. However, the difference in densitometry of

protein bands was not significantly different. Therefore, inactivation of prions by HSO_5^- is not impeded by environmentally relevant, ambient temperature changes.

3.4.5 Effect of pH. The pH of HSO_5^- solution does not affect PrP^{TSE} degradation over the time scales examined (Figure 3B). To determine the effect of pH on degradation of microparticle-bound prions by HSO_5^- , we incubated 15 μL of 10% CWD BH adsorbed with SWy-2 montmorillonite microparticles with 12.5 mM (final concentration) HSO_5^- in phosphate buffers with pH of 4, 5, 6, 7, 8 and 9. When the concentration of HSO_5^- (buffered to pH 4) was investigated in the presence of different microparticles, all samples showed significant declines of HSO_5^- concentration (Figure S5, $k_{\text{obs,HSO}_5^-}=126 \mu\text{mol/h}$, $k_{\text{obs,SWy-2}}=150 \mu\text{mol/h}$, $k_{\text{obs,SAZ-1}}=342 \mu\text{mol/h}$, $k_{\text{obs,KGa-1}}=229 \mu\text{mol/h}$, $k_{\text{obs,SHCa-1}}=190 \mu\text{mol/h}$, $k_{\text{obs,Quartz}}=190 \mu\text{mol/h}$). Some of the particles however, including iron (oxy)hydroxides and the gibbsite surface of kaolinite, have pH-dependent charge that, in principle, may have an effect on association with PrP^{TSE} (e.g., by changing the strength of attachment), and iron (oxy)hydroxides may dissolve at the low pH^{56, 57} observed in the HSO_5^- exposed samples. Disassociation of PrP^{TSE} from clay and/or iron (oxy)hydroxides particles in the presence of HSO_5^- may contribute to prion inactivation. However, the charge of montmorillonite does not change over a broad pH range found in most natural environments.⁴³

3.4.6 Effect of iron oxide. The presence of iron (oxy)hydroxides in soil is a necessary consideration for soil applications of HSO_5^- for prion remediation. Additionally, iron (oxy)hydroxides (both Fe^{II} and Fe^{III}) have previously been shown to activate peroxymonosulfate,^{53, 59} with Fe^{III} having the advantage of slower generation of sulfate radical, which, unlike in the $\text{Fe}^{\text{II}}\text{-HSO}_5^-$ system, is not quenched.⁵⁹ Although we previously showed cobalt activation enhances prion inactivation by HSO_5^- (Chapter 2), the effect of other metal

species on HSO_5^- -induced prion inactivation has not been reported. Goethite and ferrihydrite particles did not inhibit PrP^{TSE} inactivation; however, both the presence of iron (oxy)hydroxides and hectorite decreases the concentration of HSO_5^- over the course of multiple days. Unlike hectorite, the pH of the iron (oxy)hydroxides remained stable at 2.5 and the reduction in HSO_5^- concentration is likely due to activation to sulfate radical. Peroxymonosulfate-iron (oxy)hydroxides suspensions (ferrihydrite and goethite, both Fe^{III}) pre-quenched with 1 M $\text{Na}_2\text{S}_2\text{O}_3$ did not inactivate PrP^{TSE} after 1 h (Figure 4A). However, HSO_5^- solutions containing all tested concentrations (0.01-10% w/v) of both iron (oxy)hydroxides resulted in no detection of PrP^{TSE} by immunoblot (Figure 4B), indicating that iron (oxy)hydroxides do not interfere with HSO_5^- inactivation of prions. To eliminate the possibility of iron (oxy)hydroxides-induced PrP^{TSE} inactivation, the same concentrations of iron (oxy)hydroxides were exposed to 10% CWD BH for 1 h. Detection of PrP^{TSE} by immunoblot showed no differences between densitometry of immunoreactivity of the water-exposed BH control and the immunoreactivity of BH samples exposed to all concentrations of both iron (oxy)hydroxides (Figure S3).

3.4.7 Environmental implications. The development of methods for remediation of prion contaminated lands is an important and necessary component to limit the spread of CWD in captive and wild cervid populations. Our results demonstrate that prion inactivation by HSO_5^- is responsible for the reduced recovery of PrP^{TSE} from soil particles over time. These data provide strong evidence that environmentally relevant pH and temperatures does not inhibit HSO_5^- inactivation of CWD prions. Furthermore, CWD prions are degraded by HSO_5^- despite the association with clay microparticles and iron (oxy)hydroxide particles. Further work is warranted to elucidate any possible mechanism of protection from inactivation by HSO_5^- by association

with kaolinite, as well as expanding this research to additional soil components and whole soils. We show that HSO_5^- has potential for environmental applications in PrP^{TSE} decontamination.

3.5 ACKNOWLEDGEMENTS

This research was funded by NIH grant R01 NS060034. ARC was supported by NIEHS predoctoral training grant number T32ES007015. We thank Matthew Gindervogel for providing the iron (oxy)hydroxides. Article contents are solely the responsibility of the authors and do not represent official views of the sponsors.

3.6 REFERENCES

1. Prusiner, S. B., Molecular biology of prion diseases. *Science* **1991**, 252, (5012), 1515-22.
2. Prusiner, S. B., Prions. *Proc Natl Acad Sci U S A* **1998**, 95, (23), 13363-83.
3. Bolton, D. C.; Bendheim, P. E.; Marmorstein, A. D.; Potempska, A., Isolation and structural studies of the intact scrapie agent protein. *Arch Biochem Biophys* **1987**, 258, (2), 579-90.
4. Prusiner, S. B.; Groth, D. F.; Cochran, S. P.; Masiarz, F. R.; McKinley, M. P.; Martinez, H. M., Molecular properties, partial purification, and assay by incubation period measurements of the hamster scrapie agent. *Biochemistry* **1980**, 19, 4883-91.
5. Pedersen, J. A.; Somerville, R. A., Why and how are CWD and Scrapie sometimes spread via environmental routes? In *Decontamination of Prions*, Reisner, D.; Deslys, J.-P., Eds. Dusseldorf University Press: Dusseldorf Germany, 2012; pp 19-37.
6. Miller, M. W.; Williams, E. S.; Hobbs, N. T.; Wolfe, L. L., Environmental sources of prion transmission in mule deer. *Emerg Infect Dis* **2004**, 10, (6), 1003-6.
7. Brown, P.; Gajdusek, D. C., Survival of scrapie virus after 3 years' interment. *Lancet* **1991**, 337, (8736), 269-70.
8. Georgsson, G.; Sigurdarson, S.; Brown, P., Infectious agent of sheep scrapie may persist in the environment for at least 16 years. *J Gen Virol* **2006**, 87, (Pt 12), 3737-40.
9. Seidel, B.; Thomzig, A.; Buschmann, A.; Groschup, M. H.; Peters, R.; Beekes, M.; Tertytze, K., Scrapie agent (strain 263K) can transmit disease via the oral route after persistence in soil over years. *PLoS One* **2007**, 2, (5), e435.
10. Schramm, P. T.; Johnson, C. J.; Mathews, N. E.; McKenzie, D.; Aiken, J. M., Potential role of soil in the transmission of prion disease. *Rev Mineral Geochem* **2006**, 64, 135-52.
11. Smith, C. B.; Booth, C. J.; Pedersen, J. A., Fate of prions in soil: a review. *J Environ Qual* **2011**, 40, (2), 449-61.
12. Haley, N. J.; Seelig, D. M.; Zabel, M. D.; Telling, G. C.; Hoover, E. A., Detection of CWD prions in urine and saliva of deer by transgenic mouse bioassay. *PLoS One* **2009**, 4, (3), e4848.
13. Mathiason, C. K.; Powers, J. G.; Dahmes, S. J.; Osborn, D. A.; Miller, K. V.; Warren, R. J.; Mason, G. L.; Hays, S. A.; Hayes-Klug, J.; Seelig, D. M.; Wild, M. A.; Wolfe, L. L.; Spraker, T. R.; Miller, M. W.; Sigurdson, C. J.; Telling, G. C.; Hoover, E. A., Infectious prions in the saliva and blood of deer with chronic wasting disease. *Science* **2006**, 314, (5796), 133-6.

14. Race, R.; Jenny, A.; Sutton, D., Scrapie infectivity and proteinase K-resistant prion protein in sheep placenta, brain, spleen, and lymph node: implications for transmission and antemortem diagnosis. *The Journal of Infectious Diseases* **1998**, *178*, 949-53.
15. Tamgüney, G.; Miller, M. W.; Wolfe, L. L.; Sirochman, T. M.; Glidden, D. V.; Palmer, C.; Lemus, A.; DeArmond, S. J.; Prusiner, S. B., Asymptomatic deer excrete infectious prions in faeces. *Nature* **2009**, *461*, (7263), 529-32.
16. Jacobson, K. H.; Lee, S.; Somerville, R. A.; McKenzie, D.; Benson, C. H.; Pedersen, J. A., Transport of the pathogenic prion protein through soils. *Journal of Environmental Quality* **2010**, *39*, (4), 1145-52.
17. Nannipieri, P.; Smalla, K., *Nucleic acids and proteins in soil (Soil Biology)*. Springer: 2006; Vol. 8, p 458.
18. Johnson, C. J.; Phillips, K. E.; Schramm, P. T.; McKenzie, D.; Aiken, J. M.; Pedersen, J. A., Prions adhere to soil minerals and remain infectious. *PLoS Pathog* **2006**, *2*, (4), e32.
19. Cooke, C. M.; Rodger, J.; Smith, A.; Fernie, K.; Shaw, G.; Somerville, R. A., Fate of prions in soil: detergent extraction of PrP from soils. *Environ Sci Technol* **2007**, *41*, 811-817.
20. Ma, X.; Benson, C. H.; McKenzie, D.; Aiken, J. M.; Pedersen, J. A., Adsorption of pathogenic prion protein to quartz sand. *Environ Sci Technol* **2007**, *41*, 2324-2330.
21. Maddison, B. C.; Owen, J. P.; Bishop, K.; Shaw, G.; Rees, H. C.; Gough, K. C., The interaction of ruminant PrPSC with soils is influenced by prion source and soil type. *Environ Sci Technol* **2010**, *44*, 8503-8.
22. Leita, L.; Fornasier, F.; De Nobili, M.; Bertoli, A.; Genovesi, S.; Sequi, P., Interactions of prion proteins with soil. *Soil Biology and Biochemistry* **2006**, *38*, (7), 1638-1644.
23. Johnson, C. J.; Pedersen, J. A.; Chappell, R. J.; McKenzie, D.; Aiken, J. M., Oral transmissibility of prion disease is enhanced by binding to soil particles. *PLoS Pathog* **2007**, *3*, (7), e93.
24. Colby, D. W.; Prusiner, S. B., Prions. *Cold Spring Harb Perspect Biol* **2011**, *3*, (1), a006833.
25. Taylor, D. M., Inactivation of prions by physical and chemical means. *J Hosp Infect* **1999**, *43 Suppl*, S69-76.
26. Rutala, W. A.; Weber, D. J.; Society for Healthcare Epidemiology of, A., Guideline for disinfection and sterilization of prion-contaminated medical instruments. *Infect Control Hosp Epidemiol* **2010**, *31*, (2), 107-17.

27. Ding, N.; Neumann, N. F.; Price, L. M.; Braithwaite, S. L.; Balachandran, A.; Belosevic, M.; El-Din, M. G., Inactivation of template-directed misfolding of infectious prion protein by ozone. *Appl Environ Microbiol* **2012**, 78, (3), 613-20.
28. Ding, N.; Neumann, N. F.; Price, L. M.; Braithwaite, S. L.; Balachandran, A.; Mitchell, G.; Belosevic, M.; Gamal El-Din, M., Kinetics of ozone inactivation of infectious prion protein. *Appl Environ Microbiol* **2013**, 79, (8), 2721-30.
29. Lee, H.; Lee, H. J.; Sedlak, D. L.; Lee, C., pH-Dependent reactivity of oxidants formed by iron and copper-catalyzed decomposition of hydrogen peroxide. *Chemosphere* **2013**, 92, (6), 652-8.
30. Park, S. J.; Kim, N. H.; Jeong, B. H.; Jin, J. K.; Choi, J. K.; Park, Y. J.; Kim, J. I.; Carp, R. I.; Kim, Y. S., The effect of Fenton reaction on protease-resistant prion protein (PrP^{Sc}) degradation and scrapie infectivity. *Brain Res* **2008**, 1238, 172-80.
31. Paspaltsis, I.; Berberidou, C.; Poullos, I.; Sklaviadis, T., Photocatalytic degradation of prions using the photo-Fenton reagent. *J Hosp Infect* **2009**, 71, (2), 149-56.
32. Solassol, J.; Pastore, M.; Crozet, C.; Perrier, V.; Lehmann, S., A novel copper-hydrogen peroxide formulation for prion decontamination. *The Journal of Infectious Diseases* **2006**, 194, 865-9.
33. Paspaltsis, I.; Kotta, K.; Lagoudaki, R.; Grigoriadis, N.; Poullos, I.; Sklaviadis, T., Titanium dioxide photocatalytic inactivation of prions. *J Gen Virol* **2006**, 87, (Pt 10), 3125-30.
34. Zobeley, E.; Flechsig, E.; Cozzio, A.; Enari, M.; Weissmann, C., Infectivity of scrapie prions bound to a stainless steel surface. *Mol Med* **1999**, 5, 240-243.
35. Johnson, C. J.; McKenzie, D.; Pedersen, J. A.; Aiken, J. M., Meat and bone meal and mineral feed additives may increase the risk of oral prion disease transmission. *J Toxicol Environ Health A* **2011**, 74, (2-4), 161-6.
36. Anipsitakis, G. P., Cobalt/peroxymonosulfate and related oxidizing reagents for water treatment. *PhD Thesis* **2005**.
37. Anipsitakis, G. P.; Dionysiou, D. D.; Gonzalez, M. A., Cobalt-mediated activation of peroxymonosulfate and sulfate radical attack on phenolic compounds. Implications of chloride ions. *Environ Sci Technol* **2006**, 40, (3), 1000-7.
38. Violante, A.; Gianfreda, L., Role of biomolecules in the formation and reactivity toward nutrients and organics of variable charge minerals and organomineral complexes in soil environment. In *Soil Biochemistry*, Stotzky, G., Ed. Marcel Dekker, Inc: Germany, 2000; pp 207-256.

39. Norde, W.; Lyklema, J., The adsorption of human plasma albumin and bovine pancreas ribonuclease at negatively charged polystyrene surfaces. *Journal of Colloid and Interface Science* **1978**, 66, (2), 257-265.
40. Nielsen, K. M.; Calamai, L.; Pietramellara, G., Stabilization of extracellular DNA and proteins by transient binding to various soil components. In *Nucleic Acids and Proteins in Soil*, Nannipieri, P.; Smalla, K., Eds. Springer: Germany, 2006; Vol. 8, pp 142-157.
41. Johnson, C. J.; Herbst, A.; Duque-Velasquez, C.; Vanderloo, J. P.; Bochsler, P.; Chappell, R.; McKenzie, D., Prion protein polymorphisms affect chronic wasting disease progression. *PLoS One* **2011**, 6, (3), e17450.
42. Sajnani, G.; Requena, J. R., Prions, proteinase K and infectivity. *Prion* **2012**, 6, (5), 430-2.
43. Gao, J.; Pedersen, J. A., Adsorption of sulfonamide antimicrobial agents to clay minerals. *Environ Sci Technol* **2005**, 39, (24), 9509-16.
44. Chipera, S. J.; Bish, D. L., Baseline studies of the clay minerals society source clays; powder X-ray diffraction analysis. *Clays and Clay Minerals* **2001**, 49, (5), 398-409.
45. Mermut, A. R.; Cano, A. F., Baseline studies of the clay minerals society source clays: chemical analysis of major elements. *Clays and Clay Minerals* **2001**, 49, (5), 381-386.
46. Mermut, A. R.; Lagaly, G., Baseline studies of the clay minerals society source clays: layer-charge determination and characteristics of those minerals containing 2:1 layers. *Clays and Clay Minerals* **2001**, 49, (5), 393-396.
47. DuPont, DuPont oxone technical attributes. In DuPont, Ed. 2008.
48. Cai, P.; Huang, Q.; Li, M.; Liang, W., Binding and degradation of DNA on montmorillonite coated by hydroxyl aluminum species. *Colloids Surf B Biointerfaces* **2008**, 62, (2), 299-306.
49. Fiorito, T. M.; Icoz, I.; Stotzky, G., Adsorption and binding of the transgenic plant proteins, human serum albumin, β -glucuronidase, and Cry3Bb1, on montmorillonite and kaolinite: Microbial utilization and enzymatic activity of free and clay-bound proteins. *Applied Clay Science* **2008**, 39, (3-4), 142-150.
50. China Calcium Oxide. <http://csfertilizer.en.made-in-china.com/product/nejQTmsvaBrR/China-Calcium-Oxide-Cao-80-95-Industrial-Grade.html> (8/21/15),
51. DrugBank: Magnesium Oxide. <http://www.drugbank.ca/drugs/db01377> (8/21/15),
52. Davies, K. J. A., Protein damage and degradation by oxygen radicals. *The Journal of Biological Chemistry* **1987**, 262, (20), 9895-901.

53. Tan, C.; Gao, N.; Deng, Y.; Deng, J.; Zhou, S.; Li, J.; Xin, X., Radical induced degradation of acetaminophen with Fe₃O₄ magnetic nanoparticles as heterogeneous activator of peroxymonosulfate. *J Hazard Mater* **2014**, *276*, 452-60.
54. Yang, S.; Wang, P.; Yang, X.; Shan, L.; Zhang, W.; Shao, X.; Niu, R., Degradation efficiencies of azo dye Acid Orange 7 by the interaction of heat, UV and anions with common oxidants: persulfate, peroxymonosulfate and hydrogen peroxide. *J Hazard Mater* **2010**, *179*, (1-3), 552-8.
55. Liu, H.; Bruton, T. A.; Doyle, F. M.; Sedlak, D. L., In situ chemical oxidation of contaminated groundwater by persulfate: decomposition by Fe(III)- and Mn(IV)-containing oxides and aquifer materials. *Environ Sci Technol* **2014**, *48*, (17), 10330-6.
56. Shi, Z.; Bonneville, S.; Krom, M. D.; Carslaw, K. S.; Jickells, T. D.; Baker, A. R.; Benning, L. G., Iron dissolution kinetics of mineral dust at low pH during simulated atmospheric processing. *Atmospheric Chemistry and Physics* **2011**, *11*, (3), 995-1007.
57. Rubasinghege, G.; Lentz, R. W.; Scherer, M. M.; Grassian, V. H., Simulated atmospheric processing of iron oxyhydroxide minerals at low pH: roles of particle size and acid anion in iron dissolution. *Proc Natl Acad Sci U S A* **2010**, *107*, (15), 6628-33.
58. Russo, F.; Johnson, C. J.; Johnson, C. J.; McKenzie, D.; Aiken, J. M.; Pedersen, J. A., Pathogenic prion protein is degraded by a manganese oxide mineral found in soils. *J Gen Virol* **2009**, *90*, (Pt 1), 275-80.
59. Rastogi, A.; Al-Abed, S. R.; Dionysiou, D. D., Sulfate radical-based ferrous–peroxymonosulfate oxidative system for PCBs degradation in aqueous and sediment systems. *Applied Catalysis B: Environmental* **2009**, *85*, (3-4), 171-179.

3.7 Figures

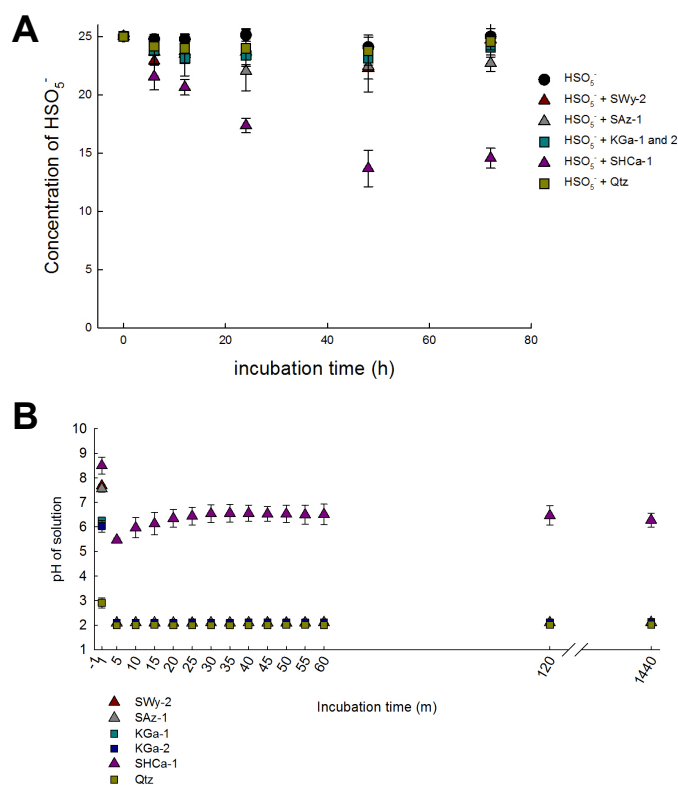


Figure 1 Concentration of HSO_5^- over time is dependent on the presence of certain microparticles and pH. Peroxymonosulfate (25 mM) was added to purified, size separated microparticles and the concentration of the HSO_5^- in solution was measured over time using idiometric titrations. After 12 hours, the concentration of HSO_5^- with hectorite was statistically different from HSO_5^- alone ($p < 0.01$) and after 24 hours, the concentration of HSO_5^- with hectorite was statistically different from all other treatments ($p < 0.01$). (B) Microparticles were added to unbuffered HSO_5^- (pH 1.86) for a final concentration of 1% weight per volume and pH was monitored over the course of 60 m (1 h) with two additional time points at 120 (2 h) and 1440 m (24 h). Peroxymonosulfate with hectorite was significantly different ($p < 0.01$) from all other solutions at all time points pH was measured.

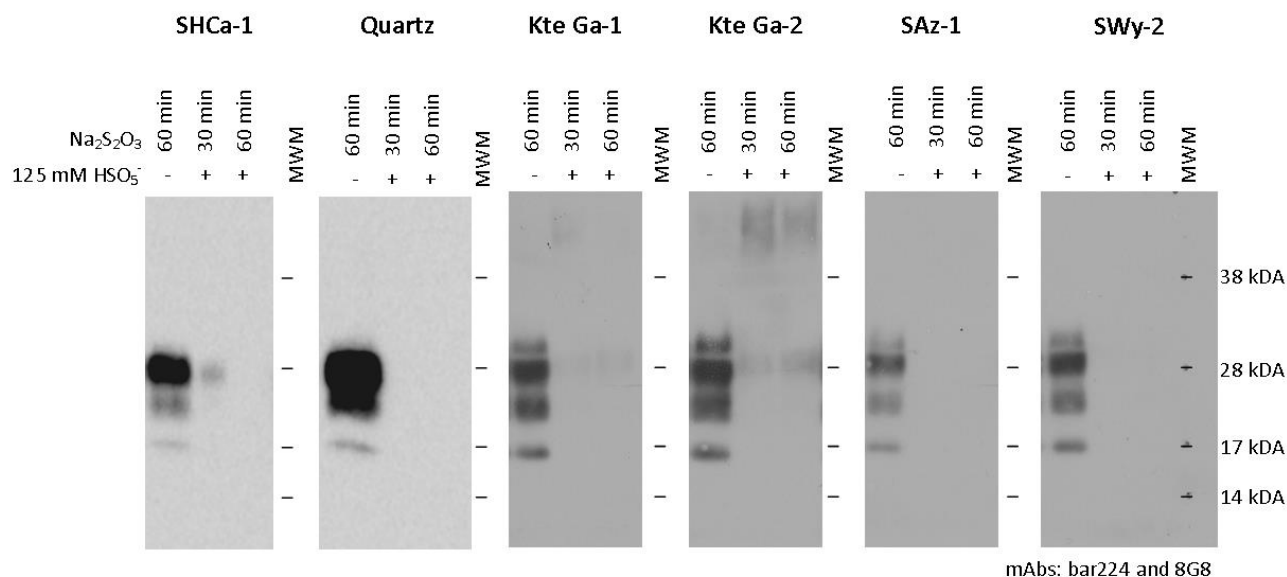


Figure 2. Clay microparticles do not inhibit inactivation of CWD prion protein by HSO_5^- . CWD prions were adsorbed to montmorillonite, kaolinite microparticles ($d_0 = 0.5\text{-}2\ \mu\text{m}$), and quartz microparticles for 2 h and then exposed to 125 mM HSO_5^- or water. Reactions were quenched with 1 M $\text{Na}_2\text{S}_2\text{O}_3$ after 30 and 60 min, as indicated. Prions were extracted in 1% SDS for 1 h (in 100 mM sodium phosphate buffer, pH 7 for Kaolinites). Exposure to 25 mM HSO_5^- shown in Figure S5. Immunoblots were probed with monoclonal antibodies bar224 and 8G8. Blots shown are representative of three replicates.

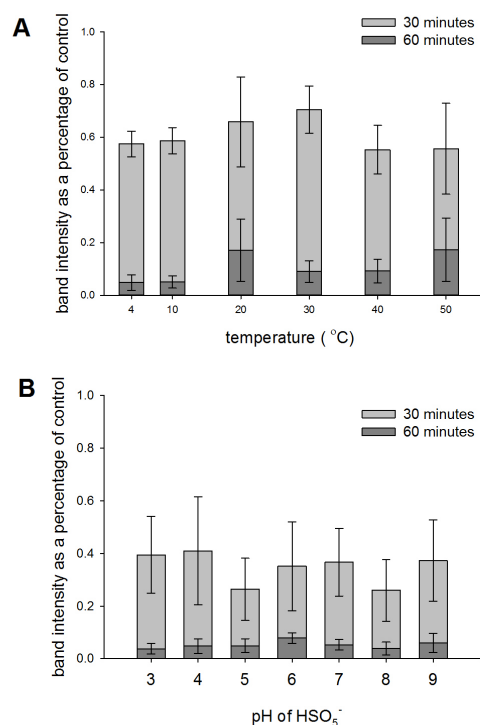


Figure 3. Inactivation of prions bound to SWy-2 microparticles by HSO_5^- is not dependent on temperature or pH. (A) Prions (15 μL of 10% CWD BH bound to SWy-2 microparticles) and 12.5 mM HSO_5^- were separately temperature equilibrated (between 4 and 50 $^{\circ}\text{C}$) for 1 h prior to HSO_5^- exposure. (B) Prions (25 μL of 10% BH) was incubated with 25 μL HSO_5^- (12.5 mM final volume) adjusted to various pH with phosphate buffer. (A and B) After 30 and 60 min, the reaction was quenched with 0.5 M sodium thiosulfate. Prions were extracted in 1% SDS for 1 h (pH 7 for Kaolinites). Densitometry was from three replicate immunoblots probed with mAbs bar224 and 8G8. Significance was determined by one-way ANOVA.

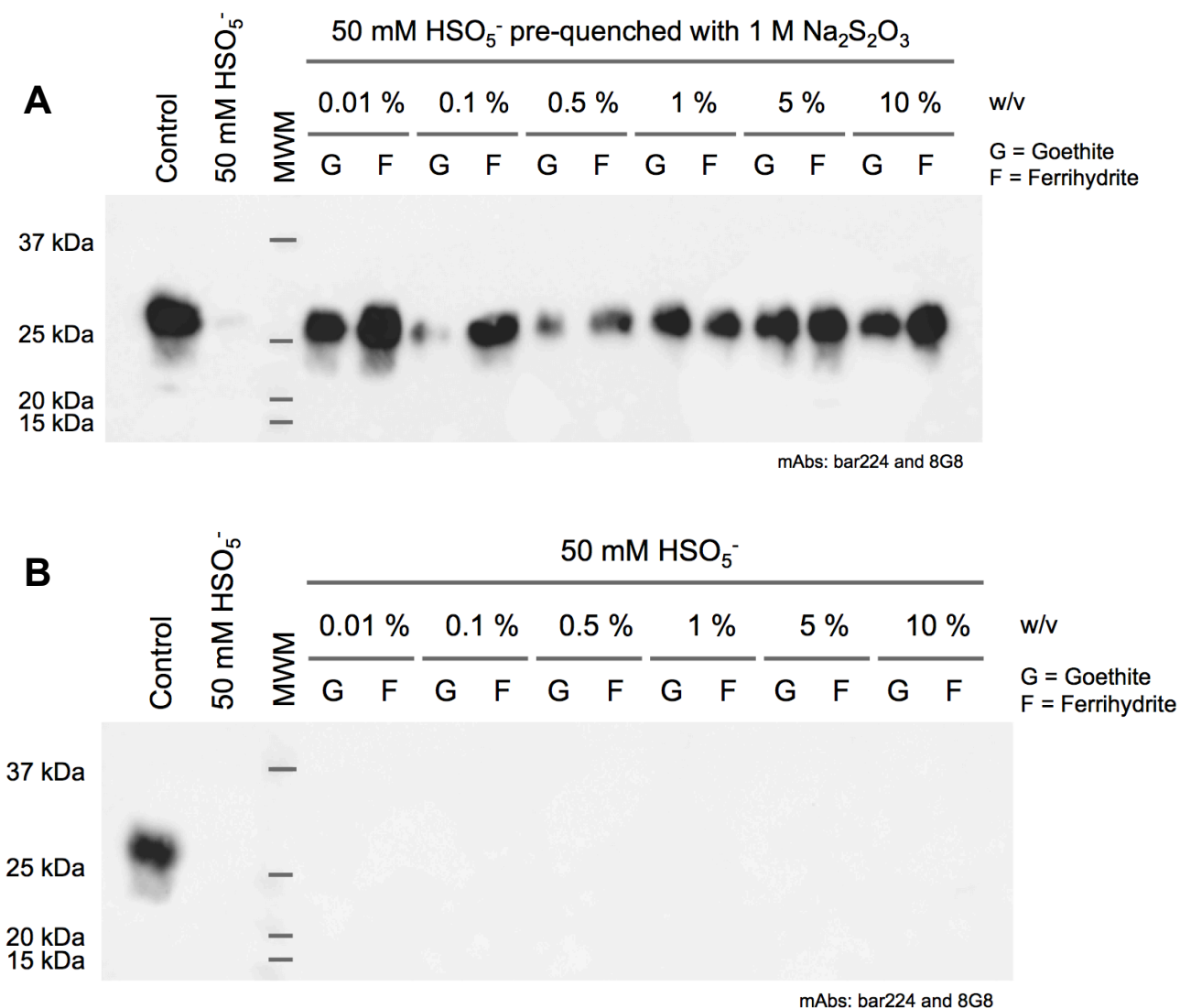


Figure 4. Iron (oxy)hydroxides presence in HSO_5^- does not impact PrP^{TSE} inactivation. CWD PrP^{TSE} (25 μL of 10% BH) was incubated with 25 mM HSO_5^- (50 mM final volume) containing various concentrations of goethite or ferrihydrite (0.01% - 10% final w/v) for 60 min before the reaction was stopped with 1 M sodium thiosulfate. The same concentrations of iron (oxy)hydroxides were pre-quenched with 1 M sodium thiosulfate for 1 h prior to exposure to CWD BH. Prions were extracted in 1% SDS for 1 h (pH 7 for kaolinites). Immunoblots probed with mAbs Bar224 and 8G8.

3.8 APPENDIX

Supporting Information for Chapter 3

Degradation of pathogenic prion protein from soil microparticles by peroxymonosulfate*

*A version of this chapter will be submitted to *Environmental Science & Technology* with Garvey, D., Epstein, G., Millevolte, R., and Pedersen, J.A. as co-authors.

Table of Contents

	Page
3.8.1 Tables	105
Table S1 Chemical composition of microparticles	105
Table S2. Characterizations of prepared smectites	106
3.8.2 Figures	107
S1. X-ray diffraction data of prepared smectites.	107
S2. SDS extraction recovered PrP ^{TSE} from soil microparticles.	108
S3. The presence of iron oxides do not inhibit detection of PrP ^{TSE} by Western blot.	109
S4. HSO ₅ ⁻ previously exposed to microparticles still degrade prions.	110
S5. Concentration decline of pH-buffered HSO ₅ ⁻ -microparticle solutions.	111
S6. Concentration of peroxymonosulfate over time in the presence of iron oxides.	112
S7. Clay microparticles do not inhibit inactivation of CWD prion protein by HSO ₅ ⁻ .	113
S8. Densitometry of PrP ^{TSE} exposed to 25 mM or 125 mM HSO ₅ ⁻ for 30 or 60 minutes.	114

3.8.1 Tables

	SiO ₂	Al ₂ O ₃	TiO ₂	Fe ₂ O ₃	FeO	MnO	MgO	CaO	Na ₂ O	K ₂ O	P ₂ O ₅	S	F	Li ₂ O
KGa-1	44.2	39.7	1.39	0.13	0.08	0.002	0.03	n.d.	0.013	0.05	0.034		0.013	
KGa-2	43.9	38.5	2.08	0.98	0.15	n.d.	0.03	n.d.	0.005	0.065	0.045	0.02		
SAz-1	60.4	17.6	0.24	1.42	0.08	0.001	6.46	2.82	0.063	0.19	0.02		0.287	
SWy-2	62.9	19.6	0.09	3.35	0.32	0.006	3.05	1.68	1.53	0.53	0.049	0.05	0.111	
SHCa-1	34.7	0.69	0.038	0.02	0.25	0.008	15.3	23.4	1.26	0.13	0.014	0.01	2.6	2.18
Qtz	100													

Table S1. Chemical composition of clay and SiO₂ microparticles.

The unpurified microparticles used had the chemical composition indicated. These data are from information provided by the Clay Minerals Society Source Clays Repository (West Lafayette, Indiana, United States).

		d_{001} (nm)	Θ Angle	Particle hydrodynamic diameter (μm)	Cation exchange capacity ($\mu\text{mol/g}$)	Cation exchange capacity ($\mu\text{mol/m}^2$)	Surface area (N_2 area, m^2/g)
Mte	SWy-2	1.26 ± 0.04	7.65 ± 0.06	0.5-2.0	764	24.01	31.82 ± 0.22
	SAz-1	1.29 ± 0.07	6.98 ± 0.27	0.5-2.0	1200	12.32	97.42 ± 0.58
Hectorite	SHCa-1	1.28 ± 0.01	6.91 ± 0.01	0.5-2.0	439	6.95	63.19 ± 0.50
Kte	KGa-1			0.5-2.0	20	1.99	10.05 ± 0.02
	KGa-2			0.5-2.0	33	1.40	23.50 ± 0.06
Quartz				180-250			

Table S2. Characterizations of prepared smectites. Characterization of microparticles used. Cation exchange capacity and surface area data was calculated from information provided by the Clay Minerals Society Source Clays Repository (West Lafayette, Indiana, United States).

3.8.2 Figures

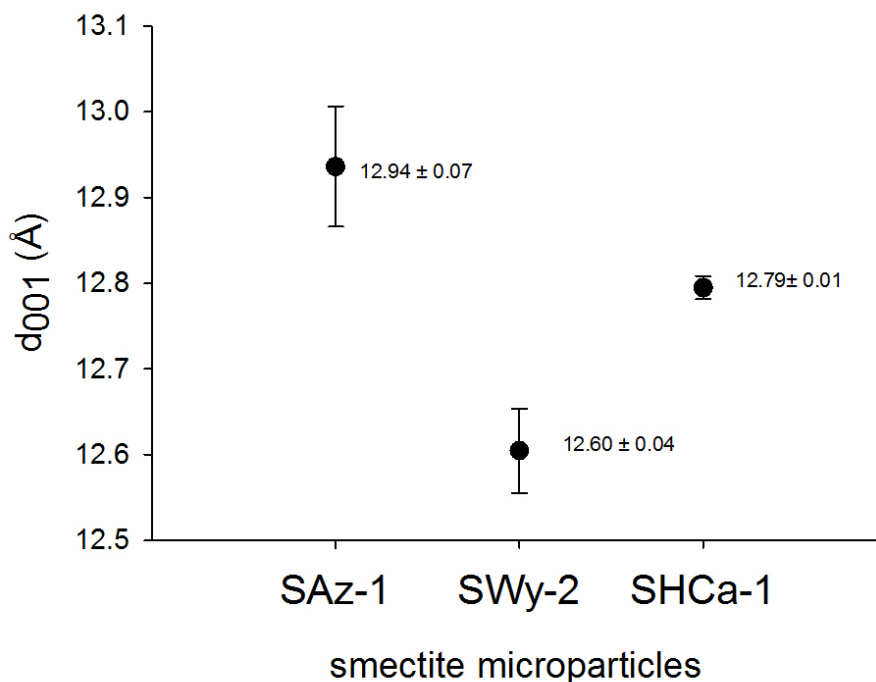


Figure S1. X-ray diffraction data of prepared smectites. A 0.01% w/v 10 mM NaCl solution of each homo-ionized smectite (SWy-2, SAz-1, and SHCa-1) was made into a slurry, vortexed, and centrifuged (10 min, 16,000g). The layer above the pellet was layered on silica wafers and dried overnight. The basal d_{001} spacings of the near homoionic smectites (Na^+ -SWy-2, Na^+ -SAz-1, and Na^+ -SHCa-1) were determined by X-ray diffraction on a Scintag PAD V diffractometer (Cupertino, California, US) using $\text{CuK}\alpha$ with a step size of 0.02° and a dwell time of 2s. Each value is an average of three replicates. Error is one standard deviation.

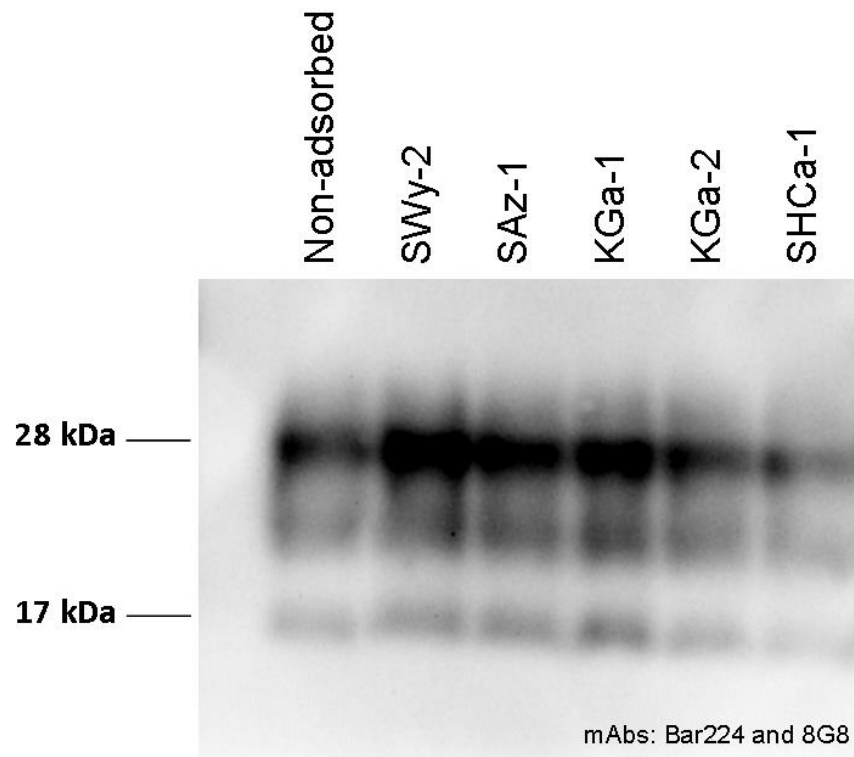


Figure S2. SDS extraction recovered PrP^{TSE} from soil microparticles. A 100 μ L volume of PK-treated CWD BH was incubated with 400 μ g of montmorillonite (SWy-2, SAz-1), kaolinite (KGa-1, KGa-2), hectroite (SHCa-1), or 20 mg quartz in 400 μ L 10 mM NaCl for 2 or 48 h. Prions were extracted in 1% SDS for 1 h (100 mM sodium phosphate buffer, pH 7 for kaolinites). Incubation of PrP^{TSE} with microparticles did not reduce detection by immunoblot. Experiments were conducted in triplicate. Immunoblots used mAb 8G8 and Bar244.

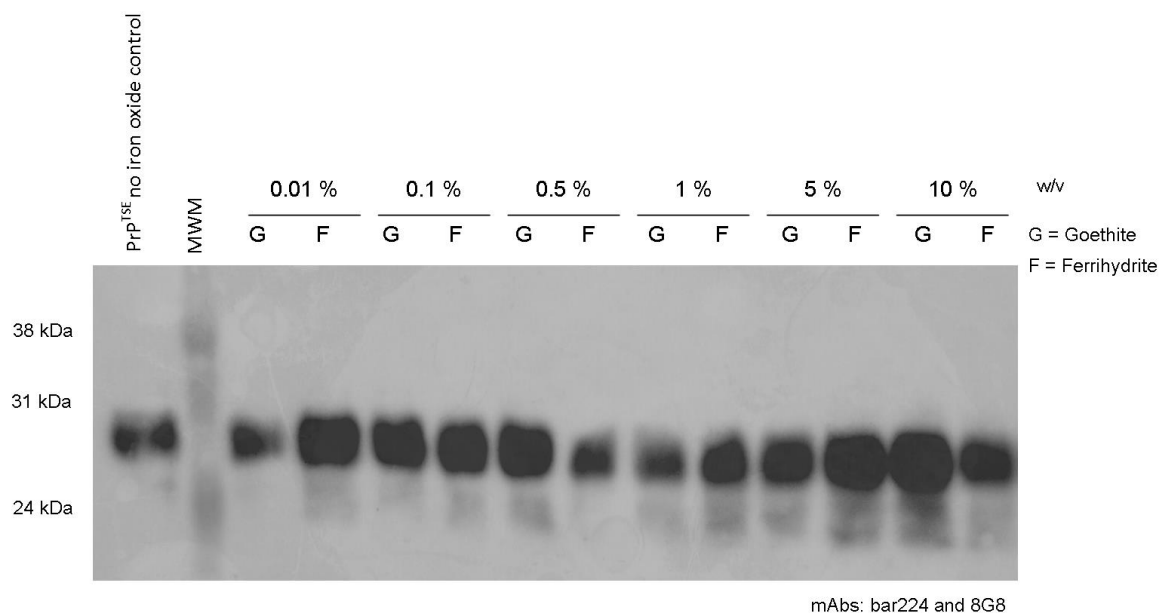


Figure S3. The presence of iron oxides do not inhibit detection of PrP^{TSE} by Western blot. CWD PrP^{TSE} (25 μ L of 10% BH) was incubated with 25 μ L of various concentrations of goethite or ferrihydrite (0.01% - 10% final w/v) for 60 min. Prions were extracted in 1% SDS for 1 h prior to preparation for SDS-PAGE. Immunoblot probed with mAbs bar224 and 8G8.



Figure S4. HSO₅⁻ previously exposed to microparticles still degrade prions.

Peroxymonosulfate (250 mM) was exposed to 10% w/v microparticles for 24 h. Microparticles were separated by centrifugation for 10 min at 800g at room temperature. The peroxymonosulfate supernatant was incubated with 20 μ L of CWD BH for a final HSO₅⁻ concentration of 125 mM. Reactions were quenched with 1 M Na₂S₂O₃ after 60 min and samples were prepped for Western blot detection. Membranes were probed with monoclonal antibodies Bar224 and 8G8. Blot shown is representative of three replicates.

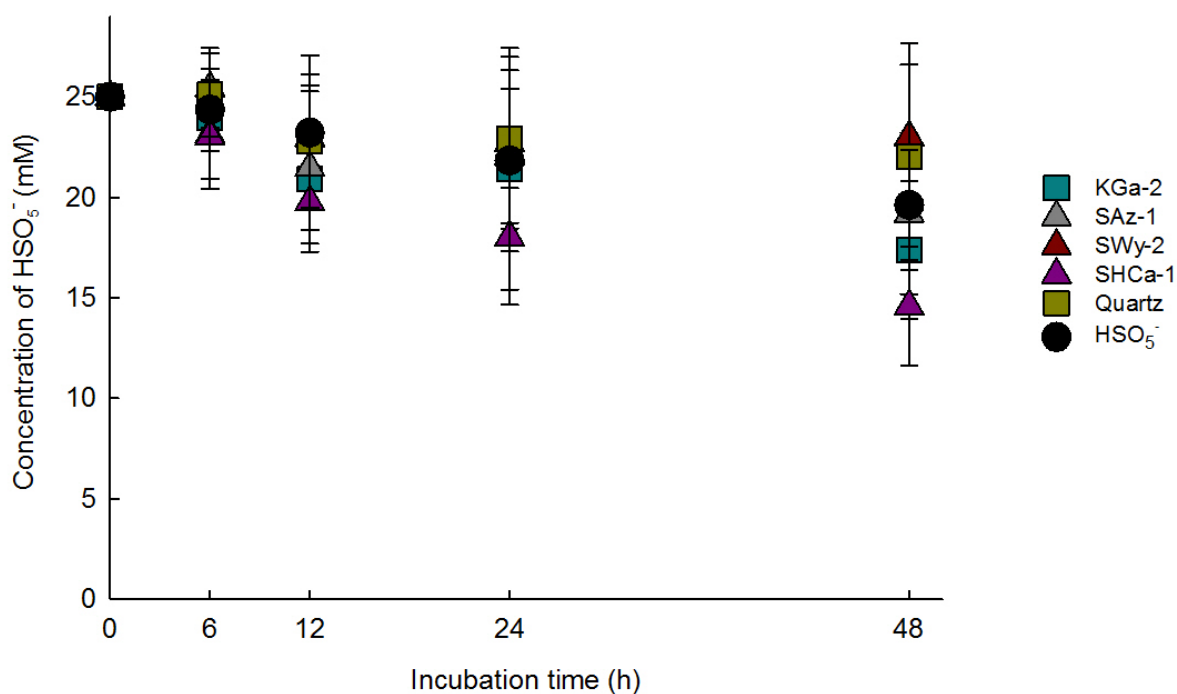


Figure S5. Concentration decline of pH-buffered HSO₅⁻-microparticle solutions.

Peroxymonosulfate (25 mM) pH adjusted to 4 with phosphate was added to purified, size separated microparticles (10% w/v) and the concentration of the HSO₅⁻ in solution was measured over time using idiometric titrations. After 48 h, the concentration of HSO₅⁻ alone or with each microparticle was not statistically different ($p > 0.05$). The HSO₅⁻ concentration between start and 48 hours incubation was statistically different for PMS ($p = 0.0270$), KGa-2 ($p = 0.0183$), and SHCa-1 ($p = 0.0037$).

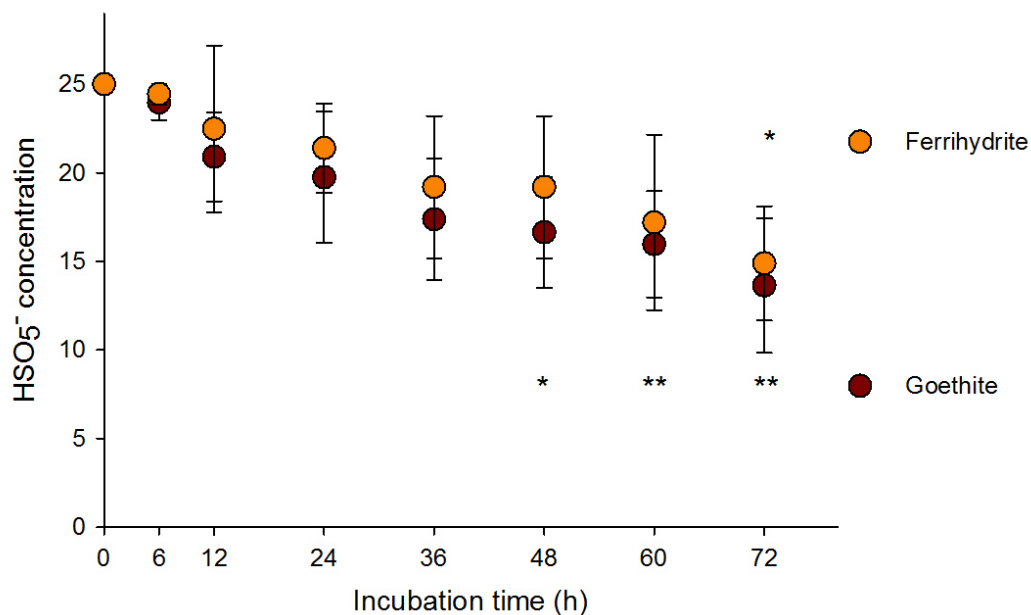


Figure S6 Concentration of peroxymonosulfate over time in the presence of iron oxides. Peroxymonosulfate (25 mM) was added to 10% w/v ferrihydrite or goethite and the concentration of the HSO_5^- in solution was measured over time using idiometric titrations. After 48 hours, the concentration of HSO_5^- in the presence of goethite was statistically significant from the original concentration ($p=0.0414$ after 48 hours, $p=0.0035$ after 60 hours $p=0.0241$ after 72 hours). After 72 hours, the concentration of HSO_5^- in the presence of ferrihydrite was statistically significant from the original concentration ($p=0.0408$).

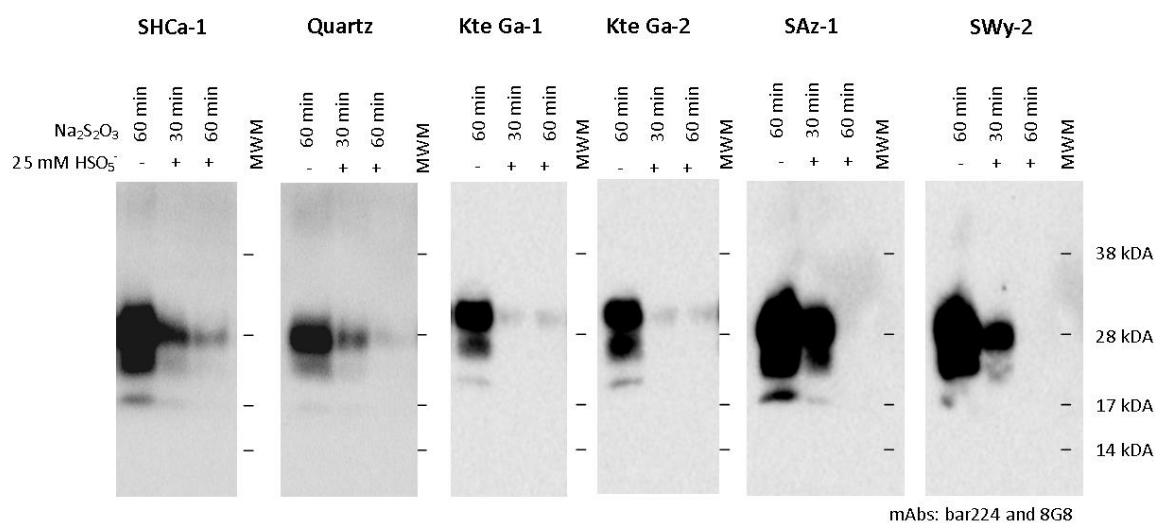


Figure S7. Clay microparticles do not inhibit inactivation of CWD prion protein by HSO_5^- . CWD prions were adsorbed to montmorillonite and kaolinite microparticles ($d_h = 0.5\text{--}2\ \mu\text{m}$), and quartz particles (0.18-0.25 mm) for 2 h and then exposed to 25 mM peroxymonosulfate or water for 30 or 60 min. Reactions were quenched with 1 M $\text{Na}_2\text{S}_2\text{O}_3$. Prions were extracted in 1% SDS for 1 h (in 100 mM sodium phosphate, pH 7 for Kaolinites). Western blots were probed with monoclonal antibodies Bar224 and 8G8. Blots shown are representative of three replicates.

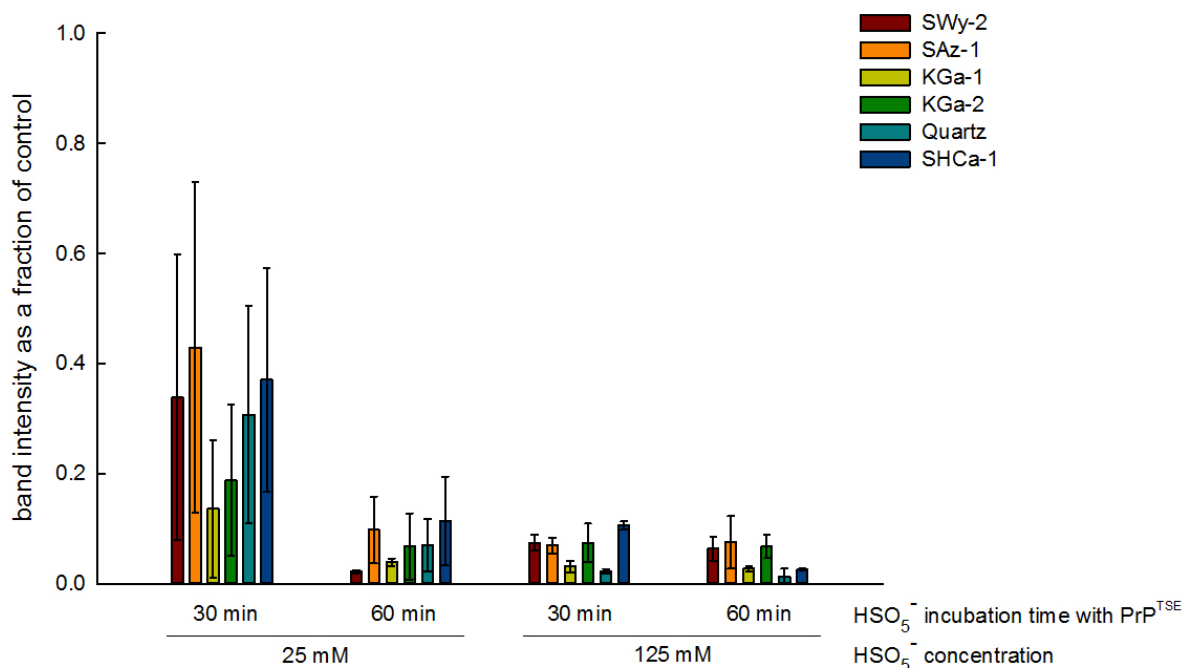


Figure S8. Densitometry of PrP^{TSE} exposed to 25 mM or 125 mM HSO₅⁻ for 30 or 60 minutes. CWD BH was incubated with either 25 or 125 mM HSO₅⁻ in the presence of CoCl₂ (125:3 molar ratio) for 30 min or 60 min. Substantial degradation of PrP^{TSE} was seen at 25 mM, with densitometry approaching background levels (0.1) for both timepoints at 125 mM HSO₅⁻ and 60 minutes for 25 mM HSO₅⁻. Error bars represent standard deviations of experimental triplicates. Immunoblots were probed with mAb 8G8/Bar224. Immunoblot densitometry values normalized to PrP^{TSE} in ultrapure water ($n = 4$). Error bars represent one standard deviation.

Chapter 4

Extraction, detection, and decontamination of chronic wasting disease agent from soil*

*A version of this chapter will be submitted to *Environmental Science & Technology* with Johnson, C.J. and Pedersen, J.A. as co-authors

4.1 ABSTRACT.

Chronic wasting disease (CWD) is a prion disease that affects North American members of the deer family (cervids). Substantial evidence implicates an environmental reservoir of infectivity as a result of excreted pathogenic agent from diseased animals. A strong interest exists for effective environmental prion decontamination methods; however, few studies have investigated the efficacy of inactivation methods when the disease agent is associated with soil or soil constituents. We have previously shown that peroxymonosulfate, (HSO_5^-) either alone as when activated to sulfate radical using a transition metal catalyst, can inactivate prions from two mammalian species, even when associated with aluminosilicate clay particles, goethite, or ferrihydrite. Here we investigated the ability of HSO_5^- to inactivate prions associated with whole soil. To achieve this objective, we optimized protocols to recover prions from different soils for detection by Western blot and amplification by an *in vitro* protein conversion assay, protein misfolding cyclic amplification (PMCA). Once optimized, we examined the extent of HSO_5^- -induced degradation by immunodetection, and reduction and reduction in the *in vitro* templating ability of the protein by PMCA, as a proxy for infectivity. We found HSO_5^- decreased the *in vitro* templating properties of CWD prions using PMCA by a factor exceeding 10^5 , indicating that HSO_5^- is effective for inactivating prions in soil matrices. We also investigated the toxicity of HSO_5^- to soil bacteria and fungi and to grass. Low concentrations of HSO_5^- substantially reduced fungal and bacterial colony formation. Furthermore, application to Kentucky bluegrass sod resulted in toxicity; nevertheless, potting soil saturated in HSO_5^- was able to produce grass at nearly the same rate and average leaf length as unexposed soil. Our results indicate that HSO_5^- may be an efficient tool in the environment to degrade prions and remediate environmental reservoirs of CWD infectivity. Furthermore, we believe our toxicity results provides a starting

point for the evaluation of long-term effects of HSO_5^- to relevant environmental species that may be exposed during prion remediation.

4.2 INTRODUCTION

Transmissible spongiform encephalopathies (TSEs) are a class of progressive neurodegenerative diseases caused by prions, a unique infectious agent that catalytically converts a normally produced, benign, cellular form of the prion protein (PrP^{C}) to the misfolded and disease-associated conformation (PrP^{TSE}).^{1,2} Most TSEs are transmitted via the oral route.^{3,4} Scrapie and chronic wasting disease (CWD) are unique among other TSEs in that indirect horizontal transmission occurs from infected to naïve animals via an environmental reservoir of infectivity.⁵⁻⁷ Chronic wasting disease affects North American members of the deer family (cervids) and is present in the United States, Canada, and South Korea.^{8,9} Strong evidence exists for environmental transmission of CWD and the maintenance of a reservoir of prion infectivity in contaminated soils.^{6,10-13} The disease agent, PrP^{TSE} , is shed from diseased animals during the lengthy course of the infection.¹⁴⁻¹⁸ Prions have been shown to bind avidly to certain soil components,^{19,20} limiting the vertical movement of prion protein in soils,^{7,21,22} and maintaining infectivity near soil surfaces. Previous works have assessed the persistence of TSE infectivity in soil for several years;^{7,21} a hamster-adapted prion strain was recovered from garden soil after burial for 3 years,²¹ and scrapie infectivity can persist in some environments for at least 16 years.²³ The capability to detect CWD agent in soil would allow identification of soil “hot spots” and thereby generating information for disease management.

To limit the further spread of the disease through environmental routes, methods to inactivate prions in the environment are necessary. Despite biological and abiotic processes that degrade proteins in soil, prion infectivity resists inactivation by methods that efficiently

inactivate conventional pathogens.²⁴ We have previously shown the ability of peroxymonosulfate (HSO_5^-) to degrade PrP^{TSE} both alone and when the PrP^{TSE} is associated with purified soil components. For use in the environment, one needs to consider the efficacy of this oxidant when prions are associated with whole soils containing components that may interfere with degradation, including natural organic matter, minerals, and other constituents. Importantly, soil contains constituents that inhibit detection by conventional means and necessitates extraction steps for immunodetection and *in vitro* amplification.

Direct detection of proteins by immunochemical techniques can be problematic due to interference by material from clays and other soil particles.²⁵ Genovesi et al. (2007) developed an direct immunologic detection method that does not require desorption of protein from soil, eliminating denaturants or detergents necessary for desorption,²⁶ however this method is not very sensitive (the limit of detection appears to be approximately equivalent to 0.25% BH), has not yet been shown to work with CWD prions, and does not allow determination of protein size as it does not use gel electrophoresis for protein band size separation, suggesting inherent challenges with verification. One solution to this problem is to increase signal by amplifying the disease agent *in vitro*. However, *in vitro* amplification can be challenging because prions can bind to soil particles and potentially to other environmental matrices.¹⁹ Two alternatives can be used to amplify PrP^{TSE} from environmental samples: direct amplification from a soil sample and extraction of PrP^{TSE} from the sample followed by amplification. However, the challenge exists that prion extraction from soil components often uses detergents that affect the secondary and higher level structure of the protein. *In vitro* PrP^{C} -to- PrP^{TSE} conversion relies upon the presence of the infectious conformation in the sample and detergent extraction may compromise this structure.

The optimization of protein misfolding cyclic amplification (PMCA), an in vitro amplification assay, could have the additional benefit of enabling the detection of prions in naturally contaminated samples. While PrP^{TSE} has been amplified directly from amended soil samples using the amyloid seeding assay²⁷ and PMCA,²⁸⁻³⁰ the amounts of soil that can be used in the PMCA reaction are limited. For example, Nagaoka et al. (2010) found the optimal sample size for PMCA to be 8 µg.³⁰ Such a small sample size raises questions about the representativeness and limits sample throughput. Extraction of PrP^{TSE} from soil followed by PMCA would allow larger amounts of soil to be tested, however, to extract PrP^{TSE} that would be reactive in PMCA, a relatively gentle extraction procedure would be necessary so as not to denature the infectious secondary and tertiary structure of the PrP^{TSE}.

The objective of this research was to evaluate the extent to which HSO₅⁻ can degrade pathogenic prion protein and inactivate prion infectivity associated with soil particles and to determine the effects of HSO₅⁻ treatment on soil microorganisms and plants. Accomplishing this objective required the optimization of methods to recover PrP^{TSE} from soils for detection by immunoblotting and PMCA. We employed the optimized methods to test the ability of HSO₅⁻ to inactivate soil-associated CWD prions. We have taken this strategy and tested a variety of potential extractants to recover PrP^{TSE} from amended soils having a range of mineral and organic compositions encompassing those likely to be encountered in environmental samples containing naturally deposited CWD PrP^{TSE}. In addition, we investigated the toxicity of HSO₅⁻ on soil microflora, on the survival of turfgrass, and the ability to grow turfgrass seeded on soil that had been exposed to HSO₅⁻.

4.3 EXPERIMENTAL

4.3.1 Ethics statement. All animals were cared for in accordance with protocols approved by the Institutional Animal Care and Use Committee of the University of Wisconsin, Madison (Assurance Number A3464-01).

4.3.2 Materials. Proteinase K (PK) from *Tritirachium album*, 30 units·mg_{protein}⁻¹) and phenylmethanesulfonyl fluoride (PMSF) (>98.5%) was purchased from Sigma-Aldrich. Peroxyonosulfate was obtained as a triplicate salt (2KHSO₅·KHSO₄·K₂SO₄, Oxone[®], 95%, manufactured by DuPont) potassium dihydrogen phosphate (≥98%) from Alfa Aesar. Sodium hydroxide (>97%), sulfuric acid (95-98%), sodium chloride (>99.9%), sodium phosphate dibasic anhydrous (>99%), and Tris base (>99.9%) were acquired from Fisher. These chemicals were used without further purification. All solutions were prepared in ultrapure water (18.2 MΩ·cm resistivity, Barnstead GenPure Pro) unless otherwise specified.

Natural organic materials (NOM) including humic acids from Elliot soil (ESHA, 1S102H), the Suwannee River (SRHA, 2S101H), Pahokee peat (PPHA, 1S103H), Leonardite (LHA, 1S104H) and fulvic acid from Elliot soil (ESFA, 1S102F) were purchased from the International Humic Substances Society (IHSS; St. Paul, Minnesota, USA) and used without further purification. The soils used were Elliot silt loam (IHSS), Defore silt loam (Outagamie County, Wisconsin, USA), and four Scottish soils (Site S topsoil (silt loam), Site S subsoil (sandy loam), Site C topsoil (sandy clay loam), and Site C Subsoil (sandy clay loam)). The Scottish soils were used in field-scale studies of the survival and migration of prions from buried cattle heads and have been extensively characterized.^{22,32,33} Concentrations of NOM was estimated as previously described.³¹ Briefly, absorbance spectra (250-700 nm) were acquired by a UV-3600 Shimadzu spectrophotometer. Triplicate samples were quantified against a five-point

calibration curve ($R^2 > 0.98$) produced with 0.005–1 g L⁻¹ ESHA for soil extraction. Samples with absorbance outside the linear range of the standard curve were diluted and reanalyzed.

4.3.3 Prion source. Brain tissue was isolated from an experimentally inoculated white-tailed deer homozygous in glycine at codon 96 (wt/wt) showing clinical symptoms of CWD prior to being euthanized.³⁴ Brain tissue was homogenized in 1× modified DPBS without Ca²⁺ or Mg²⁺ (Thermo Scientific, amended with 5 mM EDTA) to a concentration of 10% w/v and stored at –80°C until use. Prior to addition to soils, CWD-positive brain homogenate (BH; 50 µL) was treated with 50 µg·mL⁻¹ (final concentration) proteinase K (PK) for 1 h at 37 °C to eliminate PrP^C and *N*-terminally truncate PrP^{TSE}. Proteinase K activity was halted by addition of phenylmethanesulfonyl fluoride to a final concentration of 4 mM.

4.3.4 Extraction of PrP^{TSE} from Soil. Proteinase K-treated BH was allowed to interact with soils (25-50 mg) in 100 µL ultrapure water (18.2 MΩ·cm resistivity, Barnstead GenPure Pro) for 24 h at room temperature followed by a 2-h desorption step where samples were centrifuged for 10 minutes at 800 ×g (to remove any non-adsorbed, unbound PrP^{TSE}) and extraction with 200 µL of one of the following extraction buffers at room temperature (Table 1): (A) 0.1 M NaPO₄, pH 7.4; (B) 0.1 M NaPO₄, pH 8; (C) 1% nonyl phenoxypolyethoxylethanol (Tergitol-type NP-40) in 0.1 M NaPO₄, pH 7.4; (D) McDougall's buffer (NaHCO₃, 117 mM; Na₂HPO₄, 17 mM; KCl, 130 mM; NaCl, 8 mM; MgSO₄, 1 mM; CaCl₂, 1.4 mM), pH 8.23; (E) PMCA buffer (1% Triton X-100 in Ca²⁺- and Mg²⁺-free DPBS, pH 7.4 with 0.15 M NaCl, 5 mM EDTA, 0.05% saponin and miniprotease inhibitor); (F) 1% sodium lauroyl sarcosinate (sarkosyl) in 0.1 M NaPO₄, pH 7.4; or (G) 1% sarkosyl in 0.1 M NaPO₄, pH 8. The choice of these extraction buffers was driven by the need to maintain the secondary and tertiary structure of PrP^{TSE} for subsequent analysis by protein misfolding cyclic amplification.

Where indicated, eluates were precipitated with sodium phosphotungstic acid (PTA) in PMCA buffer in order to precipitate the prion protein. Sodium phosphotungstic acid (4%, pH 7.4, no MgCl) was added to a final concentration of 0.30% and incubated at 37 °C overnight. After PTA-precipitation, samples were centrifuged (30 min, 16,000g, room temperature). The pellet was washed once with 200 μ L DPBS, 0.1% sarkosyl and 50 μ L 250 mM EDTA and sedimented by centrifugation (10 min, 16,000g, room temperature). Pellets were resuspended in PBS to 50 μ L (for immunoblotting) or PMCA buffer to 100 μ L (for PMCA).

4.3.5 Inactivation of soil-bound PrP^{TSE} by peroxymonosulfate. Pathogenic prion protein in the form of 10% CWD BH was adsorbed to natural soils as described above and exposed to 25 to 125 mM HSO₅⁻ (final concentration) at room temperature (~25 °C) in polypropylene microcentrifuge tubes in the dark. Reaction with HSO₅⁻ was halted by addition of an equal volume of 1 M sodium thiosulfate. In some cases, samples were pre-treated with sodium thiosulfate to prevent oxidation by HSO₅⁻ and radical species. The pH of the HSO₅⁻ solution prior to addition in soil was stable at approximately 2 (125 mM) and 2.5 (25 mM). We have previously shown that co-extracted constituents from aluminosilicate clay mineral and iron oxide surfaces does not inhibit prion detection by immunoblot in the presence of HSO₅⁻ quenched by sodium thiosulfate (Chapter 2). Prions were extracted with 1% sarkosyl in 0.1 M NaPO₄ (pH 7.4, extraction buffer “F”) for immunoblot detection. For detection by mbPMCA, after elution with PMCA buffer (pH 7.4), prions were PTA-precipitated and resuspended with PMCA buffer.

4.3.6 Immunoblot detection of PrP^{TSE}. Prions were detected via SDS-PAGE as previously described.³¹ Briefly, a 20 μ L aliquot was mixed with 10 μ L 10 \times SDS sample buffer (100 mM Tris, pH 8, 10% SDS, 7.5 mM EDTA, 100 mM dithiothreitol, 30% glycerol), vortexed,

and heated to 100 °C for 10 min and fractionated on a 12% bis-tris polyacrylamide gels (BioRad). Proteins were electrotransferred from the gel to a 0.45 µm polyvinyl difluoride membrane (Millipore), blocked with 5% nonfat dry milk prepared in 1× Tris-buffered saline containing 0.1% Tween 20) for 1 h and probed with primary antibodies overnight at 4 °C. We used a combination of monoclonal antibodies (mAbs) 8G8 (Cayman Chemical, 1:1000, epitope: 97-102) and Bar224 (Cayman Chemical, 1:10000, epitope: 141-151) to probe the membrane-bound cervid PrP. Detection was achieved by horseradish peroxidase-conjugated goat-anti-mouse immunoglobulin G (BioRad, 1:10,000 dilution) using Super Signal West Pico chemiluminescent substrate (Pierce Biotechnology) to visualize protein bands. Densitometric analysis of immunoblot bands was conducted using Image J Software.

4.3.7 Protein misfolding cyclic amplification Protein misfolding cyclic amplification (PMCA) was conducted as previously described (Chesney et al. in review).^{35,36} Briefly, brain tissue from uninfected transgenic mice hemizygous for the cervid prion gene (Tg(CerPrP)^{153S} mice)³⁷ were used to prepare normal brain homogenate (NBH) to use as the source for the PrP^C. Mice were euthanized by CO₂ asphyxiation and immediately perfused with 1× modified DPBS without Ca²⁺ or Mg²⁺ (Thermo Scientific, amended with 5 mM EDTA). Brains were rapidly removed, flash frozen in liquid nitrogen, and stored at −80 °C until use. Brain tissue was homogenized on ice to 10% (w/v) in PMCA conversion buffer (Ca²⁺- and Mg²⁺-free DPBS, pH 7.4, supplemented with 150 mM NaCl, 1% Triton X-100, 0.05% saponin (Mallinckrodt), 5 mM EDTA, and 1 tablet Roche Complete EDTA-free protease inhibitors cocktail (Fisher) per 50 mL conversion buffer). Brain homogenates were clarified by centrifugation (2 min, 2,000g). Supernatant was transferred to pre-chilled microcentrifuge tubes, flash frozen in liquid nitrogen, and stored at −80 °C until use.

The versions of PMCA used, bead-assisted PMCA (PMCAb) and microplate-based PMCA (mbPMCA), differ in quantity of seed and NBH substrate, number of Teflon beads per reaction, and the vessel for each method. The seeds for initiating PMCA reactions were 10 μL (PMCAb) or 4 μL (mbPMCA) aliquots from CWD samples in indicated experiments added to 90 μL (PMCAb) or 36 μL (mbPMCA) NBH in 0.2 mL thin-walled PCR tubes (PMCAb) or 96-well PCR microplate (mbPMCA; Axygen, Union City, CA, USA) with two (PMCAb) or one (mbPMCA) 2.38 mm Teflon[®] bead (McMaster-Carr, #9660K12). A dilution series was prepared by serially diluting 10% CWD BH (made up in DPBS) five-fold in NBH. Sample dilutions were used to seed reactions in the same experiment and acted as positive controls. Where indicated, PrP^{TSE} was added to normal brain homogenate (NBH) from uninfected brain homogenate from Tg(CerPrP)1535[±] mice, and used as an NBH carrier to verify the success of PTA precipitation. Negative controls were NBH. Experimental plates were placed in a rack in a Misonix S-4000 microplate horn, and the reservoir was filled with ultrapure water. Each round of PMCAb or mbPMCA consisted of 96 cycles (30 s sonication at 40-60% of maximum power, 1770 s incubation at 37 °C). At the completion of 96 cycles, new NBH was reseeded with 10 μL (PMCAb) or 4 μL (mbPMCA) of the reaction product for serial PMCA. After completing the last round of PMCA, 20 μL of each sample was digested with PK (50 $\mu\text{g}\cdot\text{mL}^{-1}$, 1 h, 37 °C), and the resulting PK-resistant prion protein (PrP^{res}) was analyzed by SDS-PAGE with immunoblot detection (*vide supra*).

For analysis of the *in vitro* conversion of PrP^{TSE} extracted from soil that had been exposed to HSO₅⁻, prions (PK-treated from log 2.0 dilutions of CWD+ brain tissue) were incubated with soil (Elliot, Defore, Site S Topsoil, Site S Subsoil, Site C Topsoil and Site C Subsoil) in 100 μL ultrapure water for 24 h. Additionally, as positive controls, dilutions (log 2.0-

12) from PK-treated CWD brain tissue alone and associated with Elliot soil were pre-treated with 0.5 M $\text{Na}_2\text{S}_2\text{O}_3$. Each soil-PrP^{TSE} sample was exposed to a final concentration of 125 mM HSO_5^- . Reactions were quenched with 1 M $\text{Na}_2\text{S}_2\text{O}_3$, PTA precipitated and washed in 1:1 PMCA buffer (pH 7.4; buffer “E”). A 4 μL aliquot of the reaction mixture was then added to 36 μL NBH and subjected to two rounds of 96 cycles of mbPMCA.

4.3.8 Culture of bacteria and fungal colonies. Soils were saturated with HSO_5^- (0 – 250 mM) for 2, 4, 6, and 24 h. Samples of gravity-settled supernatant (100 μL) from the top 25 mm of the supernatant was spread on 7.5% agar plates containing 0.3% beef extract and cultured at 36 °C. Colonies were counted after 24 hours.

4.3.9 Assessment of peroxymonosulfate toxicity to grass. Kentucky bluegrass sod (from the Bruce Company, Middleton, WI) was cut into 12.5 cm × 12.5 cm squares and planted on 100 g wet weight potting soil and saturated with ultrapure water. After 48 h acclimation, 100 mL HSO_5^- solution (0-250 mM, buffered to pH 6 with phosphate where indicated) was added to each square (in 3 × 3 planting grids). The percent of green grass blades was determined, and an additional 100 mL of HSO_5^- was applied every other day for 9 days. The reactions were not experimentally quenched.

Commercial potting soil (Miracle Grow Potting Soil, purchased from the Bruce Company, Middleton, WI) was saturated with 0-250 mM HSO_5^- solution for 24 h. After draining the solution, the soil was packed into nine 3.1 × 3.1 cm pods on seed propagation trays. The soil in each pod was seeded with 30 grass seeds (Fast Grass Lawn Seed Mix, Vigoro: Home Depot SKU: 893781), watered and monitored for growth every 5 d. Grass leaf blades were counted and measured from the soil base to the tip of the blade.

4.4 RESULTS AND DISCUSSION

4.4.1 Extraction and detection of PrP^{TSE} from soil. We tested seven extraction buffers (Table 1) for their ability to recover PrP^{TSE} from amended soils. Because the presence of natural organic material (NOM) may impact the ability to extract and detect prions, we examined the amount of NOM extracted from two soils differing in organic carbon content: Elliot silt loam (fraction of organic carbon, $f_{oc} = 0.029$) and Defore silt loam ($f_{oc} = 0.133$) using seven extraction buffers (Table 1). More NOM was extracted from the Defore than the Elliot soil for all extraction buffers (Figure S1B), consistent with the higher organic carbon content of the former. The concentration of NOM extracted from the Elliot soil was 16-117 $\mu\text{g}\cdot\text{mL}^{-1}$; that from the Defore soil ranged from 56 to 1150 $\mu\text{g}\cdot\text{mL}^{-1}$. For both soils, McDougall's buffer (pH 8.23; buffer D) and PMCA buffer (pH 7.4; buffer E) removed the smallest amount of NOM from the soils (Figure S1B). Buffers containing sarkosyl (1%; buffers F and G) were the most efficient in recovering PrP^{TSE} from Elliot soil (as determined by immunoblotting) and extracted a largest amount of NOM (Figure S1B).

Natural organic matter occurs at variable concentrations in soils and may be co-extracted with PrP^{TSE}. We have previously demonstrated that NOM in soil impacts PrP^{TSE} detection by immunoblotting.³¹ Methods commonly used to extract PrP^{TSE} from soils release substantial amounts of NOM, and NOM inhibits PrP^{TSE} immunoblot signal.^{27,31} The degree of immunoblot interference for both deer and hamster prions increased with increasing NOM concentration and decreasing NOM polarity.³¹ These findings raise the concern that NOM co-extracted with PrP^{TSE} might interfere with detection by mbPMCA. We examined the degree to which NOM interferes

with mbPMCA and investigated NOM co-extracts from various buffers shown to also extract PrP^{TSE}.

We examined the effect of NOM extracts in PrP^{TSE} detection using immunoblot. Data from the interaction of NOM extracts with PrP^{TSE} illustrate a strong correlation between NOM content and inhibition of detection via immunoblot; more PrP^{TSE} is detected in the sample with extracts from Elliot soil (Figure S1C), which had less NOM (Figure S1B) than Defore soil. Extracts from Defore soil showed a strong inhibition of detection of PrP^{TSE}, except for buffers D and E (McDougal's buffer and PMCA buffer, Figure S1C), which extracted the least amount of NOM (Figure S1B). These results are consistent with prior work that demonstrates that it may be more difficult to detect prions from soils containing a large fraction of NOM,³¹ however extraction buffers containing 1% sarkosyl may help overcome this challenge.

4.4.2 Optimization of PMCA for detection of PrP^{TSE} from soils. Our first step toward optimizing PMCA to detect PrP^{TSE} in soil extracts and PrP^{TSE} associated with soil exposed to HSO₅⁻ was to determine the effect of soil extracts and extraction buffers on downstream detection using PMCAb. Extractants that allow the recovery of the largest amount of PrP^{TSE} may not be optimal for PMCA if the extractant or co-extracted constituents from soil inhibit the PMCA reaction.

To investigate the degree to which soil constituents extracted by the extraction buffers interfered with the PMCA reaction, we extracted the Elliot and Defore soils with each buffer and added extracts to a PMCA reaction. The PMCA buffer resulted in one of the lowest amounts of extracted NOM, and as expected, it allowed the highest degree of PrP^{TSE} amplification from Elliot soil (Figure S1D). The buffers containing sarkosyl (buffers F and G) had the largest

extraction of NOM and these extracts likely contain inhibitors as both samples resulted in no amplification of PrP^{TSE} (Figure S1D).

Of extractants tested, those that included 1% sarkosyl recovered the largest amount of PrP^{TSE} as determined by immunoblotting (Figure S2A). In contrast, of the extraction buffers tested, extraction buffers containing sarkosyl resulted in the poorest detection of PrP^{TSE} extracted from soil after amplification by PMCAb (Figure S2B). Sarkosyl is a detergent, it likely denatures the protein where the conversion ability is partially inhibited. Alternatively, sarkosyl may act as an inhibitor to in vitro PrP^C-to-PrP^{TSE} conversion by interaction with other components of the reaction. Although detection of PrP^{TSE} by immunoblotting is limited to samples extracted using sarkosyl, PMCAb is able to amplify prions extracted from soil in buffers that do not contain sarkosyl. Interestingly, there was no amplification of PrP^{TSE} from Defore soil (data not shown), however this is not entirely unexpected as Defore soils had the largest amount of extracted NOM.

The decrease in detection of PrP^{TSE} seen in the PMCAb containing spiked soil extracts (Figure S1D) compared to the extract buffers alone (Figure S1B) indicated a strong inhibitor of PMCAb were eluted from the soil. Because the inhibition was stronger from the Defore soil extracts and Defore soil extracts contain a much higher level of NOM (Figure S1B), we hypothesized that NOM contributed to the inhibition of PMCAb. The effect of humic (HA) and fulvic (FA) acid (major, operationally defined fractions of NOM) on amplification of PrP^{TSE} from diseased brain tissue. We used Elliot HA, Suwanee River HA, Leonardite HA, Pahokee Pete HA, and Suwannee River FA, well characterized, reference humic and fulvic acids that are frequently used in environmental chemistry studies. We examined the effect of humic and fulvic acids on amplification during the first round of PMCAb. We found that HA and FA inhibited the

first round of PMCAb in a concentration-dependent manner with the largest inhibition seen in samples with more than 0.25 μg HA and more than 1 μg FA (Figure S3).

Extracts from soil inhibit PMCA (Figure S1D). We therefore examined the ability of PTA precipitation to reduce the inhibition of these extracts. When coupled with PTA precipitation, one round of PMCA allowed detection of PrP^{TSE} with all buffers tested regardless of NBH carrier (Figure S4). Subsequent analyses of in vitro conversion using PrP^{TSE} extracted from soil as PMCA seed presented here, including those measurements from PrP^{TSE} degraded by HSO_5^- , utilized a PTA precipitation step to isolate extracted protein.

4.4.3 Degradation of soil-bound PrP^{TSE} by peroxymonosulfate. To investigate the ability of HSO_5^- to inactivate prion, we examined the ability of HSO_5^- to degrade prion protein associated with whole soils. After a 24 h incubation of PrP^{TSE} with soils, a wash with background buffer and centrifugation to separate unbound PrP^{TSE} from that associated with soil resulted in the majority of protein being found in the pellet, with a small amount in the supernatant. This indicates that although much of the PrP^{TSE} was associated with soil constituents, a fraction remained either unbound or bound to low density constituents, such as NOM, that remained in the supernatant (data not shown).

To determine if the presence of soil inhibits prion inactivation by HSO_5^- , PK-treated CWD brain homogenate (BH) was incubated with a final concentration of 25 mM or 125 mM HSO_5^- for 1 h. The reaction was quenched with 1 M $\text{Na}_2\text{S}_2\text{O}_3$, and prions were extracted by extraction buffer “F” (1% sarkosyl in 0.1 M NaPO_4 , pH 7.4) for 1 h at 37 °C before being prepared for immunoblot. Prions not exposed to HSO_5^- were extracted at amounts comparable to unbound control (Figure 1A). Prions associated with Site C Topsoil and Site C Subsoil, Site S Subsoil and Site S Topsoil, and Elliot soil exposed to 25 mM HSO_5^- had less detectable protein

compared to the unexposed control (Figure 1B), indicating incomplete degradation by HSO_5^- . Prions associated with the higher organic-content Defore soil were not detected after 1 h exposure to 25 mM HSO_5^- (Figure 1B). After 1 h exposure to 125 mM HSO_5^- , none of the soil-associated prions were detected by immunoblot (Figure 1C). These results are consistent with the inactivation of prions associated with purified clay microparticles and iron oxides (Chapter 3) and prions alone (Chapter 2), where, after 1 h, 25 mM HSO_5^- resulted in slight degradation and 125 mM HSO_5^- resulted in substantial inactivation. The decrease in detection seen from prions associated with Defore soils may be due to inhibition of immunoblot detection by the organic fraction as seen in Figure S1C and in previous work.³¹ Alternatively, prions that interact with constituents in the organic fraction may be more susceptible to inactivation by oxidation than prions associated with mineral or clay fractions. Furthermore, organic material may obstruct binding sites in soil matrices. Additionally, although prions have been shown to avidly bind montmorillonite,¹⁹ mineral oxides and organic material in natural soils may alter the surface reactivity of constituents.³⁸

4.4.4 Assessment of in vitro conversion ability of soil-bound PrP^{TSE} exposed to peroxymonosulfate. The data presented thus far demonstrate that exposure to HSO_5^- degrades soil-associated PrP^{TSE} . Using Western blot as an immunologic detection method has a detection limitation (~ 4 ng PrP) that is much higher than the amount of PrP^{TSE} needed to initiate disease (for mice, 725,000 times less sensitive than intracerebral inoculation).³⁹ Additionally, reductions in prion infectivity are not always seen with declines in immunologic detection via Western blot.^{36,40-42} To overcome these limitations in analyzing degradation, we used the reagents identified in our optimization steps to employ PMCA adapted to a microplate format (mbPMCA) to measure the *in vitro* converting ability of prions as a proxy for infectivity

and to sensitively detect PrP^{TSE} . Although we optimized PMCA for amplification of soil-associated PrP^{TSE} , the restriction on the extractants to those without detergents may lead to incomplete PrP^{TSE} extraction. Other groups have used prions still adsorbed to a surface in PMCA, including directly amplifying prions associated with soil,^{29,30} and adsorbed to metal wires.⁴⁴ However these studies either did not directly compare amplification of adsorbed prions with unbound prions,^{44,33} or the amplification was significantly reduced in certain soils.²⁹

Our objective was to detect amplified soil-extracted PrP^{TSE} that had been exposed to 125 mM HSO_5^- . We previously investigated the decrease in in vitro conversion of PrP^{C} to PrP^{TSE} after exposure to HSO_5^- and reported a decrease of $10^{5.9}$ after two rounds of mbPMCA (Chapter 2). After the second round of mbPMCA, immunoreactivity was not detected at any dilution examined in samples that had been exposed to HSO_5^- . Samples of Elliot soil- PrP^{TSE} and samples of PrP^{TSE} without soil that were pre-quenched with thiosulfate prior to HSO_5^- exposure were serially diluted and used as a positive control. Pre-treatment with thiosulfate allowed detection of PrP^{TSE} immunoreactivity for dilutions of CWD-positive deer BH to the 10^{-12} dilution in both prion dilutions in Elliot soil and prions not in the presence of soil. These results indicate that 1-h treatment with 125 mM HSO_5^- decreased the PrP^{C} -to- PrP^{TSE} converting ability of PrP^{TSE} extracted from soil by a factor of at least 10^{10} (Figure 2A, B and C). There was no detection of PrP^{TSE} from HSO_5^- -exposed samples out to the third round of mbPMCA. The first lanes in panels A, B and C of Figure 2 were from a sample from the mbPMCA reaction that was not digested with PK and represents both prion protein conformations (PrP^{TSE} and PrP^{C}). The presence of protein bands, signifying PrP immunodetection, in these lanes indicate the missing protein bands in experimental lanes are not due to problems associated with the Western blot method.

4.4.5 Toxicity of peroxymonosulfate on microorganisms. The toxicity of HSO_5^- to species that would be exposed in a decontamination effort is important to investigate prior to its application. To this end, bacterial and fungal colonies were grown on agar plates and colonies were counted to establish the effect of HSO_5^- on the survival of microorganisms amenable to culture on the medium used. The morphology of the colonies did not change regardless of the exposure time when there was no HSO_5^- in solution (Figure 3A). However at 2 h exposure, when the concentration was just 25 mM HSO_5^- , the colony branching appeared to decrease; by 250 mM, the colonies were markedly more punctate (Figure 3A). The longer exposures (4 and 6 h) resulted in far fewer and vastly smaller colonies compared to short exposure (2 h) and the lower concentration (25 mM) of HSO_5^- (Figure 3A). After just a 2 h exposure to 25 mM HSO_5^- , the number of colony forming units was significantly decreased ($p < 0.05$) and this extended to higher concentrations of HSO_5^- (Figure 3B) and for exposure times of 4 h (Figure 3C) and 6 h (Figure 3D).

We calculated the LD_{50} where the HSO_5^- concentration resulted in a reduction of colony forming units by half compared to the number of colonies grown in control solution. Peroxymonosulfate appears to be toxic to colony forming units at an LD_{50} of 118 mM for 2 hour exposure times, 109 mM for 4 hours exposure, and 87 mM for 6 hours exposure as at these concentrations half of the colony forming units survived compared to controls. We note that colonies were still able to proliferate even at higher concentrations than that needed for prion degradation (25 mM), and re-establishment of soil microflora would likely occur from the periphery of exposed soils or by deposition by air-borne cells or spores.

4.4.6 Growth of grass on soil exposed to peroxymonosulfate. Consideration of the ability of HSO_5^- -exposed soil to maintain fertility for future plant growth is important prior

to environmental application. We seeded grass seeds on soil that had been saturated with HSO_5^- solutions (0, 25, 125, and 250 mM) and measured the number and length of leaf blades at 5 and 10 d after seeding. The average length of blade for the three lowest concentrations of HSO_5^- (0, 25, and 125 mM) did not differ ($p > 0.05$, Figure 4). The highest concentration, 250 mM HSO_5^- , which was double the concentration used in any PrP^{TSE} degradation experiments, had significantly smaller average leaf blades at both 5 and 10 d after seeding ($p < 0.05$, Figure 4). However, importantly, we note that even in soil saturated with 10 times the required concentration of HSO_5^- needed to degrade PrP^{TSE} , seeded grass was able to regrow.

4.4.7 Toxicity of peroxymonosulfate on grass. As an initial evaluation of the toxicity of HSO_5^- to environmental flora, we employed Kentucky Bluegrass sod as a representative plant. Unbuffered or pH-buffered (sodium phosphate buffer, pH 6) HSO_5^- solution (0, 25, 125 and 250 mM) was applied (100 mL) to sections of sod once every two days for 9 d. The number of green grass blades as a fraction of the control (0 mM HSO_5^-) was recorded and the sections were photographed (Figure 5B). Representative sections at day 9 are presented in Figure 5A.

The sensitivity of grass to low pH was the impetus for buffering the HSO_5^- to pH 6. We had previously showed that pH does not appear to affect degradation of PrP^{TSE} by HSO_5^- (article in prep; chapter 3) In considering this sensitivity, we determined the pH changes after HSO_5^- exposure. In the presence of soil, pH decreased with increasing HSO_5^- concentration (Figure 5C); after 7 days saturation, soil solutions exposed to 25 mM HSO_5^- had a stable pH of 6.5, 125 mM had a stable pH of 5, and 250 mM HSO_5^- had a stable pH of 4 (Figure 5C).

4.4.8 Environmental Implications. The optimization of immunoblot detection of PrP^{TSE} and in vitro prion amplification by PMCA is useful beyond analysis of PrP^{TSE} degradation

by HSO_5^- or other decontamination tools; the ability to detect minute samples of naturally shed PrP^{TSE} in the environment would be a significant advancement in the struggle to confine geographic and horizontal spread of CWD. The impetus for the use of PMCA in detecting PrP^{TSE} from soil matrices using amplification steps is because naturally amended soils are expected to contain less PrP^{TSE} than can be directly detected by biochemical means. Our results indicate that amplification of PrP^{TSE} extracted from Elliot soil is possible to the 10^{10} dilution from CWD brain tissue. Additionally, we show that HSO_5^- is capable of degrading PrP^{TSE} and reducing in vitro conversion by a factor of 10^{10} in all soils tested. This level of inactivation, coupled with limited toxicity to grass seeds after exposure, implies that HSO_5^- is a promising oxidation tool for prion degradation in environmental applications.

4.5 ACKNOWLEDGEMENTS

This research was funded by NIH grant R01 NS060034. ARC was supported by NIEHS predoctoral training grant number T32ES007015. We thank Glenn Telling for the Tg(CerPrP) mice and Judd Aiken for the CWD+ white-tailed deer brain tissue. Article contents are solely the responsibility of the authors and do not represent official views of the sponsors.

4.6 REFERENCES

1. Prusiner, S. B., Prions. *Proc Natl Acad Sci U S A* **1998**, *95*, (23), 13363-13383.
2. Prusiner, S. B., Molecular biology of prion diseases. *Science* **1991**, *252*, (5012), 1515-1522.
3. Kujala, P.; Raymond, C. R.; Romeijn, M.; Godsave, S. F.; van Kasteren, S. I.; Wille, H.; Prusiner, S. B.; Mabbott, N. A.; Peters, P. J., Prion uptake in the gut: identification of the first uptake and replication sites. *PLoS Pathog* **2011**, *7*, (12), e1002449.
4. Da Costa Dias, B.; Jovanovic, K.; Weiss, S. F. T., Alimentary prion infections. *Prion* **2014**, *5*, (1), 6-9.
5. Miller, M. W.; Williams, E. S., Horizontal prion transmission in mule deer. *Nature* **2003**, *425*, 35-36.
6. Miller, M. W.; Williams, E. S.; Hobbs, N. T.; Wolfe, L. L., Environmental sources of prion transmission in mule deer. *Emerg Infect Dis* **2004**, *10*, (6), 1003-1006.
7. Seidel, B.; Thomzig, A.; Buschmann, A.; Groschup, M. H.; Peters, R.; Beekes, M.; Terytze, K., Scrapie agent (strain 263K) can transmit disease via the oral route after persistence in soil over years. *PLoS One* **2007**, *2*, (5), e435.
8. Chronic Wasting Disease.
http://www.nwhc.usgs.gov/disease_information/chronic_wasting_disease/index.jsp (Oct 26).
9. Williams, E. S.; Miller, M. W.; Kreeger, T. J.; Kahn, R. H.; Thorne, E. T., Chronic wasting disease of deer and elk: A review with recommendations for management. *Journal of Wildlife Management*. **2002**, *66*, 551-563.
10. Gough, K. C.; Maddison, B. C., Prion transmission: prion excretion and occurrence in the environment. *Prion* **2010**, *4*, (4), 275-282.
11. Mathiason, C. K.; Hays, S. A.; Powers, J.; Hayes-Klug, J.; Langenberg, J.; Dahmes, S. J.; Osborn, D. A.; Miller, K. V.; Warren, R. J.; Mason, G. L.; Hoover, E. A., Infectious prions in pre-clinical deer and transmission of chronic wasting disease solely by environmental exposure. *PLoS One* **2009**, *4*, (6), e5916.
12. Smith, C. B.; Booth, C. J.; Pedersen, J. A., Fate of prions in soil: a review. *J Environ Qual* **2011**, *40*, (2), 449-461.
13. Pedersen, J. A.; Somerville, R. A., Why and how are CWD and Scrapie sometimes spread via environmental routes? In *Decontamination of Prions*, Reisner, D.; Deslys, J.-P., Eds. Dusseldorf University Press: Dusseldorf Germany, 2012; pp 19-37.

14. Gonzalez-Romero, D.; Barria, M. A.; Leon, P.; Morales, R.; Soto, C., Detection of infectious prions in urine. *FEBS Lett* **2008**, *582*, (21-22), 3161-3166.
15. Haley, N. J.; Seelig, D. M.; Zabel, M. D.; Telling, G. C.; Hoover, E. A., Detection of CWD prions in urine and saliva of deer by transgenic mouse bioassay. *PLoS One* **2009**, *4*, (3), e4848.
16. Henderson, D. M.; Manca, M.; Haley, N. J.; Denkers, N. D.; Nalls, A. V.; Mathiason, C. K.; Caughey, B.; Hoover, E. A., Rapid antemortem detection of CWD prions in deer saliva. *PLoS One* **2013**, *8*, (9), e74377.
17. Mathiason, C. K.; Powers, J. G.; Dahmes, S. J.; Osborn, D. A.; Miller, K. V.; Warren, R. J.; Mason, G. L.; Hays, S. A.; Hayes-Klug, J.; Seelig, D. M.; Wild, M. A.; Wolfe, L. L.; Spraker, T. R.; Miller, M. W.; Sigurdson, C. J.; Telling, G. C.; Hoover, E. A., Infectious prions in the saliva and blood of deer with chronic wasting disease. *Science* **2006**, *314*, (5796), 133-136.
18. Safar, J. G.; Lessard, P.; Tamguney, G.; Freyman, Y.; Deering, C.; Letessier, F.; Dearmond, S. J.; Prusiner, S. B., Transmission and detection of prions in feces. *J Infect Dis* **2008**, *198*, (1), 81-89.
19. Johnson, C. J.; Phillips, K. E.; Schramm, P. T.; McKenzie, D.; Aiken, J. M.; Pedersen, J. A., Prions adhere to soil minerals and remain infectious. *PLoS Pathog* **2006**, *2*, (4), e32.
20. Jacobson, K. H.; Kuech, T. R.; Pedersen, J. A., Attachment of pathogenic prion protein to model oxide surfaces. *Environ Sci Technol* **2013**, *47*, (13), 6925-6934.
21. Brown, P.; Gajdusek, D. C., Survival of scrapie virus after 3 years' interment. *Lancet* **1991**, *337*, (8736), 269-270.
22. Jacobson, K. H.; Lee, S.; Somerville, R. A.; McKenzie, D.; Benson, C. H.; Pedersen, J. A., Transport of the pathogenic prion protein through soils. *Journal of Environmental Quality* **2010**, *39*, (4), 1145-1152.
23. Georgsson, G.; Sigurdarson, S.; Brown, P., Infectious agent of sheep scrapie may persist in the environment for at least 16 years. *J Gen Virol* **2006**, *87*, (Pt 12), 3737-3740.
24. Booth, C. J.; Johnson, C. J.; Pedersen, J. A., Microbial and enzymatic inactivation of prions in soil environments. *Soil Biology and Biochemistry* **2013**, *59*, 1-15.
25. Nielsen, K. M.; Calamai, L.; Pietramellara, G., Stabilization of extracellular DNA and proteins by transient binding to various soil components. In *Nucleic Acids and Proteins in Soil*, Nannipieri, P.; Smalla, K., Eds. Springer: Germany, 2006; Vol. 8, pp 142-157.
26. Genovesi, S.; Leita, L.; Sequi, P.; Andrighetto, I.; Sorgato, M. C.; Bertoli, A., Direct detection of soil-bound prions. *PLoS One* **2007**, *2*, (10), e1069.

27. Giachin, G.; Narkiewicz, J.; Scaini, D.; Ngoc, A. T.; Margon, A.; Sequi, P.; Leita, L.; Legname, G., Prion protein interaction with soil humic substances: environmental implications. *PLoS One* **2014**, *9*, (6), e100016.
28. Saunders, S. E.; Bartz, J. C.; Vercauteren, K. C.; Bartelt-Hunt, S. L., An enzymatic treatment of soil-bound prions effectively inhibits replication. *Appl Environ Microbiol* **2011**, *77*, (13), 4313-4317.
29. Saunders, S. E.; Shikiya, R. A.; Langenfeld, K.; Bartelt-Hunt, S. L.; Bartz, J. C., Replication efficiency of soil-bound prions varies with soil type. *J Virol* **2011**, *85*, (11), 5476-5482.
30. Nagaoka, K.; Yoshioka, M.; Shimozaki, N.; Yamamura, T.; Murayama, Y.; Yokoyama, T.; Mohri, S., Sensitive detection of scrapie prion protein in soil. *Biochem Biophys Res Commun* **2010**, *397*, (3), 626-630.
31. Smith, C. B.; Booth, C. J.; Wadzinski, T. J.; Legname, G.; Chappell, R.; Johnson, C. J.; Pedersen, J. A., Humic substances interfere with detection of pathogenic prion protein. *Soil Biology and Biochemistry* **2014**, *68*, 309-316.
32. Cooke, C. M.; Shaw, G., Fate of prions in soil: Longevity and migration of recPrP in soil columns. *Soil Biology and Biochemistry* **2007**, *39*, (5), 1181-1191.
33. Jacobson, K. H.; Lee, S.; McKenzie, D.; Benson, C. H.; Pedersen, J. A., Transport of the pathogenic prion protein through landfill materials. *Environ Sci Technol* **2009**, *43*, (6), 2022-2028.
34. Johnson, C. J.; Herbst, A.; Duque-Velasquez, C.; Vanderloo, J. P.; Bochsler, P.; Chappell, R.; McKenzie, D., Prion protein polymorphisms affect chronic wasting disease progression. *PLoS One* **2011**, *6*, (3), e17450.
35. Johnson, C. J.; Aiken, J. M.; McKenzie, D.; Samuel, M. D.; Pedersen, J. A., Highly efficient amplification of chronic wasting disease agent by protein misfolding cyclic amplification with beads (PMCAb). *PLoS One* **2012**, *7*, (4), e35383.
36. Moudjou, M.; Sibille, P.; Fichet, G.; Reine, F.; Chapuis, J.; Herzog, L.; Jaumain, E.; Laferriere, F.; Richard, C. A.; Laude, H.; Andreoletti, O.; Rezaei, H.; Beringue, V., Highly infectious prions generated by a single round of microplate-based protein misfolding cyclic amplification. *MBio* **2014**, *5*, (1), e00829-13.
37. Browning, S. R.; Mason, G. L.; Seward, T.; Green, M.; Eliason, G. A.; Mathiason, C.; Miller, M. W.; Williams, E. S.; Hoover, E.; Telling, G. C., Transmission of prions from mule deer and elk with chronic wasting disease to transgenic mice expressing cervid PrP. *J Virol* **2004**, *78*, (23), 13345-13350.
38. Sposito, G.; Skipper, N. T.; Sutton, R.; Park, S.-H.; Soper, A. K.; Greathouse, J. A., Surface geochemistry of the clay minerals. *Proc. Natl. Acad. Sci. USA* **1999**, *96*, 3358-3364.

39. Saa, P.; Castilla, J.; Soto, C., Ultra-efficient replication of infectious prions by automated protein misfolding cyclic amplification. *J Biol Chem* **2006**, *281*, (46), 35245-35252.
40. Klingeborn, M.; Race, B.; Meade-White, K. D.; Chesebro, B., Lower specific infectivity of protease-resistant prion protein generated in cell-free reactions. *Proc Natl Acad Sci U S A* **2011**, *108*, (48), E1244-53.
41. Shikiya, R. A.; Bartz, J. C., In vitro generation of high-titer prions. *J Virol* **2011**, *85*, (24), 13439-13442.
42. Weber, P.; Giese, A.; Piening, N.; Mitteregger, G.; Thomzig, A.; Beekes, M.; Kretzschmar, H. A., Cell-free formation of misfolded prion protein with authentic prion infectivity. *Proc Natl Acad Sci U S A* **2006**, *103*, (43), 15818-15823.
43. Belondrade, M.; Nicot, S.; Beringue, V.; Coste, J.; Lehmann, S.; Bougard, D., Rapid and Highly Sensitive Detection of Variant Creutzfeldt - Jakob Disease Abnormal Prion Protein on Steel Surfaces by Protein Misfolding Cyclic Amplification: Application to Prion Decontamination Studies. *PLoS One*. **2016**, *11*, (1), e0146833.

4.7 TABLES

Buffer	NaPO ₄	Sarkosyl	NP-40	pH	Other
A	0.1 M			7.4	
B	0.1 M			8	
C	0.1 M		1%	7.4	
D				8.23	McDougall's buffer
E				7.4	PMCA buffer
F	0.1 M	1%		7.4	
G	0.1 M	1%		8	

Table 1. Extraction buffers. McDougall's Buffer contains 117 mM NaHCO₃, 17 mM Na₂HPO₄, 130 mM KCL, 8 mM NaCl, 1 mM MgSO₄, 1.4 mM CaCl₂. PMCA buffer contains 1% Triton X-100 in Ca²⁺- and Mg²⁺-free DPBS, pH 7.4 with 0.15 M NaCl, 5 mM EDTA, 0.05% Saponin.

4.8 FIGURES

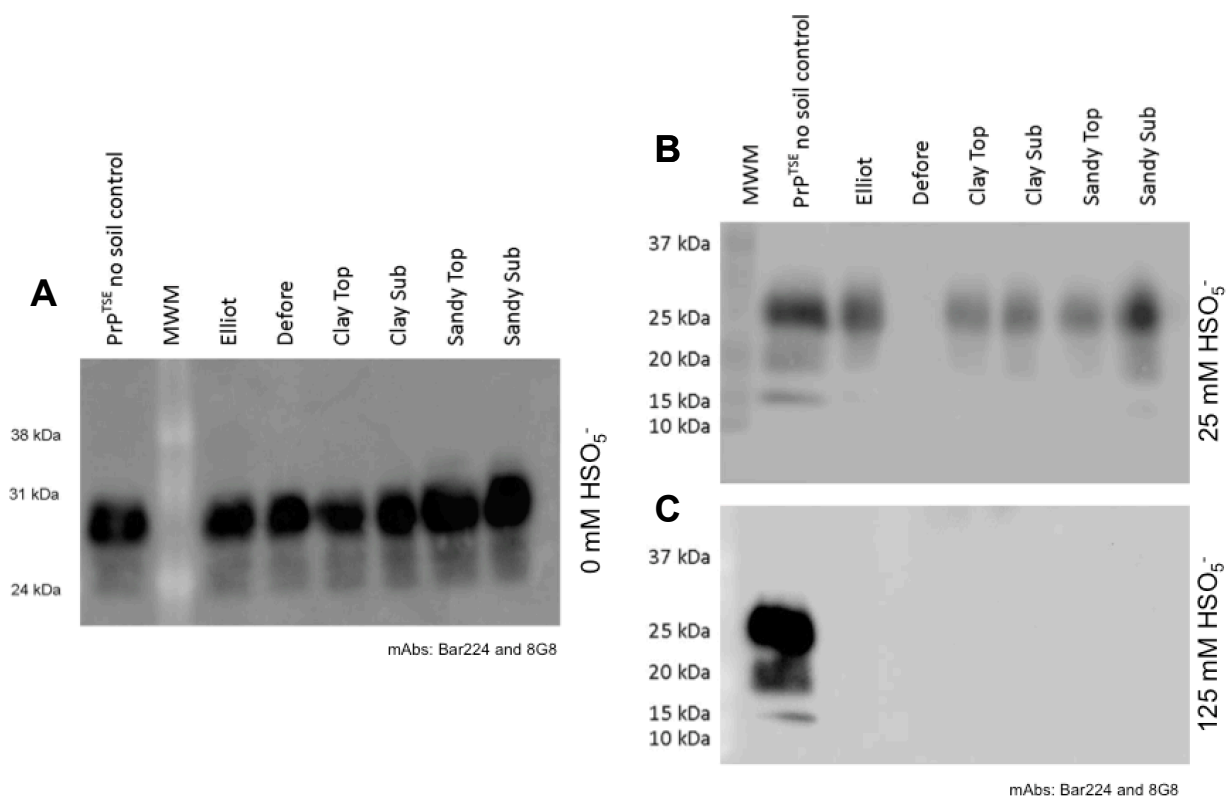
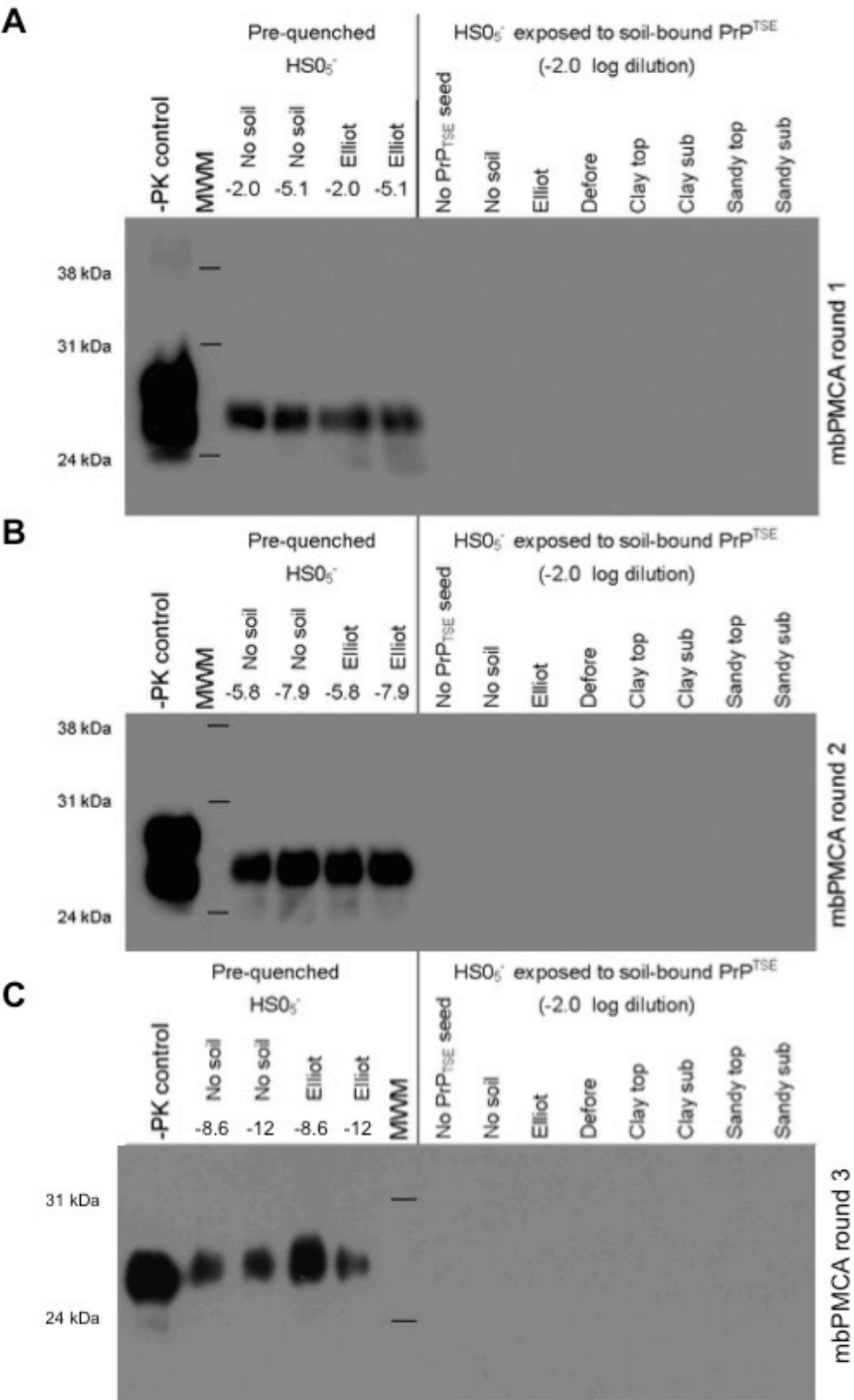


Figure 1. Degradation of CWD prions by peroxymonosulfate is not inhibited by sorption to soils. Soils (50 μg) were incubated with 50 μL CWD BH for 24 h and extracted using 1% Sarkosyl in 0.1 M NaPO_4 (pH 7.4, extraction buffer “F”). Prior to extraction, samples from each soil were exposed to (A) 0, (B) 25, or (C) 125 mM peroxymonosulfate. Reactions were quenched with 1 M $\text{Na}_2\text{S}_2\text{O}_3$. Membranes were probed with mAb Bar224 and 8G8. (Indications: Site C topsoil, Clay topsoil; Site C subsoil, Clay subsoil; Site S topsoil, Sandy topsoil; Site S subsoil, Sandy subsoil).



mAbs Bar224 & 8G8

Figure 2. In vitro converting ability of CWD PrP^{TSE} is reduced after 1 h exposure to 125 mM peroxymonosulfate. Soils (100 µg) were incubated with 50 µL 10% CWD BH for 24 h. Each soil-PrP^{TSE} sample was exposed to a final concentration of 125 mM peroxymonosulfate. Reactions were quenched with 1 M Na₂S₂O₃, PTA precipitated and incubated for 2 h in 1:1 PMCA buffer (1% Triton X-100 in Ca²⁺- and Mg²⁺-free DPBS, pH 7.4 with 0.15 M NaCl, 5 mM EDTA, 0.05% Saponin; buffer “E”) immunoblots represent the results of (A) one, (B) two, and (C) three rounds of mbPMCA. Samples exposed to 0 mM peroxymonosulfate of Elliot soil-PrP^{TSE} and samples of PrP^{TSE} without soil were serially diluted and used as a positive control. The first lanes in A, B and C was from a sample from the mbPMCA reaction that was not proteinase K digested and represents both prion protein conformations (PrP^{TSE} and PrP^C). Membranes were probed with mAb Bar224 and 8G8. (Indications: Site C topsoil, Clay topsoil; Site C subsoil, Clay subsoil; Site S topsoil, Sandy topsoil; Site S subsoil, Sandy subsoil).

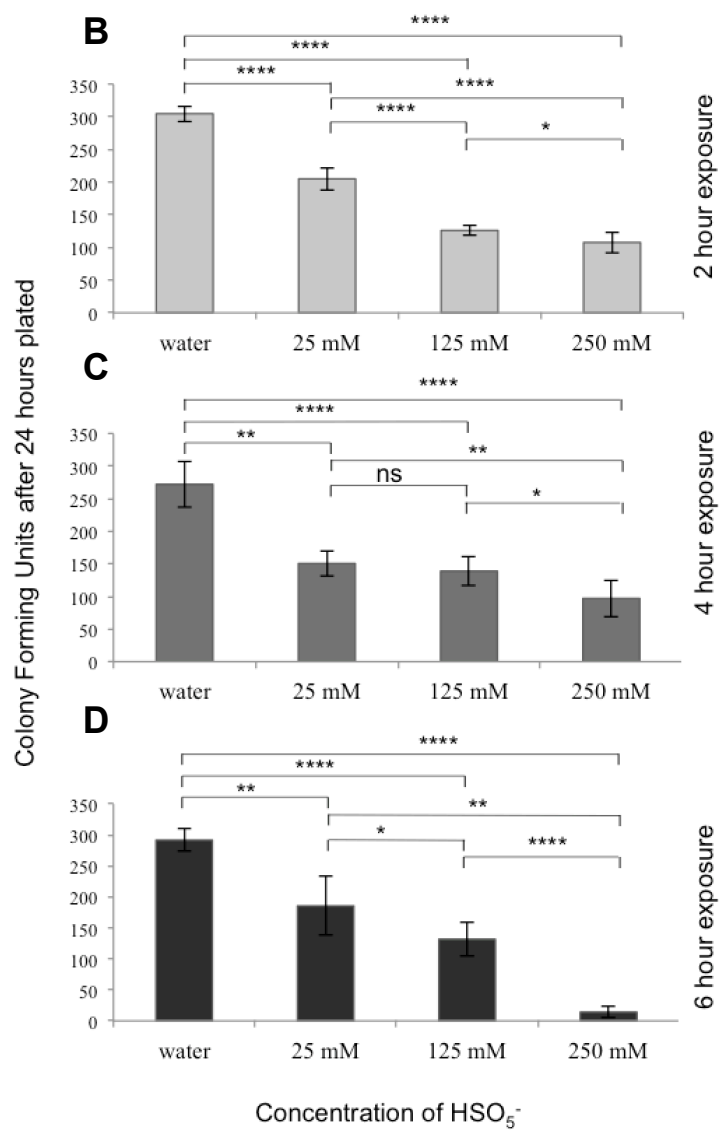
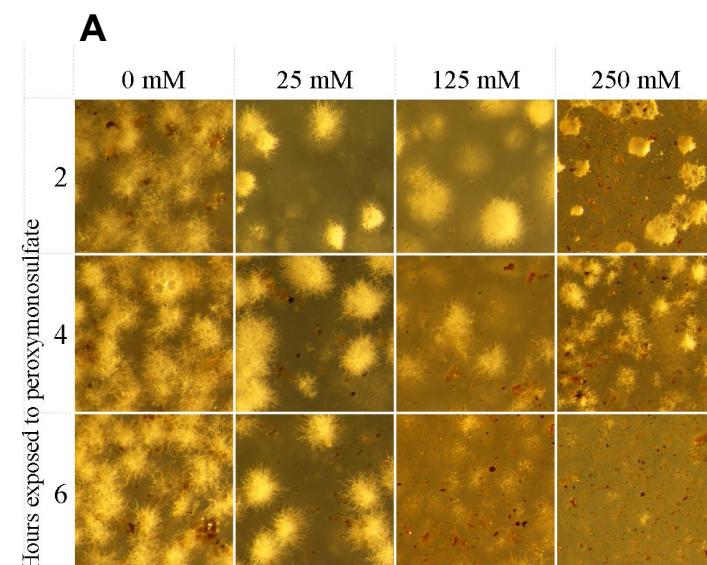


Figure 3. Colony forming units from soil after saturation in peroxymonosulfate.

Soils were exposed to HSO_5^- (0 – 250 mM) for 2, 4, and 6 h at 100% wt/v. Samples of gravity-settled supernatant (100 μL) from the top 25 mm were spread on 7.5% agar plates containing 0.3% beef extract and cultured at 36 °C. (A) Colonies were photographed and (B, C, and D) counted after 24 hours. Each value represents the average of three replicates. Error is standard deviation.

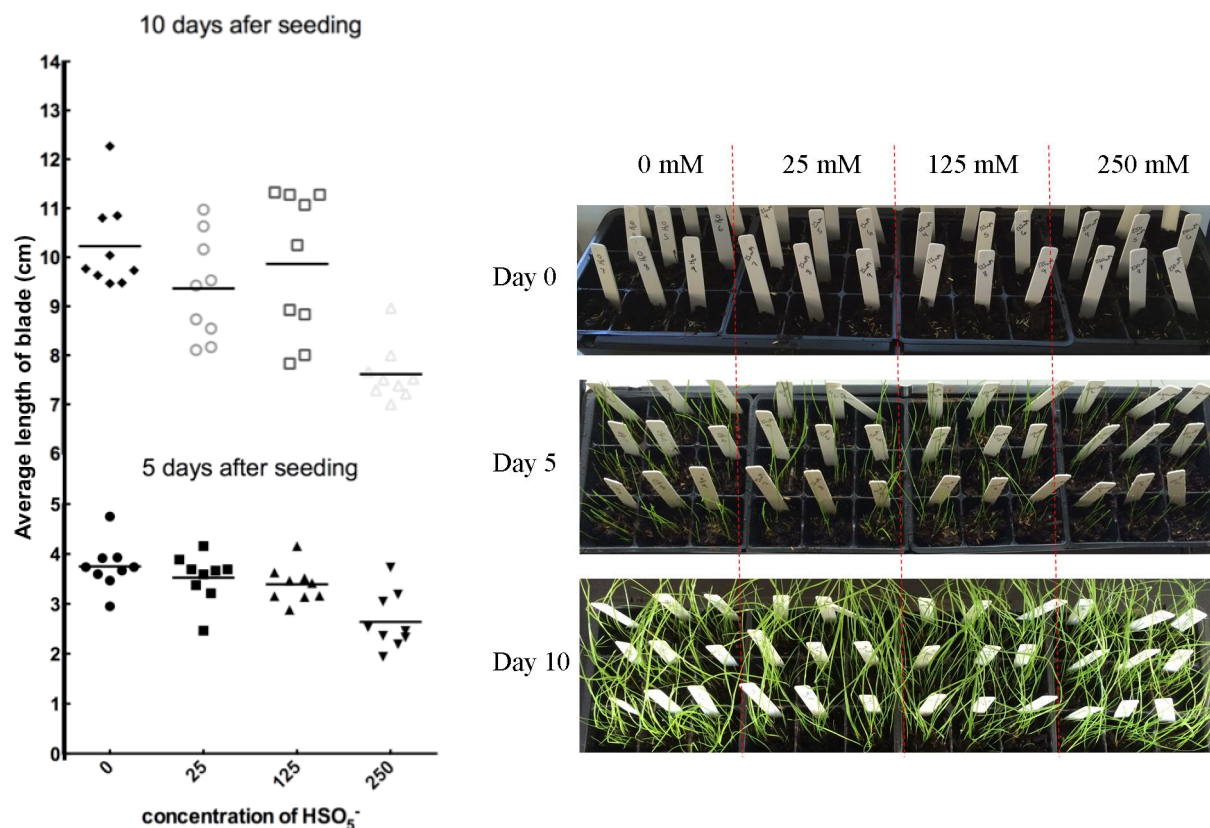


Figure 4. Soil saturated with peroxymonosulfate was able to grow grass. Potting soil was saturated (100% w/v) with unbuffered peroxymonosulfate (0mM, 25 mM, 125 mM, and 250 mM) for 48 h. Soils were drained overnight, potted in nine 4.2×4.2 cm seed starter pods per treatment, each pod was seeded with 30 seeds and each treatment was watered with 50 mL ultrapure water. After 5 and 10 days, the number and length of grass blades in each pod was counted and measured. The data here represent the average length of leaf blade from each treatment after 5 and 10 days. Each data point represents the average of each pod (9 per treatment). No significance was seen between the three lowest concentrations. The 250 mM treatment resulted in significantly shorter average grass blade lengths ($p < 0.01$) compared to all other groups for each time point.

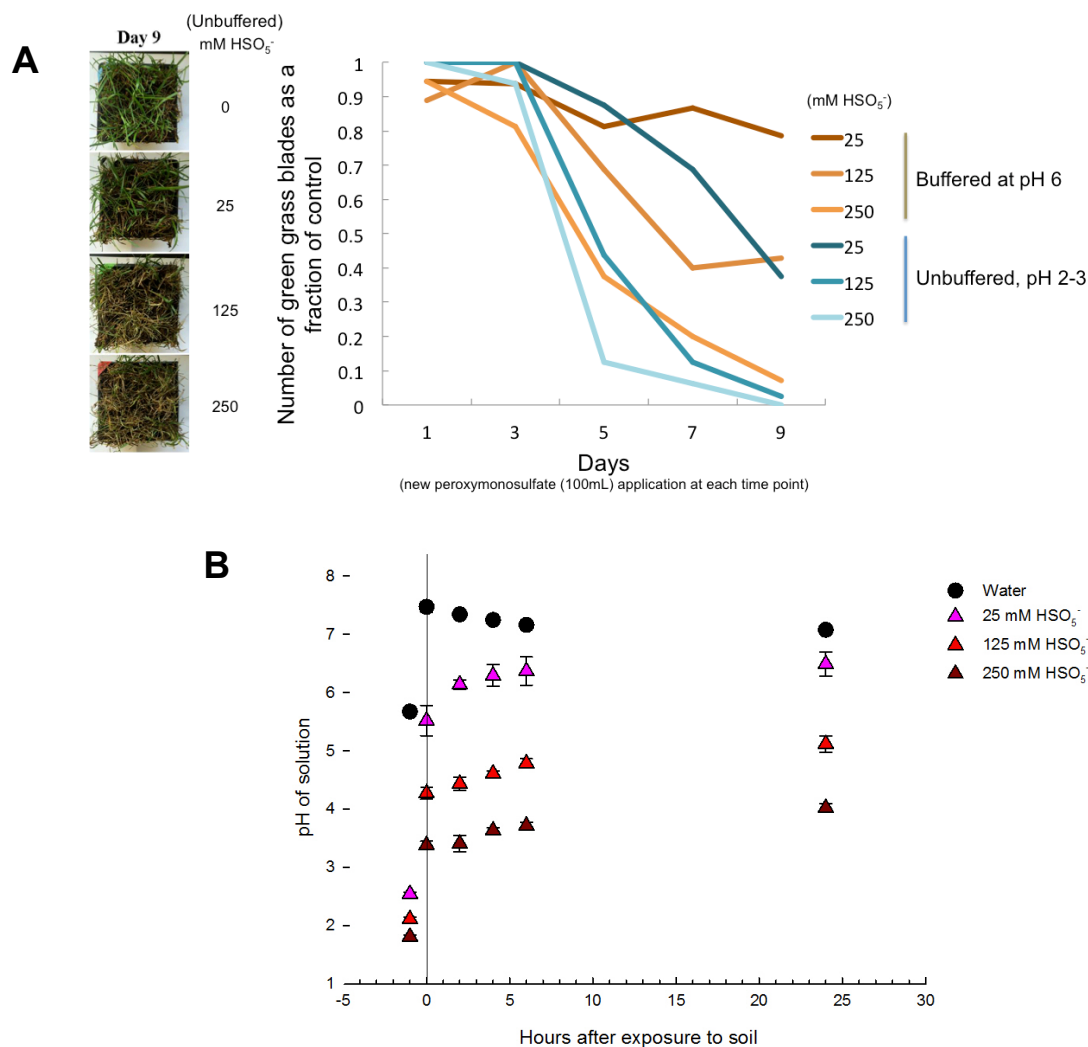


Figure 5. Sod toxicity (buffered and unbuffered). (A) Kentucky bluegrass sod was cut into 12.5 cm × 12.5 cm squares and planted on 100 g wet weight potting soil and saturated with ultrapure water. After 48 h acclimation, 100 mL peroxymonosulfate solution (0-250 mM, buffered to pH 6 with phosphate where indicated) was added to each square (in 3 × 3 planting grids). The percent of green grass blades was determined and an additional 100 mL of peroxymonosulfate was applied every other day for nine days. The reactions were not experimentally quenched. (B) Unbuffered peroxymonosulfate (0 mM, 25 mM, 125 mM, and 250

mM) was applied to potting soil (100 % w/v) and the pH was measured at the indicated times over 24 hours.

4.9 APPENDIX

Supporting Information for Chapter 4

Extraction, detection, and decontamination of chronic wasting disease agent from soil*

*A version of this chapter will be submitted to *Environmental Science & Technology* with Johnson, C.J. and Pedersen, J.A. as co-authors

Table of Contents	Page
4.9.1 Figures	150
S1. Extracts from Elliot and Defore soils reduce PMCAb amplification of PrP ^{TSE}	150
S2. Effect of extraction buffer on detection of PrP ^{TSE} associated with soil by (A) immunoblotting or (B) protein misfolding cyclic amplification.	152
S3. Effect of humic acid (HA) or fulvic acid (FA) on PMCAb	153
S4. PTA precipitation coupled with PMCAb reduce the inhibitory effect of soil extracts on PMCA	155

4.9.1 FIGURES

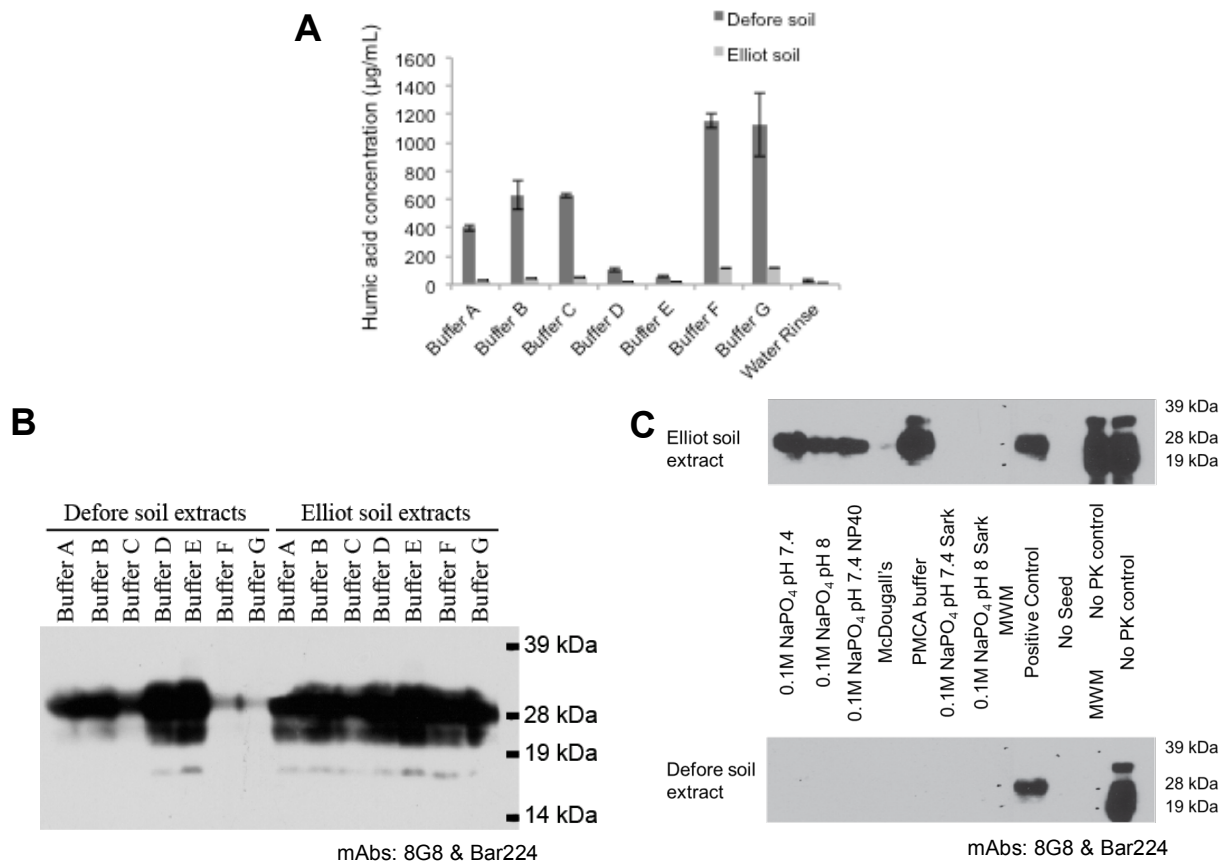


Figure S1. Extracts from Elliot and Defore soils reduce PMCAb amplification of PrP^{TSE}. (A) Samples of Defore silty loam soil or Elliot soil (25 mg) were rinsed with ultrapure water (200 µL each) with shaking 1,200 RPM for 2 h at room temperature. Samples were centrifuged (1000g, 10 min), and the supernatant was removed and saved as water rinse. The indicated buffers were added (200 µL) to each of the soil pellets and vortexed at 1,200 RPM (2 h, room temperature). Soil particles were sedimented (1000g, 10 min), and the supernatants were retained. Extractions were done in triplicate, and 100 µL of each extraction and the water rinses were used to assay the absorbance at $\lambda = 465$ nm. Absorbances were compared to dilution series of Elliot soil humic acid in each of the above buffers and concentration of humic acid calculated

for each of the buffer extractions. Shown are the mean humic acid concentrations for the three replicates with the standard deviations for each. (B) Extracts (20 μ L) were mixed with PK-treated brain homogenate from an end-stage CWD infected deer (10 μ L) and allowed to interact for 2 h at room temperature. Each sample was boiled for 15 min with 10 μ L LDS sample buffer containing reducing agent. An 18- μ L aliquot of each sample was resolved on a 15 well 10% NuPAGE gel, transferred to PVDF and PrP was detected using Bar 224 and 8G8 mAbs. (C) An 8- μ L aliquot of each extract was mixed with 2 μ L of 0.4% CWD BH from an end-stage CWD positive wt/wt deer. NBH (90 μ L) was added with two Teflon® beads in a 200- μ L thin-walled PCR tube. Samples were sonicated for 96 cycles (30 s sonication with 1770 s incubation at 37 °C between sonications). PrP^{res} was detected by immunoblotting with antibodies 8G8 and Bar224.

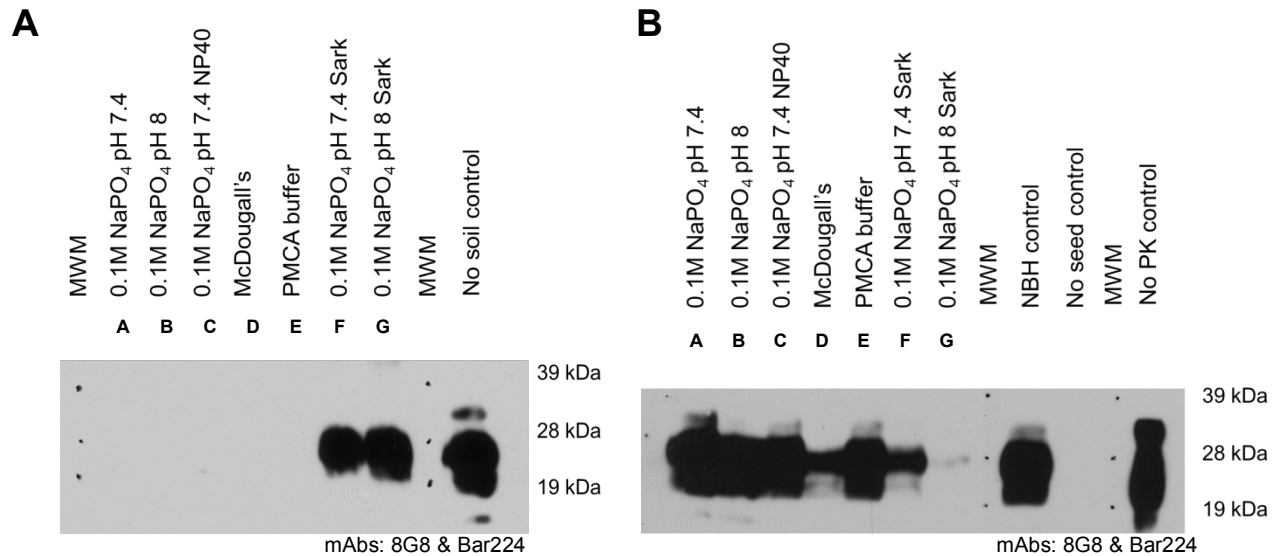


Figure S2. Effect of extractant on detection of PrP^{TSE} extracted from soil by (A) immunoblotting or (B) protein misfolding cyclic amplification. (A) PK-treated 10% CWD+ white-tailed deer brain homogenate (40 μ L) was adsorbed to 25 mg Elliot silt loam soil in 100 μ L ultrapure water for 24 h followed by a 2-h desorption step in 100 μ L water (to remove any non-adsorbed unbound PrP^{TSE}) and extraction at room temperature with 200 μ L extraction buffer (indicated). Eluates were PTA-precipitated and suspended in 100 μ L PMCA buffer prior to detection by immunoblotting. (B) Extraction buffers (8 μ L) were mixed with 2 μ L dilutions of CWD BH equivalent to 0.4% from an end-stage CWD positive wt/wt deer. NBH (90 μ L) was added with two Teflon® beads in a 200- μ L thin-walled PCR tubes. Samples were subjected to 96 cycles of PMCAb (one cycle consisted of 30 s sonication followed by 27 min 30 s incubation at 37 °C). (A & B) PrP^{res} was detected by immunoblotting with antibodies 8G8 and Bar224. MWM, molecular weight marker.

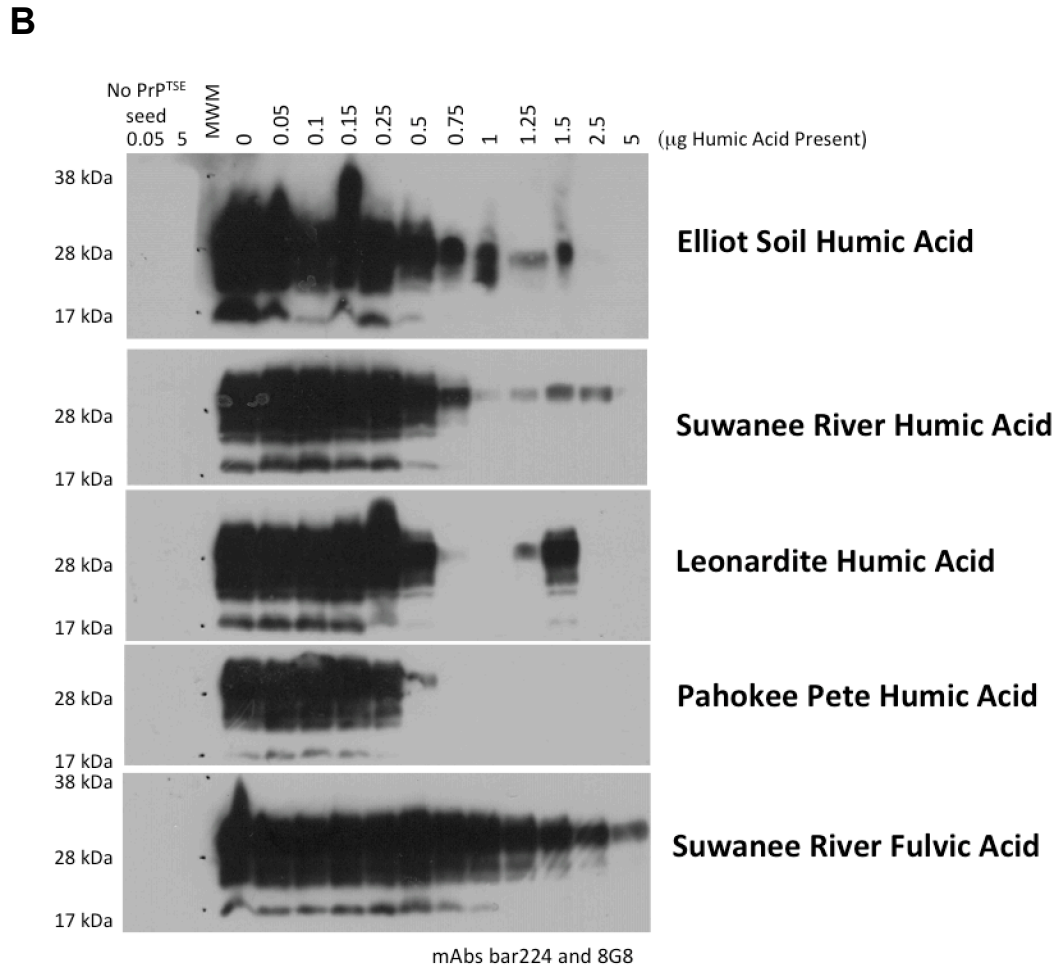
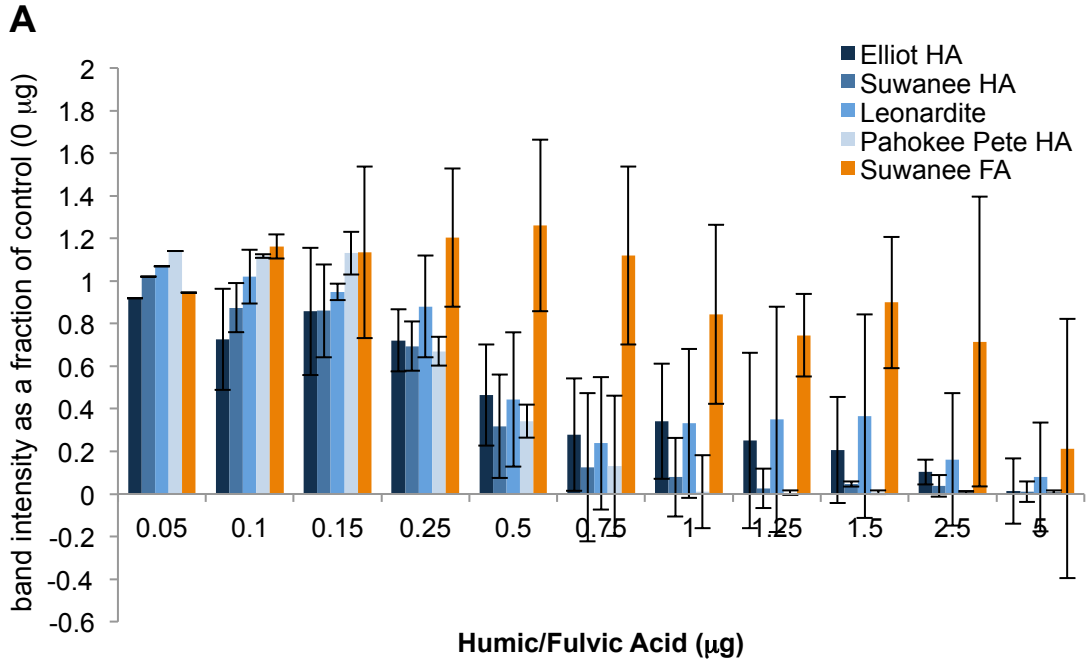


Figure S3. Effect of humic acid (HA) or fulvic acid (FA) on amplification of PrP^{TSE}

by PMCAb. Prions (10% CWD brain homogenate) were diluted using four serial fivefold dilutions in NBH. The seed dilution (2 μ L) was transferred into 36 μ L NBH with saponin, and 2 μ L humic acid (dissolved in ultrapure water) was added for a total mass of 5, 2.5, 1.5, 1.25, 1, 0.75, 0.5, 0.25, 0.15, 0.1, 0.05 or 0 μ g Elliot Soil HA, Suwanee River HA, Leonardite HA, Pahokee Pete HA, or Suwannee River FA. Controls lacked infectious seeds and contained 5 or 0.05 μ g humic or fulvic acid. All samples were subjected to a single round of mbPMCA for 96 cycles. (A) Densitometry was measured with ImageJ and represents the intensity of PrP immunoblot signal as a fraction of the control (0 μ g humic or fulvic acid). (B). Immunoblots shown are representative of three replicates and are probed with mAbs Bar224 and 8G8.

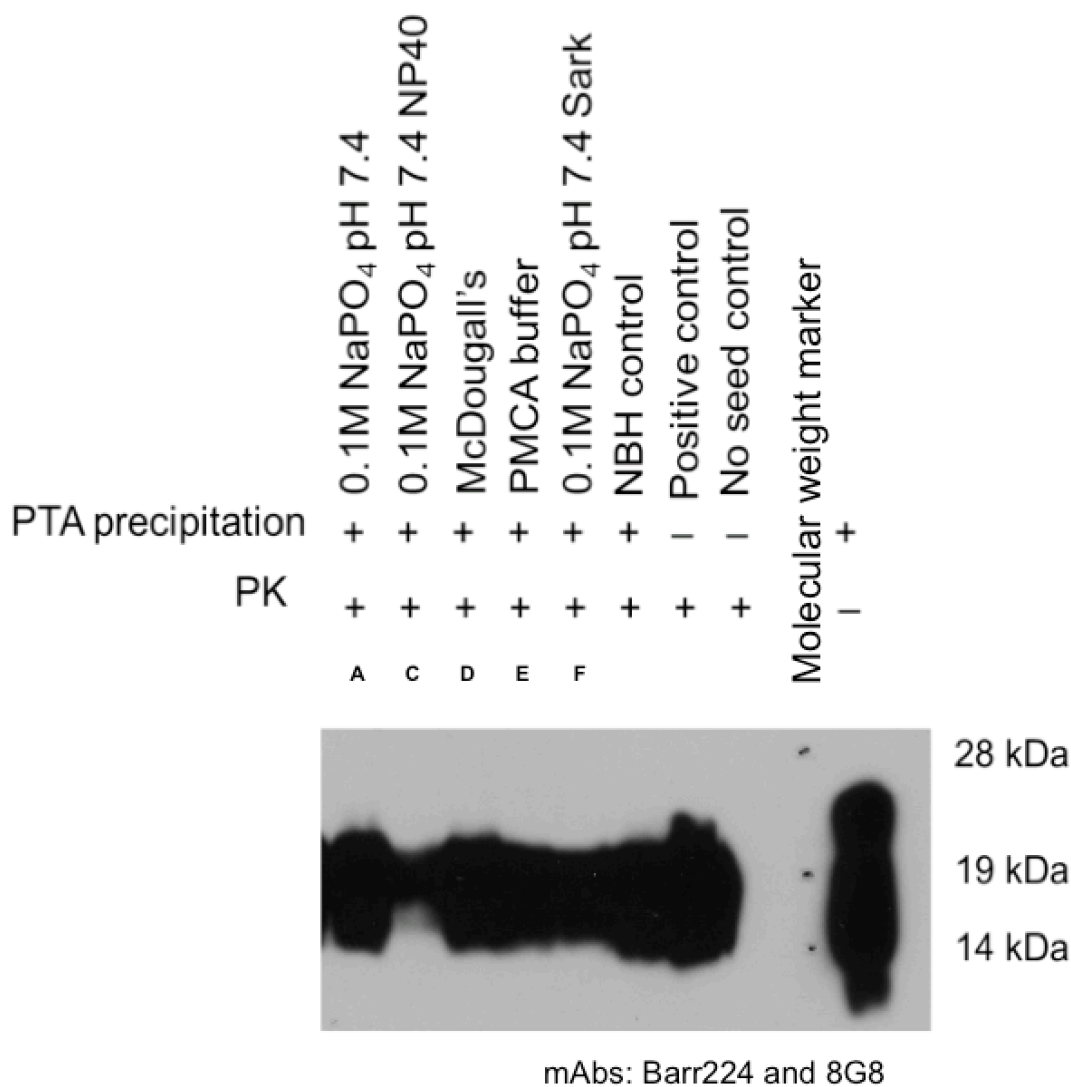


Figure S4. PTA precipitation coupled with PMCAb reduce the inhibitory effect of soil extracts on PMCA. After PTA precipitation, 10 μ L samples from extractions using each buffer were added to a PMCAb reaction. Extraction buffers are listed in Table 1. NBH carrier was uninfected brain homogenate added to PrP^{TSE} prior to PTA precipitation. Samples were added with two Teflon® beads in a 200- μ L thin-walled PCR tubes. Samples were sonicated for 96 cycles (30 s sonication with 27:30 incubation at 37 °C between sonications). PrP^{res} was detected using immunoblotting with antibodies 8G8 and Bar224.

Chapter 5

Microparticles Alter Early Disease Tissue Tropism and Accumulation of Chronic Wasting Disease Prions in White-Tailed Deer*

Microparticles Alter Early Prion Disease Pathogenesis

*A version of this chapter will be submitted to *PLoS Pathogens* with Johnson, C.J., Nichols, T.A., Kornely, H.J., Shoukfeh, D., and Pedersen, J.A. as co-authors.

* Guilherme Ludwig assisted with statistical analysis

5.1 ABSTRACT

Environmental reservoirs of infectivity contribute to the spread of prion diseases of sheep and of North American members of the deer family (cervids). Soil has been implicated in the environmental transmission of both diseases. Oral transmission of prion disease in the hamster model can be enhanced when the disease agent is bound to mineral microparticles present in soils. The layered aluminosilicate mineral montmorillonite exhibited the strongest potentiation of disease transmission in hamsters of the particles studied to date. The digestive systems of ruminants and hamsters differ, leaving open the question of whether the enhanced transmission of disease by microparticle-bound prions observed in rodents also occurs in ruminants. Here, we tested the hypothesis that association of cervid chronic wasting disease (CWD) prions with montmorillonite microparticles alters the early tissue tropism and accumulation of the disease agent following oral inoculation of white-tailed deer (*Odocoileus virginianus*). At 42 days post inoculation (dpi), pathogenic prion protein (PrP^{TSE}) accumulated to a larger extent in lymphatic and ileal tissues and was present at detectable levels in more tissues in animals orally inoculated with prions associated with montmorillonite microparticles relative to those inoculated with prions alone as determined by microplate-based protein misfolding cyclic amplification. Only deer inoculated with CWD agent associated with montmorillonite had detectable PrP^{TSE} in the palatine tonsil at 42 dpi. These findings indicate enhanced oral transmission of CWD by montmorillonite-bound prions consistent with prior findings in rodent models. The potentiation of disease transmission by the association of CWD prions with microparticles warrants consideration in evaluating the relative importance of direct and indirect disease transmission and in developing strategies to manage CWD in free-ranging and captive cervid populations.

5.2 AUTHOR SUMMARY

Prion diseases affect a variety of mammalian species, including humans. Prions are unique infectious agents composed predominately, if not solely, of misfolded forms of the normally benign prion protein. Chronic wasting disease (CWD) is a prion disease that affects North American members of the deer family. A distinctive aspect of CWD is that environmental routes contribute to transmission of the disease. Soil is considered a plausible reservoir of prion infectivity in the environment. We previously demonstrated that when bound to certain microparticles found in soil, disease transmission is enhanced in a rodent model upon oral exposure. In this work we show that the enhancement of disease transmission by microparticle-bound prions extends to deer. When CWD prions associated with the common clay mineral montmorillonite are orally administered to white-tailed deer, the infectious agent accumulates to a larger extent and in more tissues during early stages of the disease relative to deer inoculated with prions alone. Enhanced transmission of microparticle-bound CWD agent warrants consideration in modeling disease dynamics and in designing strategies to limit the spread of the disease.

5.3 INTRODUCTION

Prions are the etiological agents in transmissible spongiform encephalopathies (TSEs), a class of inevitably fatal, progressive neurodegenerative diseases.^{1, 2} These diseases affect cattle (bovine spongiform encephalopathy; BSE), scrapie (sheep and goats), North American cervids (chronic wasting disease; CWD), and humans (e.g., Creutzfeldt-Jakob disease (CJD), and kuru).¹ Substantial evidence implicates consumption of BSE-contaminated beef in the acquisition of variant CJD,³ raising concern about the zoonotic potential of other prion diseases. Prions are composed primarily, if not solely, of misfolded conformers of the prion protein (PrP).^{1, 4} The central molecular event underlying the progression of these diseases is the seeded or template-driven conformational conversion of the benign, normally folded conformer (PrP^C) to disease-associated forms (PrP^{TSE}) and subsequent assembly into β -sheet-rich aggregates.⁵ The conformational changes alter the susceptibility of the protein to proteolysis^{6, 7} and confers remarkable resistance to decontamination methods that are effective against conventional pathogens, including boiling, autoclaving, or treatment with alcohols or formalin.⁸

Chronic wasting disease, initially believed to be isolated to the front range of the Rocky Mountains in Colorado and Wyoming, has spread dramatically across North America. Animals infected with CWD shed prions into the environment during the course of disease, including the pre-symptomatic stage through saliva,⁹⁻¹¹ urine,¹¹ feces,¹²⁻¹⁵ and antler velvet.¹⁶ Prions can also enter the environment via decomposition of infected animal carcasses¹⁷ and in blood shed from wounds.⁹ For both CWD and scrapie, environmental reservoirs of infectivity contribute to horizontal disease transmission.¹⁷⁻¹⁹ Prions are resistant to many decontamination methods effective against conventional pathogens and can retain infectivity after exposure to alcohols, formalin, and standard autoclaving conditions.⁸ The stability of prions contributes to their

persistence in the environment^{20, 21} and thus their transmission to naïve hosts. Under at least some conditions, prion infectivity can persist in the environment for over a decade.²² Prions released to soil environments are expected to associate strongly with soil particle surfaces.²³⁻²⁷ Although vertical movement appears to be limited,²⁸ a potential consequence of prion attachment to clay particles may result in transport in overland flow to streams, resulting in movement to distant locations.²⁹

Soil has been implicated in transmission of CWD and scrapie.^{30, 31} Association of prions with microparticles in soils or used as food and feed additives can enhance the oral transmission of prion disease in rodent (hamster) models.²³⁻²⁵ These microparticles include the aluminosilicate clay minerals montmorillonite and kaolinite, silicon dioxide, and meat and bone meal microparticles.²³⁻²⁵ The digestive systems of hamsters and ruminants such as cervids differ. Hamsters possess a non-glandular forestomach, glandular stomach compartment, and a large cecum. Cervids have a four-chambered stomach comprised of the rumen, reticulum, omasum, and abomasum.³² Whether the enhanced transmission of TSE by prions associated with microparticles occurs in cervids has not been investigated.

The objective of this study was to test the hypothesis that association of CWD agent with microparticles alters the early tissue tropism and accumulation of prions following oral inoculation of white-tailed deer (*Odocoileus virginianus*). To accomplish this objective, we used montmorillonite as a model because microparticles of this aluminosilicate mineral produced the largest enhancement of disease transmission in prior studies.^{23, 24} White-tailed deer fawns were orally inoculated with CWD PrP^{TSE} either bound to montmorillonite microparticles or in the absence of microparticles. Tissues were harvested at 42 days post infection (dpi), and the accumulation of prions in tissues was examined by microplate-based protein misfolding cyclic

amplification (mbPMCA)³³ and immunohistochemistry (IHC). Oral exposure to CWD agent associated with Mte altered early tissue tropism (prions accumulated in the palatine tonsils only in those animals orally exposed to CWD agent + montmorillonite) and in substantially higher accumulation of PrP^{TSE} in retropharyngeal and submandibular lymph nodes relative to deer exposed to PrP^{TSE} alone. These observations are consistent with enhanced transmission of CWD by prions associated with microparticles and could help explain the efficiency of environmental transmission of this disease.¹⁷⁻¹⁹

5.4 MATERIALS AND METHODS

5.4.1 Ethics Statement. All procedures involving animals were approved by the Institutional Animal Care and Use Committee of the University of Wisconsin, Madison (Assurance Number A3464-01) and the Institutional Animal Care and Use Committee (protocol # QA-2004) at the USDA National Wildlife Research Center in accordance with the USDA Animal Welfare Act Regulation. CFR, title 9, chapter 1, subchapter A, parts 1-4.

5.4.2 Preparation of inoculum and oral dosing of white-tailed deer fawns.

Brain tissue was isolated from a homozygous wild-type (95QQ 96GG) white-tailed deer that had been experimentally infected with CWD prions via the oral route and showed clinical symptoms of CWD prior to euthanization.³⁴ Brain tissue was homogenized in 1× Dulbecco's phosphate buffered saline (PBS) without Ca²⁺ or Mg²⁺ (137 mM NaCl, 8.1 mM HPO₄²⁻, 1.47 mM H₂PO₄; pH 7) to a concentration of 10% w/v and stored at -80 °C until use. Two CWD-positive inocula were prepared: 10% brain homogenate from a CWD-positive white-tailed deer with or without montmorillonite (Mte) microparticles. For the negative control deer, we prepared 10% w/v brain homogenate from a CWD-negative control white-tailed deer and administered it without montmorillonite microparticles. Brain homogenate samples were clarified by centrifugation (2

min, 1000g) prior to inoculum preparation. The montmorillonite (SWy-2, Crook County, Wyoming, USA; Clay Minerals Society Source Clays Repository, West Lafayette, Indiana, United States) was size-fractionated by wet sedimentation to obtain particles with hydrodynamic diameters of 0.5–2 μm and homoionized with sodium as previously described.³⁵ Brain homogenates for the inoculum containing montmorillonite were prepared by allowing PrP^{TSE} to adsorb to 0.1% Mte for 4 h with shaking at ambient temperature. These samples were then centrifuged over a 1 M sucrose cushion containing 10 mM NaCl to separate montmorillonite-bound from free prions.²⁵

Seven white-tailed deer were purchased from a CWD-free, private deer facility in Missouri, USA and transported to the USDA National Wildlife Research Center (NWRC) in Fort Collins, CO for the study. Fawns were between 2 and 14 days of age upon arrival, were bottle-fed and weaned by 16 weeks of age. Deer were orally inoculated with 130 mL of normal brain homogenate or normal brain homogenate containing 10 mL of a 10% CWD+ brain homogenate (equivalent to 1 g brain tissue) with or without montmorillonite at 3 months of age via syringe by inserting tubing through the diastema into the oral cavity. Fawns were genotyped at codon 95 and 96 by the USDA Agricultural Research Laboratory in Pullman, WA. All deer were homozygous wild-type (QQ)³⁴ at codon 95, and either GS or GG at codon 96. Both genotypes were represented in each treatment group (Table 1): one GS and two GG deer. The control animal was GS at codon 96. After 42 d, animals were euthanized and tissues (Table S1) were harvested. Tissues were halved; one half was fixed in buffered formalin for 2 weeks, and the other was frozen in liquid nitrogen and stored at –80 °C until use.

5.4.3 Tissue homogenization and phosphotungstic acid precipitation.

Tissues were homogenized to a 10 % w/vol concentration in DPBS (pH 7.4) containing Roche

complete protease inhibitor in a Fastprep 24 bead beater using 2 mm glass beads and 1.6 mm silicon carbide particles. Sodium *N*-lauroylsarcosinate (sarkosyl) was added to a final concentration of 1%, and samples were incubated for 1 h under constant mild agitation. Tissue homogenates were centrifuged (60 min, 15000g, 10 °C), the supernatant was transferred and centrifuged again under the same conditions. After the second centrifugation, the supernatant was removed and diluted 1:1 with DPBS (15 mM KH₂PO₄, 81 mM Na₂HPO₄, 137 mM NaCl, and 3 mM KCl) containing 4% sarkosyl. Sodium phosphotungstic acid (4% with 170 mM MgCl) was added to a final concentration of 0.57% and incubated overnight at 37 °C. After precipitation, samples were centrifuged (30 min, 15000g, room temperature). The pellet was washed once with 200 µL PBS, 0.1% sarkosyl and 50 µL 250 mM EDTA and centrifuged (10 min, 16000g). Pellets were resuspended in PMCA buffer (150 mM NaCl, 4 mM EDTA, pH 8.0, 1% (v/v) Triton X-100 and miniprotease inhibitor) and brought to 100 µL.

5.4.4 Microplate-based protein misfolding cyclic amplification. Microplate-based protein misfolding cyclic amplification (mbPMCA) was conducted according to our previously published PMCAb protocol³⁶ adapted to a microplate format.³³ Uninfected transgenic mouse ((Tg(CerPrP)1536^{+/0})³⁷ brain homogenate served as the substrate for the PMCA reaction. Transgenic mice (cared for in accordance with protocols approved by the Institutional Animal Care and Use Committee of the University of Wisconsin, Madison (Assurance Number A3464-01)) were euthanized by CO₂ asphyxiation and immediately perfused with 1× modified Dulbecco's phosphate buffered saline without Ca²⁺ or Mg²⁺ (Thermo Scientific, amended with 5 mM EDTA). Brains were then rapidly removed, flash frozen in liquid nitrogen, and stored at -80 °C until use. Brains were homogenized on ice to 10% (w/v) in PMCA conversion buffer (Ca²⁺- and Mg²⁺-free DPBS supplemented with 150 mM NaCl, 1% Triton X-100, 0.05% saponin

(Mallinckrodt), 5 mM EDTA, and one tablet Roche Complete EDTA-free protease inhibitors cocktail (Fisher) per 50 mL conversion buffer). Brain homogenates were clarified by centrifugation (2 min, 2,000g). Supernatant was transferred to pre-chilled microcentrifuge tubes, flash frozen in liquid nitrogen, and stored at -80°C until use.

Positive control samples for mbPMCA were made from a 10% CWD BH diluted five-fold in series. Briefly, a dilution series was prepared from clinically affected white-tailed deer³⁴ by serial five-fold dilution of 10% BH in normal brain homogenate (NBH) to generate a dilution series. Samples from the dilution series were used to seed 36 μL NBH (4 μL seed) in a 96-well PCR microplate (Axygen, Union City, CA, USA).

Microplates containing samples for mbPMCA were placed in a rack in a Misonix S-4000 microplate horn, and the reservoir was filled with ultrapure water (18.2 $\text{M}\Omega\cdot\text{cm}$ resistivity, Barnstead GenPure Pro). Each round of mbPMCA consisted of 96 cycles of 30 s sonication (40-60% of maximum power) and 29 min, 30 s incubation (37°C). At the completion of 96 cycles, 20 μL of each sample was digested with PK ($50\text{ }\mu\text{g}\cdot\text{mL}^{-1}$, 1 h, 37°C) and prepared for SDS-PAGE for detection by immunoblotting. For serial mbPMCA, 4 μL of the reaction mixture was transferred to fresh NBH to seed a new round.

Samples were prepared for SDS-PAGE by adding NuPAGE lithium dodecyl sulfate sample buffer (7.5 μL) and NuPAGE sample reducing agent (2.5 μL) containing 500 mM dithiothreitol (Invitrogen), and heating for 10 min to 100°C . Protein samples were fractionated on 12% bis-tris polyacrylamide gels (Invitrogen) and electrotransferred to 0.45 μm polyvinyl difluoride membranes. Membranes were blocked in 5% non-fat dry milk in Tris-buffered saline containing 0.1% Tween 20 (overnight, 4°C). PrP was probed with mAb 8G8 (1:10,000 dilution, Cayman Chemical) and Bar224 (1:5000 dilution, Cayman Chemical). Detection was achieved

with HRP-conjugated goat anti-mouse immunoglobulin G (1:10,000; BioRad) and Super Signal West Pico chemiluminescent substrate (Pierce Biotechnology, Rockford, IL).

5.4.5 Immunohistochemistry. Immunohistochemical staining was performed by the Wisconsin Veterinary Diagnostic Laboratory. Tissues fixed in formalin were dehydrated, embedded in paraffin, sectioned via microtome (5 μ m thickness), placed on positively charged slides, deparaffinized, and rehydrated. Antigen retrieval was performed by hydrated autoclaving in retrieval buffer using the PrP specific Anti-Prion 99 antibody (Roche-Ventana, Cat# 06914713001), and a biotinylated secondary goat anti-mouse antibody, followed by horseradish peroxidase-streptavidin conjugate, chromagen substrate and hematoxylin counterstain. Three blinded evaluators, unfamiliar with the study, assessed the stained tissue sections. Tissue sections were assigned a ranking of 0 (“staining absent”) to 4 (“strong staining”), with zero denoting a complete lack of PrP staining (minus obvious background) and four indicating intense PrP signal. Scores were averaged among evaluators and divided by the maximum score (4), to arrive at a normalized IHC score between 0 and 1.

5.4.6 Data and Statistical Analysis. The comparison of treatment in regard to prion detection was computed using Fisher’s exact test. Prion detection as a relative value was computed based on the round of mbPMCA where detection was first seen; a relative PMCA detection value is calculated as the mbPMCA round where detection is first seen, subtracted from the total number of rounds (4), plus one. No detection was indicated with a relative detection value of 0. The nonparametric Kruskal-Wallis H test was used to test differences among medians with Dunn’s correction; pair-wise comparisons were made using the nonparametric Mann-Whitney U test with Bonferroni’s correction. The significance level was set at $\alpha = 0.05$.

5.5 RESULTS

At 42 days after oral inoculation, tissues were collected (Table S1) from six asymptomatic white-tailed deer that had been orally inoculated with CWD-infected brain homogenate (BH; 10% w/v in 1× phosphate-buffered saline, PBS) with ($n = 3$) or without ($n = 3$) 0.1% wt/vol Mte as well as from a control animal given BH (10% w/v in 1× PBS) generated from a CWD-negative white-tailed deer. Pathogenic prion protein accumulated to a larger extent in lymphatic and ileal tissues and was present at detectable levels in more tissues in animals orally inoculated with PrP^{TSE} associated with montmorillonite (Mte) microparticles relative to those inoculated with PrP^{TSE} alone ($p = 0.0039$, Fisher's exact test, Table 1). An odds ratio from Fisher's exact test of 4.0690 indicates that it is 4 times more likely to detect prions in the tissues from the deer inoculated with Mte than from the deer inoculated with only CWD BH. Association of CWD prions with microparticles in the inoculum resulted in detection of PrP^{TSE} in a larger number of tissues in CWD-infected white-tailed deer than in deer challenged with CWD prions alone. Detectable PrP^{TSE} was present in the retropharyngeal (RPLN) and submandibular (SMLN) lymph nodes, and in the ileum of deer orally exposed to CWD prions in the absence or presence of montmorillonite (Table 1). All animals orally inoculated with CWD agent (\pm montmorillonite) had detectable PrP^{TSE} in the RPLN. Detectable PrP^{TSE} was present in the SMLN of all deer inoculated with CWD agent bound to Mte, but in only one animal inoculated with PrP^{TSE} alone (one of three replicate samples). Only deer inoculated with CWD agent associated with montmorillonite had detectable PrP^{TSE} in the palatine tonsil (two of three animals, both 96GG; Table 1). Furthermore, PrP^{TSE} was detected in earlier rounds of mbPMCA and in more replicates in lymph nodes and the palatine tonsil when inoculated with microparticles, indicating enhanced accumulation (Table 1). Pathogenic prion protein was

detected in the ilea of all deer inoculated with PrP^{TSE} associated with montmorillonite, and in two of three animals inoculated with PrP^{TSE} alone. Control deer did not exhibit PrP^{TSE} in any analyzed tissues.

The round of mbPMCA in which PrP^{TSE} was first detected for each sample provides an estimate the amount of prion accumulation in each tissue. Samples in which PrP^{TSE} is detectable in the first round of mbPMCA contain more prions than do samples for which detection is first achieved in subsequent rounds. In Figure 1, we express the amount of pathogenic prion protein in a tissue sample in a manner yielding a higher value for detection at an earlier round of mbPMCA, which corresponds to a larger amount of PrP^{TSE}. The relative amount of PrP^{TSE} is calculated as the round of first detection subtracted from the total number of rounds (4) plus one, with no detection assigned a value of zero. The median values for the PrP^{TSE} + Mte treatment differed from the control treatment for the RPLN ($p = 0.013$, Kruskal Wallis with Dunn's post hoc correction; Figure 1A) and the two experimental treatments differed for the SMLN ($p = 0.005$, Kruskal Wallis with Dunn's post hoc correction; Figure 1B). Prions were detected in the palatine tonsil from only animals inoculated with prions associated with montmorillonite (Figure 1C). The experimental treatments for the ileum and palatine tonsil did not differ in the round of first detection of PrP^{TSE} ($p > 0.05$; Figure 1D).

The PrP^{TSE} in tissues positive for CWD prions by mbPMCA were not detectable by immunohistochemical analysis (Figure S1). Three independent evaluators blind to the study reviewed and ranked stained tissues. All experimental tissues, including those from the control animal, had no staining that would be considered indicative of accumulation of PrP^{TSE}. This result is consistent with previous reports of the higher sensitivity of serial PMCA relative to IHC.^{38, 39}

To allow an estimation of the amounts of PrP^{TSE} in tissue samples, we analyzed dilutions of CWD-infected brain tissue by mbPMCA in parallel with experimental samples (Figure S2A). Comparison of the round at which PrP^{TSE} was first detected in a tissue against the dilution series provided an estimate of the amount of PrP^{TSE} in terms of an equivalent dilution of brain tissue from a clinical CWD-infected white-tailed deer (Figure S2B). Results from this analysis are presented in Figure 2 and clearly indicate higher prion accumulation in tissues from animals dosed with CWD prions associated with montmorillonite microparticles compared to those inoculated with CWD prions alone. Accumulation of PrP^{TSE} differed between treatment groups ($p = 0.0086$, Kruskal-Wallis H test with Dunn's multiple comparison's test), with significantly larger amounts of prions detected in tissues from deer given the CWD BH inoculum containing microparticles compared to detection in tissues from deer in the control treatment ($p = 0.0081$, Mann-Whitney U with Bonferroni's correction). Differences in PrP^{TSE} accumulation based on tissue types, excluding treatment type, were not significant. These comparisons are presented graphically in Figure S4.

5.6 DISCUSSION

Association of prions with mineral microparticles can enhance disease transmission in the hamster model.²³⁻²⁵ In this contribution, we investigated early tissue accumulation patterns of PrP^{TSE} in white-tailed deer orally inoculated with CWD prions alone or bound to montmorillonite microparticles. Microplate-based PMCA,^{33, 40} a new, high-throughput variation of bead-assisted PMCA,^{33, 36, 41} allowed detection of differences in prion accumulation patterns in tissues of white-tailed deer between the two treatments 42 days after oral inoculation with CWD agent. At 42 dpi, PrP^{TSE} was detected in the ileum, RPLN, and SMLN in animals in both

treatment groups with higher accumulation the RPLN and SMLN in animals in the prion + montmorillonite treatment than in the group receiving prions alone. Furthermore, PrP^{TSE} was detected in the palatine tonsils from two deer in the treatment group inoculated with CWD agent bound to montmorillonite. Detection of PrP^{TSE} in the RPLN and ileal tissue of the deer is in agreement with prior work using IHC to investigate the tissue tropism of PrP^{TSE} in mule deer orally inoculated with CWD agent (inoculated with 10× more CWD-infected brain homogenate than used in the present study).⁴² To our knowledge, the detection of PrP^{TSE} in the palatine tonsil and SMLN at 42 dpi represents the earliest detection of prion accumulation in these tissues in deer inoculated by the oral route. In the study mentioned above, PrP^{TSE} was first detected in the tonsil of orally inoculated mule deer at 78 dpi (in one of 205 follicles examined) and was not detected in the SMLN of any animal (maximum 80 dpi investigated).⁴² Alimentary tract-associated lymphoid tissue, including the palatine tonsils, retropharyngeal lymph nodes, and intestinal lymphoid tissue, has long been implicated as the primary route of prion uptake and early prion replication sites.⁴²⁻⁴⁵ Our results confirm the RPLN as a site of early accumulation of CWD prions in orally inoculated cervids,⁴² and demonstrates that SMLN and palatine tonsils can also figure importantly in early disease pathogenesis. Tonsil-derived human follicular dendritic-like cells resist prion infection by trafficking PrP^{TSE} to lysosomes.⁴⁶ The association of PrP^{TSE} with montmorillonite microparticles may interfere with this trafficking. Uptake of prions through the intestine does not appear to be necessary to initiate disease via the oral route; scrapie prions injected into the palatine tonsils of sheep caused widespread prion replication throughout the body and subsequent neuroinvasion.⁴⁷

All deer used in the study were homozygous at codon 95 (95QQ). Deer homozygous for glycine (96GG) and heterozygous at this position (96GS) were represented in each treatment

group (Table 1). The 96GS individuals appeared to accumulate PrP^{TSE} to smaller extent than did the 96GG animals, but the restricted sample sizes used in this study preclude statistically testing the hypothesis that tissue accumulation differed between animals with these genotypes. We note that upon intranasal inoculation, white-tailed deer with the 96GG *PRNP* genotype had a broader PrP^{TSE} distribution, measured by IHC-positive follicles in the SMLN, RPLN, parotid lymph nodes, palatine tonsils and Peyer's patches during the asymptomatic stage compared to 96GS deer.⁴⁸

The *PRNP* genotype at codon 96 influences detection of PrP^{TSE} by PMCA. A study comparing detection of PrP^{TSE} by PMCA and IHC suggested that PMCA was the more sensitive technique for 96GG but not for 96GS white-tailed deer, although the comparison of PMCA and IHC detection of 96GS deer was constrained by sample size.³⁹ The effect of PrP primary sequence on PMCA may have been due to sequence mismatch between PrP^{TSE} in the tissues and PrP^C used as substrate in the PMCA reaction. The primary sequence of PrP influences susceptibility to TSE infection *in vivo*^{34, 49, 50} and the efficiency of PMCA *in vitro*.⁵¹ If the *PRNP* genotype of deer included in our study influenced the efficiency of mbPMCA, the tissues of the 96GS animals may have harbored higher levels of PrP^{TSE} than our results indicate.

Potential explanations for enhanced transmission of prions bound to montmorillonite microparticles include protection from degradation in the gastrointestinal tract, induction of inflammation in the intestinal tract, increased residence time in the gastrointestinal tract, and enhanced sampling by alimentary-tract associated lymphatic tissue. Experiments using an *in vitro* rumen model suggest that prions resist degradation in this intestinal digestive compartment whether or not they are bound to soil particles.⁵² This is consistent with our results where the detection of PrP^{TSE} is similar between the two control groups in the ileum.

Inflammation can enhance or alter prion disease progression,⁵³⁻⁵⁶ possibly by inducing the release of tight junction proteins and increasing initial PrP^{TSE} uptake across the epithelium by protruding, PrP^C-rich dendritic cells sampling the intestinal lumen contents.^{45, 55} To our knowledge, no published studies have suggested that smectite particles (e.g., montmorillonite) induce intestinal inflammation. To the contrary, Ca²⁺-montmorillonite particles do not promote inflammation in healthy humans⁵⁷ and have been shown to adsorb inflammatory proteins and diminish inflammation in a rodent model.^{58, 59} Furthermore, montmorillonite does not alter intestinal permeability in weanling pigs,⁶⁰ and has been shown to counteract the intestinal disruption caused by the pro-inflammatory cytokine tumor necrosis factor- α in intestinal inflammation.⁶¹ Oral administration of montmorillonite alone is therefore not expected to induce intestinal inflammation. In the present study, the montmorillonite microparticles were coated in biomolecules from PK-digested brain homogenate, altering the surface properties of the particles. Whether montmorillonite particles bearing such a coating would induce inflammation awaits experimental determination. We note that whereas neither dietary TiO₂ microparticles nor a high dose bacterial lipopolysaccharide alone induced inflammatory response in human intestinal organ cultures, when administered together with sufficient calcium, concentrations of the pro-inflammatory cytokine IL1-B were increased.⁶²

Smectites have been previously investigated for reducing the duration of diarrhea in children,^{63,64} and has been shown to increase the adsorptive capacity of the intestinal lumen.⁶⁵ These studies show that, in addition to decreasing the duration of intestinal evacuation events without increasing the permeability of the epithelium,⁶¹ smectites adsorbed pathogens such as rotavirus and other diarrhea-inducing agents.⁶⁵ Indigestible endogenous microparticles engulfed by macrophages in intestinal tissues are retained in the immobilized cells.^{66,67} Adsorption of

cations to the surface of ingested microparticles may facilitate the binding of organic molecules, such as proteins.⁶² Prions associated with these microparticles could in principle have a longer residence time in the intestine than un-bound prions, reducing elimination through the intestines and increasing the potential for uptake of both prion and microparticle into intestinal tissue rich with M-cell lymphoid aggregates (e.g., Peyer's patches in the small intestine).^{62,68}

In deer, prions accumulate in the lymphatic system, including lymph nodes and the spleen, prior to accumulation in neural tissue.⁴⁴ Lymphatic intestinal sampling may select exogenous aluminosilicate microparticles.⁶² The detection of prions in the palatine tonsils from deer dosed with montmorillonite may indicate that sampling occurs in the oral cavity and is enhanced when prions are bound to microparticles. Prions accumulate in nasal mucosa-associated lymphoid tissue and SMLN of Syrian hamsters as early as 4 weeks after inoculation via the nasal cavity.⁶⁹ Accumulation of prions in the palatine tonsil and the proximity of this mucosa-associated lymphoid tissue to the salivary glands may lead to increased prion shedding in saliva. Determining the relationship between prion accumulation in tonsils and shedding of prions in saliva requires additional research; the presence of prions in the palatine tonsil early in pathogenesis suggests that soil microparticles may expedite the re-entry of prions into the environment.

PMCA is an extremely sensitive method for detecting PrP^{TSE}.^{36,70,71} Relatively few comparisons with IHC have been published. The present study shows that mbPMCA is more sensitive than IHC in RPLN and SMLN, palatine tonsils, and ileal tissues. Although the highest dilution of CWD-positive brain homogenate detectable in the first to third rounds may vary, we are able to routinely detect the 10^{-13.6} dilution from CWD BH (18th 5-fold dilution of 10% CWD BH) after four rounds of mbPMCA. No further detection occurred in the fifth round (Figure S2).

We expected mbPMCA to be more sensitive than immunohistochemistry (IHC) to determine prion accumulations in tissues. Significantly earlier detection of CWD prions in white-tailed deer by serial PMCA compared to IHC (mean of 2.78 months) has been reported, although the genotype at codon 96 influenced the result; heterozygous 96GS deer exhibited congruous PrP^{TSE} detection by both serial PMCA and IHC.³⁹ We found that mbPMCA to be more sensitive than IHC by at least a factor of $10^{6.3}$, as calculated by the smallest corresponding brain dilution that was positive by mbPMCA. mbPMCA resulted in detection of CWD PrP^{TSE} in multiple tissue types that were negative by IHC (Figures 2, S1). In our IHC examination of the lymph nodes and tonsils, particular attention was directed toward the nodular germinal centers of the cortex and medulla. In the ileal tissues, gut-associated lymphoid tissue was inspected in addition to intestinal crypts. No prion antibody staining was determined for any tissue at 42 dpi.

At 42 dpi CWD prions were present in more tissues and at higher concentrations in the fawns dosed with prions associated with montmorillonite microparticles than in those inoculated with prions alone. This finding is consistent with the enhanced transmission of prion disease in hamsters when the agent is bound to montmorillonite (and other microparticles).^{23,24} These data suggest that soil and dietary microparticles may have a similar effect on transmission and early disease pathogenesis in deer, although differences in particle size, shape, and surface chemistry may influence the effect of particles in disease transmission. We note is that humans consume exogenous microparticles via food and pharmaceutical additives^{66,72} at a rate of ~40 mg/d (approximately 10^{12} particles/d).⁶² Although microparticles have not been implicated in the transmission of human TSEs, our data suggest that investigation of microparticles as a risk factor in oral TSE acquisition is warranted. Contamination of soil environments with CWD prions has been proposed to contribute to the spread and maintenance of the disease in both wild and

captive cervid populations.^{17,30} Our results suggest that management decisions must consider the role local soils may play in CWD transmission and pathogenesis, of shed infectious agent in the environment.

5.7 ACKNOWLEDGEMENTS

We thank Dr. Delwyn Keane, Ben Johnson, and Dan Barr (Wisconsin Veterinary Diagnostic Laboratory); Judd Aiken for the CWD-positive white-tailed deer tissue; Glenn Telling for the Tg(CerPrP) mice; Natalie Kirk, Rose Millevolte, and Gabriel Epstein for their assistance with tissue analysis; Dr. Terry Spraker, Dr. Thomas Gidlewski and the animal care staff for their excellent care of the deer, and Dr. Katherine O'Rourke from the USDA Agricultural Research Service, Pullman, WA, for genetic analysis. Thank you to Guilherme Ludwig for assistance with statistical analysis. This work was funded by the National Institutes of Health grant R01 NS060034. ARC was supported by NIEHS T32 ES007015.

5.8 REFERENCES

1. Prusiner, S. B., Prions. *Proc Natl Acad Sci U S A* **1998**, *95*, (23), 13363-13383.
2. Prusiner, S. B., Molecular biology of prion diseases. *Science* **1991**, *252*, (5012), 1515-1522.
3. Hope, J., Bovine spongiform encephalopathy: a tipping point in One Health and Food Safety. *Curr Top Microbiol Immunol* **2013**, *366*, 37-47.
4. Soto, C., Prion hypothesis: the end of the controversy? *Trends Biochem Sci* **2011**, *36*, (3), 151-158.
5. Prusiner, S. B., Novel proteinaceous infectious particles cause Scrapie. *Science* **2011**, *216*, (4542), 136-144.
6. Silva, C. J.; Vazquez-Fernandez, E.; Onisko, B.; Requena, J. R., Proteinase K and the structure of PrPSc: The good, the bad and the ugly. *Virus Res* **2015**, *207*, 120-126.
7. Bolton, D. C.; Bendheim, P. E.; Marmorstein, A. D.; Potempska, A., Isolation and structural studies of the intact scrapie agent protein. *Arch Biochem Biophys* **1987**, *258*, (2), 579-590.
8. Taylor, D. M., Inactivation of prions by physical and chemical means. *J Hosp Infect* **1999**, *43 Suppl*, S69-76.
9. Mathiason, C. K.; Powers, J. G.; Dahmes, S. J.; Osborn, D. A.; Miller, K. V.; Warren, R. J.; Mason, G. L.; Hays, S. A.; Hayes-Klug, J.; Seelig, D. M.; Wild, M. A.; Wolfe, L. L.; Spraker, T. R.; Miller, M. W.; Sigurdson, C. J.; Telling, G. C.; Hoover, E. A., Infectious prions in the saliva and blood of deer with chronic wasting disease. *Science* **2006**, *314*, (5796), 133-136.
10. Henderson, D. M.; Manca, M.; Haley, N. J.; Denkers, N. D.; Nalls, A. V.; Mathiason, C. K.; Caughey, B.; Hoover, E. A., Rapid antemortem detection of CWD prions in deer saliva. *PLoS One* **2013**, *8*, (9), e74377.
11. Haley, N. J.; Seelig, D. M.; Zabel, M. D.; Telling, G. C.; Hoover, E. A., Detection of CWD prions in urine and saliva of deer by transgenic mouse bioassay. *PLoS One* **2009**, *4*, (3), e4848.
12. Tamgüney, G.; Miller, M. W.; Wolfe, L. L.; Sirochman, T. M.; Glidden, D. V.; Palmer, C.; Lemus, A.; DeArmond, S. J.; Prusiner, S. B., Asymptomatic deer excrete infectious prions in faeces. *Nature* **2009**, *461*, (7263), 529-532.
13. Haley, N. J.; Mathiason, C. K.; Zabel, M. D.; Telling, G. C.; Hoover, E. A., Detection of sub-clinical CWD infection in conventional test-negative deer long after oral exposure to urine and feces from CWD+ deer. *PLoS One* **2009**, *4*, (11), e7990.

14. Safar, J. G.; Lessard, P.; Tamguney, G.; Freyman, Y.; Deering, C.; Letessier, F.; Dearmond, S. J.; Prusiner, S. B., Transmission and detection of prions in feces. *J Infect Dis* **2008**, *198*, (1), 81-89.
15. Tamguney, G.; Miller, M. W.; Wolfe, L. L.; Sirochman, T. M.; Glidden, D. V.; Palmer, C.; Lemus, A.; DeArmond, S. J.; Prusiner, S. B., Asymptomatic deer excrete infectious prions in faeces. *Nature* **2010**, *466*, (7306), 652-652.
16. Angers, R. C.; Seward, T. S.; Napier, D.; Green, M.; Hoover, E.; Spraker, T.; O'Rourke, K.; Balachandran, A.; Telling, G. C., Chronic wasting disease prions in elk antler velvet. *Emerg Infect Dis* **2009**, *15*, (5), 696-703.
17. Miller, M. W.; Williams, E. S.; Hobbs, N. T.; Wolfe, L. L., Environmental sources of prion transmission in mule deer. *Emerg Infect Dis* **2004**, *10*, (6), 1003-1006.
18. Mathiason, C. K.; Hays, S. A.; Powers, J.; Hayes-Klug, J.; Langenberg, J.; Dahmes, S. J.; Osborn, D. A.; Miller, K. V.; Warren, R. J.; Mason, G. L.; Hoover, E. A., Infectious prions in pre-clinical deer and transmission of chronic wasting disease solely by environmental exposure. *PLoS One* **2009**, *4*, (6), e5916.
19. Miller, M. W.; Wild, M. A.; Williams, E. S., Epidemiology of chronic wasting disease in captive Rocky Mountain elk. *J Wildl Dis* **1998**, *34*, (3), 532-538.
20. Brown, P.; Gajdusek, D. C., Survival of scrapie virus after 3 years' interment. *Lancet* **1991**, *337*, (8736), 269-270.
21. Seidel, B.; Thomzig, A.; Buschmann, A.; Groschup, M. H.; Peters, R.; Beekes, M.; Tertytze, K., Scrapie agent (strain 263K) can transmit disease via the oral route after persistence in soil over years. *PLoS One* **2007**, *2*, (5), e435.
22. Georgsson, G.; Sigurdarson, S.; Brown, P., Infectious agent of sheep scrapie may persist in the environment for at least 16 years. *J Gen Virol* **2006**, *87*, (Pt 12), 3737-3740.
23. Johnson, C. J.; McKenzie, D.; Pedersen, J. A.; Aiken, J. M., Meat and bone meal and mineral feed additives may increase the risk of oral prion disease transmission. *J Toxicol Environ Health A* **2011**, *74*, (2-4), 161-166.
24. Johnson, C. J.; Pedersen, J. A.; Chappell, R. J.; McKenzie, D.; Aiken, J. M., Oral transmissibility of prion disease is enhanced by binding to soil particles. *PLoS Pathog* **2007**, *3*, (7), e93.
25. Johnson, C. J.; Phillips, K. E.; Schramm, P. T.; McKenzie, D.; Aiken, J. M.; Pedersen, J. A., Prions adhere to soil minerals and remain infectious. *PLoS Pathog* **2006**, *2*, (4), e32.
26. Jacobson, K. H.; Kuech, T. R.; Pedersen, J. A., Attachment of pathogenic prion protein to model oxide surfaces. *Environ Sci Technol* **2013**, *47*, (13), 6925-6934.

27. Cooke, C. M.; Rodger, J.; Smith, A.; Fernie, K.; Shaw, G.; Somerville, R. A., Fate of prions in soil: detergent extraction of PrP from soils. *Environ Sci Technol* **2007**, *41*, 811-817.
28. Jacobson, K. H.; Lee, S.; Somerville, R. A.; McKenzie, D.; Benson, C. H.; Pedersen, J. A., Transport of the pathogenic prion protein through soils. *J Environ Qual* **2010**, *39*, (4), 1145-1152.
29. Nichols, T. A.; Pulford, B.; Wyckoff, A. C.; Meyerett-Reid, C.; Michel, B.; Gertig, K.; Hoover, E. A.; Jewell, J. E.; Telling, G.; Zabel, M. D., Detection of protease-resistant cervid prion protein in water from a CWD-endemic area. *Prion* **2009**, *3*, (3), 171-183.
30. Schramm, P. T.; Johnson, C. J.; Mathews, N. E.; McKenzie, D.; Aiken, J. M., Potential role of soil in the transmission of prion disease. *Rev Mineral Geochem* **2006**, *64*, 135-152.
31. Pedersen, J. A.; Somerville, R. A., Why and how are CWD and Scrapie sometimes spread via environmental routes? In *Decontamination of Prions*, Reisner, D.; Deslys, J.-P., Eds. Dusseldorf University Press: Dusseldorf Germany, 2012; pp 19-37.
32. Stevens, C. E.; Hume, I. D., Contributions of microbes in vertebrate gastrointestinal tract to production and conservation of nutrients. *Physiol Rev* **1998**, *78*, (2), 393-427.
33. Moudjou, M.; Sibille, P.; Fichet, G.; Reine, F.; Chapuis, J.; Herzog, L.; Jaumain, E.; Laferriere, F.; Richard, C. A.; Laude, H.; Andreoletti, O.; Rezaei, H.; Beringue, V., Highly infectious prions generated by a single round of microplate-based protein misfolding cyclic amplification. *MBio* **2014**, *5*, (1), e00829-13.
34. Johnson, C. J.; Herbst, A.; Duque-Velasquez, C.; Vanderloo, J. P.; Bochsler, P.; Chappell, R.; McKenzie, D., Prion protein polymorphisms affect chronic wasting disease progression. *PLoS One* **2011**, *6*, (3), e17450.
35. Gao, J.; Pedersen, J. A., Adsorption of sulfonamide antimicrobial agents to clay minerals. *Environ Sci Technol* **2005**, *39*, (24), 9509-9516.
36. Johnson, C. J.; Aiken, J. M.; McKenzie, D.; Samuel, M. D.; Pedersen, J. A., Highly efficient amplification of chronic wasting disease agent by protein misfolding cyclic amplification with beads (PMCAb). *PLoS One* **2012**, *7*, (4), e35383.
37. Browning, S. R.; Mason, G. L.; Seward, T.; Green, M.; Eliason, G. A.; Mathiason, C.; Miller, M. W.; Williams, E. S.; Hoover, E.; Telling, G. C., Transmission of prions from mule deer and elk with chronic wasting disease to transgenic mice expressing cervid PrP. *J Virol* **2004**, *78*, (23), 13345-13350.
38. Wyckoff, A. C.; Galloway, N.; Meyerett-Reid, C.; Powers, J.; Spraker, T.; Monello, R. J.; Pulford, B.; Wild, M.; Antolin, M.; VerCauteren, K.; Zabel, M., Prion amplification and hierarchical Bayesian modeling refine detection of prion infection. *Sci Rep* **2015**, *5*, 1-8.

39. Haley, N. J.; Mathiason, C. K.; Carver, S.; Telling, G. C.; Zabel, M. D.; Hoover, E. A., Sensitivity of protein misfolding cyclic amplification versus immunohistochemistry in ante-mortem detection of chronic wasting disease. *J Gen Virol* **2012**, *93*, (Pt 5), 1141-1150.
40. Lacroux, C.; Comoy, E.; Moudjou, M.; Perret-Liaudet, A.; Lugan, S.; Litaize, C.; Simmons, H.; Jas-Duval, C.; Lantier, I.; Beringue, V.; Groschup, M.; Fichet, G.; Costes, P.; Streichenberger, N.; Lantier, F.; Deslys, J. P.; Vilette, D.; Andreoletti, O., Preclinical detection of variant CJD and BSE prions in blood. *PLoS Pathog* **2014**, *10*, (6), e1004202.
41. Gonzalez-Montalban, N.; Makarava, N.; Ostapchenko, V. G.; Savtchenko, R.; Alexeeva, I.; Rohwer, R. G.; Baskakov, I. V., Highly efficient protein misfolding cyclic amplification. *PLoS Pathog* **2011**, *7*, (2), e1001277.
42. Sigurdson, C.; Williams, E. S.; Miller, M. W.; Spraker, T.; O'Rourke, K., Oral transmission and early lymphoid tropism of chronic wasting disease PrPres in mule deer fawns (*Odocoileus hemionus*). *J Gen Virol* **1999**, *80*, 2757-2764.
43. Beekes, M.; McBride, P. A., The spread of prions through the body in naturally acquired transmissible spongiform encephalopathies. *FEBS J* **2007**, *274*, (3), 588-605.
44. Fox, K. A.; Jewell, J. E.; Williams, E. S.; Miller, M. W., Patterns of PrPCWD accumulation during the course of chronic wasting disease infection in orally inoculated mule deer (*Odocoileus hemionus*). *J Gen Virol* **2006**, *87*, (Pt 11), 3451-3461.
45. Press, C. M.; Heggebo, R.; Espenes, A., Involvement of gut-associated lymphoid tissue of ruminants in the spread of transmissible spongiform encephalopathies. *Adv Drug Deliv Rev* **2004**, *56*, (6), 885-899.
46. Cancedda, M. G.; Di Guardo, G.; Chiocchetti, R.; Demontis, F.; Marruchella, G.; Sorteni, C.; Maestrale, C.; Lai, A.; Ligios, C., Role of palatine tonsils as a prion entry site in classical and atypical experimental sheep scrapie. *J Virol* **2014**, *88*, (2), 1065-1070.
47. Krejciova, Z.; De Sousa, P.; Manson, J.; Ironside, J. W.; Head, M. W., Human tonsil-derived follicular dendritic-like cells are refractory to human prion infection in vitro and traffic disease-associated prion protein to lysosomes. *Am J Pathol* **2014**, *184*, (1), 64-70.
48. Nichols, T. A.; Spraker, T. R.; Rigg, T. D.; Meyerett-Reid, C.; Hoover, C.; Michel, B.; Bian, J.; Hoover, E.; Gidlewski, T.; Balachandran, A.; O'Rourke, K.; Telling, G. C.; Bowen, R.; Zabel, M. D.; VerCauteren, K. C., Intranasal inoculation of white-tailed deer (*Odocoileus virginianus*) with lyophilized chronic wasting disease prion particulate complexed to montmorillonite clay. *PLoS One* **2013**, *8*, (5), e62455.
49. Windl, O.; Dempster, M.; Estibeiro, J. P.; Lathe, R.; de Silva, R.; Esmonde, T.; Will, R.; Springbett, A.; Campbell, T. A.; Sidle, K. C. L.; Palmer, M. S.; Collinge, J., Genetic basis of Creutzfeldt-Jakob disease in the United Kingdom: a systemic analysis of predisposing mutations and allelic variation in the PRNP gene. *Hum Genet* **1996**, *98*, 259-264.

50. Hunter, N.; Goldmann, W.; Foster, J. D.; Cairns, D.; Smith, G., Natural scrapie and PrP genotype: case-control studies in British sheep. *Vet Rec* **1997**, *141*, 137-140.
51. Bucalossi, C.; Cosseddu, G.; D'Agostino, C.; Di Bari, M. A.; Chiappini, B.; Conte, M.; Rosone, F.; De Grossi, L.; Scavia, G.; Agrimi, U.; Nonno, R.; Vaccari, G., Assessment of the genetic susceptibility of sheep to scrapie by protein misfolding cyclic amplification and comparison with experimental scrapie transmission studies. *J Virol* **2011**, *85*, (16), 8386-8392.
52. Saunders, S. E.; Bartelt-Hunt, S. L.; Bartz, J. C., Resistance of soil-bound prions to rumen digestion. *PLoS One* **2012**, *7*, (8), e44051.
53. Combrinck, M. I.; Perry, V. H.; Cunningham, C., Peripheral infection evokes exaggerated sickness behaviour in pre-clinical murine prion disease. *Neuroscience* **2002**, *112*, (1), 7-11.
54. Heikenwalder, M.; Zeller, N.; Seeger, H.; Prinz, M.; Klohn, P. C.; Schwarz, P.; Ruddle, N. H.; Weissmann, C.; Aguzzi, A., Chronic lymphocytic inflammation specifies the organ tropism of prions. *Science* **2005**, *307*, (5712), 1107-1110.
55. Jeffrey, M.; Gonzalez, L.; Espenes, A.; Press, C. M.; Martin, S.; Chaplin, M.; Davis, L.; Landsverk, T.; MacAldowie, C.; Eaton, S.; McGovern, G., Transportation of prion protein across the intestinal mucosa of scrapie-susceptible and scrapie-resistant sheep. *J Pathol* **2006**, *209*, (1), 4-14.
56. Sigurdson, C. J.; Heikenwalder, M.; Manco, G.; Barthel, M.; Schwarz, P.; Stecher, B.; Krautler, N. J.; Hardt, W. D.; Seifert, B.; MacPherson, A. J.; Cortesy, I.; Aguzzi, A., Bacterial colitis increases susceptibility to oral prion disease. *J Infect Dis* **2009**, *199*, (2), 243-252.
57. Mitchell, N. J.; Kumi, J.; Aleser, M.; Elmore, S. E.; Rychlik, K. A.; Zychowski, K. E.; Romoser, A. A.; Phillips, T. D.; Ankrah, N. A., Short-term safety and efficacy of calcium montmorillonite clay (UPSN) in children. *Am J Trop Med Hyg* **2014**, *91*, (4), 777-785.
58. Zychowski, K. E.; Elmore, S. E.; Rychlik, K. A.; Ly, H. J.; Pierezan, F.; Isaiah, A.; Suchodolski, J. S.; Hoffmann, A. R.; Romoser, A. A.; Phillips, T. D., Mitigation of colitis with NovaSil clay therapy. *Dig Dis Sci* **2015**, *60*, (2), 382-392.
59. Zychowski, K. A. Calcium montmorillonite for the mitigation of aflatoxicosis and gastrointestinal inflammation. Texas A&M University, 2014.
60. Hu, C. H.; Gu, L. Y.; Luan, Z. S.; Song, J.; Zhu, K., Effects of montmorillonite-zinc oxide hybrid on performance, diarrhea, intestinal permeability and morphology of weanling pigs. *Anim Feed Sci Tech* **2012**, *177*, (1-2), 108-115.
61. Mahraoui, L.; Heymann, M.; Plique, O.; Droy-Lefaix, M. T.; Desjeux, J. F., Atypical effect of diosmectite on damage to the intestinal baffle induced by basal tumour necrosis factor- α . *Gut* **1997**, *40*, 339-343.

62. Powell, J. J.; Thoree, V.; Pele, L. C., Dietary microparticles and their impact on tolerance and immune responsiveness of the gastrointestinal tract. *Br J Nutr* **2007**, *98 Suppl 1*, S59-63.
63. Szajewska, H.; Dziechciarz, P.; Mrukowicz, J., Meta-analysis: Smectite in the treatment of acute infectious diarrhoea in children. *Aliment Pharmacol Ther* **2006**, *23*, (2), 217-227.
64. Madkour, A. A.; Madina, E. M. H.; El-Azzouni, O. E. Z.; Amer, M. A.; El-Walili, T. M. K.; Abbass, T., Smectite in acute diarrhea in children: a double blind placebo-controlled clinical trial. *J Pediatr Gastroenterol Nutr* **1993**, *17*, 176-181.
65. Dupont, C.; Foo, J. L.; Garnier, P.; Moore, N.; Mathiex-Fortunet, H.; Salazar-Lindo, E.; Peru; Malaysia Diosmectite Study, G., Oral diosmectite reduces stool output and diarrhea duration in children with acute watery diarrhea. *Clin Gastroenterol Hepatol* **2009**, *7*, (4), 456-462.
66. Lomer, M. C. E.; Thompson, R. P. H.; Powell, J. J., Fine and ultrafine particles of the diet: influence on the mucosal immune response and association with Crohn's disease. *Proc Nutr Soc* **2002**, *61*, (01), 123-130.
67. Powell, J. J.; Ainley, C. C.; Harvey, R. S. J.; Mason, I. M.; Kendall, M. D.; Sankey, E. A.; Dhillon, A. P.; Thompson, R. P., Characterisation of inorganic microparticles in pigment cells of human gut associated lymphoid tissue. *Gut* **1996**, *38*, 390-395.
68. Powell, J. J.; Faria, N.; Thomas-McKay, E.; Pele, L. C., Origin and fate of dietary nanoparticles and microparticles in the gastrointestinal tract. *J Autoimmun* **2010**, *34*, (3), J226-233.
69. Kincaid, A. E.; Bartz, J. C., The nasal cavity is a route for prion infection in hamsters. *J Virol* **2007**, *81*, (9), 4482-4491.
70. Saa, P.; Castilla, J.; Soto, C., Ultra-efficient replication of infectious prions by automated protein misfolding cyclic amplification. *J Biol Chem* **2006**, *281*, (46), 35245-35252.
71. Saborio, G. P.; Permanne, B.; Soto, C., Sensitive detection of pathological prion protein by cyclic amplification of protein misfolding. *Nature* **2001**, *411*, (6839), 810-813.
72. Lomer, M. C. E.; Hutchinson, C.; Volkert, S.; Greenfield, S. M.; Catterall, A.; Thompson, R. P. H.; Powell, J. J., Dietary sources of inorganic microparticles and their intake in healthy subjects and patients with Crohn's disease. *Br J Nutr* **2007**, *92*, (06), 947-955.

5.9 TABLES

Table 1. Prions were detected in four of eleven tissues tested at 42 dpi.

Inoculum	Mte	<i>PRNP</i> Genotype (codon 96)	Sex	Retropharyngeal Lymph Node <i>n</i> = 4	Palatine Tonsil <i>n</i> = 3	Submandibular Lymph Node <i>n</i> = 3	Ileum <i>n</i> = 4
Uninfected BH	–	GS	F	–,–,–,–	–,–,–	–,–,–	–,–,–,–
CWD BH	–	GG	M	4,–,–,–	–,–,–	–,–,–	–,–,–,–
CWD BH	–	GG	F	2,2,3,–	–,–,–	3,–,–	2,3,3,–
CWD BH	–	GS	F	4,–,–,–	–,–,–	–,–,–	2,2,–,–
CWD BH	+	GS	F	2,2,2,–	–,–,–	2,3,3	3,4,–,–
CWD BH	+	GG	F	1,2,2,2	2,2,–	3,3,–	1,2,2,–
CWD BH	+	GG	F	1,2,–,–	2,–,–	3,3,–	3,–,–,–

Abbreviations: Mte, montmorillonite; *PRNP*, prion protein gene; BH, brain homogenate; *n*, number of individual samples tested for each tissue type listed.

Numbers indicate first round of mbPMCA (out of 4) where sample was positive by Western blot.

Information represented graphically in Figure S3.

PRNP genotype at codon 96 is reported; genotype at codon 95 was QQ for all animals.

5.10 FIGURES

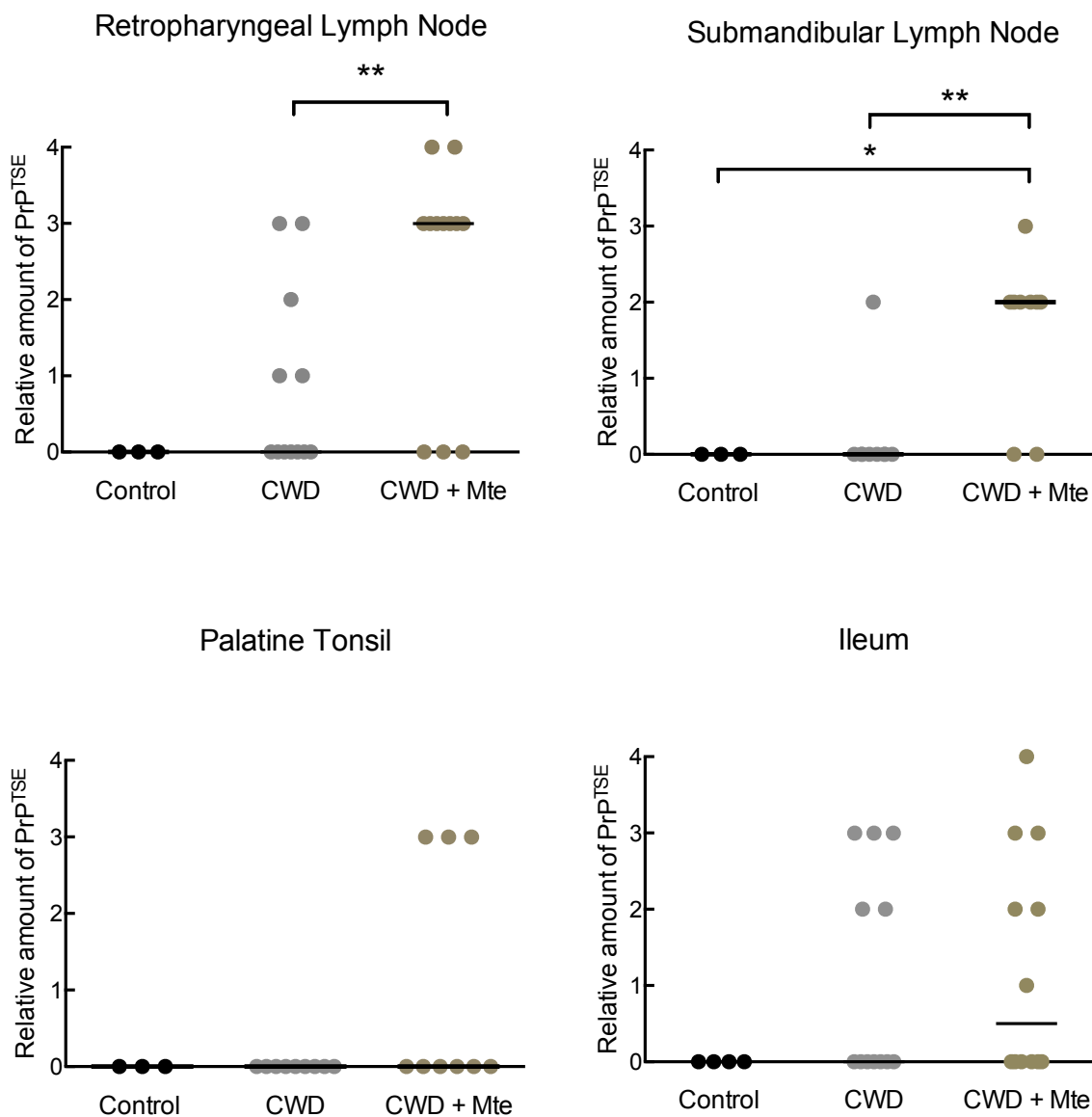


Figure 1. Accumulation of disease-associated prion protein (PrP^{TSE}) is higher in white-tailed deer orally exposed to chronic wasting disease (CWD) prions + montmorillonite (Mte) relative to those inoculated with prions alone. The round of microplate-based protein misfolding cyclic amplification (PMCA) in which PrP^{TSE} was first detected in samples was subtracted from the maximum number of rounds (4), plus one to yield a metric reflecting the relative amount of PrP^{TSE}. Each dot denotes a replicate sample. No

detection was assigned a value of zero. Lines indicate median values; differences among medians were tested by the nonparametric Kruskal-Wallis H test for each tissue with Dunn's multiple-comparison posttest and pair-wise comparisons were made with one tailed Mann-Whitney U test (*, $p < 0.05$).

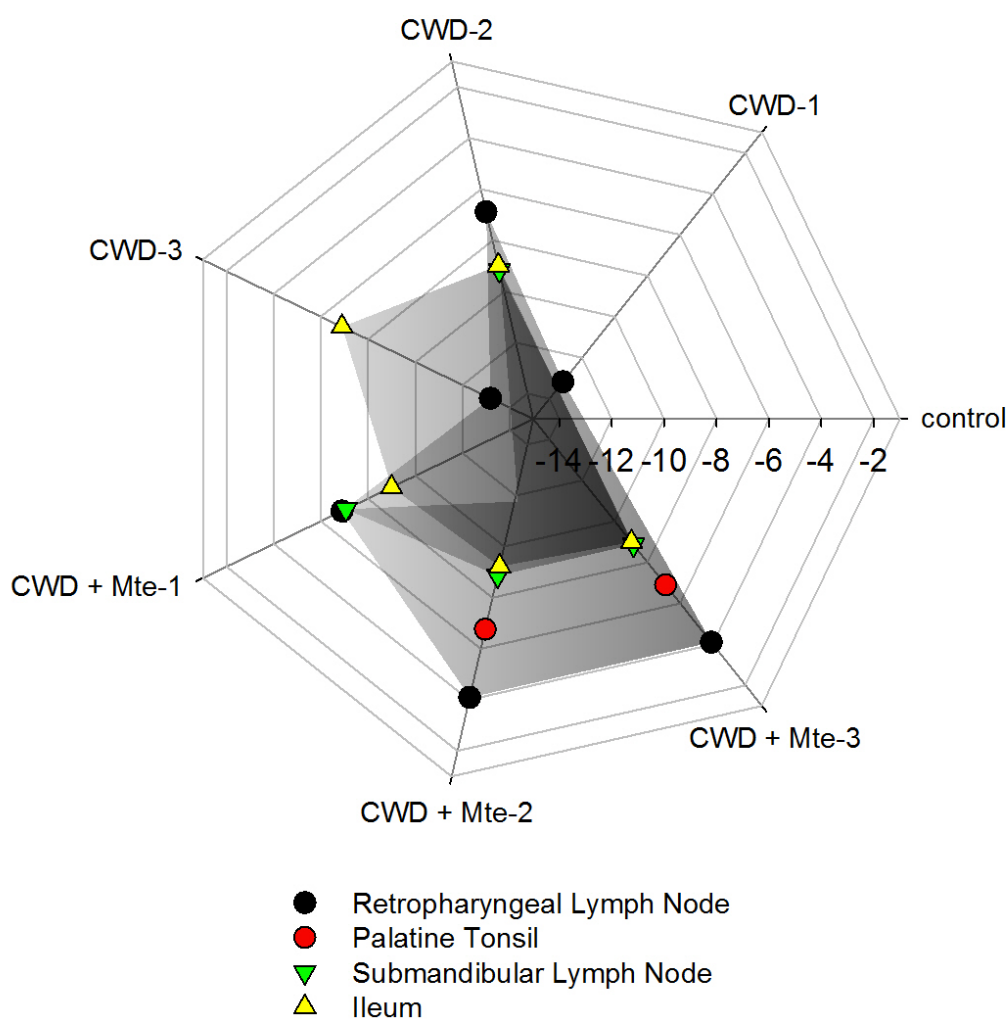


Figure 2. The amount of prions was higher in animals inoculated with chronic wasting disease (CWD) prions associated with montmorillonite (Mte) microparticles than in those dosed with CWD prions alone. The axis expresses amount of prions as an equivalent dilution of deer brain tissue from a clinical CWD-infected white-tailed deer (Figure S2). Details of the analysis are described in the text. Values represent means of all replicates for each tissue type per animal.

5.10 APPENDIX

Supporting Information for Chapter 5

Microparticles Alter Early Disease Tissue Tropism and Accumulation of Chronic Wasting Disease Prions in White-Tailed Deer*

Microparticles Alter Early Prion Disease Pathogenesis

*A version of this chapter will be submitted to *PLoS Pathogens* with Johnson, C.J., Nichols, T.A., Kornely, H.J., Shoukfeh, D., and Pedersen, J.A. as co-authors.

Table of Contents

	Page
5.10.1 Tables	187
Table S1. Tissues analyzed by mbPMCA for the presence of PrP ^{TSE}	187
5.10.2 Figures	188
S1. Immunohistochemical analysis fails to detect pathogenic PrP in white-tailed deer tissues harvested at 42 dpi that test CWD-positive by mbPMCA.	188
S2. Dilution series of PrP ^{TSE} in CWD-infected brain tissue analyzed by mbPMCA.	189
S3. Detection of PrP ^{TSE} by mbPMCA in tissues of white-tailed deer at 42 days post oral challenge with CWD in the presence and absence of montmorillonite.	190
S4. Variation of estimated PrP ^{TSE} content due to treatment rather than tissue type.	191

5.10.1 TABLES

Table S1. Tissues analyzed by mbPMCA for the presence of PrP^{TSE}

Lymphatic	Intestinal	Neural	Peripheral
Retropharyngeal lymph node	Duodenum	Lumbar spinal cord	Forelimb muscle
Submandibular lymph node	Ileum	Thoracic spinal cord	
Palatine tonsil	Cecum		
Spleen	Colon		

5.10.2 FIGURES

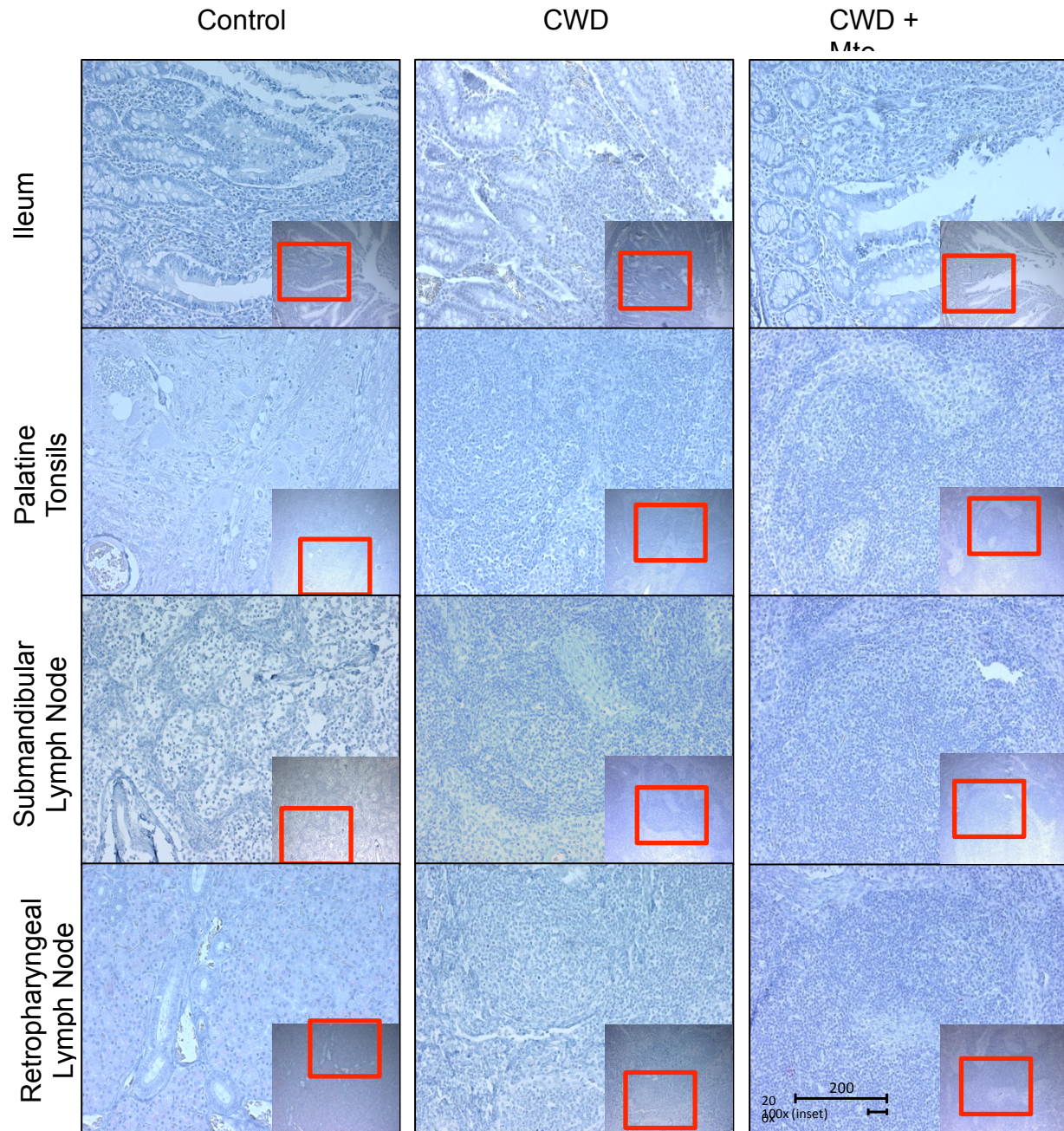
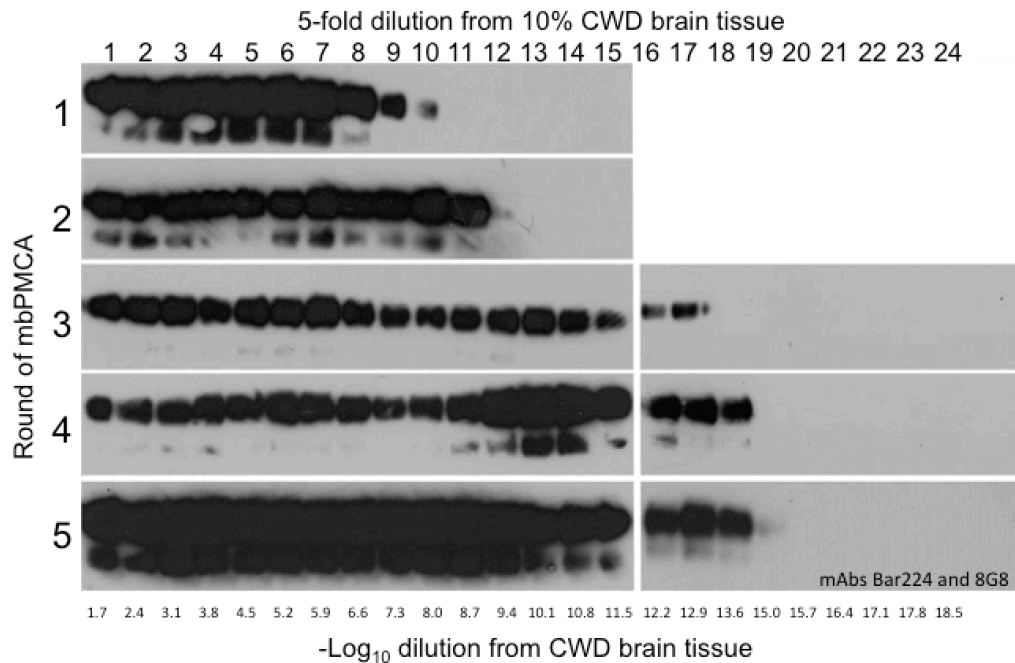


Figure S1. Immunohistochemical analysis fails to detect pathogenic PrP in white-tailed deer tissues harvested at 42 dpi that test CWD-positive by mbPMCA. Representative samples of tissue thin sections immunohistochemically stained for PrP using PrP-specific monoclonal antibody Anti-Prion 99. Control tissues from deer orally inoculated with uninfected brain homogenate. Magnification 20× (Inset 10×).



B

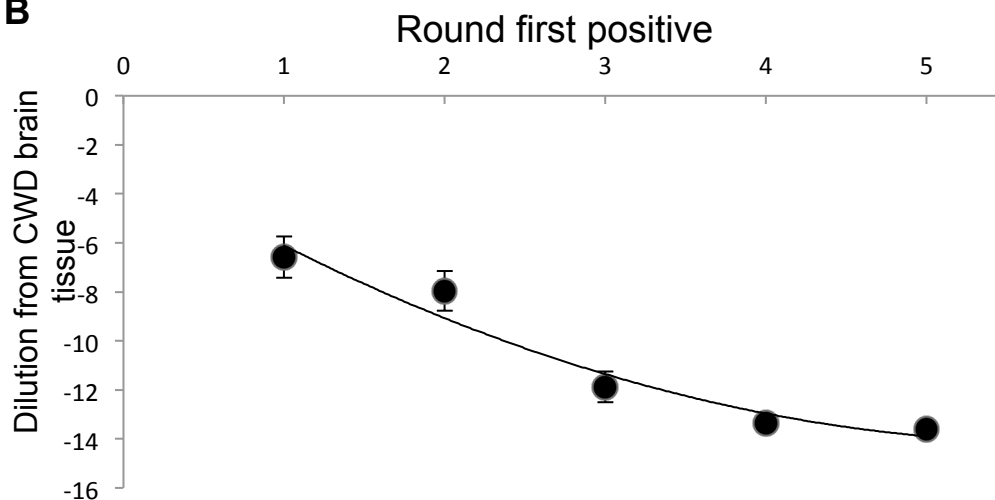


Figure S2. Dilution series of PrP^{TSE} in CWD-infected brain tissue analyzed by mbPMCA. The brain homogenate (BH) from a clinical CWD-infected white-tailed deer was serially diluted 5-fold in normal BH (NBH) to a maximum dilution of $10^{-18.5}$ relative to the original deer brain tissue. (A) Diluted samples CWD+ BH (4 μ L) were used to seed NBH (96 μ L) in the mbPMCA reaction. Detection was achieved by immunoblotting using monoclonal antibodies Bar224 and 8G8. Representative blots are shown ($n = 6$). (B) Calibration curve constructed from mbPMCA results. Data points are the mean of six replicates of the mbPMCA round at which detection was first observed; error bars represent one standard deviation. The line fit to the data is $y = 0.3387x^2 - 3.9778x - 2.4725$ ($R^2 = 0.95$).

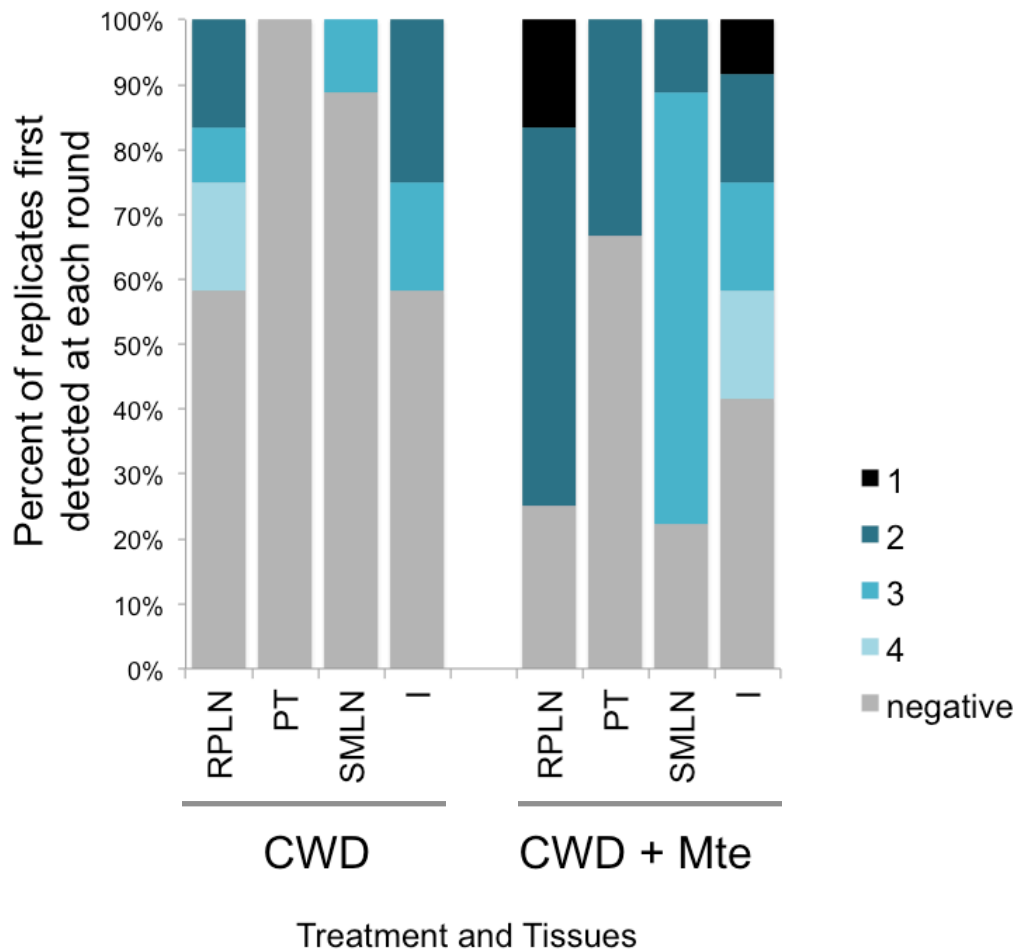


Figure S3. Detection of PrP^{TSE} by mbPMCA in tissues of white-tailed deer at 42 days post oral challenge with CWD in the presence and absence of montmorillonite. Numbers indicate the round of mbPMCA yielding the first detection of PrP^{TSE}. Tissues from the control animal were negative for all rounds of mbPMCA. Abbreviations: RPLN, retropharyngeal lymph node; PT, palatine tonsil; SMLN, submandibular lymph node; I, ileum.

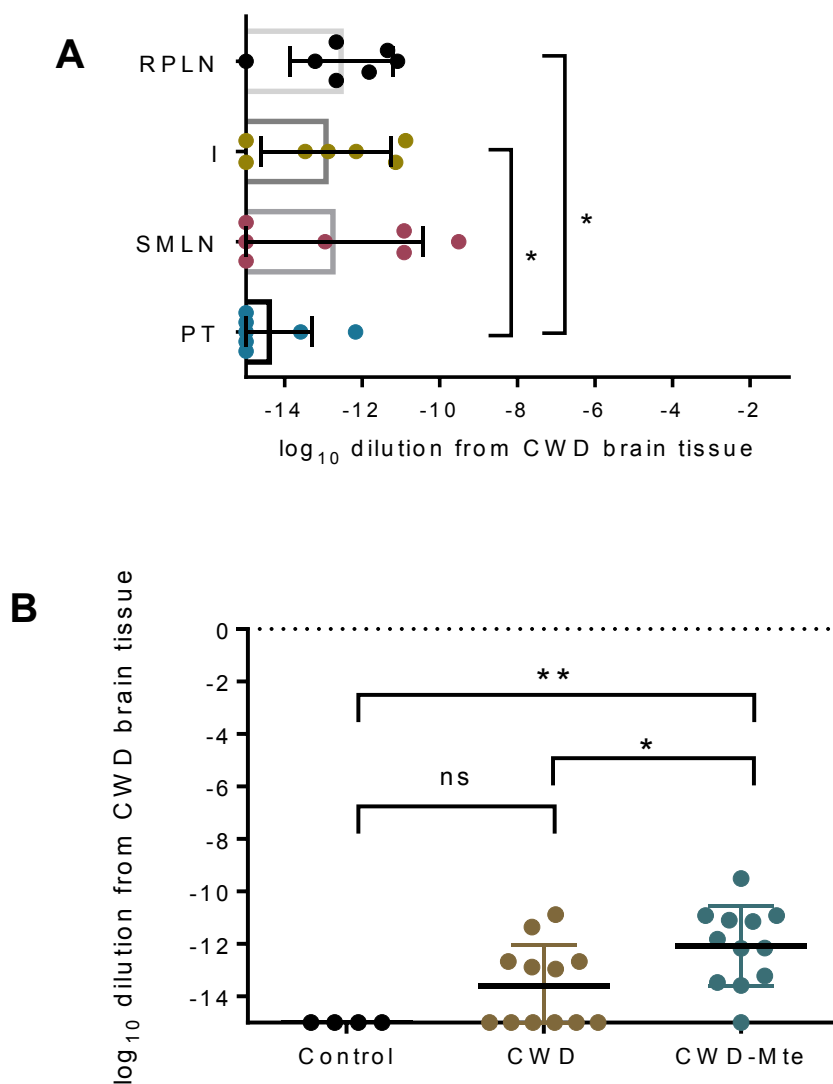


Figure S4. Variation of estimated PrP^{TSE} content due to treatment rather than tissue type. (A) A nonparametric Friedman test indicates no difference between tissue types when treatment is excluded, except for RPLN and PT, where the RPLN had more PrP^{TSE} than did the PT ($p = 0.0256$, Mann-Whitney U). (B) The effect of treatment type differed between treatments (CWD \pm Mte treatments vs. control) ($p < 0.0086$) when tissue type was excluded (i.e., all tissue types pooled for each treatment). The CWD + Mte treatment resulted in production of more PrP^{TSE} than the CWD treatment ($p = 0.0406$) and the control ($p = 0.0044$) (both Mann-Whitney U). Replicates without prion detection by mbPMCA are indicated with a value of $-15 \log_{10}$ dilution (lowest dilution of CWD+ BH that was not detectable after five rounds of mbPMCA). *, $p < 0.05$; **, $p < 0.01$, ns, not significant ($p > 0.05$).

Chapter 6

Overall conclusions and future research needs.

While many of the conclusions that can be drawn from the individual experiments and studies contained in this thesis can be found at the end of each chapter the overarching themes from this body of work can be summarized as follows:

- . Although to our knowledge there is currently no use of chemical decontamination of prion-contaminated land, the need exists to curtail the environmental spread of chronic wasting disease. Peroxymonosulfate is an advanced chemical oxidation process that may have application in inactivating prions shed into the environment by diseased animals, thereby limiting the transmission to naïve animals.
- . We show that peroxymonosulfate is able to inactivate two different strains of prions. It is also able to inactivate CWD prions at environmentally relevant pH and temperatures and when PrP^{TSE} is associated with whole soils and clay and iron oxide particles.
- . The challenge of environmental use of peroxymonosulfate for prion decontamination is the risk of toxicity. We show that, although peroxymonosulfate is toxic to soil microflora and turfgrass, grass can be regrown in soils exposed to high concentrations of peroxymonosulfate. Further work is warranted to determine methods of application to increase time of contact with PrP^{TSE} “hot spots” while reducing toxicity to non-target species.
- . Additional work is needed to build on our basic understanding of prion structures, and furthermore, how prions interact with soil components. This information would improve

our understanding of the molecular level interactions that govern the behavior of infectious units in environmental systems.

- . In white tailed deer, CWD prions have higher accumulation and accumulate in a larger number of tissues when the prions are associated with montmorillonite.
- . In vitro amplification of PrP^{TSE} by microplate-based PMCA is more sensitive in detecting prions in infected tissues by a factor exceeding $10^{6.3}$.
- . Supplemental analytical and theoretical work in early prion disease pathogenesis when prions are associated with clay microparticles is warranted and critical to understand the mechanism of montmorillonite-enhanced prion disease transmission seen in rodent studies and what was recapitulated here in deer. A crucial study would be to track clay-bound prions from the intestinal lumen across the intestinal epithelium; clay additives are often included in animal feed to increase nutrient retention time and the same effect could hold true for clay particle-bound prions. It is also possible that the lymphatic sampling and uptake of clay particle-bound prions is increased relative to the unbound prion. Additionally, it would be sensible to investigate macrophage-mediated attack of Mte-bound and unbound PrP^{TSE}. Suggested approaches for these studies could be using radiolabelled or dye conjugated PrP^{TSE} bound to clay.